



EARLY MESOZOIC DETRITAL AND EVAPORITIC SYNRIFT SERIES OF MOHAMMEDIA-BENSLIMANE-EL GARA-BERRECHID BASIN (WESTERN MESETA, MOROCCO): SEDIMENTARY AND PALAEOENVIRONMENTAL EVOLUTION AND COMPARISON WITH THE BASINS OF THE NORTHEASTERN AMERICAN MARGIN

Afenzar, Abdelkrim¹ and Rachid, Essamoud¹

¹Dynamics of Sedimentary Basins and Geological Correlations Laboratory, Faculty of Sciences, Ben M'Sik Hassan II University of Casablanca. B.P. 7955, Sidi Othmane, Casablanca, Morocco, r_essamoud@gmail.com

In the early Mesozoic, the northwestern part of the African continent was affected by the initial breakup associated with the early stages of the opening of the Central Atlantic (Central Atlantic rifting). During this phase, the Moroccan Meseta was subjected to an extensive tectonic regime. This extension led to the opening of a set of rift basins, including the Mohammedia-Benslimane-El Gara-Berrechid basin (MBEB) and the focus of our study.

Sedimentological analysis, which is the objective of our work, has shown that during the synrift phase (Upper Triassic-Lower Jurassic), the MBEB basin is characterized by detrital and evaporite sediment filling. This study made it possible to characterize fifteen types of facies and eight architectural elements and facies associations. A gradual decrease of palaeoslope over time led to the evolution of paleoenvironments during this filling from a proximal alluvial fan system to braided rivers, and then to an anastomosing system. These environments eventually evolve to an alluvial plain associated with a coastal plain where playa lakes, mudflats, and lagoons developed. The pure and massive halitic facies at the top of the series probably indicates an evolution of the depositional setting towards a shallow to deep subtidal environment. The presence of evaporites indicates a hot and arid climate that favored their precipitation.

This work allowed a comparison of the sedimentary series of this basin with those of the other basins of the northeastern North American margin. Regarding sedimentary filling history, the American basins belong to the southern segment and the central segment resemble to the Moroccan Atlasic basins as well as the basal detrital formation of the Mesetian and Moroccan Atlantic margin basins. These basins are characterized by continental sedimentation during the Upper Triassic (fluvial deposits interbedded with lacustrine and playa deposits). The basins of the North Atlantic segment have a similarity with our study basin and with the other basins of the Moroccan Atlantic margin concerning the presence of evaporites.

Introduction

The studied basin is one of the most important Triassic basins in Morocco. This importance is reflected in its role to understand the geodynamic and paleogeographic history of the Central Atlantic domain during the Triassic. Usually, These Triassic basins generally show a similar sedimentological evolution, dominated by continental deposits (Withjack et al., 1998; Withjack et al., 2012; Leleu et al., 2016).

The classification and interpretation of deposits are based on several criteria: hierarchies of strata and their boundary surfaces, lithofacies, geometry of sedimentary bodies and architectural elements (Miall, 2006). The main objective of this study is to reconstruct the paleoenvironment and the synrift sedimentological filling history of the MBEB basin and compare this basin and the other Triassic basins belonging to the Central Atlantic domain.



Geological Setting

The Triassic MBEB basin is part of the Moroccan north western Meseta (**Figure 1**). Structural studies present this basin as a vast shallow depression that seems to have originated from N-S to NE-SW half-graben structure (Fadli, 1990; El Wartiti et al., 1992; Medina, 1994). This area is characterized by a Paleozoic basement deformed during the Hercynian orogeny. At the end of the Paleozoic and the early Mesozoic, a half-graben was developed and during Late Triassic-Early Jurassic filled by detrital and evaporitic synrift sediments and associated magmatic activity belonging to CAMP (Afenzar and Essamoud, 2017; Afenzar, 2018).

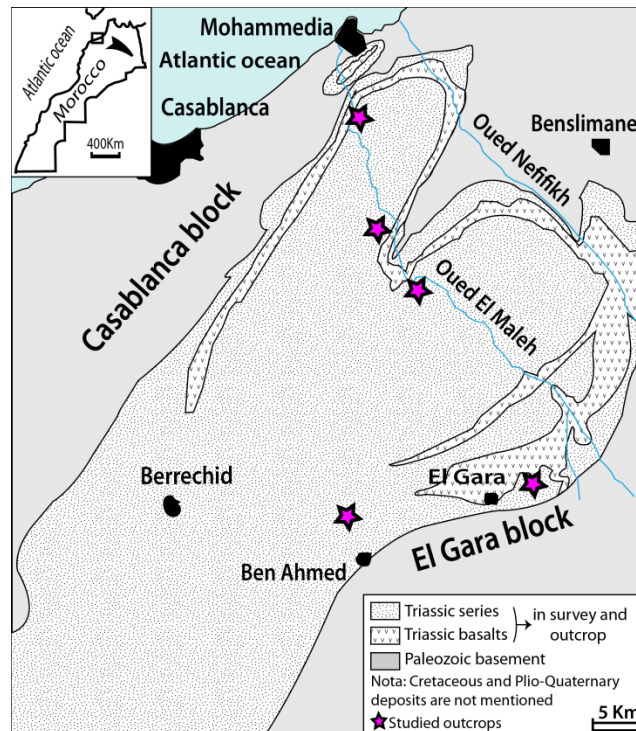


Figure 1. Geographical and geological situation of the Mohammedia-Benslimane-El Gara-Berrechid basin.

In the Late Triassic, this basin was subjected to a NW-SE extension regime with a slight deformation component (El Wartiti et al., 1992; Medina, 1994). According to these authors, this structure is controlled by a deep detachment, which is probably an ancient Hercynian weakness zone, and which plunges slightly towards the NNW (Medina, 1996). This is related to the opening of the proto-Atlantic domain flooded by the Tethys which probably crossed the fracture zone of Gibraltar (E-W or NE-SW: Medina, 1996).

Facies Analysis

In this study, fifteen facies were identified, described, and interpreted in terms of depositional processes (**Tables 1 and 2**).

Conglomerates facies

The conglomerates facies are located in the basal part of the Triassic series of the basin. They have a purple color and present a matrix-supported fabric. The matrix is formed by sand and silt, and the pebble gravels are centimeter to decimeter-sized, showing angular to subangular shapes. Sometimes, these conglomerates do not



show any sedimentary structures (Gms lithofacies: debris flow), other times the stratification may be apparent (Gm lithofacies: characterized by horizontal bedding, imbrication) or (Gp lithofacies: planar crossbeds).

Sandstone Facies

Four sandstone facies were identified, and are located at the base and middle of the series. The sandstones facies range from 0.2 to 4 m thick and consisting of medium- to very coarse-grained sandstone.

1. Massive sandstone (Sm lithofacies) interpreted as rapid deposition and sediment gravity flow.
2. Planar cross-stratified sandstone (Sp lithofacies) representing linguoid, transverse bars, lower flow regime deposits.
3. Horizontally stratified sandstone (Sh lithofacies) interpreted as a planar bed flow/upper flow regime.
4. Fine sandstone, low angle (< 10 °) crossbeds (Sl lithofacies) representing crevasse splays deposits.

Siltstone and Mudstone Facies

Siltstones: Reddish siltstones are the predominant lithofacies throughout the studied sections. Siltstones can be laminated or massive, and up to 20 m thick. These siltstones alternate with sandstone and sometimes with gypsum. They correspond to facies F1 of Miall (2006).

Mudstones: Massive reddish mudstones showing mottling spots. This facies is identified in all outcrops and correspond to facies Fm of Miall (2006) interpreted as overbank deposition in a flood plain or abandoned channel deposits (Miall, 1985, 1996; Einsele 2000; Afenzar and Essamoud 2016; 2017).

Table 1. Description and interpretation of the sedimentary facies identified in the basin and their correspondence with those defined by Miall, (1978, 1985, and 2006).

Lithofacies	Characteristics	Interpretation
Conglomeratic		
Fc1: Gms	Massive disorganized conglomerates, matrix-supported gravel, without sedimentary structures	Mass flows, debris flows deposits
Fc2a: Gm	Clast-supported stratified conglomerates, horizontal bedding imbrication	Longitudinal bar
Fc2b: Gm	Organized conglomerate, Poor matrix	Sieve deposits, lag deposit
Fc3: Gp	Clast-supported planar cross-stratified conglomerate	Linguoid bar, transverse bar
Sandstone		
Fc4: Sm	Massive sandstone, fine to coarse-grain size	Rapid deposition, sediment gravity flow
Fc5: Sp	Planar cross-stratified sandstone, very fine to coarse	Linguoid, transverse bars, lower flow regime
Fc6: Sh	Horizontally stratified sandstone	Planar bed flow, upper flow regime
Fc7: Sl	Fine sandstone, low angle (< 10 °) crossbeds	Crevasse splays deposits
Siltstone and Mudstone		
Fc8: F1	Laminated to massive siltstone	Overbank deposit
Fc9: Fm	Massive to laminated mudstone	Overbank or abandoned channel deposits



Evaporite Facies

Throughout the basin, five evaporitic facies have been identified. The description and interpretation are summarized in **Table 2**.

Table 2. Description and interpretation of the evaporitic facies identified in the basin (Afenzar and Essamoud, 2017, and Afenzar, 2018).

Lithofacies	Characteristics	Interpretation
Fc10	Gypsum bed	Mudflats/lagoon deposits
Fc11	Fibrous gypsum	Diagenetic origin
Fc12	Milky halite	Lagoon, playa and mudflats deposits
Fc13	Phenoblastic halite	Diagenetic deposit
Fc14	Fibrous halite	Diagenetic origin

Architectural Elements and Facies Associations

In this study, we have characterized six architectural elements (AE1–AE6) and two facies associations (AFP: Playa Facies Association, and AFE: Evaporite Facies Association).

Table 3. Description and interpretation of architectural elements (modified after Miall, 2006).

Element	Element code	Lithofacies	Interpretation
Sediment gravity flow	AE1 (SG)	Gm, Gms	Alluvial fans deposits
Channels	AE2 (CH)	Any combination	Fluvial channel deposits
Gravel bars and bedforms	AE3 (GB)	Gm, Gp	Channel deposits/channel floor lag
Sandy bedforms	AE4 (SB)	Sp, Sh, Sl	Channel deposits
Laminated sand sheets	AE5 (LS)	Sh, Sl	Distal overbank sheet
Overbank fines	AE6 (OF)	Sh, Fm, Fl	Floodplain deposits
Facies Association of Playa	AFP	Fm, Fl	Playa lake deposits
Evaporite Facies Association	AFE	Fc10...Fc14	Lagoon, playa and mudflats deposits

Depositional Environment

Facies identification and the characterization of the architectural elements allows reconstruction of the palaeoenvironment in the MBEB basin during the Triassic period:

Alluvial Fan System

In most outcrops, this fluvial model is essentially characterized by the coarse deposits Fc1 (Gms), Fc2a (Gm), Fc2b (Gm), Fc3 (Gp), and medium deposits Fc4 (Sm) and Fc6 (Sh). These lithofacies are associated in three architectural elements: AE1 (sediment gravity flow SG), AE2 (channels CH) and AE3 (gravel bars and bedforms GB). We deduce that this depositional environment is similar to the model No.1 of Miall (1985, 2006). This model corresponds to alluvial fans with gravity flows of gravelly rivers and proximal braided rivers.

Braided River System / Shallow Channels

This fluvial system is represented by conglomeratic facies and sandstone facies. The association of these facies forms the architectural element AE3 (GB: gravel bars) and AE4 (SB: sandy bedforms). By comparing the



architectural elements of this fluvial style with the depositional models of Miall (1985 and 2006), we noticed that model No. 2 is like our case, i.e. braided river system with gravel bars.

Anastomosed Rivers / Floodplains

This depositional environment is characterized by thick deposits fine to very fine grain sandstones and mudstones. They are associated and organized into two architectural elements: AE4 (SB: Sand Bedforms) deposited in the crevasse splays, and architectural element AE6 (OF: Overbank Fine) formed in flood plains and abandoned channels. According to Farrell (1987), Kraus and Bown (1988), and Miall, (1985, 2006), this type of depositional environment is poorly studied unlike other types of depositional environment, and is linked to an anastomosed environment characterized by low-energy floods with crevasse channels and crevasse splays (Miall, 2006).

Coastal Plain / Playa Lakes / Mudflats and Lagoons

This depositional environment is characterized by very fine sandy facies, mudstone facies, siltstone facies and evaporites facies. Two facies associations are identified: playa and evaporitic. This model probably corresponds to the large coastal plain downstream characterized by the development of playas lakes, mudflats and lagoons where the evaporite facies are formed by the evaporation of marine waters under a hot climate and in relation to a pellicular sea that covered the domain during the Upper Triassic time.

Northeast North American Margin VS Northwest African Margin

The opening of the northeast North American and northwest African margin (Moroccan) margins basins is synchronous with the Central Atlantic rifting (Withjack et al., 1998; Piqué et al., 1998; Leleu et al., 2016). They are subject to almost the same tectonic regime at the Triassic time, and present a set of common and contrasting features (**Figure 2**). The North American basins are characterized by a half-graben geometry (Manspeizer and Cousminer, 1988; Olsen et al., 1989; Schlische, 1993; Withjack et al., 1998, 2012). It is almost the same geometry as a set of Moroccan basins, including the MBEB basin.

North American onshore and offshore basins in the southern and the central Atlantic segments have a sedimentary fill resembling the Moroccan Atlasic basins, as well as the basal detrital strata of the Mesetian and Moroccan Atlantic margin basins. These basins include the southern Deep River, Culpeper, Newark, Franklin, and Hartford basins, and central Fundy Basins as described by Wade et al., (1996), Keen et al. (1987), Welsink et al. (1989), Withjack and Callaway (2000), Withjack et al. (2012), and Leleu et al. (2016). They are characterized by continental sedimentation during the Upper Triassic with strata composed of alluvial, fluvial, playa, and lacustrine deposits.

Based on the stratigraphy and published seismic sections of North American margin rift basins, we conclude that the Orpheus, Flemish Pass, and Jeanne d'Arc basins are the only ones with a significant evaporitic component (e.g. Keen et al., 1987; Welsink et al., 1989; Sinclair, 1995; Withjack and Callaway, 2000); Tanner and Brown, 2003; Syamsir et al., 2010; Withjack et al., 2012; and Leleu et al., 2016). These basins thus have a similarity with our study basin and with the other basins of the Moroccan Atlantic margin concerning the presence of evaporites (**Figure 2**). In the Orpheus Basin, the age of magmatic activity (CAMP) is about 200 Ma (Syamsir et al., 2010, his Figure 1C). This is the same CAMP age in the Mohammedia-Benslimane-El Gara-Berrechid Basin (Peretsman-Clement, 1985).

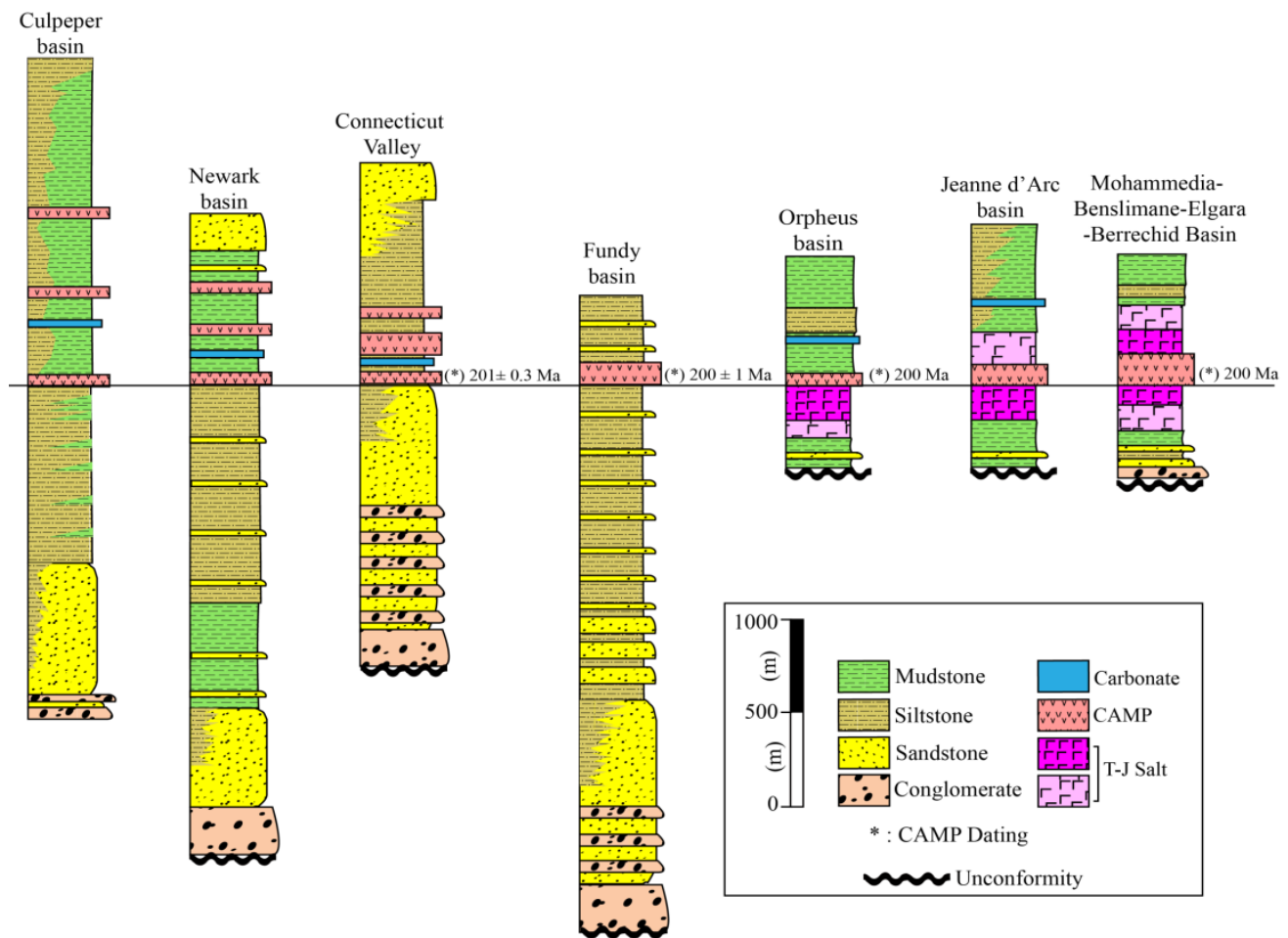


Figure 2: Comparison of the sedimentary series of the MBEB basin with those of some Triassic basins of the Northeastern American margin.

Discussion and Conclusions

Through the sedimentological analysis of Triassic successions of the MBEB basin, we conclude:

- Detrital sedimentation in the MBEB basin can be interpreted as resulting from the filling of a half-graben, and extensional reactivation of Hercynian faults that caused subsidence and associated rift margin erosion.
- This basin is, therefore, an open continental zone, which has favored the formation of alluvial fans and high-energy fluvial systems, and as the basin filled transitioning to lakes, and to playa-evaporitic settings. It is a typical succession associated with the geodynamic context of rift basins.
- The presence of evaporites indicates an arid climate that has favored their precipitation.
- In the Moroccan Atlantic margin, the sedimentary series show a great similarity in all the basins of this margin. They are all composed of a detrital fluvio-lacustrine formation at the base surmounted by another saliferous formation covered by Late Triassic-Early Jurassic CAMP tholeiitic basalt.
- The comparison with the basins of the northeastern North American margin reveals a similarity of the MBEB basin with the basins of the North Atlantic segment (Orpheus, Flemish Pass, and Jeanne Arc basins). In these basins, the synrift sedimentary series consists of detrital deposits at the base with a salt series capped by and/or interbedded with basalts. It is almost the same case as the basins of the Moroccan margin.



References

- Afenzar, A., and Essamoud, R., 2016. Facies analysis, architectural elements and environmental reconstruction of Triassic deposits of the Western Meseta (Mohammedia-Benslimane-Berrechid-El Gara area), Morocco. In: J.A. Morales Gonzales, B.M.C. Flores, A.M. Sarmiento, and M.A.C. Cerro (eds), *Geo-Temas, Sociedad Geologica de Espana*, **16**(1), 196-200.
- Afenzar, A., and Essamoud, R., 2017. Sédimentologie de facies des dépôts triasiques de la région d'Oued el Maleh et El Gara (Meseta, Maroc). *International Journal of Advanced Research*, **5**(5), 1938-1949.
- Einsle, G., 2000, *Sedimentary Basins: Evolution, Facies, and Sediment Budget*. Berlin: Springer-Verlag, 792p.
- El Wartiti, M., Medina, F., and Fadli, D. 1992, Effects of the Central Atlantic early rifting in the northern border of the Berrechid-El Gara basin (Morocco). *Gaia*, **4**, 31-38.
- Fadli, D., 1990, Evolution sédimentaire et structurale des massifs de Mdakra et du Khatouat: deux segments hercyniens de la Meseta marocaine nord-occidentale. Thèse ès Sciences, Univ. Mohammed V, Fac. Sci. Rabat, 294 p.
- Farrell, K.M., 1987. Sedimentology and facies architecture of overbank deposits of the Mississippi River, False River region, Louisiana. In: F.G. Ethridge, R.M. Flores, and M.D. Harvey (eds), *Recent Developments in Fluvial Sedimentology*. Society of Economic Paleontologists and Mineralogists Special Publication, **39**, 111-120.
- Keen, C.E., Boutilier, R., de Voogd, B., Mudford, B., and Enachescu, M.E., 1987. Crustal geometry and extensional models for the Grand Banks, eastern Canada: constraints from deep seismic reflection data. *Canadian Society of Petroleum Geologists, Memoir*, **12**, 101-115.
- Kraus, M.J., and Bown, T.M., 1988. Pedofacies analysis; a new approach to reconstructing ancient fluvial sequences. *Geological Society of America Special Paper*, **216**, 143-152.
- Leleu, S., Hartley, A.J., Oosterhout, C.V., Kennan, L., Ruckwied, K., and Gerdes, K. 2016. Structural, stratigraphic and sedimentological characterization of a wide rift system: The Triassic rift system of the Central Atlantic Domain. *Earth Science Reviews*, **158**, 89-124.
- Manspeizer, W., and Cousminer, H.L., 1988. Late Triassic–Early Jurassic synrift basins of the U.S. Atlantic margin. In: R.E. Sheridan and J.A. Grow (eds), *The Atlantic Continental Margin*, **2**, 97-216.
- Medina, F., 1994. Evolutions structurale du Haut Atlas occidental et des régions voisines du Trias à l'Actuel, dans le cadre de l'ouverture de l'Atlantique central et de la collision Afrique-Europe. State Thesis, University Mohammed, Rabat, Morocco.
- Medina, F., 1996. Le Trias du Maroc introduction. In: F. Medina (ed), *Le Permien et le Trias du Maroc: état des connaissances*. Pumag, Marrakech, 139-153.
- Miall, A.D., 1978. Lithofacies types and vertical profile models in braided river deposits: a summary. In: A.D. Miall (ed), *Fluvial sedimentology*, Canadian Society of Petroleum Geologists Memoir, **5**, 597-604.
- Miall, A.D., 1985. Architectural-element analysis: a new method of facies analysis applied to fluvial deposits. *Earth-Science Reviews*, **22**, 261-308.
- Miall, A.D., 2006. *The geology of fluvial deposits, sedimentary facies, basin analysis and petroleum geology*. 4th edition, Springer-Verlag, Berlin, 582p.
- Olsen, P.E., Schlische, R.W., and Gore, P.J.W., 1989. Chapter 5: Newark Basin, Pennsylvania and New Jersey. In: P.E. Olsen, R.W. Schlische, and P.J.W. Gore (eds), *Field Guide to the Tectonics, stratigraphy, sedimentology, and paleontology of the Newark Supergroup, eastern North America*. 28th International Geological Congress, Guidebooks for Field Trips T351, American Geophysical Union, Washington, DC, 69-152.



- Peretsman, C.G., 1985. A geochemical and petrographic analysis of early Mesozoic evaporites from Morocco: implications for the history of the North Atlantic. Unpublished MSc. Thesis, University of Oregon, 87p.
- Peretsman, C.G., and Holser, T.W., 1988. Geochemistry of Moroccan evaporites in the setting of the North Atlantic rift. *Journal of African Earth Sciences*, **7**(2), 375-383.
- Piqué, A., Le Roy, P., and Amrhar, M., 1998. Transtensive synsedimentary tectonics associated with ocean opening: the Essaouira-Agadir segment of the Moroccan Atlantic margin. *Journal of the Geological Society*, **155**, 913-928.
- Sinclair, I.K., 1995. Sequence stratigraphic response to Aptian-Albian rifting in conjugate margin basins: a comparison of the Jeanne d'Arc basin, offshore Newfoundland, and the Porcupine basin, offshore Ireland. In: R.A. Scrutton, M.S. Stoker, G.B. Shimmield, and A.W. Tudhope, A.W. (eds), *The Tectonics, Sedimentation and Paleoceanography of the North Atlantic Region*. Geological Society Special Publication, **90**, 29-49.
- Syamsir, Z., Withjack, M.O., Durcanin, M.A., Schlische, R.W., and Monteverde, D.H., 2010. The Mesozoic Orpheus rift basin, offshore Nova Scotia and Newfoundland, Canada: Synrift and early post rift evolution of a well imaged North Atlantic rift basin. Extended Abstracts: II Central and North Atlantic Conjugate Margins Conference, Lisbon, Portugal, 29 September to 1 October 2010, "Re-discovering the Atlantic, New winds for an old sea", 279-283.
- Tanner, L.H., and Brown, D.E., 2003. Tectonostratigraphy of the Orpheus graben, Scotian basin, offshore eastern Canada, and its relationship to the Fundy rift basin. In: P.M. LeTourneau, and P.E. Olsen (eds.), *The Great Rift Valleys of Pangea in Eastern North America, Volume 2: Sedimentology, Stratigraphy and Paleontology*. Columbia University Press, New York, 59-68.
- Wade, J.A., Brown, D.E., Fensome, R.A., and Traverse, A., 1996. The Triassic-Jurassic Fundy Basin, Eastern Canada: regional setting, stratigraphy and hydrocarbon potential. *Atlantic Geology*, **32**(3), 189-231.
- Welsink, H.J., Dwyer, J.D., and Knight, R.J., 1989. Tectono-stratigraphy of the passive margin off Nova Scotia. In: A.J. Tankard, and H.R. Balkwill (eds), *Extensional Tectonics and Stratigraphy of the North Atlantic Margins*. American Association of Petroleum Geologists Memoir, **46**, 215-231.
- Withjack, M.O., and Callaway, S., 2000. Active normal faulting beneath a salt layer: an experimental study of deformation patterns in the cover sequence. *Bulletin of the American Association of Petroleum Geologists*, **84**(5), 627-651.
- Withjack, M.O., Schlische, R.W. and Olsen, P.E., 2012. Development of the passive margin of Eastern North America: Mesozoic rifting, igneous activity, and breakup. In: D.G. Roberts, and A.W. Bally (eds), *Regional geology and tectonics: Phanerozoic rift systems and sedimentary basins*. Amsterdam: Elsevier, 301-335.



CHEMOSTRATIGRAPHY AND SEDIMENTARY PROVENANCE ANALYSIS FOR THE JEANNE D'ARC AND FLEMISH PASS BASINS, GRAND BANKS, EAST COAST CANADA

Barbarano, Marta¹, Fairey, B. ¹, Martin, John¹, Riley, David¹ and Pearce, Tim¹

¹ Chemostrat Ltd., 1 Ravenscroft Court, Buttington Cross Enterprise Park, Welshpool, SY21 8SL, United Kingdom, martabarbarano@chemostrat.com

The sediment provenance of the Jurassic and Cretaceous successions of the Flemish Pass and Jeanne d'Arc Basins is the focus of this study. Preliminary data relating to the successions contemporaneously deposited in the Orphan and Carson basins are also given.

In this study, we coupled Raman heavy mineral (HM) analysis and detrital zircon U-Pb geochronology on an extensive number of samples, with the aim of increasing the available dataset and reconstructing the sediment provenance of the Grand Banks basins.

From our multidisciplinary dataset it is possible to recognize provenance changes occurring both stratigraphically and spatially, and our provenance dataset supports our chemostratigraphic correlations. The Humber and Dunnage zones of western Newfoundland are interpreted to be sediment contributors. It is possible that the Variscan granites of Iberia indirectly provided sediment to the eastern part of the Jeanne d'Arc Basin and to the Outer Ridge Complex: sediment from this source would have been reworked from local Paleozoic highs before final deposition into the Grand Banks basins. We also show that this approach can help in ground-truthing existing sediment provenance models and gross depositional environment (GDE) maps for the study area.

Introduction

The formation of the Grand Banks basins is associated with the opening of the North Atlantic Ocean, with late Palaeozoic paleogeographic reconstructions placing it close to the conjugate Porcupine and Rockall basins (offshore Ireland) and to the landmasses of Greenland and Iberia. Possible sedimentary sources include these landmasses, the Avalon Zone, located to the west of the depositional area, and the Flemish Cap, located to the east of the Flemish Pass Basin.

Mainly based on detrital zircon U-Pb geochronology analysis, Lowe et al. (2011) suggested provenance from the Central Mobile Belt and the Avalon Zone of onshore Newfoundland, as well as from areas located to the north and the south of the Grand Banks basins. For the material deposited in the Flemish Pass Basin, they did not find any evidence supporting derivation from Iberia, the Flemish Cap, or Grenvillian plutonic rocks. However, provenance from Iberia was inferred by McDonough et al. (2011), who observed a zircon population comprising grains aged between ca. 325 Ma and ca. 300 Ma in Jurassic sandstones encountered by Flemish Pass Basin wells Baccalieu I-78 and Mizzen O-16. Having observed abundant spinel grains and late Mesoproterozoic to early Neoproterozoic zircon grains, Tsikouras et al. (2011) indicated the Lower Cretaceous sedimentary rocks of the Scotian Basin, located to the southwest of the Grand Banks basins, were largely derived from rocks like those in the Humber Zone of western Newfoundland.

Methods

Cuttings and core samples of sedimentary rocks were disaggregated with agate mortar and pestle; the disaggregated material was sieved to obtain a 40 µm to 250 µm grain-size window. After carbonate digestion in a 10% acetic acid solution, the 'light' and 'heavy' grains contained in the 40-250 µm grain-size window were separated using a lithium metatungstate solution (density 2.89 g/cm³), using the funnel separation technique as



indicated in Mange and Maurer (1992). HM grains were mounted on a glass slide and each slide was analyzed with a Horiba LabRam Raman Microscope, using a 532 nm green laser.

A Frantz magnetic separator was employed to further concentrate zircon grains. To determine the U-Pb age of each grain we used a laser ablation inductively coupled plasma mass spectrometer (ICP-MS). The Plesovice zircon standard (Sláma et al., 2008) was used to correct for downhole U-Pb fractionation, mass bias and instrument drift. Any age data that was more than $\pm 10\%$ discordant was filtered from the dataset.

Currently, the provenance database for the Grand Banks includes more than 250 samples analyzed via Raman spectroscopy and more than 300 detrital zircon geochronology samples. Additional samples are being processed.

In addition to Raman heavy mineral analysis and detrital zircon U-Pb geochronology, we also performed two additional analyses. ICP-MS analysis (ca. 10K samples) was done to determine the chemical composition of the sediment and build-up a chemostratigraphic subdivision and correlation of the study succession. Analyses of stable isotope ($\delta^{13}\text{C}$ and $\delta^{18}\text{O}$) (ca. 5K samples) on the inorganic carbonate fraction of the same succession was completed in order to have a chronological reference for the chemostratigraphic interpretation. The correlation was mainly based on variations in the concentration of elements such as Si, Zr, Ti, Nb, Ta, Rb, U, Th, Ga, V and the REEs and on up-section variations in the value of ratios of some of these elements – these variations being associated with changes in the relative proportions of quartz, feldspar, heavy minerals, clays and organic matter. Elemental data obtained via ICP-MS analysis also gave some information for reconstructing the sediment provenance, as indicated below. Additionally, petrographic analysis was performed on a selection of sandstones of the Flemish Pass and Jeanne d'Arc basins.

Results and Discussion

Examples of the obtained results are given below, together with the interpretation of the data.

Within the Flemish Pass Basin, we recognize different sediment provenances for correlative sandstones intersected by wells in the eastern part of the basin. For example, Upper Tithonian sandstones intersected by wells Mizzen O-16 and Mizzen F-09 contain large proportions of ultrastable minerals (zircon, tourmaline and rutile) relative to the rest of the heavy mineral assemblage, coupled with predominance of late Neoproterozoic and Paleozoic ages in the zircon grain populations. The correlative sandstones in well Baccalieu I-78, to the south of the 'Mizzen wells', contain abundant metamorphic lithic clasts (either not observed at all or observed only in small proportions in other wells of the study area) and higher proportions of epidote and rutile grains than in most of the correlative sandstones. Wells located to the west of Baccalieu I-78 – Bay de Verde F-67Z and Bay du Nord C-78Z – contain a higher frequency of garnet grains and Paleoproterozoic to Mesoproterozoic zircon ages and less important Paleozoic zircon age peaks than observed in wells O-16, F-09 and I-78.

Different provenances and, therefore, different sediment entry points into the basin are suggested, during the Late Tithonian, for the three locations corresponding to the indicated wells of the Flemish Pass Basin. As a result, one might expect to see variations in reservoir quality associated with the different provenance of the sediment of the 'Mizzen wells', well Baccalieu I-78 and the 'Bay wells'. Moreover, the Upper Jurassic sandstones of the 'Mizzen wells' seem to have a similar provenance to the Upper Jurassic sandstones intersected by Orphan Basin wells Cupids A-33 and Margaree A-49, but the important difference is that zircon grains of Silurian to Devonian age are more frequent in the 'Mizzen wells' than in A-33 and A-49 (**Figure 1**).

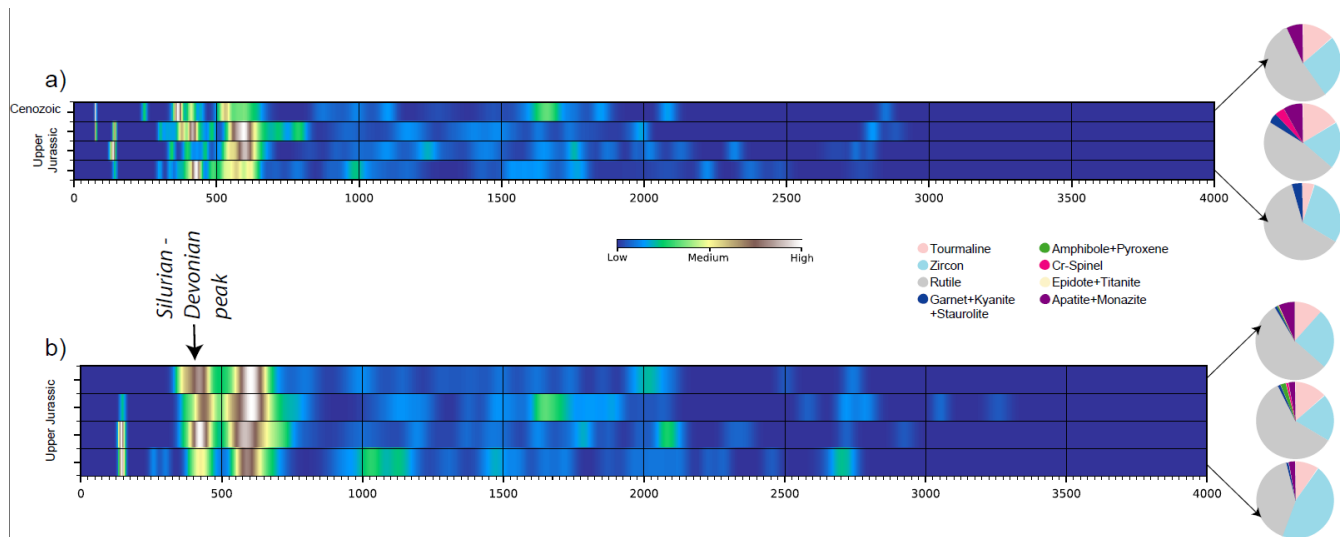


Figure 1. A similar provenance is suggested for the Upper Jurassic sandstones of the eastern Orphan Basin and the Flemish Pass Basin ‘Mizzen wells’ (data for one well of each basin in “a” and “b”, respectively) from results of detrital zircon U-Pb geochronology (probability density heat-maps) and heavy mineral analysis (pie-charts).

The sedimentary rocks penetrated by some Outer Ridge Complex wells may have been derived from the recycling of sediment originally eroded from Iberia. This is suggested because Callovian to Kimmeridgian sandstones intersected by well Golconda C-64, and Upper Tithonian to Lower Cretaceous sandstones intersected by well Aster C-93A, show predominance of ultrastable minerals and significant Carboniferous to Permian zircon age peaks. Zircon grains of this age are also observed in Jurassic sandstones in wells Lancaster G-70 and Panther P-52 and in Lower Cretaceous sandstones deposited in the eastern area of the Jeanne d’Arc Basin.

Carboniferous to Permian zircon age peaks are observed in samples containing only very small proportions of Silurian to Devonian aged zircon grains (**Figure 2**). As detrital material coming from Iberia is characterized by having very few zircon grains of Ordovician to Devonian age and many grains of Carboniferous age (Dinis et al., 2017), provenance from the Variscan granites of Iberia is indicated for these samples by results of zircon geochronology. However, very high concentrations of ultrastable heavy minerals, suggesting sediment recycling rather than derivation from granitic rocks, are noted in some sandstones that contain Carboniferous to Permian zircon grains (**Figure 2**), such as those drilled by wells Golconda C-64 and Aster C-93 and, further to the south, by wells Amethyst F-20 and Gros Morne C-17.

Elemental data obtained via ICP-MS analysis were plotted on the well-established Th/Sc vs. Zr/Sc diagram proposed by McLennan et al. (1993). Almost all the analyzed sandstones from the Grand Banks basins have large amounts of material plotting along the ‘recycling trend’ and are therefore interpreted as having derived from older sedimentary rocks. In contrast, quite a few Upper Cretaceous sandstones intersected by wells located in the western area of the Jeanne d’Arc Basin plot on the ‘compositional trend’. They presumably contain abundant detrital material derived from igneous or metamorphic rocks, rather than from sedimentary rocks.

One of these wells is Egret K-36. Provenance data collected for the sandstones penetrated by well Egret K-36 point to an important change in provenance occurring after the deposition of the Lower Cretaceous sandstones and before the Upper Cretaceous sandstones were deposited. Lower Cretaceous sandstones are characterized by high concentration of ultrastable minerals associated with late Neoproterozoic zircon ages, suggesting erosion of sedimentary rocks of the Avalon Zone of eastern Newfoundland, whereas Upper Cretaceous sandstones have abundant metamorphic minerals (including kyanite and andalusite) and Cr-spinel, associated with Silurian to Devonian zircon ages (**Figure 3**). Progressive erosion of the sedimentary cover resulted in the gradual



exposure and unroofing of Paleozoic granites, which presently are extensively exposed in the Gander Zone (Geological Map of Newfoundland, 1990). For the Upper Cretaceous sandstones intersected by well Egret K-36, occurrence of ca. 10% Cr-spinel in the heavy mineral assemblages suggests provenance from rocks similar to those found in the ophiolite complexes of the Humber and Dunnage zones and / or from other mafic and ultramafic intrusive rocks present in Newfoundland. A similar up-section provenance change is observed in well Terra Nova I-97, as Upper Jurassic sandstones have late Neoproterozoic and Paleozoic zircon grains associated with large proportions of ultrastable minerals, whereas Upper Cretaceous sandstones have predominance of Paleozoic zircon grains associated with relatively frequent Cr-spinel.

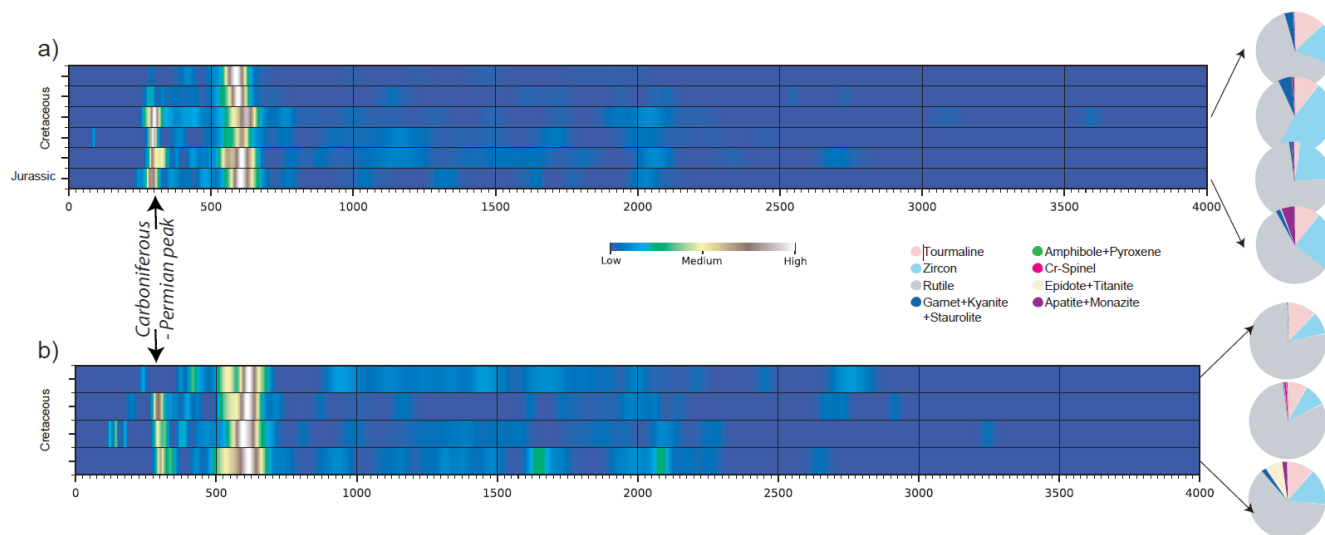


Figure 2. Provenance from multiple sources, including recycling of material originally derived from the Variscan granites of Iberia in sandstones deposited in the Outer Ridge Complex and in the eastern area of the Jeanne d’Arc Basin (data for one well of each basin in “a” and “b”, respectively).

Based on our elemental, isotopic and detrital zircon U-Pb geochronological data, a correlation was established between the Hibernia sandstones penetrated by Jeanne d’Arc Basin well Terra Nova I-97 and Hibernia equivalent sandstones penetrated by Carson Basin well St. George J-55. Sandstones intersected by well St. George J-55 contain an important Lower Cretaceous zircon component which could be interpreted as related to the volcanism documented at this time in the Scotian Basin (e.g. Bowman et al., 2012 and references therein). Although less significant, a component Lower Cretaceous zircon grains is also observed in the correlative sandstones drilled by well Terra Nova I-97. The sandstones penetrated by well Riverhead N-18 also contain abundant Lower Cretaceous zircon grains, although a detailed correlation between this well and well St George J-55 is, so far, unestablished.

Summary

In the Flemish Pass Basin, different sediment entry points are suggested, during the Upper Tithonian, for the locations corresponding to wells (i) Mizzen O-16 and Mizzen F-09, (ii) Baccalieu I-78, (iii) Bay de Verde F-67Z and Bay du Nord C-78Z. The sandstones intersected by wells O-16 and F-09 and the correlative sandstones in Orphan Basin wells Cupids A-33 and Margaree A-49 might have a similar provenance.

Ultimate provenance from the Variscan granites of Iberia is indicated for some sandstones deposited in the Outer Ridge Complex and in the eastern area of the Jeanne d’Arc Basin. However, these sandstones may have been derived from sediment recycling, rather than directly from landmasses of Iberia.



In the western area of the Jeanne d'Arc Basin, an important provenance change had occurred before the deposition of the Upper Cretaceous sandstones. These sandstones probably derived from rocks similar to the Paleozoic granites of the Gander Zone and within ophiolite complexes of the Humber and Dunnage zones.

Additional data and interpretation for the provenance of the succession deposited in the Orphan and Carson basins will soon be available.

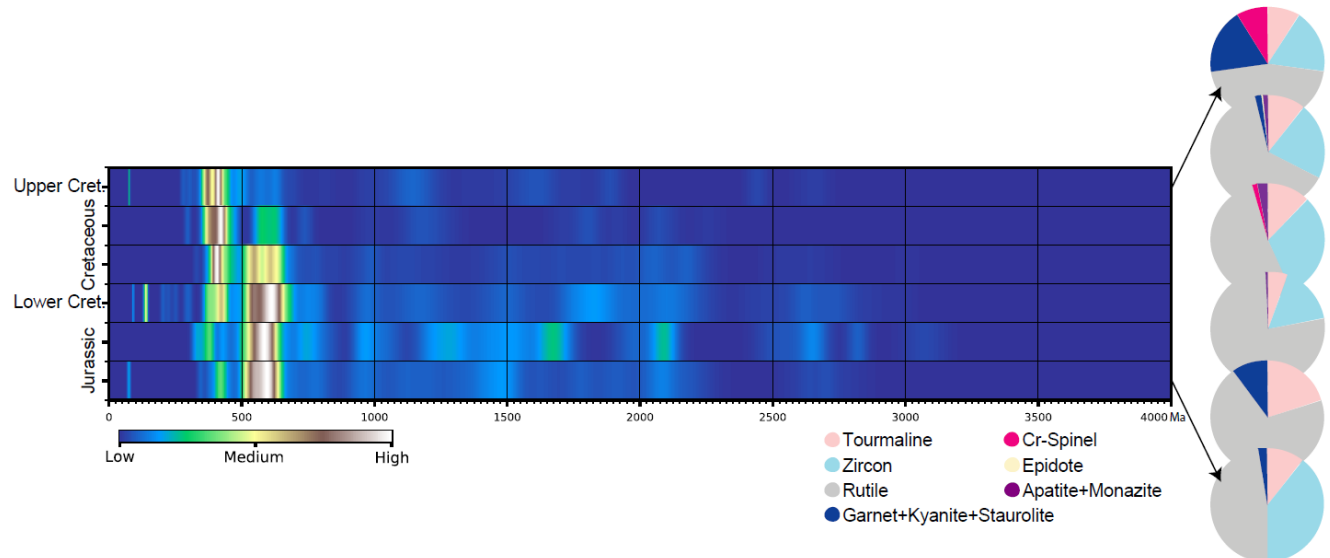


Figure 3. Up-section provenance change indicated by results of detrital zircon U-Pb geochronology (heat-map) and heavy mineral analysis (pie charts) obtained in sandstones deposited in the western area of the Jeanne d'Arc Basin (data for a single well shown in figure).

References

- Bowman, S.J., Pe-Piper, G., Piper, D.J.W., Fensome, R.A., and King, E.L., 2012. Early Cretaceous volcanism in the Scotian Basin. *Canadian Journal of Earth Sciences*, **49**(12), 1523-1539.
- Colman-Sadd, S.P., Hayes, J.P. and Knight, I., 1990. Geology of the Island of Newfoundland. Map 90-01. Government of Newfoundland and Labrador, Department of Mines and Energy, Geological Survey Branch. Scale: 1:1 000 000. http://www.nr.gov.nl.ca/nr/mines/investments/geology_map_nl.pdf
- Dinis, P. A, Fernandes, P., Jorge, R.C. G.S, Rodrigues, B., Chew, D.M., and Tassinari, C.G., 2017. The transition from Pangea amalgamation to fragmentation: Constraints from detrital zircon geochronology on West Iberia paleogeography and sediment sources. *Sedimentary Geology*, **375** 172-187. doi.org/10.1016/j.sedgeo.2017.09.015.
- Lowe, D.G., Sylvester, P.J., and Enachescu, M.E., 2011. Provenance and paleodrainage patterns of Late Jurassic and Early Cretaceous synrift sandstones in the Flemish Pass Basin, offshore Newfoundland, east coast of Canada. *Bulletin of the American Association of Petroleum Geologists*, **95**(8), 1295-1320.
- Mange, M.A., and Maurer, H.F.W., 1992. *Heavy Minerals in Colour*. Chapman and Hall, London, 147p.
- McDonough, M., Sylvester, P., Bruder, N., Lo, J., and O'Sullivan, P., 2011. Provenance of reservoir sandstones in the Flemish Pass and Orphan Basins (Canada): U-Pb dating of detrital zircons using the laser ablation method. Extended Abstracts: II Central and North Atlantic Conjugate Margins Conference, Lisbon, Portugal, 29 September to 1 October 2010 "Re-discovering the Atlantic, New winds for an old sea", 181-184.



- McLennan, S.M., Bock, B., Compston, W., Hemming, S.R., and McDaniel, D.K., 2001. Detrital zircon geochronology of Taconian and Acadian foreland sedimentary rocks in New England. *Journal of Sedimentary Research*, **71**, 305-317.
- Sláma, J., Kosler, J., Condon, D.J., Crowley, J.L., Gerdes, A., Hanchar, J.M., Horstwood, M.S A., Morris, G.A., Nasdala, L., Norberg, N., Schaltegger, U., Schoene, B., Tubrett, M.N., and Whitehouse, M.J., 2008. Plešovice zircon - A new natural reference material for U–Pb and Hf isotopic microanalysis. *Chemical Geology*, **249**, 1-35.
- Tsikouras, B., Pe-Piper, G., Piper, D.J.W., and Schaffer, M., 2011. Varietal heavy mineral analysis of sediment provenance, Lower Cretaceous Scotian Basin, eastern Canada. *Sedimentary Geology*, **237**, 150-165.
-



STRUCTURAL STYLE AND FAULT EVOLUTION IN THE GREATER BAY DU NORD AREA, FLEMISH PASS BASIN, OFFSHORE NEWFOUNDLAND

Bernal, Asdrúbal J.¹, Tonn, Rainer¹, Novoa, Enrique², and Söderstrøm, Bo³

¹ Equinor Canada Ltd., 2 Steers Cove, St. John's, NL A1C 6J5, Canada, asbp@equinor.com

² Equinor Gulf Services LLC, 2107 Citywest Boulevard, Houston, Texas 77042, USA

³ Equinor ASA, Martin Linges vei 33, Fornebu 1330, Norway

The structural style, timing of deformation and interaction of fault sets in the Greater Bay du Nord Area, Flemish Pass Basin, is presented and discussed using seismic and borehole data. The structural style in the study area is dominated by rollover anticlines with erosion in the up-dip, crestal areas. These rollovers are related to complex interactions of low angle listric and associated synthetic and antithetic faults; some of them displaying conjugate geometry. We interpret three Mesozoic fault populations:

1. Relatively long, NE-SW-striking faults with dominant vergence to the east and high displacement and height that extend into pre-Jurassic strata.
2. NW-SE-striking faults, with no clear dominant vergence and confined within the Jurassic-to-Cretaceous succession, has much less displacement and length.
3. Faults with NNE-SSW to NNW-SSE strike and variable displacement, lateral extent, and height. A major E-W striking normal fault bounds the Greater Bay du Nord Area to the south.

Integration of structural and isopach maps, growth strata analysis, and evaluation of fault interactions allows us to propose a timing of fault activity and relate it to the rotation of extension direction throughout the Mesozoic. We suggest three pulses of tectonic activity. The first pulse relates to a rift climax phase of Oxfordian-Kimmeridgian in the Flemish Pass, with the major E-W-striking and NE-SW-striking fault population accommodating this deformation. A period of relative tectonic quiescence is observed in the Upper Tithonian, where differential subsidence and minor faulting is interpreted. The second pulse develops in the Early Cretaceous with most of the fault growth and propagation occurring during the Berriasian to Hauterivian (?) with a NNE-SSW to NNW-SSE orientation and dominant vergence to the east. These developed west-dipping rollover anticlines and associated west-verging half-graben depocentres. The NW-SE-oriented fault population develops during the Aptian-Albian. The E-W-striking bounding fault and the NNE-SSW fault sets re-activate during this time, with different degrees of strike-slip displacement expected during fault reactivation in Early Cretaceous time. The third phase of tectonic deformation comprises mild inversion in the transition of Early to Late Cretaceous, followed by westward subsidence of the basin during Tertiary and the development of polygonal faulting.

Introduction

The greater Bay du Nord Area is in the Flemish Pass Basin, offshore Newfoundland, ca. 450 km (280 mi.) from the city of St. John's (**Figure 1**). The Flemish Pass Basin is bound to the east and southeast by the Flemish Cap (Avalon Zone according to Williams et al., 1999), the Beothuk Knoll, and Flemish Pass Graben. To the north and northwest it is constrained by the eastern extension of the Cumberland Arch and southern portion of the East Orphan Basin, and to the south and southwest by the Central Ridge and the continental-oceanic transition zone of the South Bank High (Williams et al., 1999). The Flemish Pass Basin corresponds to one of the NE-SW oriented Tithonian depocentres, interpreted as a rift arm of the North Atlantic rift system, and encompasses an area in excess of 10,000 km² (3,860 mi.²) with Mesozoic and Cenozoic sedimentary packages up to 10 km (6.2 mi.) in



thickness (based on estimates from Equinor Canada Ltd.). Together with the Orphan Basin, the Flemish Pass Basin represents one of the younger, northerly extensions of the Grand Banks province, which is a northeast-trending assemblage of Mesozoic cratonic basins and intervening basement ridges that originated in the latest Triassic and Middle Jurassic.

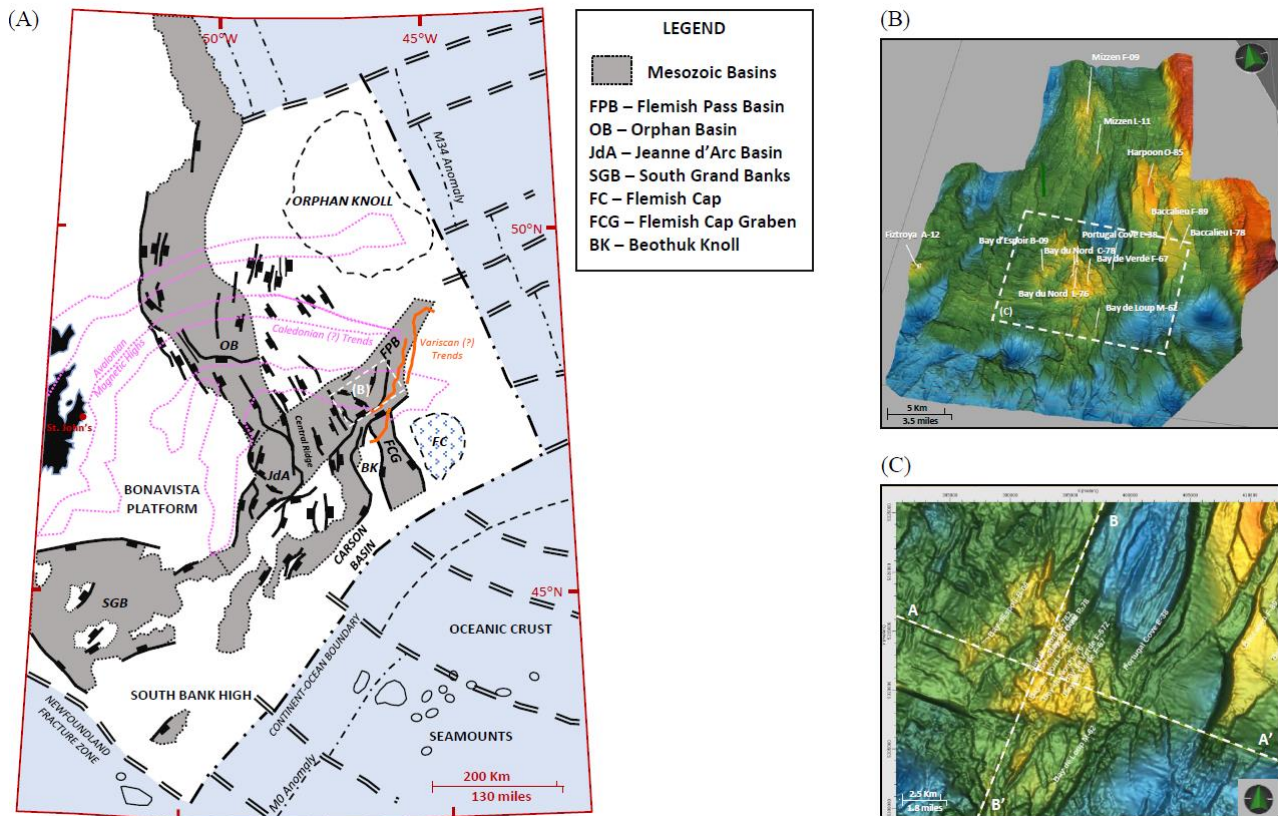


Figure 1. A) Paleozoic to Mesozoic composite structural elements map. Basement trends are integrated with seismic observations and gravimetric data. White rectangle indicates the location of the figure presented in B). Modified and simplified from Foster and Robinson (1993), and Sharp et al. (2018). B) 3D view, structural map of the Base Cretaceous seismic horizon in a section of the Baccaieu Subbasin. White rectangle indicates the location of the figure presented in C). C) Structural map of the Base Cretaceous seismic horizon in the Greater Bay du Nord Area. A-A’ and B-B’ indicate the locations of the seismic vertical sections presented in **Figure 2**.

An overall agreement exists on the identification and timing of major tectonic events during the rifting-drifting process on the North Atlantic (e.g. Enchescu, 1987; Ziegler, 1989; Roest et al., 1992; Driscoll et al., 1995; Srivastava et al. 2000; Sibuet et al. 2007; Skogseid, 2010; Withjack et al., 2012; and Sharp et al., 2018). Two rift phases have been proposed offshore Newfoundland (East Coast Canada) by Sharp et al. (2018); phase 1 in the Triassic, characterised by wide distributed basins, and phase 2 in the Mid/Late Jurassic to Cretaceous displaying different degrees of faulting and subsidence. Sharp et al. (2018) suggest that crustal lineaments (Variscan meta-sediments fold trends and Caledonian terrane boundaries) partially controlled the location and configuration of these rift systems (Figure 1). Late Triassic rifting into the Flemish Pass has been proposed previously (Ziegler, 1989; Foster and Robinson, 1993; Withjack et al., 2012) but no stratigraphic controls exist to support this interpretation.

More stratigraphical control exists for the Jurassic and Cretaceous rifting events and their transition toward continental drifting. In the Flemish Pass Basin, Foster and Robinson (1993) propose that the beginning of the rift/post-rift transition occurs at Mid-Aptian time (120 Ma) while Sinclair (1995a) suggests this transition occurs



near the end of Albian time. Sharp et al. (2018) propose that the drift phase in the North Atlantic begins in Aptian/Albian time from an integrated study that includes the Jeanne d'Arc, Flemish Pass and Orphan basins.

Structural Setting in the Greater Bay du Nord Area

The Greater Bay du Nord Area comprises the Bay d'Espoir, Bay du Nord, Bay de Verde, Bay de Verde East, Bay de Loop, Portugal Cove, and Baccalieu structures (**Figure 1b** and **Figure 2**). A Lower Cretaceous basin is present to the northeast of the Bay du Nord and Bay de Verde structures and to the west of the Baccalieu structure. A major east-west lineament separates the Bay de Loup structure to the south from the other structures to the north.

Structural Styles

Figure 2 displays interpreted seismic sections through the Greater Bay du Nord Area, with faults and seismic horizons from seabed to the economic basement (Top Paleozoic?). The seismic horizons from Base Pleistocene Miocene to the Base Cenozoic Unconformity show a fanning geometry, with increasing in dip from east to west (**Figure 2a**). Seismic horizons from the base Pleistocene to seabed display a parallel geometry, except for the mass transport complexes observed within this interval.

The structures in the Greater Bay du Nord Area comprise rollover anticlines with different degrees of erosion in the up-dip, crestal areas (fault scarps). These rollover anticlines are genetically linked to a system of cross-cutting, listric faults and associated synthetic and antithetic faults, which create highly segmented structures. Some of the listric faults stop propagating within the Kimmeridgian sediments whereas others extend deeper into the stratigraphy, offsetting the economic basement (**Figure 2a**).

Relative structural highs of the economic basement (A_B , B_B , C_B in **Figure 2a**) coincide with, but are not fully aligned to, areas of base Cretaceous erosion (A_C , B_C , C_C), suggesting that detachments within the Jurassic section (B_J , C_J) also contribute to the location of base Cretaceous erosion. This situation is evident in the Bay d'Espoir structure.

The major east-west lineament separating the Bay de Loup structure to the south from the other structures to the north has a pronounced normal fault expression and strata geometry in the hangingwall and footwall that resembles those observed in strike-slip settings (**Figure 2b**). This fault could be genetically linked to a major transform fault (with some listric component) separating the Baccalieu Subbasin from the Gabriel Subbasin (sensu Enachescu, 1987) observed in regional seismic sections further to the south of the Bay de Loup structure.

Fault Sets

Three main faults sets are identified with the following mean strike directions: NE-SW, NNE-SSW to NNW-SSE, and NW-SE (**Figure 3**). The NW-SE set develops in the western portion of the Greater Bay du Nord area (Bay du Nord and Bay d'Espoir structures) while the NNE-SSW and NE-SW striking fault sets are observed throughout the Greater Bay du Nord area. Most of the NNW-SSE fault set separates the Portugal Cove and Bay de Verde East fault blocks to the east from Bay de Verde and Bay du Nord fault blocks to the west.

The NW-SE fault set usually offsets the other faults sets but intersecting geometries are also observed. Few cases were observed where the NW-SE oriented fault set might be offset by another fault set while in other cases, the NW-SE fault set seems to link to other faults sets. In addition, the NNE-SSW and NE-SW striking fault sets display a segmented geometry, with fault bifurcations, relays, and lenses.

Three different kinds of fault intersections are observed: (1) cross-cutting intersection without major changes of fault strike, (2) cross-cutting intersection with changes in fault strike, and (3) abrupt change of fault strike at fault tip (L-shape faults).

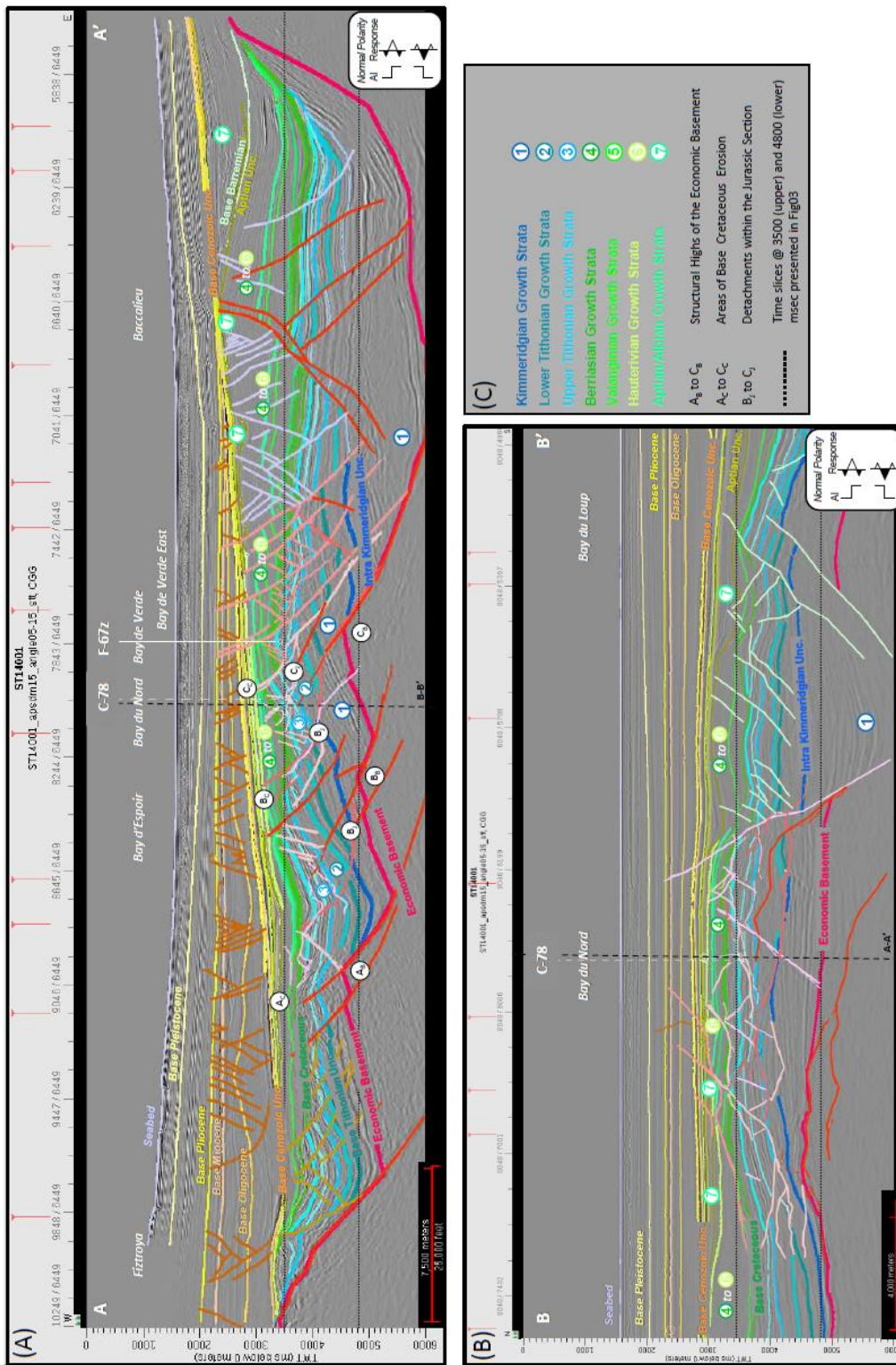


Figure 2. A) NW-SE and B) NE-SW seismic vertical sections through the Greater Bay du Nord area. The location of the vertical seismic sections is presented in **Figure 1**. Seismic horizons are colour coded by age. Tertiary: yellow and brown; Cretaceous: green; Upper Tithonian: light blue; Intra-Kimmeridgian: dark blue; and economic basement; red. The colour coding for faults is presented in **Figure 3**. (C) Legend for growth strata age and structural style observations (see text for details).

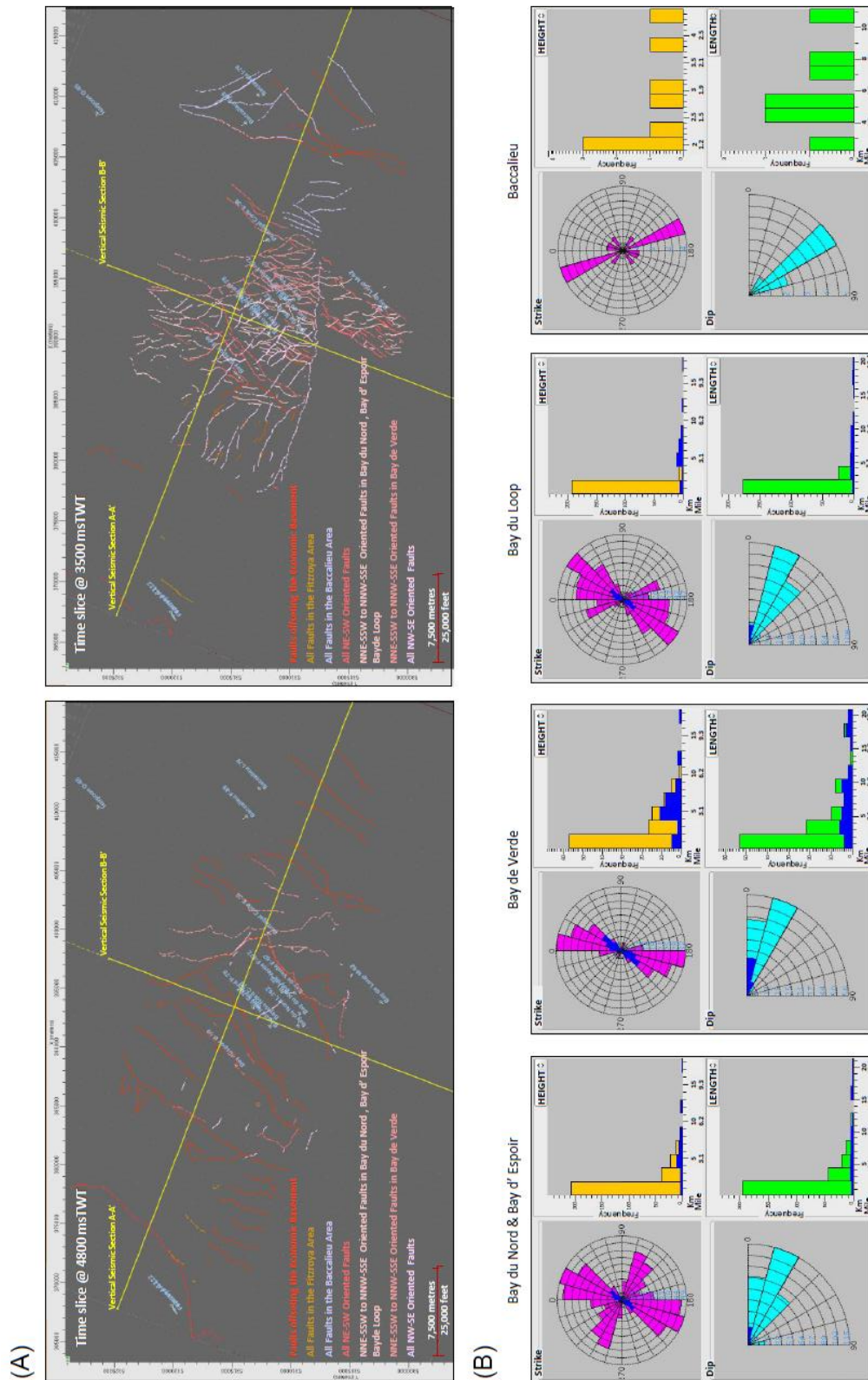


Figure 3. A) Time slice at 4800 msec (left) and 3500 msec (right) in the Greater Bay du Nord area displaying the fault strikes, colour coded by orientation and structure. The locations of the vertical seismic sections presented in **Figure 2** are indicated. B) Strike, dip, height, and length for the faults in each structure in the Greater Bay du Nord area. The blue color are the dimensions of the faults that extend down to the economic basement.



Growth Strata and Tectonic Phases

Seismic termination analysis permits the identification of growth strata in the Jurassic and Cretaceous sections (**Figure 2**) while the analysis of isochron thickness maps of the Jurassic, Cretaceous, and Tertiary sequences allow visualization on how depocentres are distributed in the study area and change through time.

The integration of seismic sequence and growth strata analysis together with the nature of the fault intersection patterns allow us to propose the timing of deformation for the various fault sets in the Greater Bay du Nord area, and a field-scale tectonic evolution model. A summary of the tectonic evolution of the Greater Bay du Nord area is presented in **Figure 4**.

1. The first pulse of extensional deformation observed in the study area is related to an episode of major fault activity in Late Jurassic (from Callovian to Lower Tithonian climaxing in the Oxfordian/Kimmeridgian. This is Rift Phase 2 according to Sharp et al. (2018). The major E-W striking fault to the south of the Greater Bay du Nord area and the NE-SW striking fault population accommodate this deformation.
2. A period of relative tectonic quiescence is observed in the Upper Tithonian, where minor faulting or differential subsidence and compaction are interpreted.
3. The second pulse develops in the Early Cretaceous with most of the fault growth and propagation occurring from Berriasian to (?)Hauterivian time. The faults growing at this time have a NNE-SSW to NNW-SSE orientation with a dominant vergence to the east. Some of these faults are kinematically linked to west-dipping rollover anticlines and associated west-verging half-graben depocentres.
4. The third pulse of extensional deformation is accommodated by the NW-SE oriented fault population, propagating mainly during the Aptian-Albian. The E-W striking bounding fault and the NNE-SSW fault sets re-activate during this time. Different degrees of strike-slip displacement are expected during fault reactivation in Early Cretaceous time.
5. The last phase of tectonic deformation comprises localised inversion in the Early to Late Cretaceous transition. This is followed by westward subsidence of the basin during Tertiary and the development of polygonal faulting. Foster and Robinson (1993) proposed the inversion of Early Cretaceous subbasins in the Flemish Pass during the Aptian due to strike-slip movements associated to plate reorganization. A similar model of episodic tectonic evolution has been proposed for some structures of the Jeanne d'Arc Basin (e.g. Sinclair, 1995b; Sinclair, 1999). In addition, the inversion phase identified in the Greater Bay du Nord area is interpreted in the east coast of USA and Canada (e.g. Withjack et al., 2012).

Summary

The structures interpreted in the Greater Bay du Nord area correspond to rollover anticlines, characterized by different degrees of erosion on the crests and a complex interaction of multiple listric faults. Antithetic faults developed on most of these rollover structures, which grew mainly during the Lower Cretaceous.

The strike of these listric faults show two main orientations: NW-SE and NNE-SSW. They display both hard-link and soft-link relations with the main fault(s) developed during the rift climax phase of Oxfordian/Kimmeridgian in the Flemish Pass. A population of NW-SE striking faults, growing during the (?)Barremian-Albian and younger than and usually offsetting the NW-SE and NNE-SSW populations, developed in the western portion of the Greater Bay du Nord area (Bay du Nord and Bay d'Espoir structures). The NW-SE-striking fault population do not develop extensively in the eastern portion of the Greater Bay du Nord area (Bay de Verde and Bay de Verde East structures), where a more coeval growth with conjugate geometry is observed.



The i) rotation of the regional stress field through time, ii) episodic fault activity, iii) fault populations with variable strike orientation, iv) type of cross-cutting and termination of fault interactions, and v) abrupt changes on fault displacement along strike together suggests the kinematics of the extensional evolution in the Greater Bay du Nord area responds to three phases of extension. These three phases have different extension directions, with variable degrees of strike-slip displacement expected along major faults. Localised inversion in the Early to Late Cretaceous transition is observed in some of the structures of the Greater Bay du Nord area.

Acknowledgements

We thank our colleagues James Carter, Stephen Kearsey, and Iain Sinclair from Husky Energy, whose ideas and fruitful discussions helped to improve not only the conceptual model presented here but also the documentation. Comments from Alejandro Amilibia-Cabeza, Ian Sharp, Geoff Rait, and Jakob Skogseid improved our understating of the basin scale and plate tectonics processes offshore Newfoundland. Jon Dexter provided the fault interpretation in the Bay du Loup area, while Scott Hess and Torbjørn Fristad provided some of the pre-Tithonian seismic horizons. Comments from Irene Kelly improved the quality of this manuscript.

References

- Driscoll, N.W., and J.R. Hogg, 1995. Stratigraphic response to basin formation: Jeanne d’Arc Basin, offshore Newfoundland. In: J.J. Lambiase (ed), *Hydrocarbon habitat in rift basins*, Geological Society of London, Special Publication, **80**, 145-163.
- Enachescu, M.E., 1987. Tectonics and structural framework of the northeast Newfoundland continental margin. In: C. Beaumont and A.J. Tankard (eds), *Sedimentary basins and basin-forming mechanisms*: Canadian Society of Petroleum Geologists Memoir, **12**, 117-146.
- Foster, D.G., and Robinson, A.G., 1993. Geological history of the Flemish Pass Basin, offshore Newfoundland: *Bulletin of the American Association of Petroleum Geologists*, **77**(4), 588-609.
- Roest, W.D., Dañobeitia, J.J., Verhoef, J., and Collette, B.J., 1992. Magnetic anomalies in the Canary Basin and the Mesozoic evolution of the Central North Atlantic: *Marine Geophysical Research*, **14**, 1-24.
- Sharp, I.R., Higgins, H., Scott, M., Freitag, U., Allsop, C., Kane, K., Sultan, A., Doubleday, P., Leppard, C., Bloomfield, J., Cody, J., Rait, G., and Haynes, S., 2018. Rift to drift evolution and hyper- extension in the North Atlantic – insights from a super-regional approach. Program and Short Abstracts: 6th Conjugate Margins Conference, Halifax, Nova Scotia, Canada, 19-22 August 2018 “Celebrating 10 Years of the CMC: Pushing the Bounadies of Knowledge”, 48.
- Sibuet, J.-C., Srivastava, S.P., Enachescu, M., and Karner, G.D., 2007. Early Cretaceous motion of Flemish Cap with respect to North America: implications on the formation of Orphan Basin and SE Flemish Cap–Galicia Bank conjugate margins. In: G.D. Karner, G. Manatschal, and L.M. Pinheiro (eds), *Imaging, mapping and modelling continental lithosphere extension and breakup*, Geological Society of London, Special Publication, **282**, 63-76, doi: <https://doi.org/10.1144/SP282.4>.
- Sinclair, I., 1995a, Sequence stratigraphic response to Aptian-Albian rifting in conjugate margin basins: a comparison of the Jeanne d’Arc Basin, offshore Newfoundland, and the Porcupine Bain, offshore Ireland. In: R.A. Scrutton, M.S. Stoker, G.B. Shimmield, and A.W. Tudhope (eds), *The tectonics, sedimentation and palaeoceanography of the North Atlantic region*, Geological Society of London Special Publication, **90**, 29-49.
- Sinclair, I., 1995b, Transpressional inversion due to episodic rotation of extensional stresses in Jeanne d’Arc Basin, offshore Newfoundland. In: J.G. Buchanan and P.G. Buchanan (eds), *Basin Inversion*, Geological Society of London, Special Publication, **88**, 249-271.



- Sinclair, I.K., Evans, J.E., Albrechtsons, E.A., and Sydora, and L.J., 1999. The Hibernia Oilfield-effects of episodic tectonism on structural character and reservoir compartmentalization. In: A.J. Fleet and S.A.R. Boldy (eds), *Petroleum Geology of Northwest Europe: Proceedings of the 5th Conference*, London, U.K., October 26–29, 1997, 517-528.
- Skogseid, J., 2010. The Orphan Basin – a key to understanding the kinematic linkage between North and NE Atlantic Mesozoic rifting. Extended Abstracts: II Central and North Atlantic Conjugate Margins Conference, Lisbon, Portugal, 29 September to 1 October 2010, “Re-discovering the Atlantic, New winds for an old sea”, 13-23, <http://metododirecto.pt/CM2010/>.
- Srivastava, S.P., Sibuet, J.-C., Cande, S., Roest, W.R., and Reid, I.D., 2000. Magnetic evidence for slow seafloor spreading during the formation of the Newfoundland and Iberian margins: *Earth and Planetary Science Letters*, **182**, 61-76, doi: [https://doi.org/10.1016/S0012-821X\(00\)00231-4](https://doi.org/10.1016/S0012-821X(00)00231-4)
- Williams, H., Dehler, S.A., Grant, A.C., and Oakey, G.N., 1999. Tectonics of Atlantic Canada: *Geoscience Canada*, **26**, 51-70.
- Withjack, M.O., Schische, R.W., and Olsen, P.E., 2012. Development of the passive margin of Eastern North America: Mesozoic rifting, igneous activity, and breakup. In: D.G. Roberts, and A.W. Bally (eds), *Regional geology and tectonics: Phanerozoic rift systems and sedimentary basins*, Elsevier, 300-335, <https://doi.org/10.1016/B978-0-444-56356-9.00012-2>.
- Ziegler, P.A., 1989. Evolution of the North Atlantic: An Overview. In: A.J. Tankard and H.R. Balkwill (eds), *Extensional Tectonics and Stratigraphy of the North Atlantic Margins*, American Association of Petroleum Geologists Memoirs, **46**, 111-129.
-





SEISMIC STRATIGRAPHY AND ARCHITECTURE OF THE JURASSIC ABENAKI MARGIN, AND POTENTIAL FOR DISTAL ORGANIC-RICH FACIES

Campbell, Taylor J.¹; Wach, Grant. D.¹; Richards, F.W.¹; and Silva, Ricardo. L.¹

¹ Basin and Reservoir Lab, Department of Earth Sciences, Dalhousie University, Halifax, NS B3H 4R2, Canada, taylor.campbell@dal.ca

Well and core data, 3D seismic data, and geologic analogs (Portugal and Morocco) are used to test and extend stratigraphic concepts of a mixed clastic-carbonate depositional setting during the Middle Jurassic to Early Cretaceous in the Sable Subbasin, offshore Nova Scotia. The study focuses on basinward mapping of third-order depositional sequences in the Abenaki Formation carbonate bank margin, and addresses:

1. source rock potential in coeval basinal calcareous mudstones,
2. changes in bank margin morphology related to the basement,
3. transition from a dominantly carbonate to fluvio-deltaic system extending into the Late Cretaceous, and
4. the presence of thick fluvio-deltaic sediments adjacent to basinal mudstones outboard of the carbonate bank.

Geological, petrophysical, and geophysical methods are used to interpret the depositional cycles and stratigraphic framework of limestones and calcareous shales deposited in deeper water outboard of the Abenaki margin. This framework formed the basis for a 3D geocellular model populated with lithologies from well data via a seismic inversion. This model was interpreted in terms of environments of deposition and source rock potential.

The third-order sequence stratigraphic framework was modified from a framework established by Encana at their Deep Panuke gas field. This third-order ascending chronostratigraphic (Abenaki 1-7) framework incorporates multiple litho-stratigraphically defined formations: the Mohican, Mohawk, Mic Mac, Abenaki, Missisauga, and Verrill Canyon. Thick fluvio-deltaic successions adjacent to basinal mudstones, as seen in the Migrant N-20 well, are structurally controlled, with deposition in local depocentres in response to sediment loading and listric faulting above a deeper mobile salt substrate (latest Triassic Argo Formation).

Based on published carbonate depositional models, distal condensed sections in the Abenaki 1-4 sequences (Bajocian–Kimmeridgian) have the potential for accumulations of organic-rich sediments. The basinal shales of these sequences are estimated to have been deposited in up to 200 m water depths and have potential as Type II source rocks. A change in seismic signatures and facies occurs between Abenaki 1-4 and Abenaki 5-7 sequences reflecting encroachment of the Sable Delta from the east. Abenaki 5-7 sequences (Kimmeridgian–Berriasian) are interpreted to have potential for a predominantly Type III source, with some potential for Type II sources in intervening calcareous mudstones.

Introduction

The Middle Jurassic to Early Cretaceous succession within the Scotian Basin, offshore Nova Scotia, comprises a floodplain and delta complex (Mic Mac and Missisauga formations), carbonate platform (Abenaki Formation) and associated basinal sediments (**Figure 1**). The Abenaki Formation carbonate bank lies at the northern end of a continental-scale giga-platform extending south to modern-day carbonates in the Caribbean (Jansa, 1981). It has been studied extensively by the petroleum industry, academia, and the Geological Survey of Canada (e.g. Eliuk, 1978, 2016; Wade and MacLean, 1990; Weissenberger et al., 2000; and Kidston et al., 2005). Available data is sourced from 127 exploration wells, extensive 3D and 2D seismic surveys (29,512 km² and



400,954 km respectively (CNSOPB, 2008), and production information from the commercial gas field at Deep Panuke. The connection between the platform margin and associated basinal sediments has received far less attention, due to lack of well penetrations and less direct commercial interest. Hydrocarbons are found all along the Scotian margin, therefore understanding the relationships between the units and related depositional facies might help better understand and predict the elements and processes of the area's petroleum system (e.g. Enachescu and Wach, 2005).

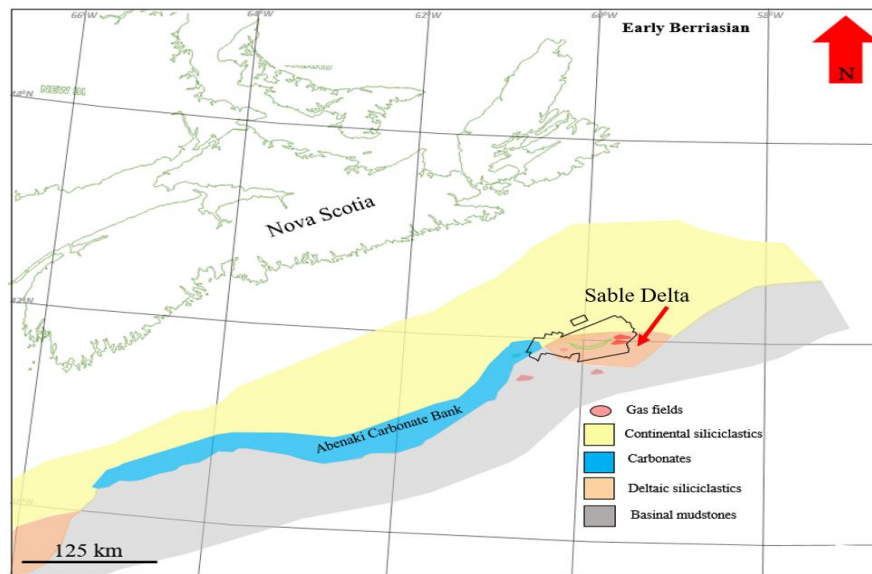


Figure 1. Generalized facies distribution map of the Abenaki Formation carbonate bank (blue), distal shales of the Verrill Canyon Formation (grey), Sable Delta of the Lower Missisaga fFormation (orange), and siliciclastics of the Mic Mac and Mohawk formations (yellow). This map shows approximate facies distribution during the Early Berriasian based upon 2D and 3D seismic data (modified from Wade and Maclean, 1990). The ExxonMobil 3D Sable MegaMerge polygon area is outlined in black. The five red polygons are gas fields associated with the ExxonMobil-Shell Sable Gas Project.

The Cohasset-Migrant area within the ExxonMobil 3D Sable MegaMerge seismic survey can be tied to the Cohasset L-97, Dominion J-14, and Migrant N-20 wells. The provides the opportunity to study: i) the stratigraphic architecture of the carbonate platform-basin transition in detail seismically; ii) the possible source-prone intervals; and iii) the stratigraphic and structural relationship between the carbonate depositional system and the deltaic depositional system that subsequently overwhelms it. The source rock potential of the Abenaki margin has been interpreted by Mukhopadhyay (1991, 1994) and Kidston et al. (2005), although there is very little well control outboard of the platform margin. However, with sufficient seismic imaging and resolution, it is possible to infer potential source rocks from stratigraphic and structural architectures.

Geological Background and Analogous Basins

Comparing the Scotian Basin to its conjugate margin offshore Morocco, and to the onshore Lusitanian Basin in Portugal, was crucial to aid in the understanding of a large-scale carbonate depositional environment with siliciclastic influence as exhibited within the Sable Subbasin. Through fieldwork within the Lusitanian Basin, and a comparison of stratigraphic charts of the Moroccan Margin and the Lusitanian Basin to that of the Sable Subbasin, it is evident that similar structural and depositional processes were taking place on all three margins from the Late Triassic to Early Cretaceous. All margins developed synrift grabens and half-grabens during the Middle to Late Triassic that were flooded with marine waters from the Tethys paleo-ocean. Terrestrial and



restricted shallow marine conditions deposited synrift redbeds and salt on all three margins in the Late Triassic (e.g. Brown, 1980; Wade and MacLean, 1990).

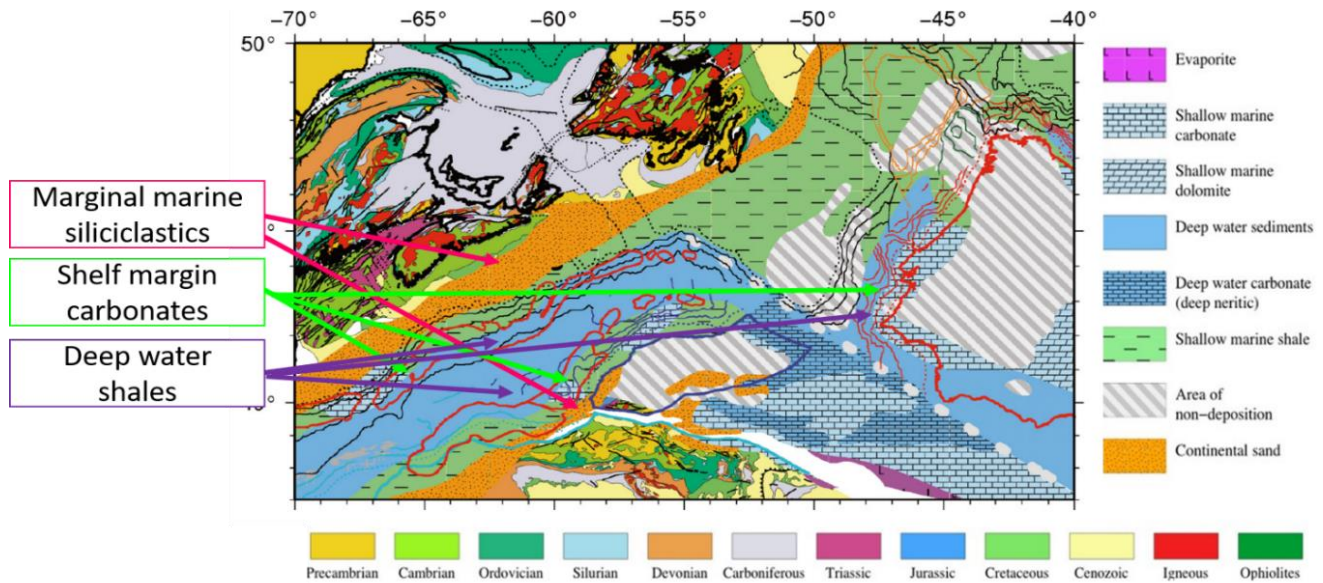


Figure 2. Paleogeographic map of the Middle Jurassic at Middle Bajocian, 170 Ma modified from Sibuet et al. (2011) to show similar depositional facies trends taking place on all three margins (Scotian, Moroccan, Iberian). The typical basinward facies transition within the Central Atlantic during the Middle Jurassic consists of marginal marine siliciclastics, shelf margin carbonates, and deep-water shales. The Iberian Margin (within the Lusitanian Basin in Portugal) did not experience as much siliciclastic influence due to inferred sediment starvation, perhaps due to more arid conditions.

From the Early to Middle Jurassic, on all three margins occurred deposition of marginal marine clastics prograding into carbonates and transitioning basinward into distal shales (**Figure 2**). From the Middle to Late Jurassic, in the Scotian and Moroccan margins, another basinward transitioning facies progression of clastics to carbonates to distal shales was deposited (e.g. Brown, 1980; Wade and MacLean, 1990; Broughton and Trepaniér, 1993). Within the Lusitanian Basin, there are considerably less siliciclastics during this time as compared to the other two margins, due to an inferred sediment starvation, with carbonates deposited well into the late Oxfordian (Ellis et al., 1990).

During the Cretaceous, existing carbonate depositional systems on the Scotian and Moroccan margins subsequently were overwhelmed by siliciclastic deposition from the east. This sediment pulse was in response to the Avalon uplift, a Late Jurassic rift flank uplift associated with the initiation of seafloor spreading between the Grand Banks and Western Europe (Iberia) (Wade and MacLean, 1990) on the Scotian Margin and from an unexplained, inferred uplift on the Moroccan Margin, which allowed episodic sedimentation along the Moroccan margin. The depositional systems of the two margins differ after the Early Cretaceous.

There are known source rock intervals within the Lower Triassic, and Lower and Upper Jurassic in Morocco, and the Lower and Middle Jurassic in the Lusitanian Basin. Both areas underwent similar depositional processes to that of the Scotian Basin within a similar timeframe (Broughton and Trepaniér, 1993; Silva et al., 2014). These analogies were considered when interpreting the potential source prone intervals down-dip of the carbonate bank, where there are limited well penetrations within the Scotian Basin.



Methodology

This study was completed using a combination of geological, geophysical, and petrophysical analyses. Two carbonate depositional models were used to interpret the Abenaki carbonate bank (Weissenberger et al., 2000; Encana 2006) and the inferred basinal sediments (Kidston et al., 2005).

The Abenaki Formation within the Scotian Basin has been interpreted here to comprise seven depositional sequences, ranging from the Bajocian to the Berriasian (Weissenberger et al. 2000; Encana 2006) (**Figure 3**). The boundaries between the depositional sequences are defined by major flooding surfaces mapped throughout the study area, where foreslope and basinal microbial limestones are overlain by basinal mudstones. All sequences were interpreted from one bounding flooding surface to the next throughout the 2D and 3D seismic. All third-order depositional sequences represent marine regression, defined by a basinward progradation when the rate of sediment flux exceeds the rate of new space added. This allows the sequences to transition from siliciclastics/carbonates on the shelf, to carbonates on the margin/slope, prograding basinward into distal mudstones.

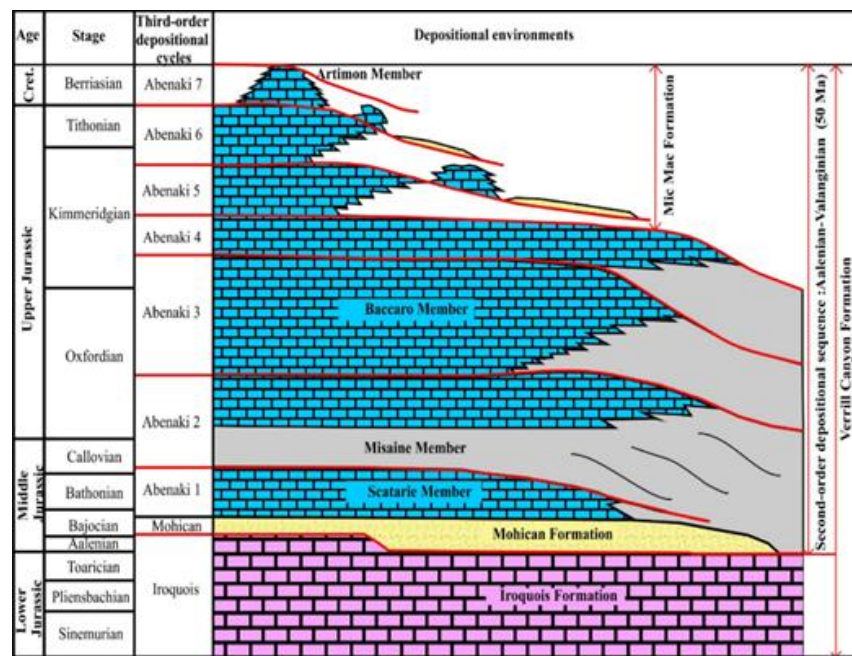


Figure 2. Refined schematic of the third-order depositional sequences of the Abenaki Formation based upon results from this study, using seismic, core, and well logs. Modified from Weissenberger et al., (2000) and Encana (2006).

The Wilson carbonate sequence stratigraphic model presented by Kidston et al. (2005) (**Figure 4**) was also used since there are no deep well penetrations in the study area which sample the basinal equivalents of the Abenaki carbonate bank. This sequence stratigraphic model is applied to the distal facies of the third-order depositional sequences, (Middle Jurassic to Early Cretaceous). From this model, the assumption is made that there is potential for organic-rich facies within the distal shales of the Abenaki carbonate bank.

Core and microfacies analysis was performed on ten cored intervals of the Abenaki Formation to examine the different minerals and lithologies that help determine their depositional environment. Eliuk (2016) proposed a modern analog of Australia’s Great Barrier Reef system, the longest modern coral reef in the world, terminating to the north in the large Fly River Delta in the Gulf of Guinea. Both the Fly River Delta/Great Barrier Reef and the Abenaki Margin/Sable Delta comprise a mixed siliciclastic and carbonate depositional system. The evolution of passive margins from rifting, development, and termination of carbonate systems, and the burial of carbonates



by prograding siliciclastics, is not unique to the Fly River/Great Barrier Reef and is observed in other low-latitude regions over geological time (Tcherepanov et al., 2008).

Petrophysical analysis included stratigraphic correlation and log analysis of ten key wells penetrating the Middle Jurassic within the study area. These were used to aid in the interpretation of depositional environments, and how the depositional environments changed laterally. The total organic content values for six of the ten key wells were also examined from log reports to determine if there was any potential for organic-rich facies based on previous work done by Mukhopadhyay (1991, 1994).

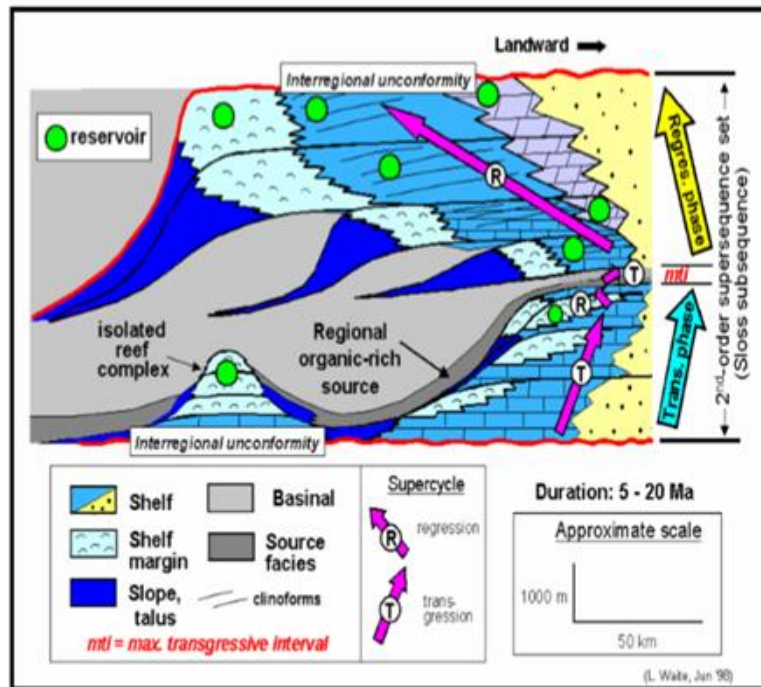


Figure 4. Schematic of Wilson carbonate sequence stratigraphic model from Kidston et al. (2005). This model identifies where potential organic-rich materials can be deposited within a carbonate ramp environment.

Most of the study comprised of geophysical analyses, including seismic interpretation of 2D and 3D seismic using seismic facies analysis and seismic stratigraphy. Seismic horizons and faults were correlated throughout the study area, from the Early Triassic to the Early Cretaceous. A genetic seismic inversion was also performed to aid in the discrimination between limestones and sandstones, which was then used to interpret depositional environment down-dip of the carbonate bank. A geocellular model was also defined from the seismic and fault correlations, which was then depth-converted and infilled with lithological properties.

Results and Discussion

Using the carbonate depositional model of the Abenaki carbonate bank (**Figure 3**), 18 seismic horizons and 14 faults (**Figure 5**) were interpreted throughout the study area. From seismic interpretation, well log analysis, and populating a depth converted geocellular model with lithologies, it was concluded that two main depositional environments were present from the Middle Jurassic to Early Cretaceous. From the Bajocian to middle Kimmeridgian (Abenaki 1-4; **Figure 3**), a normal, prograding carbonate depositional environment where all sequences downlap one another distally. This system has a facies progression of erosion-resistant frame builders on the bank margin, to limestones on the proximal foreslope, and mudstones on the distal foreslope, were deposited in water depths of 75 to 200 m (Encana, 2006).



The second depositional environment comprises a mixed carbonate and siliciclastic environment, from the middle Kimmeridgian to the Berriasian (Abenaki 5-7; **Figure 3**). This is approximately when the Sable Delta of the Mic Mac-Missisauga formations began encroachment from the northeast and influencing the growth of the Abenaki's fifth, sixth, and seventh depositional sequences. During this period, only minor patch reefs could develop as sea level kept up with siliciclastic deposition. Siliciclastics of the Mic Mac Formation interfinger with the carbonates just outboard of the carbonate bank. Basinward of the Missisauga Formation, the laterally equivalent mudstones of the Verrill Canyon Formation dominated (**Figure 3**).

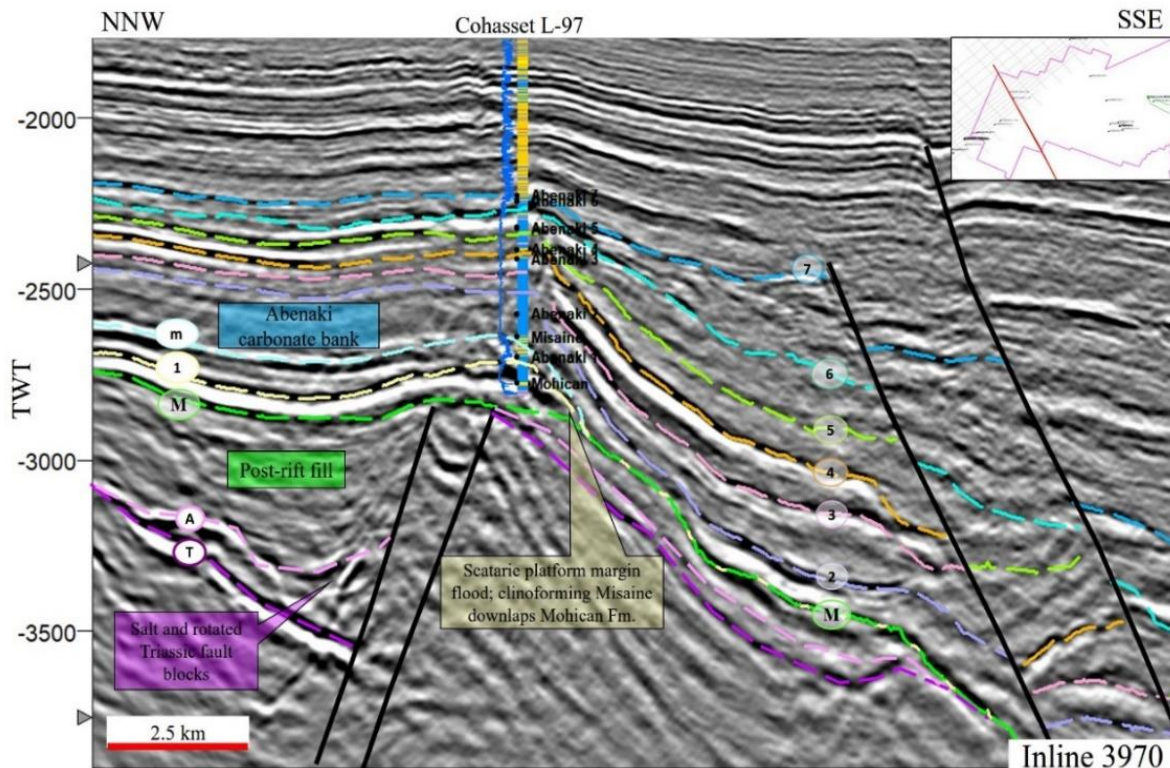


Figure 3. Seismic line from the ExxonMobil 3D Sable MegaMerge dataset. The yellow horizon (1) to blue horizon (7) interval contains the interpreted seven third-order sequences Abenaki 1-7, deposited over approximately 20 million years (Weissenberger et al., 2000). Abenaki 4 (orange) is the most regressive of these sequences and can be mapped distally. These limestone seismic markers can be mapped confidently basinwards. Third-order sequences are labeled 1-7, the top of the Misaine Member is marked as “m”, the top of the Triassic is marked by Tm, the top of the Argo salt is marked by A, and the top of the Mohican is marked by M.

From this study, a revised stratigraphic chart of the Late Jurassic to Early Cretaceous was created for the siliciclastics outboard of the Abenaki carbonate bank (**Figure 6C**). Directly outboard of the carbonate bank, the carbonates interfinger with siliciclastics of the Mic Mac Formation, which could have bypassed the carbonate bank, or siliciclastics could have come in around the carbonate bank from the north during highstands. **Figure 5** shows the beginning of the expansion trend (large normal faulting, highlighted in **Figure 5** as black lines) interpreted to be a result of the siliciclastic influx from the northeast causing loading and consequential subsidence, normal faulting, and salt movement. The carbonates and distal carbonate facies of the third-order sequences are correlated below the Migrant N-20 well within the 3D MegaMerge area, signifying that the siliciclastics within the expansion trend do not interfinger with the carbonate bank and are separate and younger, and associated with the Missisauga Formation. Figure 6C shows the revised stratigraphic chart where a fault is placed between the



siliciclastics of the Mic Mac and Missisauga formations as compared to past interpretations of this interval (**Figures 6A** and **6B**).

Source Rock potential of distal third-order depositional sequences of the Abenaki carbonate bank

Deposition of Abenaki 1, 2, 3, and 4 (**Figure 3** and **Figure 5**) took place during the Middle to Late Jurassic (middle Bajocian to middle Kimmeridgian) in a predominately carbonate depositional environment. Abenaki 2 contains shale designated the Misaine Member, which was interpreted to have been deposited in an inner to outer neritic environment on the continental shelf at Cohasset L-97 (Beicip-Franlab, 2016). Although there are many potential uncertainties in the total organic content values recorded in the well logs, the intervals with the most potential to contain organic-rich facies are the distal shales of the Abenaki 2 to 4 sequences of Bajocian to Kimmeridgian age.

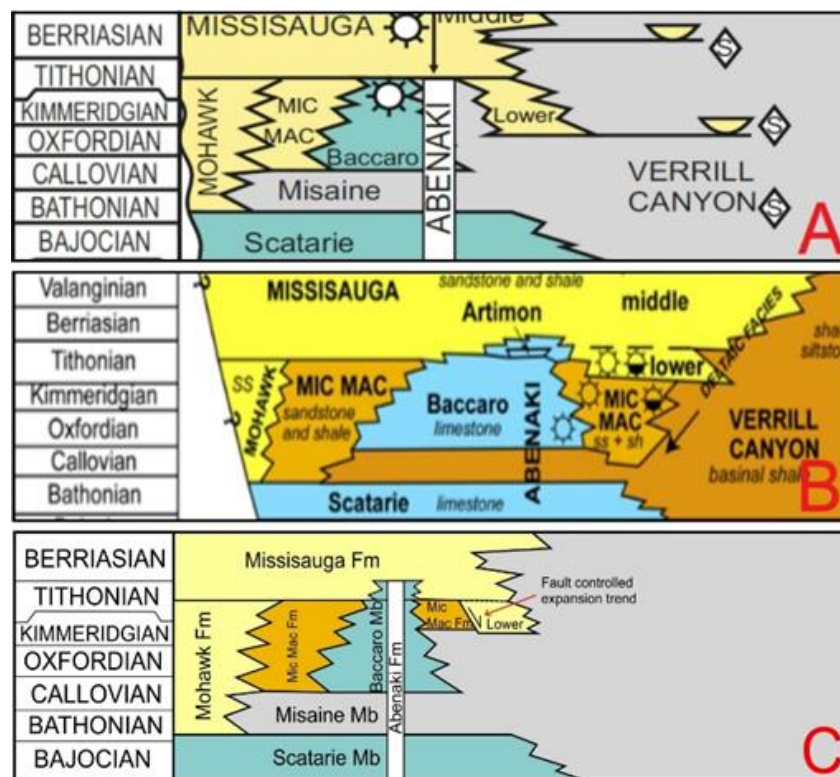


Figure 6. A) Stratigraphic chart of the Scotian Basin from Weston et al. (2012). The authors interpreted the siliciclastics outboard of the Abenaki carbonate bank to be sourced from the Missisauga Formation and to interfinger with the distal shales of the Abenaki carbonate bank. B) Stratigraphic chart created by Tari et al. (2012) from Wade and MacLean (1990). The authors interpreted the siliciclastics just outboard of the carbonate bank to be part of the Mic Mac Formation, which interfingers with both the Missisauga Formation and the Verrill Canyon Formation distally. C) Revised stratigraphic chart created from interpretations from this study. The siliciclastics just outboard of the carbonate bank are interpreted to be from the Mic Mac Formation that interfinger with the carbonates, which are then juxtaposed against siliciclastics of the Missisauga Formation due to faulting, creating the expansion trend around Migrant N-20.

The condensed sections of marine mudstones and argillaceous deep-water carbonates that were deposited in the distal foreslope to deep shelf environments during the middle Oxfordian and the middle to early Kimmeridgian (Abenaki 2, 3, and 4) (e.g. **Figure 7A** and **7B**), would have been starved of terrigenous materials during a period of maximum relative sea-level rise. This would result in deposition of sediments that primarily comprise skeletal remains of pelagic fauna. These sediments deposit in water depths of approximately 200-500 m



(Figure 7A, 7B, and 7C) (Tyson, 1987). If anoxia and high organic productivity prevailed during times of organic deposition, these intervals have potential to contain kerogen of predominately Type 2 source.

Similarly, on the Moroccan Margin, Oxfordian shales present in the onshore fields of the Essaouira Basin have Type II kerogen, reaching up to 4.3% TOC in an approximate 10 m thick interval (Broughton and Trepaniér 1993). This is a good indication that anoxic conditions could also prevail at a similar water depth on the Scotian Margin due to both margins hosting similar depositional environments from the Early Triassic to Early Cretaceous.

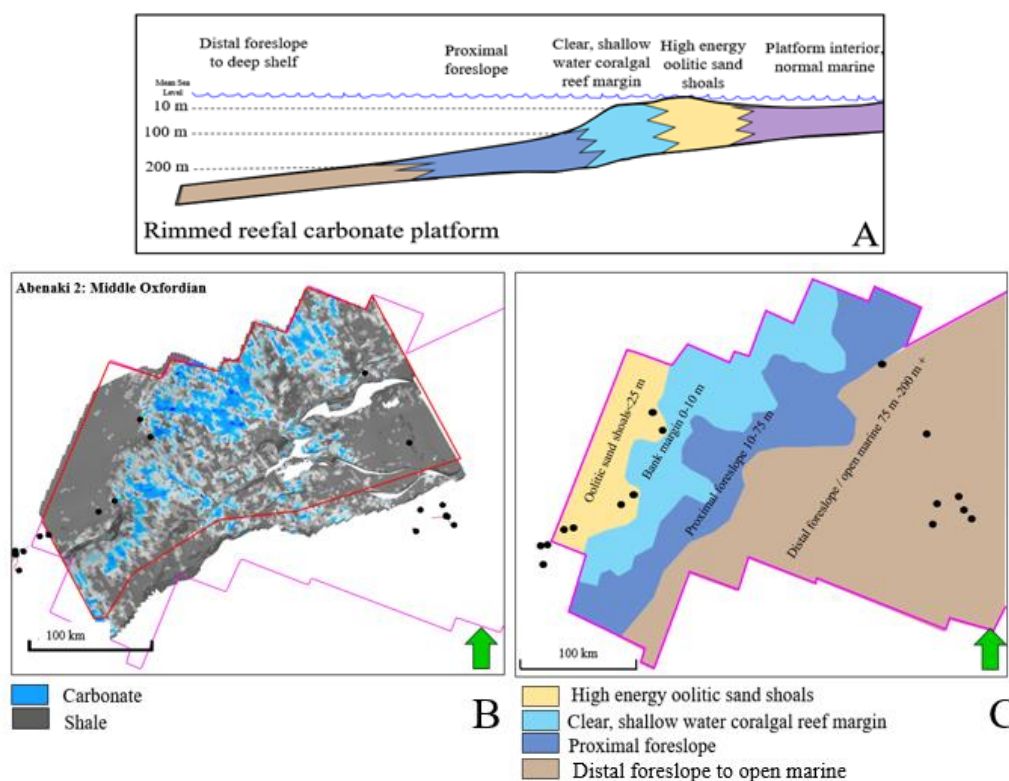


Figure 7. A) Carbonate depositional model in which the environment of deposition maps were created for Abenaki 2, 3, and 4 sequences. The boundary between the distal foreslope to outer neritic was unable to be determined throughout the seismic, therefore it is just interpreted as being deposited in water depths greater than 200 m (modified from Beicip-Franlab, 2016). B and C represent map views of Abenaki 3 during the middle Oxfordian. B) Geocellular model populated with lithologies from the genetic seismic inversion (blue=carbonates, grey=shales). C) Environment of deposition map interpreted from the geocellular model and from the stratigraphic framework. The potential organic-rich intervals are interpreted to have been deposited on the distal foreslope to deep shelf (outer neritic).

The distal foreslope to deep shelf environments of Abenaki 5, 6, and 7 (Figure 8) are less likely to contain Type II kerogen due to having a mixed marine and terrigenous source. The distal foreslope of the carbonate platform was influenced by sediments associated with deposition of the prodelta strata of the Sable Delta. The conditions normally associated with a marine petroleum source rock formation typically result from low contents of terrestrial organic matter except in the immediate proximity of fluvial sources. The Sable Delta was approximately 10-20 km from the distal intervals (within the study area) in which Abenaki 5, 6, and 7 sequences were deposited. This may have allowed terrestrial organic matter to be preserved, or organic matter could have degraded during transport. The depositional environment in which the mudstones of these third-order sequences were deposited was most likely of higher energy and in relatively shallower water depths compared to the older depositional sequences (Abenaki 1–4). If anoxic conditions at this water depth prevailed, there may be potential to host a mixed Type II/III kerogen source with the terrigenous detritus sourced from the Sable Delta having



potential to provide significant organic content basinward of the platform margin. Within the Late Jurassic in the Lusitanian Basin onshore Portugal, the Cabaços Formation has kerogen assemblages of mostly continental origin, with minor influxes of marine influence, and averages approximately 4% TOC (Silva et al., 2014). The deposition of the source prone intervals of the Cabaços Formation is interpreted to have been in calm and proximal environments, close to the source area.

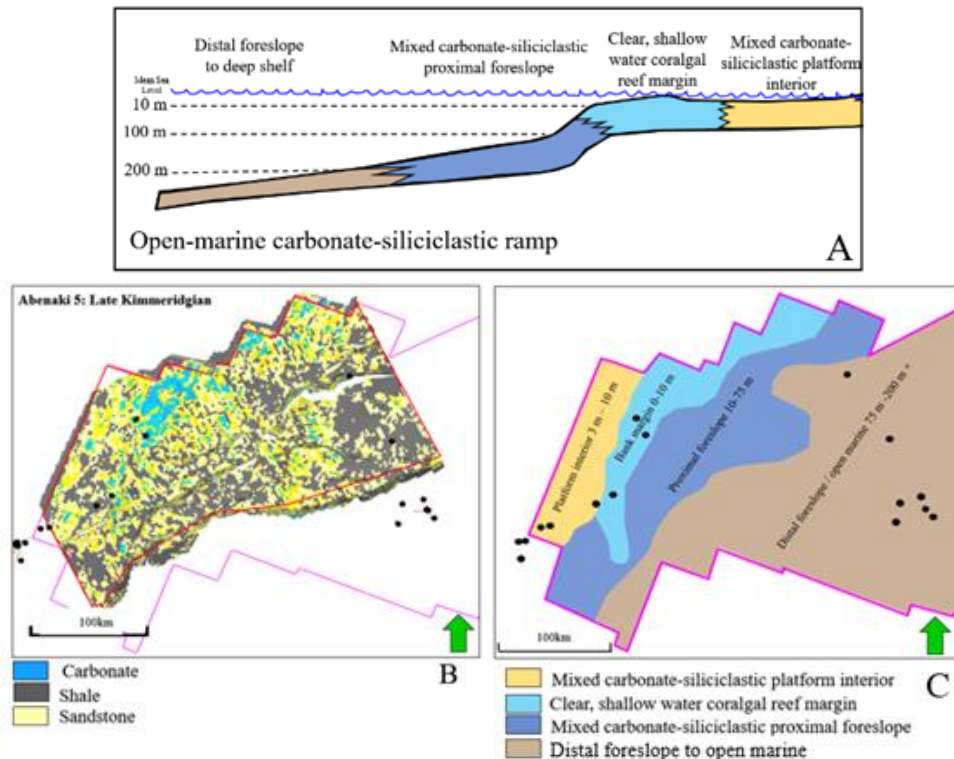


Figure 8. A) carbonate depositional model from which the environment of deposition maps were created for the Abenaki 5, 6, and 7 sequences (modified from Beicip-Franlab, 2016). Figure B and C shows the map view of Abenaki 5 during the Late Kimmeridgian. B) Geocellular model, which was populated with lithological data from the genetic seismic inversion. C) Environment of deposition map interpreted from the geocellular model, and the seismic stratigraphic framework. The potential source intervals of these third-order depositional sequences are interpreted as being deposited on the distal foreslope to open marine.

Conclusions

The depositional environments, interpreted in each third-order depositional sequences of the Abenaki Formation carbonate bank, support the conclusion that terrigenous, siliciclastic material from the Sable Delta to the northeast began influencing the growth of the carbonate bank in the middle Kimmeridgian. The third-order depositional sequences below the middle Kimmeridgian (Abenaki 1–4) were deposited as a normal, shelf-margin carbonate system, outboard of siliciclastics of the fluvial Mic Mac and Mohican formations. The younger third-order depositional sequences, extending from the middle Kimmeridgian to the early Berriasian (Abenaki 5–7) were deposited as an increasingly mixed siliciclastic-carbonate depositional system in both the inboard and outboard settings. The carbonates in the Abenaki 5–7 sequences were aggradational and grew predominately as patch reefs at the shelf margin, however they were not able to prograde as far into the basin as the progradational sequences below. These upper sequences represent increasing influx of siliciclastics sourced from the Sable Delta.

From this geological model and analog studies, the calcareous shales deposited on the distal foreslope/deep basin of the middle Callovian, middle Oxfordian, and middle Kimmeridgian were in water depths



with the potential for preservation of organic matter in anoxic conditions. If organic matter could be preserved, it would likely be Type II kerogen. If all conditions to produce a successful source rock were met in Abenaki sequences 5–7, and anoxic conditions at this water depth prevailed, there may be potential to host a mixed Type II/III kerogen source, with the terrigenous detritus sourced from the Sable Delta having potential to provide significant organic content basinward of the platform margin. Anoxic condition at this depth in the Scotian Margin may be inferred from analogous studies of the Moroccan Margin and the Lusitanian Basin, both of which have analogous source prone intervals within the Middle to Late Jurassic.

At Migrant N-20, the deltaic siliciclastics within the interpreted expansion trend are interpreted to be from the younger Missisauga Formation and are fault juxtaposed against the clastics of the Mic Mac and Verrill Canyon formations. Based on seismic correlation of the third-order depositional sequences interpreted below the Migrant N-20 well, the siliciclastics above must be younger as they do not interfinger with the distal shales of the Abenaki carbonate bank as illustrated in published stratigraphic charts (CNSOPB, 2008; Weston et al., 2012, and Beicip-Franlab, 2016).

References

- Beicip-Franlab, 2016, Central Scotian Slope Play Fairway Analysis (PFA). Nova Scotia Department of Energy, accessed May 31, 2018. <http://www.oera.ca/offshore-energy-research/geoscience/central-scotian-slope-atlas-2016>
- Broughton P., and Trepaniér, A., 1993. Hydrocarbon generation in the Essaouira Basin of Western Morocco. *Bulletin of the American Association of Petroleum Geologists*, **77**(6), 999-1015.
- Brown, R.H., 1980. Triassic Rocks of Argana valley, Southern Morocco, and their structural implications. *Bulletin of the American Association of Petroleum Geologists*, **64**(7), 988-1003.
- Canada-Nova Scotia Offshore Petroleum Board. 2007. Canada-Nova Scotia Offshore Petroleum Board Call for Bids NS2007-1 Information Package (Regional Geology). Accessed September 23, 2017. http://www.callforbids.cnsopb.ns.ca/2007/01/regional_geology.html
- Eliuk, L.S., 1978. The Abenaki Formation, Nova Scotia Shelf, Canada - A depositional and diagenetic model for a Mesozoic carbonate platform. *Bulletin of Canadian Petroleum Geology*, **26**(4) 424-514.
- Eliuk, L.S., 2016. Abenaki carbonate platform in relation to the Jurassic-Cretaceous Sable Island Delta, offshore Nova Scotia, Canada. Unpublished PhD. thesis, Department of Earth Sciences, Dalhousie University, Halifax, N.S., Canada, 560p.
- Ellis, P.M., Wilson, R.C.L., and Leinfelder, R.R., 1990. Tectonic, palaeogeographic and eustatic controls on Upper Jurassic carbonate buildup development in the Lusitanian Basin, Portugal. *International Association of Sedimentologists Special Publication*, **9**, 169-202.
- Enachescu, M., and Wach, G.D., 2005. Exploration Offshore Nova Scotia: Quo Vadis? (Where do we go from here?). *Ocean Resources*, June-July 2005, 23-25.
- Encana Corporation., 2006, Deep Panuke Offshore Gas Development: Development Plan, Volume 2, 293p. https://www.cnsopb.ns.ca/sites/default/files/inline/dp_dpa_vol2.pdf
- Jansa, L.F., 1981. Mesozoic carbonate platforms and banks of the eastern North American margin. *Marine Geology*, **44**, 97-117.
- Kidston, A.G., Brown, D.E., Smith, B.M., and Altheim, B., 2005. The Upper Jurassic Abenaki Formation Offshore Nova Scotia: A Seismic and Geologic Perspective: Canada-Nova Scotia Offshore Petroleum Board, Halifax, NS, Canada, 165p. http://www.cnsopb.ns.ca/sites/default/files/pdfs/Abenaki_report_06_2005.pdf



- Morrison, N.M., 2017. Seismic inversion and source rock evaluation on Jurassic organic rich intervals in the Scotian Basin, Nova Scotia. Unpublished M.Sc. thesis, Department of Earth Sciences, Dalhousie University, Halifax, N.S., Canada, 216p.
- Mukhopadhyay, P.K., 1991. Evaluation of organic facies of the Verrill Canyon Formation, Sable Subbasin, Scotian Shelf. Geologic Survey of Canada, Open File Report 2435, 99p.
- Mukhopadhyay, P.K., 1994. Organic Petrography and Kenetics of Limestone and Shale Source Rocks in Wells Adjacent to Sable Island, Nova Scotia and the Interpretation on Oil-Oil or Oil-Source Rock Correlation and Basin Modeling: Geologic Survey of Canada, Open File Report 3167, 100p.
- Sibuet, J.-C., Rouzo, S., and Srivastava, S., 2011. Plate tectonic reconstructions and paleogeographic maps of the central and North Atlantic oceans. *Canadian Journal of Earth Sciences*, **49**(12), 1395-1415, doi:10.1139/e2012-071.
- Silva, R.L., Mendonça Filho, J.G., Azerêdo, A.C., and Duarte, L.V., 2014. Palynofacies and TOC analysis of marine and non-marine sediments across the Middle-Upper Jurassic boundary in the central northern Lusitanian Basin (Portugal). *Facies*, **60**, 255-276.
- Tari, G.C., Brown, D.E., Jabour, H., Hafid, M., Louden, K., and Zizi, M., 2012. The conjugate margins of Morocco and Nova Scotia. In: D.G. Roberts and A.W. Bally (eds), *Regional Geology and Tectonics: Phanerozoic Rift Systems and Sedimentary Basins – Volume 1C – Passive Margins*. Elsevier, Amsterdam, 265-300.
- Tcherepanov, E.N., Droxler, A.W., Lapointe, P., Dickens, G.R., Bentley, S.J., Beaufort, L., Peterson, L.C., Daniell, J., and Opdyke, B.N., 2008. Neogene evolution of the mixed carbonate-siliciclastic system in the Gulf of Papua, Papua New Guinea. *Journal of Geophysical Research Atmospheres*, **113**(F1), F01S21 (15p.), doi:10.1029/2006JF000684.
- Tyson, R.V., 1987. The genesis and palynofacies characteristics of marine petroleum source rocks. In: J. Brooks, and A.J. Fleet (eds), *Marine Petroleum Source Rocks: Geological Society Special Publication*, **26**, 47-67.
- Wade, J.A., and MacLean, B.C., 1990. Chapter 5 - The geology of the southeastern margin of Canada, Part 2: Aspects of the geology of the Scotian Basin from recent seismic and well data. In: M.J. Keen and G.L. Williams (eds), *Geology of Canada No.2 - Geology of the continental margin of eastern Canada*. Geological Survey of Canada, 190-238 (also Geological Society of America, *The Geology of North America*, Vol.I-1).
- Weissenberger, J., Harland, N.L., Hogg, J. and Syloonyk, G., 2000. Sequence stratigraphy of Mesozoic Carbonates, Scotian Shelf, Canada. In: *GeoCanada 2000 – The Millennium Geoscience Summit, Joint Convention of the CSPG, CSEG, GAC, MAC, CGU and CWLS, Conference CD-ROM, Paper No.1262*, 5p.
- Weston, J.F., MacRae, R.A., Ascoli, P., Cooper, M.K.E., Fensome, R.A., Shaw, D., and Williams, G.L., 2012. A revised biostratigraphic and well-log sequence stratigraphic framework for the Scotian Margin, offshore eastern Canada. *Canadian Journal of Earth Sciences*, **49**(12), 1478-1503.
-





FRONTIER EXPLORATION IN THE PENICHE BASIN (WEST IBERIA MARGIN): NEW INSIGHTS FROM RECENT 3D SEISMIC AND GRAV-MAG MODELING

Casacão, João¹, Fernandes, Susana¹, Silva, Francisco¹, and Rocha, João¹

¹ Galp Energia, Rua Tomás da Fonseca, Torres de Lisboa, Torre Galp - 5º Andar, 1600-209, Lisbon, Portugal, joao.casacao@galp.com

A recent 3D seismic dataset was acquired on the northern sector of the Peniche Basin (West Iberia Margin) to investigate the petroleum potential on the northern depocentre of the basin. This survey revealed outstanding geological features that were poorly imaged in previous 2D seismic surveys. Interpreted 3D seismic was coupled with gravity-magnetic-derived analysis to investigate the structural controls and the lithological nature of the basement. The main lineament directions suggest a strong control of the Late-Hercynian basement fabric. No volcanic features were observed in the 3D seismic, in contrast with several salt features, which include well-developed diapirs and detached salt stocks. These are determined to control sedimentation dynamics through the Early Cretaceous subsidence phase. Thermal modelling of Early and Late Jurassic source rocks indicate point present-day mature to over-mature intervals. These outcomes contribute to enhanced geological knowledge of this sector of the West Iberia Margin, as well as having direct implications for petroleum prospectivity.

Introduction

The deepwater Peniche Basin, located along the West Iberia Margin (WIM), has been one of the exploration focus area on the southern Central Atlantic, especially during the last decade, driven by some oil and gas indications and proven petroleum systems on the Lusitanian and Porto basins. The basins of the WIM have been broadly compared to other hydrocarbon prolific conjugates (**Figure 1**), such as the Jeanne d'Arc, Flemish Pass, and Scotian basins on the Canadian counterpart, the Porcupine and Rockall Trough basins in the western Irish margin, and the Essaouira/Aaiun-Tarfaya basins in Morocco (Wach et al., 2014; Pimentel and Pena dos Reis, 2016). Still underexplored and lacking proper stratigraphic control, the northern sector was recently surveyed with ca. 3,200 km² of 3D seismic and gravity-magnetic data. New insights were drawn from these surveys concerning the most likely stratigraphic record that should be relatively similar to the contiguous Lusitanian and Porto basins. Yet, some lithological variations are expected, reflecting the continuous basinward deepening particularly from the rift-climax phase onwards, as is recognized on the DSDP Site 398, and overall sedimentary infill thicker than the recorded in contiguous basins.

Framework

The study area is located in deep water about 50 km to the west of the Portuguese coastline (**Figure 2**). It lies over thinned continental crust on the inner/outer proximal margin of West Iberia, and broadly classified as a 'magma-poor' margin (Péron-Pinvidic and Manatschal, 2008). Its evolution reflects sequences of extensional pulses interposed with shorter periods of tectonic quiescence, which ultimately led to the lithospheric breakup during Aptian-Albian times. The rift-to-drift evolution of the WIM is associated with a diachronous northward opening (Alves et al., 2006), controlled by the ENE-WSW Nazaré and Aveiro strike-slip faults. The 'magma-poor' nature of NW Iberia's Mesozoic evolution, given by the apparent lack of volcanic features, and the absence of post-rift inversion structures, were confirmed by 3D seismic.



The lack of volcanic features on 3D seismic suggest an non-existent magma-plumbing system to the north of the transcurrent Nazaré Fault, which could be explained using the alternating crustal architecture hypothesis along the WIM (Pereira et al., 2016), in which the study area would lie on a lower continental plate footwall.

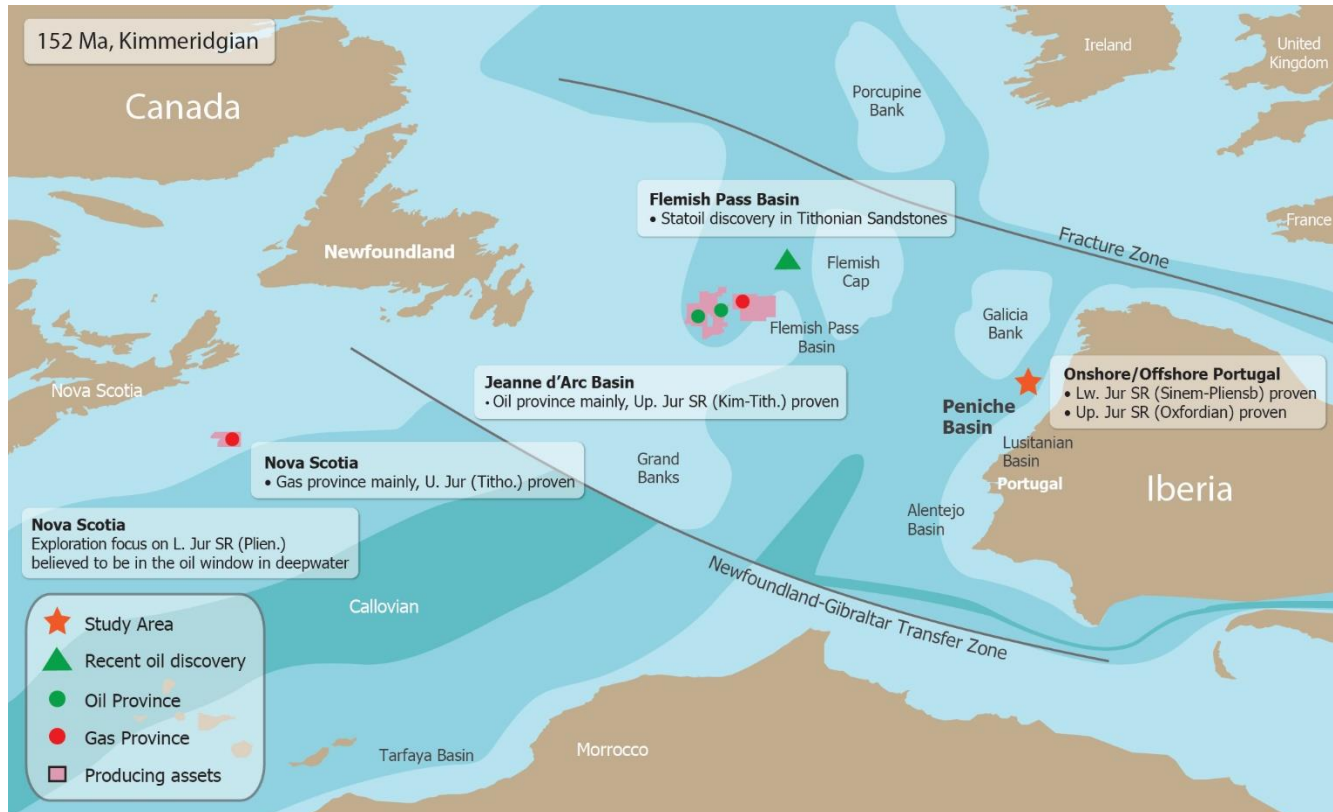


Figure 1. Paleogeographic reconstruction of the southern North Atlantic margins at Kimmeridgian times.

Structural Setting and Nature of Basement

Structurally, the opening of this half-graben trough at the northern sector of the Peniche Basin seems to be mostly controlled by tectonic subsidence associated with both horizontal and vertical interactions, between the deeply-rooted ENE-WSW Aveiro Fault and NNW-SSE and NE-SW structures. Its main rotation phase is related with the rift-climax phases during the Late Jurassic to Early Cretaceous, probably associated with local crustal thinning. Potential field data modelling was incorporated into the assessment, helping to identify the main structural families, showing the character of each anomaly, and incorporating the latter with regional geological knowledge. This gave some insights on the magnetic signature and geometry of the pre-Mesozoic basement within the study area. The area is characterized by a low magnetic response suggesting it may be composed of low-grade metamorphic lithologies such as schists and metaquartzites found in the mainland Paleozoic terranes. The only high magnetic responses are in the northern part of the area, which can be attributed to a local Late-Hercynian granitoid emplacement, and along the Aveiro Fault. A fissural volcanic emplacement may explain this magnetic correspondence along the deeply-rooted Aveiro Fault, which can be contemporaneous to the Late Cretaceous regional volcanic event.

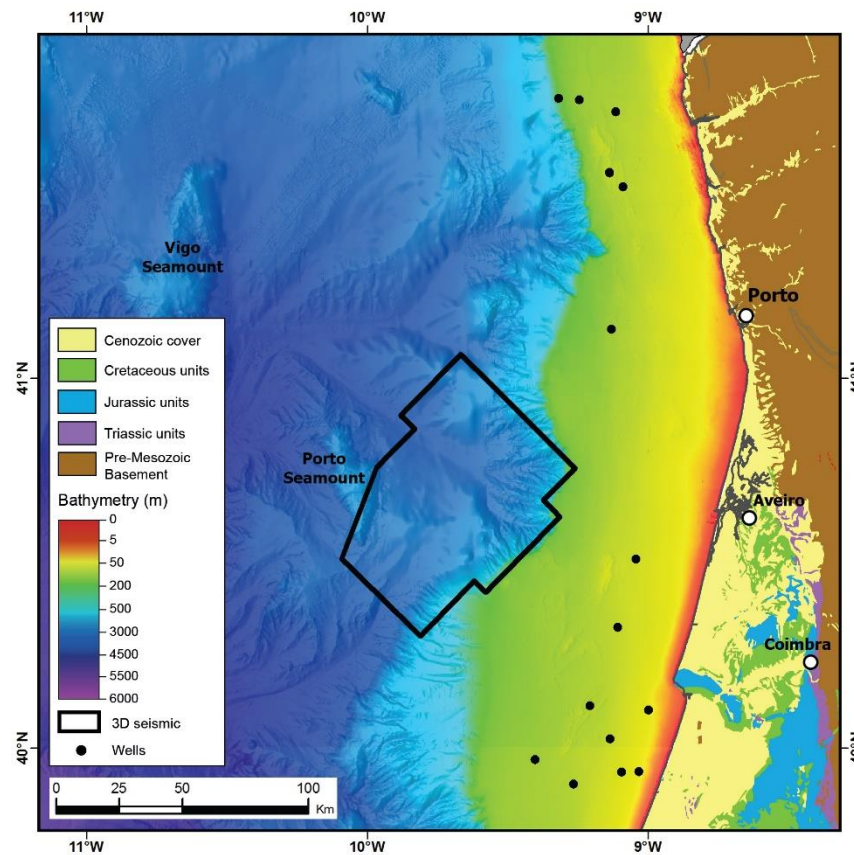


Figure 2. Location of the 3D seismic dataset and nearby wells on the continental platform. Bathymetry from EMODNET (2016).

Seismic Interpretation

The interpreted seabed to near-top basement seismic horizons define the main megasequences based on the tectono-stratigraphic record from the Peniche Basin. Seismic interpretation was particularly challenging due to the numerous occurrences of salt pillows and diapirs, which impose deformation on the Early/Mid-Jurassic(?) thick sag-related carbonates, and significantly control the Early Cretaceous clastic depositional systems. Whenever present, autochthonous salt represents a regional stratigraphic marker, below which is observed a pre-salt sequence, variable in thickness and likely composed of Triassic synrift continental siliciclastics. Our interpretation indicate thick Upper Jurassic wedge sequences developed within the hanging-walls of the Porto Seamount horst and the Aveiro Fault, prior to a roughly uniform Cretaceous and Tertiary cover. Notwithstanding, complex salt tectonics seem to accompany the main subsidence pulses with associated higher sedimentation, and diapiric reactivations during the Tertiary compressive phases until present-day, locally evidenced by supra-salt seabed deformation.

Petroleum Systems Modeling

Based on regionally proven petroleum systems and conjugate analogues, Jurassic source rocks were identified and % Ro-equivalent maturity and expulsion modelling performed. In addition to the Sinemurian-Pliensbachian and Oxfordian source rock intervals recognized in the contiguous Lusitanian Basin, the presence of a thick Upper Jurassic interval allowed consideration of a marine 'Kimmeridge Clay'-type source rock hypothesis in the modelling exercises. These marine shales can be found within strata of analogue basins, such as the conjugate Egret Member (Jeanne d'Arc and Flemish Pass basins), and the Kimmeridge Clay Formation



(Porcupine, South Celtic Sea, Wessex, and North Sea basins) (Scotchman et al., 2016; **Figure 3**). Contrary to the inboard Lusitanian Basin where transitional to coastal fluvio-deltaic facies occur, the outboard Peniche Basin should reflect a deepwater setting with relatively higher subsidence and sedimentation rates, and prone to the deposition and accumulation of shales and other marine hemipelagic facies.

According to the estimated thermal regime in this region, with present-day surface Heat Flow ca. 47 mW/m² (average measured value derived from a piston core survey), thermal modelling results indicate source rocks are currently mature to overmature that should have expelled most of their hydrocarbons.

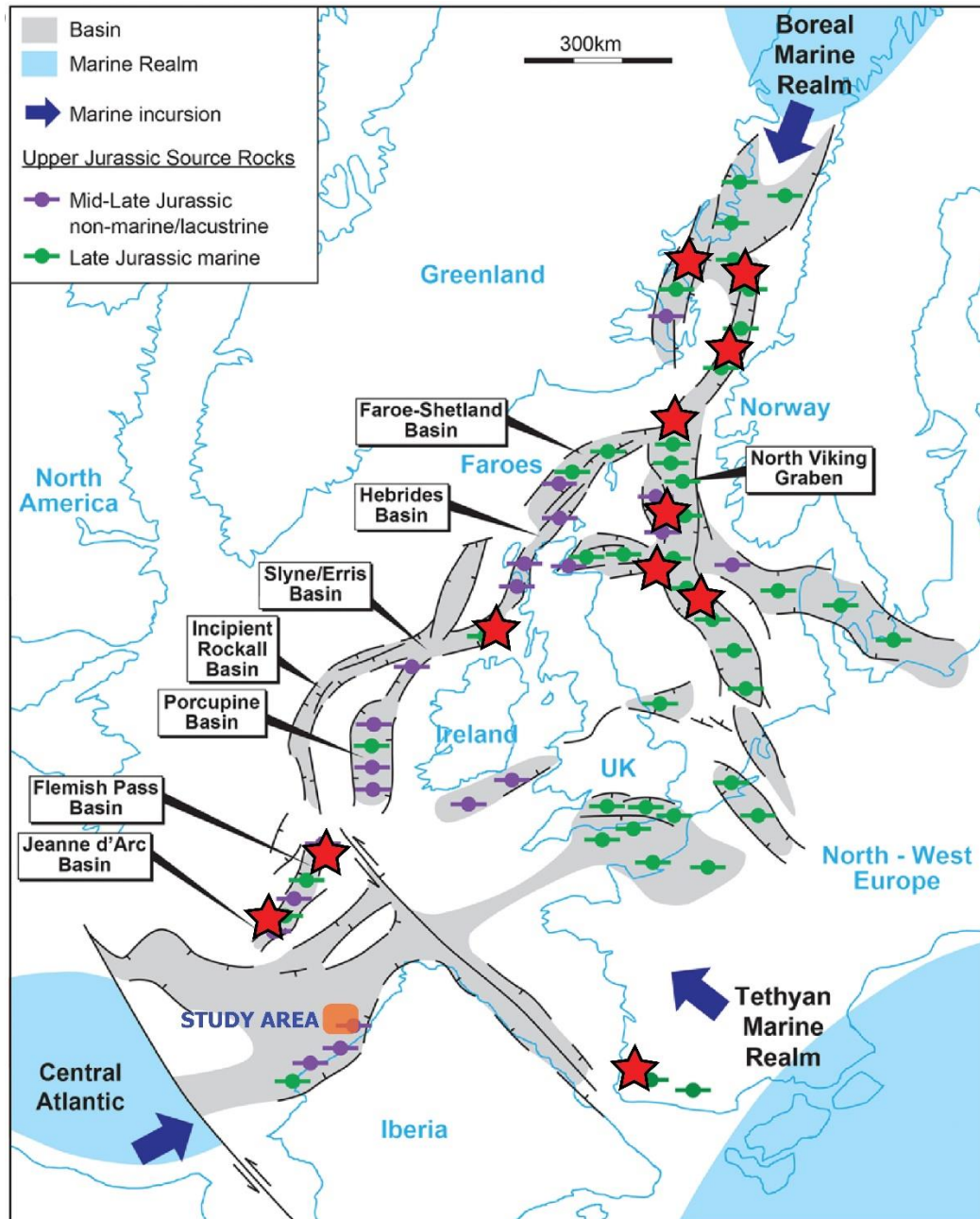


Figure 3. Late Jurassic paleoreconstruction with the distribution of marine source-rocks in the North Atlantic and southern boreal realm. Red stars indicate oil and gas fields with hydrocarbons sourced from the Upper Jurassic marine shales (adapted from Scotchman et al., 2016).



Summary and Conclusions

The recent 3D seismic dataset allowed a clearer imaging over the Peniche Basin depocentre where complex structuring and remarkable salt features are observed. Gravity-magnetic analysis reveal a low magnetic response from the basement and support the idea of strong structural control imposed from the basement up until the Cretaceous sequence. The interpreted Late Jurassic strata is remarkably thick, which has implications for petroleum systems modelling. Besides the Sinemurian-Pliensbachian and Oxfordian intervals, a conceptual ‘Kimmeridgian Clay’-type source rock was considered for hydrocarbon expulsion scenarios. Consequently, modelling results indicate that Late Jurassic sourcerocks are mature that should already have charged the Cretaceous reservoirs. These results, coupled with regional geology integration, enrich both geological understanding and petroleum potential within the Peniche Basin. Nevertheless, some issues still lack proper characterization and include:

- 1) The actual basement geometry and composition that is still open to interpretation, and the thermo-mechanical lithospheric constraints that lead to the creation of this depocentre.
- 2) The actual lithostratigraphic record of the sub-Cretaceous sequences.
- 3) The presence, thickness, and lithological character of the Late Triassic clastic sequence.
- 4) A more detailed analysis on the multi-stage evolution of salt diapirs.
- 5) Proof of concept for a hypothetical Kimmeridgian source rock interval preserved in thick Late Jurassic synrift wedges along the outer West Iberia Margin equivalent to prolific source rocks in the Canadian margins.

Acknowledgements

The authors thank Repsol, Kosmos, Partex, and the Portuguese petroleum regulator (ENMC) for authorizing this publication and the permission to show some 3D seismic lines at the Halifax 2018 Conjugate Margin Conference. The authors would also like to thank the team colleagues at Galp involved in this project.

References

- Alves, T.M., Moita, C., Cunha, T., Monteiro, J.H., and Pinheiro, L., 2006. Meso-Cenozoic evolution of North-Atlantic continental slope basins: the Peniche Basin, Western Iberian margin. *Bulletin of American Association of Petroleum Geologists*, **90**(1) 31-60.
- Pereira, R., Alves, T.M., and Mata, J., 2016. Alternating crustal architecture in West Iberia: a review of its significance in the context of NE Atlantic rifting. *Journal of the Geological Society, London*, **174**(3), 522-540. doi.org/10.1144/jgs2016-050
- Péron-Pinvidic, G., Manatschal, G., 2008. The final rifting evolution at deep magma-poor passive margins from Iberia-Newfoundland: a new point of view. *International Journal of Earth Sciences*, **98**(7), 1581-1597. doi:10.1007/s00531-008-0337-9
- Scotchman, I.C., Doré, A.G., Spencer, A.M., 2016, Petroleum systems and results of exploration on the Atlantic margins of the UK, Faroes and Ireland: what have we learnt? Geological Society, London, Petroleum Geology Conference Series, **8**, 187-197, 27 October 2016. doi.org/10.1144/PGC8.14
- Pimentel, N., and Pena dos Reis, R.P., 2016. Petroleum Systems of the West Iberian Margin: a review of the Lusitanian basin and deep offshore Peniche basin. *Journal of Petroleum Geology*, **39**(3), 305-326, doi: 10.1111/jpg.12648
- Wach, G.D., Pimentel, N., and Pena dos Reis, R., 2014. Petroleum Systems of the Central Atlantic Margins, from Outcrop and Subsurface Data. 33rd Annual GCSSEPM Foundation Bob F. Perkins Research Conference, January 26-28, 2014, Houston, Texas. doi.org/10.5724/gcs.14.33.0197





EARLY RIFT ARCHITECTURE AND THE CREATION OF ACCOMMODATION SPACE: INSIGHTS FROM THE NOVA SCOTIA MARGIN, ATLANTIC CANADA

Cervantes, Pablo¹, Whitehouse, Paul¹, Grow, Tim¹, Loureiro, Patrick¹, and Fitzsimmons, Roy¹

¹Hess Corporation, 1501 McKinney Street, Houston, TX 77010, USA, pcervantes@hess.com

The Nova Scotia Margin is a passive continental margin that developed during a period of sustained stretching as North America rifted and started separating from northwestern Africa. Rifting occurred between Late Triassic to Early Jurassic. During this time, restricted basins were formed, their orientation and architecture controlled by the inherited structural grain within the crust. Basin orientation follows a NE-SW trend across Nova Scotia with similar orientations observed in the Moroccan conjugate margin. The width and depth of these early basins is controlled by the amount of stretching and crustal thinning, which we define by discrete crustal domains (stretched, necked, hyper-extended, exhumed, and oceanic crust). Salt deposition concentrated in these early basins prior to break-up.

In this study, observations were focused on the area basinward of the LaHave Platform. This area is characterized by a salient called the Abenaki Nose, and bounded by reentrants where the Shelburne and Sable subbasins are developed. Using 2D and 3D reflection seismic, tied to gravity and refraction datasets, the extent of discrete crustal domains has been mapped (**Figures 1 and 2**). In each, their seismic architecture has been characterized and described, and their spatial development around the Abenaki Nose is:

- West of Abenaki Nose: Salt is present in a narrow band deposited on necked crust that transitions into hyper-extended crust. Salt structures suggest a thin, original, autochthonous layer. Autochthonous salt ends sharply against a zone of SDR's that become normal oceanic crust basinward. The Jurassic section deposited on top of the SDRs is thin.
- Abenaki Nose: Around this salient, salt is present in a wide zone with structures suggesting a thick original autochthonous layer in the deepest parts of the basin. The west side of the nose is defined by a NW-SE lineament. Immediately west of the lineament crustal domains progressed basinward from necked to hyper-extended to oceanic crust. An exhumed domain is not observed. East of the lineament crustal domains progressed from necked to hyper-extended to exhumed to oceanic crust. This area is covered by 3D seismic and the transition between domains is well imaged. The Jurassic section interpreted in both areas is thick. The earliest part of the Jurassic is thicker to the east of the Abenaki Nose, in the region of hyper-extended and exhumed domains.
- East of Abenaki Nose: Salt is present to the north within the Orpheus Graben and basinward ends sharply where it launches as a canopy to form the Banquereau Synkinematic Wedge. There is no autochthonous salt under the wedge. Crustal domains transition from necked, to hyper-extended, to exhumed under the wedge and finally to normal oceanic crust. The transition between hyper-extended crust and exhumed mantle is marked by a step-up basinward (where the canopy is launched). The transition between exhumed mantle and oceanic crust is also marked by a step-up basinward. Observations suggest that the SDRs to the west and the exhumed domain to the east of the nose were formed after salt deposition by two different processes reflecting two different opening/spreading rates.

Observation in crustal evolution portray a complex opening history for this part of the margin. Crustal architecture and associated changes in dominant crustal rock type resulted in changes in isostatic expression which



manifested themselves as changes to the developing paleo-bathymetry. The evolving basin architecture controlled sediment entry points, which in-turn responded to paleo-bathymetry. Loading of sediment, into basins which had previously been loci of salt deposition, resulted in the development of discrete sediment fairways. Detailed mapping within the Jurassic stratigraphy offers insights into how these complex salt basins developed in response.

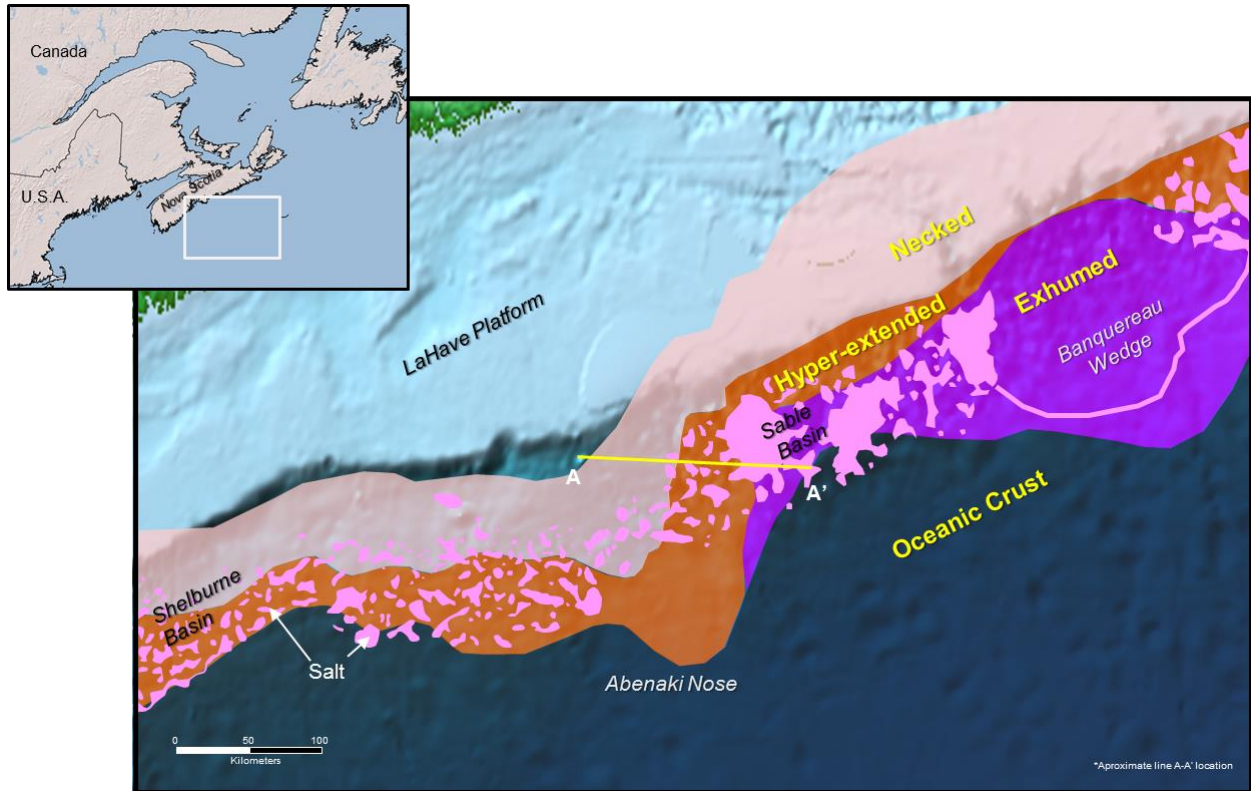


Figure 1. Area of Study. Map shows the distribution of crustal elements in the area (necked, hyper-extended, exhumed and oceanic crust) as well as the distribution of salt structures.

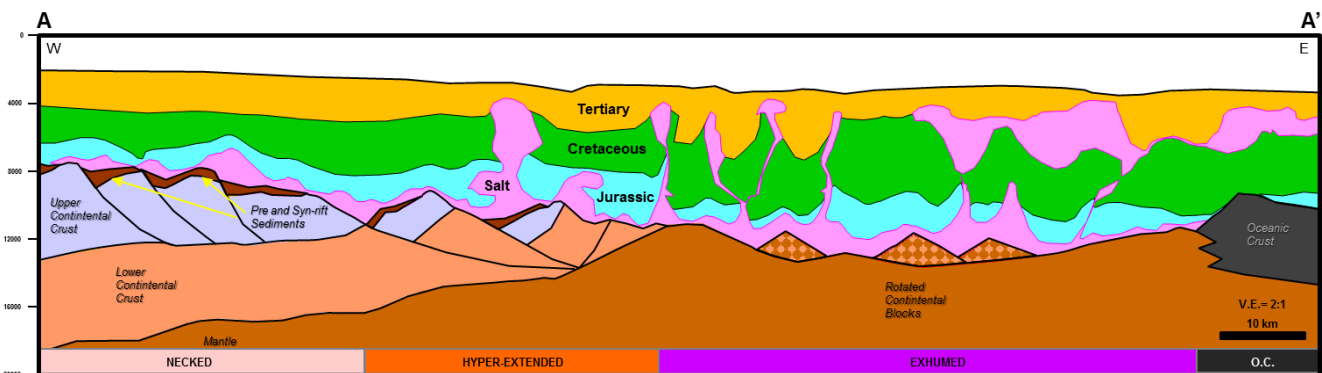


Figure 2. Cross-section oriented East-West across the Abenaki Nose (see figure 1 for approximate location) showing the interpreted crustal structure and the stratigraphic packages.



HYDROCARBON AND AQUEOUS FLUID INCLUSION SIGNATURES IN WELL CUTTINGS FROM NEWFOUNDLAND AND LABRADOR OFFSHORE BASINS

Costanzo, Alessandra¹, Hunt, J.¹, Feely, M.¹, Wilton, D.H.², and Norris, D.³

¹ Earth and Ocean Sciences, School of Natural Sciences, National University of Ireland, University Road, Galway LL32 8FA, Ireland, Alessandra.costanzo@nuigalway.ie

² Department of Earth Sciences, Memorial University of Newfoundland, St. John's, NL A1B 3X5 Canada

³ Nalcor Energy Limited, 500 Columbus Drive, St. John's, NL A1B 0C9, Canada

The offshore basins of Newfoundland and Labrador are part of a series of conjugate sedimentary basins formed by the rifting and seafloor spreading that began in the Late Triassic, leading to the opening of the Atlantic Ocean. Basins of this study contain kilometric scale sequences of Upper Jurassic to Tertiary sediments and form part of a system of basins extending from the southeastern USA to the north of Baffin Bay off southwest Greenland. Rifting occurred from south to north with the oldest (Late Triassic/Early Jurassic) in the south and the youngest (Lower Cretaceous) in northeast Newfoundland and Labrador Sea.

Fluid signatures of quartz-hosted fluid inclusions were obtained from 167 samples of well cuttings collected from seven wells in the Newfoundland and Labrador offshore basins. The sampled wells (C-NLOPB well No.) and their respective basins are:

- Saglek Basin, Labrador Shelf: Gilbert F-53 (No.64), Skolp E-07 (No.55), and Ogmund E-72 (No.70)
- Hopedale Basin, Labrador Shelf: Snorri J-90 (No.47) and Herjolf M-92 (No.53)
- East Orphan Basin, NE Newfoundland Shelf: Margaree A-49 (No.384)
- South Whale Basin, Grand Banks Shelf: Lewis Hill G-85 (No.283)

Five fluid inclusion types (aqueous and hydrocarbon fluids) were recognised: Type 1, Type 2 and Type 3 are aqueous fluid inclusions, pseudosecondary to secondary in origin and occur in all wells. Type 4 and Type 5 are hydrocarbon-bearing fluid inclusions that are either primary, pseudosecondary, or secondary in origin. They are present in some samples from the Gilbert, Herjolf and Margaree wells. Ultra-violet (UV) light microscopy of the hydrocarbon-bearing fluid inclusions reveal an API gravity range from ca. 30°–35° (yellow/green fluorescence; Margaree A-49) to 45°–50° (blue/white fluorescence; Gilbert F-53 and Herjolf M-92) suggesting the trapping of medium to light oils.

Type 1 two-phase (Liquid+Vapour=L+V; L>V) aqueous fluid inclusions predominate in all well samples. They generally homogenise to the liquid phase between 60°C and 150°C and have low to moderate salinities (<10 eq.wt.% NaCl). However, two sub-populations (Population A and Population B) of Type 1 fluid inclusions, defined by differing T_H values (Population A: 80°C to 120°C; Population B: 120°C to 160°C), occur in the Saglek Basin (Skolp E-07), the Hopedale Basin (Snorri J-90 and Herjolf M-92) and the East Orphan Basin (Margaree A-49). Most of the well samples have either the high-T or the low-T population present. These fluid temperature differences reflect temperature changes during basin development. High salinity (~20 eq.wt.% NaCl) Type 1 fluids are uncommon and were only recorded in the samples from the Saglek and Hopedale Basins. Similar temperatures recorded from Type 1 and Type 5 fluid inclusions present within the Gilbert F-53 well may indicate a coeval trapping relationship between these two fluids. FIT-Oil generated isochores for the Type 5 together with the Type 1 fluid isochore indicates oil and aqueous fluid trapping pressures ranging between ca. 380 and 460 bars at temperatures of ca. 110° C.



Introduction

Fluid inclusions (FI) represent fluids (hydrocarbons and water) trapped either during cementation, or later, as fluids migrated through and interacted with host rocks during the evolution of a sedimentary basin. Studies of aqueous FI and hydrocarbon-bearing FI (HCFI) can facilitate the reconstruction of the P-T-x (pressure, temperature and fluid compositions) conditions associated with petroleum systems in oil prospective offshore basins (Roedder, 1984; Shepherd et al., 1985; Goldstein and Reynolds, 1994; Hurai et al., 2015). In other words, FI studies are critical to the understanding of petroleum migration and accumulation.

We report the results of FI studies conducted on 167 cuttings samples from seven exploration wells from the following basins: a) Labrador Shelf - Saglek Basin (61 samples from two wells) and Hopedale Basin (81 samples from three wells), b) Northeast Newfoundland Shelf - East Orphan Basin (13 samples from one well), and c) the Grand Banks Shelf - South Whale Basin (12 samples from one well) (**Figure 1**). The samples are from Upper Jurassic to Lower Cenozoic horizons.

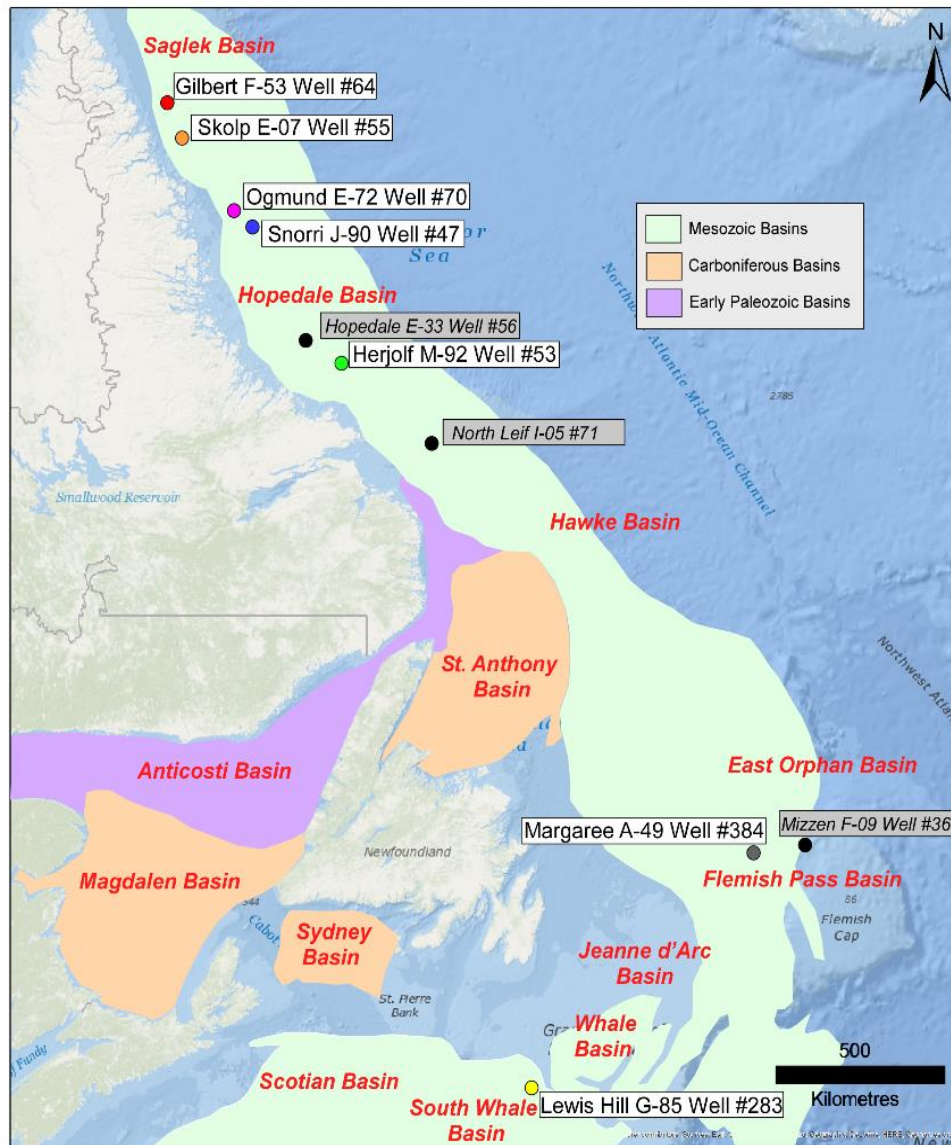


Figure 4. Location of the wells investigated in this study. Ten wells were sampled initially but three contained unsuitable material for fluid inclusion studies. These wells are shaded in grey above. Basin locations are after Enachescu (2006).



Materials and Methods

One hundred and sixty-seven doubly polished fluid inclusion wafers (ca. 100–150µm thick) were prepared at petrographic thin section preparation laboratories in the UK (InRock, ALS Petrophysics and British Geological Survey) and the USA (Wagner Petrographic). The wafers were then subjected to fluid inclusion analyses in the Geofluids Research Laboratory, National University of Ireland Galway. A paragenetic classification of the fluid inclusions was developed using transmitted light microscopy. Samples were then examined using UV light microscopy (Nikon Eclipse E200 microscope with an epifluorescence attachment) to determine the presence of hydrocarbon bearing fluid inclusions. The fluorescence colour emitted by hydrocarbon bearing FI in UV light is related broadly to API gravity (George et al., 1997, 2001; Bodnar, 1990). Microthermometric analyses were performed on the wafers using a Linkam THMGS 600 heating-freezing stage, mounted on an Olympus BX51 transmitted light microscope. The microscope is equipped with several special extra-long working distance objective lenses ranging up to 100 times magnification. Calibration of the stage was performed using synthetic fluid inclusion standards (pure CO₂ and water). Precision is ± 0.2°C at -56.5°C and ± 2°C at 300°C.

Results

Five fluid inclusion types were recorded: Types 1, 2, and 3 are aqueous FI that are pseudosecondary to secondary in origin and occur in all wells. Types 4 and 5 are HCFIs that are either primary, pseudosecondary, or secondary in origin. They are present in several samples from the Gilbert, Herjolf and Margaree wells (see Table 1). The general distribution of each type is summarised in **Figure 2** and **Table 2** shows the distribution of each type across the suite of well samples.

Table 1. Classification of fluid inclusions.

TYPES	1	2	3	4	5
PHASES PRESENT	L + V (L>V)	L	L + V + S	L	L + V (L>V)
LIQUID COMPOSITION	aqueous	aqueous	aqueous	HC*	HC
SIZE	3-20µm	2-10µm	5-15µm	2-15µm	5-20µm
OCCURRENCE	Detrital quartz	Detrital quartz	Detrital quartz	Detrital quartz	Detrital quartz
DISTRIBUTION	Trails, clusters	Trails, clusters, dust rings	Trails, isolated	Trails	Trails, isolated
UV FLUORESCENCE COLOUR	-	-	-	Blue	Blue

*Includes HCFI observed in dust rings in Margaree A-49 Well #384 that are irresolvable using transmitted light microscopy.

L=liquid, V=vapour, S=solid, HC=hydrocarbon.

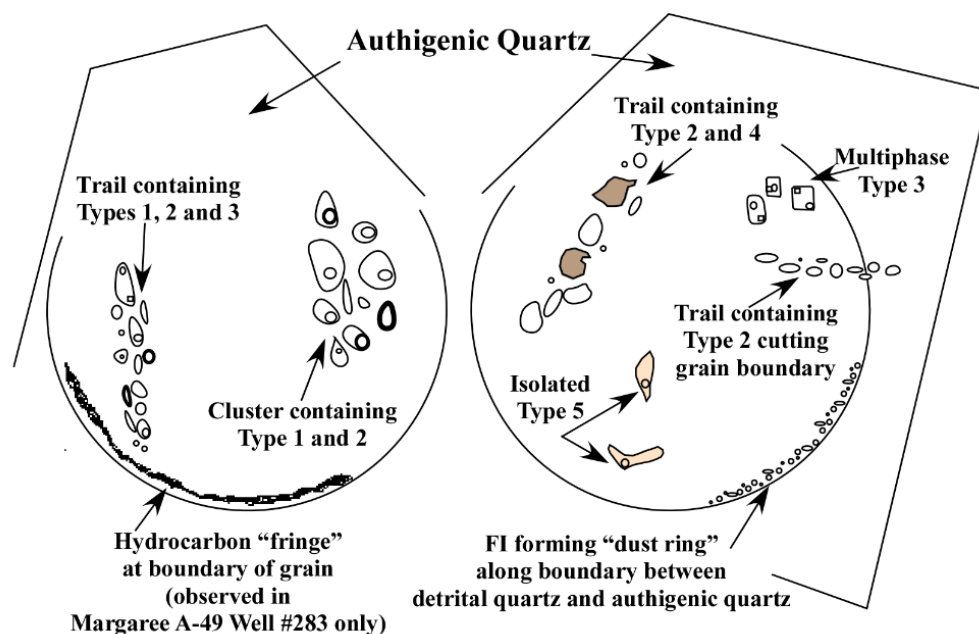


Figure 2. Schematic representation of the occurrence of each FI type.

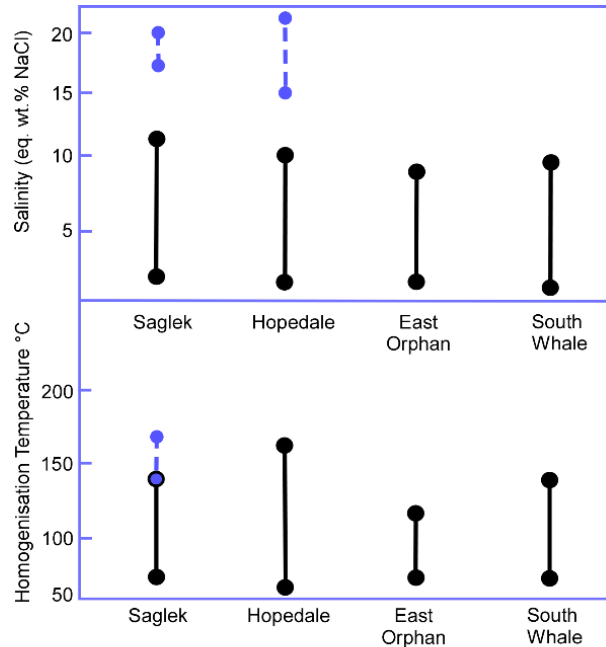
Table 1. Fluid Inclusion Types observed in each of the seven wells.

Shelf	Basin	Well	FI Type				
			1	2	3	4	5
			Aqueous			HCFI	
Labrador	Saglek	Gilbert F-53	X	X	X	X	X
		Skolp E-07	X	X	X	-	-
	Hopedale	Ogmund E-72	X	X	X	-	-
		Snorri J-90	X	X	X	-	-
		Herjolf M-92	X	X	X	X	X
Northeast Newfoundland	East Orphan	Margaree A-49	X	X	X	X	-
Grand Banks	South Whale	Lewis Hill G-85	X	X	X	-	-

Type 1 are the most common type found in all samples. They are two-phase (L+V; L>V) aqueous inclusions (~10µm) occurring in trails that cross-cut detrital quartz grains. They are pseudosecondary to secondary in origin and predominate in all samples. They are consistently of low to moderate salinity (~ <10 eq. wt.% NaCl; **Figure 3**). This salinity range is comparable to that found elsewhere on the Atlantic margins (e.g. further north in the UK Rockall and in the West of Shetland region; see Parnell et al. (1999)] and the Jeanne d'Arc Basin offshore Newfoundland (Parnell et al., 2001). Type 1 fluid inclusions have low to moderate T_H values (<150°C) indicative of basinal fluids. However, within the overall Type 1 population two sub-populations of Type 1 fluid inclusions, defined by differing T_H values (high-T and low-T, occur in the Saglek Basin (Skolp E-07), Hopedale Basin (Snorri J-90 and Herjolf M-92) and the East Orphan Basin (Margaree A-49). Most of the well samples have either the high-T or low-T population present. Furthermore, there are no correlations between these T-based populations and sample depth. These fluid temperature differences may reflect cyclical temperature



changes during basin development. High salinity (~20 eq.wt.% NaCl) Type 1 fluids are uncommon and were recorded only in the Saglek and Hopedale Basins. Type 3 solid bearing aqueous fluid inclusions recorded in all wells may also indicate trapping of high salinity fluids.



Microthermometry of Type 1 Aqueous Fluids

Figure 3. T_H and salinity ranges of Type 1 fluids from the four basins. The blue bars reflect the relatively high salinities (Saglek and Hopedale basins) and temperatures (Saglek Basin) that have been recorded during microthermometry.

Type 2 are monophasic (liquid) aqueous inclusions that occur in trails cross-cutting detrital quartz grains. They are pseudosecondary to secondary in origin and occur in all samples. They indicate fluid trapping temperatures of $<50^\circ\text{C}$ (Goldstein and Reynolds, 1994) and record low-T migration of aqueous fluids.

Type 3 are three phase (L+V+S) aqueous FI that occur in trails commonly and are secondary in origin. They occur in all wells and have temperatures of homogenisation between 100°C and 160°C like the high temperature Type 1 population. The presence of halite reflects high salinity fluid migration during basin evolution.

Type 4 are monophasic liquid HCFIs and occur as either isolated individuals or along microfractures. They are either secondary or pseudosecondary in origin. They were recorded in samples from Gilbert F-53, Herjolf M-92 and Margaree A-49 wells.

Type 5 are two-phase liquid rich (L+V; $L>V$) HCFI. They are pseudosecondary in origin. They yield homogenisation temperatures (to the L phase) from $\sim 75^\circ\text{C}$ to 86°C in a sample from the Gilbert F-53 well. Similar temperatures recorded from Type 1 FI present within this well may indicate a coeval trapping relationship between these two fluids (**Figure 4**). FIT-Oil generated isochores for the Type 5 together with the Type 1 fluid isochore (using FLUIDS™ software, Bakker, 2003) indicates oil and aqueous fluid trapping pressures ranging from ~ 380 bars to 460bars at temperatures of $\sim 110^\circ\text{C}$ (**Figure 4**).

Finally, it should be noted that HCFIs were recorded in samples from the Gilbert F-53, Herjolf M-92, and Margaree A-49 wells where they occur in trails indicative of hydrocarbon migration. API gravities in the range 40° - 50° (blue-white fluorescence) characterise the HCFIs in samples from Gilbert F-53 and Herjolf M-92, and the Margaree A-49 samples have API gravities of 30° to 35° (yellow-green fluorescence).

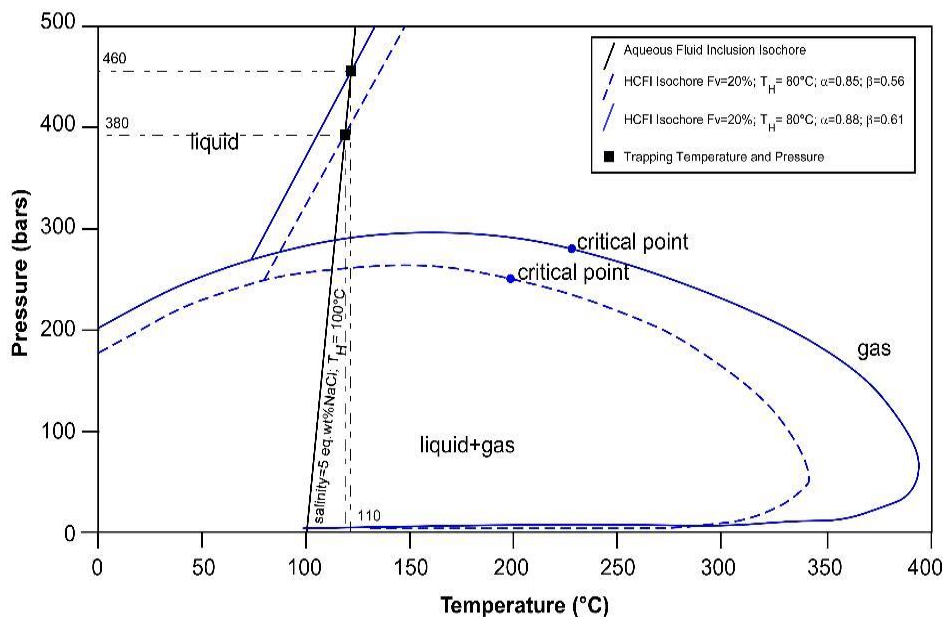


Figure 4. FIT-Oil generated isochores for the HCFI observed in Gilbert F-53 Well #64. The isochores are generated after the method outlined in Thiéry et al., (2000). The critical point (the bubble point), which appears on each of the two hydrocarbon phase envelopes, mark the phase change from liquid to gas. Fluids trapped above the critical point are referred to as supercritical fluids (neither gas nor liquid).

Conclusions

The recorded range of T_H values from aqueous and hydrocarbon bearing fluid inclusions in sandstone samples recovered from basins across the world (Walderhaug 1994; i.e. India, Canada, Gabon, North Sea, and Mid-Norway) are displayed in **Figure 5A**.

The range of T_H values for two-phase aqueous inclusions are similar in range to those recorded from the Type 1 FI in this study. Similar T_H values for HCFI across global basins are also indicated (Figure 5a and 5b). Furthermore, **Figure 5B** compares T_H ranges for Type 1 and Type 5 fluid inclusions with data recorded by Feely and Parnell (2003) and Conliffe et al. (2010) from the Irish offshore massif (i.e. Porcupine Basin). These plots reflect the relatively narrow range of fluid trapping temperatures that have been recorded across a global sample of oil prospective basins.

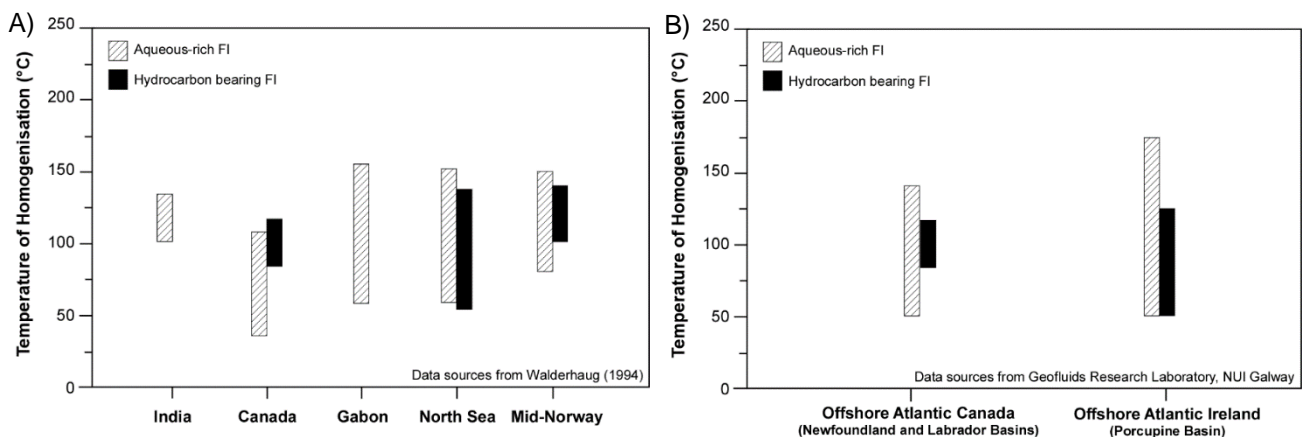


Figure 5. A) Temperature of homogenisation of aqueous and hydrocarbon bearing fluid inclusion studies from across the world. B) Temperature of homogenisation of aqueous and hydrocarbon bearing fluid inclusion studies from the North Atlantic. Data for the Porcupine Basin are from Feely and Parnell, (2003), and Conliffe et al., (2010).



Acknowledgements

The fluid inclusion studies of the Labrador and Newfoundland offshore basins are funded by the Offshore Geoscience Data Program (OGDP) jointly administered by Nalcor Energy Oil and Gas, and the Department of Natural Resources, Government of Newfoundland and Labrador.

References

- Bakker R.J., 2003. Clathrates: computer programs to calculate fluid inclusion V-X properties using clathrate melting temperatures. *Computers and Geosciences* **23**(1), 1-18.
- Bodnar R.J., 1990. Petroleum migration in the Miocene Monterey formation, California, USA: constraints from fluid inclusion studies. *Mineralogical Magazine*, **54**, 295-304.
- Conliffe, J., Feely, M., Parnell, J., and Ryder, A., 2010. Hydrocarbon migration in Jurassic sandstones from the Porcupine Basin, offshore Ireland: evidence from fluid inclusion studies. *Petroleum Geoscience*. **16**(1), 67-76.
- Enachescu, M., 2006. Favorable Geology, advanced technology may unlock Labrador's substantial resource. *Exploration and Development. Oil and Gas Journal*, **104**, 29-34.
- Feely, M., and Parnell, J., 2003. Fluid inclusion studies of well samples from the hydrocarbon prospective Porcupine Basin, offshore Ireland. *Journal of Geochemical Exploration*, **78-79**, 55-59.
- George, S.C., Krieger, F.W., Eadington, P.J., Quezada, R.A., Greenwood, P.F., Eienberg, L.I., Hamilton, P.J., and Wilson, M.A. 1997. Geochemical comparison of oil-bearing fluid inclusions and produced oil from the Toro sandstone, Papua New Guinea. *Organic Geochemistry*, **26**(3), 155-173.
- George S.C., Ruble, T.E., Dutkiewicz, A., and Eadington, P.J. 2001. Assessing the maturity of oil trapped in fluid inclusions using molecular geochemistry data and visually determined fluorescence colours. *Applied Geochemistry*, **16**(4), 451-473.
- Goldstein, R.H., and Reynolds, T.J., 1994. Systematics of Fluid Inclusions in Diagenetic Minerals. *SEPM Short Course*, **31**, 199p.
- Hurai, V., Huraiova, M., Slobodnik, M., and Thomas, R., 2015. *Geofluids – Developments in Microthermometry, Spectroscopy, Thermodynamics and Stable Isotopes*. Elsevier Press. ISBN: 978-0-12-803241-1.
- Parnell, J., Carey, P.F., Green, P., and Duncan, W., 1999. Hydrocarbon migration history, west of Shetland: Integrated fluid inclusion and fission track studies. In: A.J. Fleet and S.A.R. Boldy (eds.), *Geological Society, London, Petroleum Geology Conference Series*, **5**, 613-625.
- Parnell, J., Middleton, D., Chen, H., and Hall, D., 2001. The use of integrated fluid inclusion studies in constraining oil charge history and reservoir compartmentation: examples from the Jeanne d'Arc Basin, offshore Newfoundland. *Marine and Petroleum Geology*, **18**, 535-549.
- Roedder, E., 1984. Fluid Inclusions. *Mineralogical Society of America, Reviews in Mineralogy*, 12: 644.
- Shepherd, T.J., Rankin, A.H., and Alderton, D.H.M., (1985). *A practical guide to fluid inclusion studies*. Glasgow and London, Distributed in the USA by Chapman and Hall, New York.
- Thiéry, R., Pironon, J., Walgenwitz, F., and Montel, F., 2000. PIT (Petroleum Inclusion Thermodynamic): a new modelling tool for the characterization of hydrocarbon fluid inclusions from volumetric and microthermometric measurements. *Journal of Geochemical Exploration*, **69-70**, 701-704.
- Walderhaug, O., 1994. Temperatures of quartz cementation in Jurassic sandstones from the Norwegian continental shelf; evidence from fluid inclusions. *Journal of Sedimentary Research*, **64**(2a), 311-323.





SALT SEDIMENT INTERACTION IN THE CENTRAL BASIN OF THE NOVA SCOTIA PASSIVE MARGIN, OFFSHORE EASTERN CANADA.

Decalf, Carole C.¹, Bondurant, Charles H.¹, and Bunting, Philip¹

¹ BP, 225 Westlake Park Boulevard, Houston, TX 77079, USA, Carole.decalf@bp.com

On the passive margin of Nova Scotia (offshore Eastern Canada), salt tectonics play a significant role regarding the occurrence of trapped hydrocarbons. Latest Triassic salt deposition and its subsequent movement influenced the structural framework and the sediment distribution along the margin since the last 200 Ma. Complex tectonic activities and the concurrent development of major delta systems influenced the distribution, timing, and style of potential hydrocarbon-bearing structures and inherent reservoir intervals on the paleo-slope especially during the Jurassic and Cretaceous time range.

In the Scotian Basin, the Triassic Argo (salt) Formation is interpreted to be late synrift to possibly earliest post-rift in age (Wade and MacLean, 1990). Its deposition, thickness, and potentially also its composition varies from the northeastern to the southwestern part of the Scotian Basin depending on the original rift structure and orientation (Ings and Shimeld, 2006). Allochthonous salt canopies initiated as early as Middle to Late Jurassic in the Banquereau synkinematic wedge and are interpreted to appear at a later stage in the central part of the margin.

Recently, modern 3D wide azimuth towed streamer (WATS) seismic survey acquisition data over an area of approximately 7,000 km², was processed with latest techniques such as reflection full waveform inversion (FWI). This process generated a major uplift in the imaging and resulted in better definition of the salt structure in the central basin. It supports the view that the Argo salt experienced early deformation and allochthonous canopy emplacement by Middle to Late Jurassic not only in the eastern but also in the central part of the basin. Following this is a period of active diapirism responding to Cretaceous sediment loading, and a subsequent final shallow canopy formation by Late Cretaceous time.

Additionally, seismic facies observations correlated between salt minibasins within a stratigraphic framework and tied with sparse well control, provides a better understanding of the sediment deposition between the paleo-salt highs, especially in the central part of the Scotian Basin but also all along the wider passive margin.

This study proposes an integrated approach on salt deformation and sediment interaction using the latest 3D seismic processing technology as well as Moroccan outcrop analogues to understand better the distribution and evolution of the salt. It identifies and discusses various salt trap domains and their implication on sediment transport in the Central Scotian Basin of Nova Scotia.

Introduction

On the passive margin of Nova Scotia, offshore Eastern Canada, salt tectonics play a significant role regarding the occurrence of trapped hydrocarbons. Late Triassic salt deposition and its subsequent movement influenced both the structural framework and sediment distribution along the margin for the last 200 Ma. Complex tectonic activities and the concurrent development of major Cretaceous delta systems influenced the distribution, timing, and style of potential hydrocarbon-bearing structures and inherent reservoir intervals on the paleo-slope especially during the Jurassic and Cretaceous timeframe.

In the Scotian Basin, the Triassic Argo salt is interpreted to be late synrift to earliest post-rift in age (Wade and MacLean, 1990). Salt deposition, thickness and potentially its composition varies from the eastern to the southern part of the Scotian margin depending on the original rift structure and orientation. Allochthonous salt



canopies initiated as early as Middle to Late Jurassic in the Banquereau Synkinematic Wedge (BSW) and are interpreted to appear at a later stage in the central part of the margin (Ings and Shimeld, 2006) (Figure 1).

This study proposes an integrated approach on salt deformation and sediment interaction using the latest 3D seismic processing technology as well as Moroccan outcrop analogues to better understand the distribution and evolution of the salt.

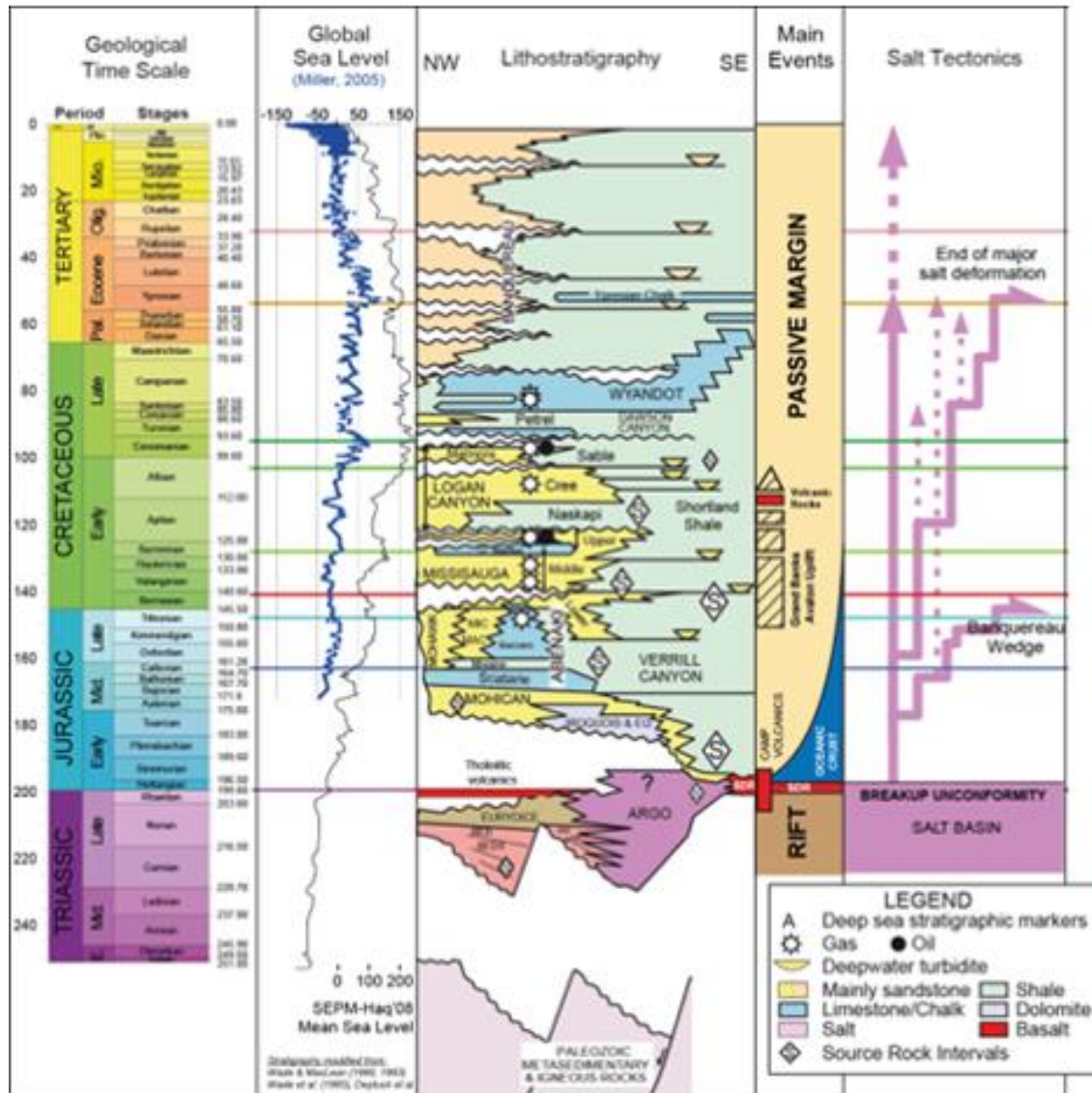


Figure 1. Chronostratigraphy of the northern part of the Scotian Basin (OETRA, 2011). The Argo salt is deposited during the late phase of the Triassic rifting and deformed through Jurassic (BSW) to Early Tertiary.

Seismic Acquisition and Processing

In 2015, BP launched a modern 3D wide azimuth towed streamer (WATS) seismic acquisition program over an area of approximately 7,000 km². The Tangier survey is located across the four license blocks acquired by BP in 2014. About 350 TB of seismic data was acquired in multi-azimuth with high fold coverage to handle complex salt geology. After the initial phase of regional processing, BP and their partners initiated a complex seismic processing “enhancement” phase allowing for the latest seismic processing techniques to be applied.



One important process resulting in the successful imaging of the area of interest was the interaction between tomography and the latest reflection full waveform inversion (RFWI) technique. This processing step introduced a major imaging uplift resulting in more well defined geologic and salt structures in the central basin. Even the upper/lower crust and Mohorovičić (Moho) discontinuity was imaged and had flat gathers.

Results and Discussion

The Tangier 3D seismic revealed a relatively well-imaged Moho reflector beneath the extended and hyperextended crust. It appears to be climbing up from northeast to southwest towards the basement with the presence of an interpreted mid-crustal boundary reflector. The Moho reflector is shallowest in the southern part of the 3D coverage area where it reaches a depth of less than 12 km. Continental crust is less than 2 km thick at this location. This elevated Moho geometry and thin crust suggests the creation of a rift that failed but was eventually successful further outboard. To the south of the failed rift, the distinction between lower and upper crust is challenging, suggesting that the lower crust might not be present. On this southern side, we also observed high amplitude discontinuous (“broken”) reflectors that are located at the top of the basement reflector composed mainly of horst blocks. We suggest these volcanic events were deposited synrift and then overlain by Argo salt at the end of rifting, similar to the conjugate margin of Morocco. Volcanics in this stratigraphic interval are confirmed on the adjacent LaHave Platform only within Glooscap G-63 well northwest of the Tangier area (MacLean and Wade, 1993). Deptuck and Kendell (2017) discuss their regional relationship with Argo Formation salts.

Contrary to the southern side of the failed rift, the northern side has a well-imaged crust and seaward dipping faults that appear sole into the mid crustal boundary. The fairly well imaged synrift sequence appears to be filled with sediments, perhaps the same Triassic clastics as seen (and penetrated by wells) on the shelf (Figures 1 and 2). Argo salt appears to be deposited at the late stage of the Triassic rift and could be interbedded with clastics and volcanics. Salt deformation style varies from east to west, but also inboard to outboard of the “failed rift”.

Mohorovičić discontinuity interpretation

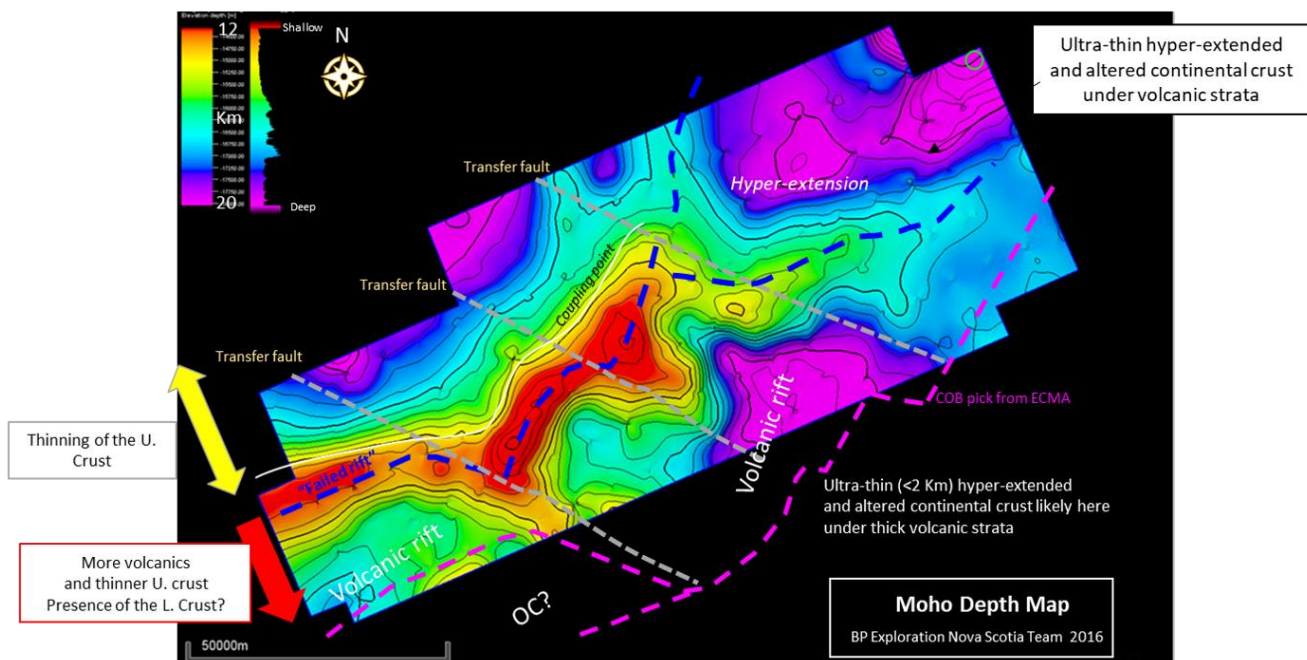


Figure 2. Interpretation of the Mohorovicic discontinuity over the Tangier 3D seismic showing the failed rift location and the hyper-extended domains.



Within the Tangier 3D survey area, we observe a basement structural inheritance influencing salt deposition:

1) In the southern part, north of the failed rift, the salt is relatively thin and forms salt pillows, whereas south of the failed rift, the salt formed salt walls and locally, completely infilled the failed rift grabens (salt diamond shape).

2) In the northern portion, the salt forms diapirs and canopies. Central Scotian Basin salt has similar deposition, geometries, and deformation as the Moroccan salt basin that extends from the Talfeney Plateau to the onshore, including the Essaouira Basin and the Taфраout Diapir in the Atlas Mountains (Tari et al., 2012).

We interpret local basement highs and rotated fault blocks, combined with sediment loading from the Jurassic and Cretaceous, provided launching points for Argo salt deformation. In the central part of the Scotian Basin, the Argo salt has experienced an early phase of deformation and allochthonous salt canopy formation initiated by Mid to Late Jurassic, comparable to the BSW formation time frame. Jurassic salt canopies are mostly present in the Sable Subbasin canopy area where they formed near deep-buried grabens. The Early Jurassic canopy was followed by a period of active salt diapirism responding to Cretaceous sediment loading (Sable Delta; Mississauga, Logan Canyon formations) with subsequent shallow canopy formation in the Tertiary (**Figure 3**).

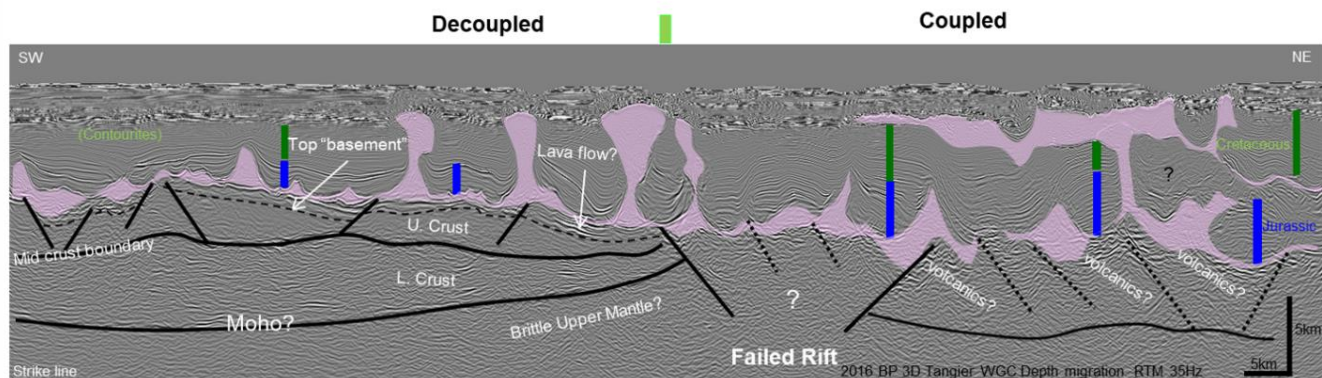


Figure 3. Strike line across BP License blocks showing the a) failed rift, b) mid-crustal boundary and moho reflectors c) the salt deformation style and d) interpreted volcanic events.

Conclusions

The acquisition, processing and interpretation of this high-resolution 3D seismic has allowed us to investigate the crustal domain as well as the impact basement had on salt deposition and deformation in the central part of the Scotian Basin. We observed a genetic link between salt deposition and deformation with basement morphology.

- The Argo salt increases in thickness where the basement is deeper, and the continental crust is highly extended.
- Several salt domains are identified coinciding with differences in basement versus “failed rift” structures. While the eastern area is defined as a complex salt-tongue canopy with multiple Jurassic and Cretaceous canopy levels, the southwestern area is dominated by simpler diapir and salt pillow structures. Salt wall and complex canopies on the south side of the failed rift show the maturity of the salt deformation moving seaward
- There is seismic evidence in the reflectivity on the top of the basement suggesting volcanic intervals could be extended to the central portion of the Scotian Basin (**Figures 2 and 3**).
- Finally, the central part of the Nova Scotia salt basin presents similarities with its Moroccan conjugate in deposition and emplacement.



Acknowledgments

The authors would like to thank Hess, our partner in the license blocks for good seismic discussion and brainstorming sessions. We also recognize BP Nova Scotia Team, H. Liu from Seismic Delivery Team, and T. Heyn and J. Evenick from Regional Team. Finally, we would like to thank BP for permission to share this work. Thanks also go to D. Steinhoff and J. Evenick for editing this article.

References

- Deptuck, M.E., and Kendell, K.L., 2017. A review of Mesozoic-Cenozoic salt tectonics along the Scotian Margin, Eastern Canada (Chapter 13). In: J.I. Soto, J. Flinch, and G.C. Tari (eds), *Permo-Triassic Salt Provinces of Europe, North Africa and the Atlantic Margins – Tectonics and Hydrocarbon Potential*, Elsevier, Amsterdam, 287-312.
- Ings, S.J., and Shimeld, J.W., 2006. A new conceptual model for the structural evolution of a regional salt detachment on the northeast Scotian margin, offshore eastern Canada. *American Association of Petroleum Geologists Bulletin*, **90**(9), 1407-1423.
- MacLean, B.C., and Wade, J.A., 1993. Seismic Markers and Stratigraphic Picks in the Scotian Basin Wells. East Coast Basin Atlas Series, Geological Survey of Canada, 276 p.
- Offshore Energy Technical Research Association (OETRA), 2011. Scotian Basin Play Fairway Analysis Study. [http://www.oera.ca/offshore-energy-research/geoscience/play-fairway-analysis/Play Fairway Analysis-atlas/](http://www.oera.ca/offshore-energy-research/geoscience/play-fairway-analysis/Play%20Fairway%20Analysis-atlas/)
- Tari, G.C., Brown, D.E., Jabour, H., Hafid, M., Loudon, K., and Zizi, M., 2012. The conjugate margins of Morocco and Nova Scotia. In: D.G. Roberts and A.W. Bally (eds), *Regional Geology and Tectonics: Phanerozoic Rift Systems and Sedimentary Basins – Volume 1C – Passive Margins*. Elsevier, Amsterdam, 265-300.
- Wade, J.A. and MacLean, B.C., 1990. Chapter 5 - The geology of the southeastern margin of Canada, Part 2: Aspects of the geology of the Scotian Basin from recent seismic and well data. In: M.J. Keen and G.L. Williams (eds), *Geology of Canada No.2 - Geology of the continental margin of eastern Canada*. Geological Survey of Canada, 190-238 (also Geological Society of America, *The Geology of North America*, Vol.I-1).
-





A CONTINENTAL-SCALE DELTA'S EFFECT ON THE NORTH END OF A JURASSIC-CRETACEOUS GIGAPLATFORM: THE ABENAKI CARBONATE-SABLE DELTA STUDY A DECADE OR SO LATER, OFFSHORE NOVA SCOTIA

Eliuk, Leslie S.¹

¹GeoTours Consulting Inc., Box 852, Lunenburg NS, B0J 2C0, Canada, leslie.eliuk@gmail.com

My study was to describe and understand the strange relationship of a thick extensive carbonate platform co-existing for a long time (15 Ma) beside a continental-scale delta. After finding no analogues in the modern world oceans but some interesting examples of reefs in or near deltas, an explanation was proposed to address two questions with the results not wholly convincing for the first and more satisfactory for the second.

1. Morphology, nature and origin of a big delta/thick carbonate platform juxtaposition and lateral ramp carbonates. A bathymetric 'Gap' best explains the systems' juxtaposition with their very different styles of carbonates. This interpretation is supported by vintage seismic data and the nature of the transition shown in well sections and cores. More work can be done using newer and better seismic data sets, and by considering with modelling the effect of deltaic sediment loads on creating a lateral moat and potential compensatory distal highs. Another possible control in the modern is favourable ocean currents but not easily proved in the ancient.

2. Possible lateral effects on platform margin carbonates due to proximity of deltaic sedimentation depends on location and can be nearly non-existent within the platform, subtle on the slope and profound, long continued and variable on the top during the expansion of the delta. This explanation is supported by the presence of rare, thin quartz sandstone beds or oolite nuclei on the main platform, the increasing influence of slope onlap prodelta shales, and some lateral changes in slope carbonates. There are also wholesale reef mound community changes at top of the Abenaki succession, but without presence of coarse terrigenous clastics. Further features such as common reworked microfossils, Neptunian dykes, and condensed marine redbeds indicate that the distal sedimentary section may be more gap than record with both submarine and subaerial hiatuses even including suspect mixing zone dolomite. There seems to be a consistent diachronous relationship to prodeltaic siliciclastic, sponge-rich, and marine redbed successions.

Imperfect modern analogues. The world's longest modern coral reef tract, Australia's Great Barrier Reef, ends in the Fly River Delta of the Gulf of Guinea (Tcherepanov et al. 2008, 2010). The world's largest river, Brazil's Amazon, has a long, narrow but cryptic reef tract on the edge of its wide continental shelf (Moura et al. 2016). While not platforms, these modern examples give insight into the deltaic termination of the Phanerozoic's longest carbonate platform.

Introduction

Note: **Table 1** is a list of cores used in this thesis and particular ones shown in the Halifax 2018 CMC Core Workshop at the Canada-Nova Scotia Offshore Petroleum Board's Geoscience Research Centre (CNSOPB-GRC, Dartmouth, NS). These demonstrate the changes in carbonate facies particularly near the top of the Abenaki Formation resulting from the progressive enlargement of the Sable Delta over time.

Figure 1A illustrates simplified stratigraphic columns of the Scotian Basin versus the northern Gulf of Mexico, and **Figure 1B** a schematic map of the eastern seaboard of North America in the Late Jurassic. Together they are used to contrast the two major deltaic areas at either end of the world's longest Phanerozoic reef-tract carbonate platform – Poag's (1991) gigaplatfrom. These continental-scale deltas are of very different ages and even extent. **Figure 2** shows the wells and general facies relations of the Abenaki carbonate platform and the Sable



Island delta in the Late Jurassic. **Figure 3** schematic shows controls that are often used to explain or allow two, typically inimical, major sediment groups – siliciclastics and carbonates (deltas and carbonate platforms) - and very different complexes of depositional environments to coexist.

Table 1: ABENAKI FORMATION REEFAL (margin-slope) CORE
(Baccaro, Artimon and Roseway members; MicMac Formation limestones)

WELL	CORE # ('reefal')	CORE INTERVAL (original units)	FACIES NUMBERS	COMMENTS
West Venture C-62	12,13	<5255-5276.5 m	3C/4B in 8	thin shoaling facies - thrombolitic to coral-sponge reef mound
South Desbarres O-76	1,2	3799-3827 m	8 (reeflet 5B)	Smallest coral reeflet in bottom of marine deltaic channel (~15cm)
Penobscot L-30	1	11231-11269 feet	5D(5A/B/C)	minor thin layers corals-chaetetics amongst oolite
	2	13285-13316 feet	1/3C	slope stromatactis-thrombolitic/microbial 'mud' mound-depauparate
Cohasset L-97	1	3407-3426 m	5B(?3B)	very large in situ corals (complicated diagenetic overprint)
Margaree F-70	1	3434-3458.6 m	5B, 3B, 4B (3C?) pinnacle -W side	deepening trend - coral reef rubble to slope sands with reeflets of microsolenids corals up to lithistid sponge with ?microbialite
Panuke PI-1A (J-99)	1	4029.3-4030.3 m	vuggy dolomite	dolomitized questionable coral reef
Panuke H-08	1	3446-3449 m	5B (3B)	recrystallized (micro-porous) crinoid- and chaetetic-rich
Demascota G-32	1	11228-11251 feet	4A	sponge reef mound in Artimon Member type section
	2	11836-11862 feet	5B	coral-stromatoporoid reef with marine filled ?cave (HTD altered)
	3	12704-12720.5 feet	5B	coral-stromatoporoid reef
	5	14400-14424 feet	3C(5C)	thrombolitic-stromatactis slope mound
Moheida P-15	1	2562-2564 m	4A	Marly sponge reef mound debris over coated red ironstone
Acadia K-62	(1, 2, 3)	2811.4-2822 m	5D?	Dolomitized oolite?, possible dedolomite cements
	4	3380.8-3399.2 m	5E(5A,B,D)	reef flat – back reef (oolitic, oncologic and mollusk-rich)
	5	3736.8-3753 m	3C-5C	thrombolitic/microbial mud mound (shallower than G-32 C5)
Albatross B-13	(1)	2511.5- 2517 m cutting-sidewall core	5D red-white 3C	White oolite; vertical open fractures = ?neptunian dykes, geopetals? cyclic red-pink-white slope thrombolitic-microbial slope carbonates
Shelburne G-29	(1 lost)	3991-4005.5 m lost	5D reddened	Sample – lost bottom of hole and core; light oolites, some reddened
OCS-A0317 (Hyena)	4	<u>BALTIMORE</u>	<u>CANYON</u>	<u>TROUGH (USA)</u>
		11563-11586 feet	3C	slope 'microbialite' -near base well in top of seismic clinofolds
OCS-A336 (Rhino)	3	14882-14912 feet	3B	shoaling? proximal foreereef (corals & crinoids) argillaceous
	4	15970-15999 feet	5B	in situ and debris coral-coraline sponge reef

Note: about 180 m of core listed above. No core is listed for the Scatarie Member or for any shelf interior wells unless reefal. Of the most recent wells, Panuke M-79 did have a core in the Scatarie Member (4532.7-3535.7m) consisting of mixed quartz sandstone and oolitic limestone probably in a shoal, not porous. FACIES NUMBERS: 1=bathyal shale, 2=neritic shale, 3=foreereef-channel, 3A= foreslope channel, 3C= distal foreslope (microbial mud mound), 3B= proximal foreslope (foreereef), 4= sponge reefal, 4A= 'deep' siliceous sponge reef & intermound, 4B= 'shallow' siliceous sponge reef, 4C= 'shallow' siliceous sponge-coral reef, 5= open marine carbonate bank 5A =skeletal rich, 5B=coralgal-stromatoporoid reefal, 5C=mud/pelleted; 5D=oolitic, 5E= oncologic, 5F= sandstone, 6= 'moat' (open inner shelf), 7= mixed carbonate siliciclastic platform interior (nearshore ridge), 8= coastal deltaic (lagoonal-continental), 9= mixed carbonate-deltaic, 10= deltaic/interdeltaic SEE Chapter 4 on the Abenaki carbonate facies template for details and illustrations of these cores as well as Chapters 5 and Appendices.

Problem #1 Conclusions – Nature of Northeast/Deltaic/Ramp Carbonates (Non-platform as compared with Platform Carbonates) and the Gap between the Delta and Platform

1. Large scale vertical styles and interbedded siliciclastics show two major groups of Late Jurassic carbonate wells. Those within and flanking the Sable Delta area, and on the shelf northeast of the Sable Island area, are variable and usually have greater amounts of siliciclastics than carbonates (typically oolitic) versus those of the southwest Abenaki platform margin. The latter consist of a kilometre or more thick carbonates with no or only minor amounts of thin beds of coarse siliciclastics except for the topmost interval in the Panuke Trend. The contrast between the two groups is stark and occurs over a short distance between the Penobscot L-30 well in the Sable Delta area, and Marquis L-35 - the northernmost platform margin well.

2. This lithologic subdivision is reflected in shelf morphology differences. The Sable Delta area and the shelf to the northeast have ramp and distally steepened ramp profiles with major progradation during the Late Jurassic. The northeast shelf prograded as a mixed carbonate siliciclastic system over 30 km, on a +≥200 km wide front, into an oceanic basin as part of the Sable-Laurentian deltaic complex. The southwest Abenaki platform has a steep slope mainly following the basin hinge line and is aggradational moving basinward less than a kilometre but extending laterally over 500 km to the USA-Canada boundary.

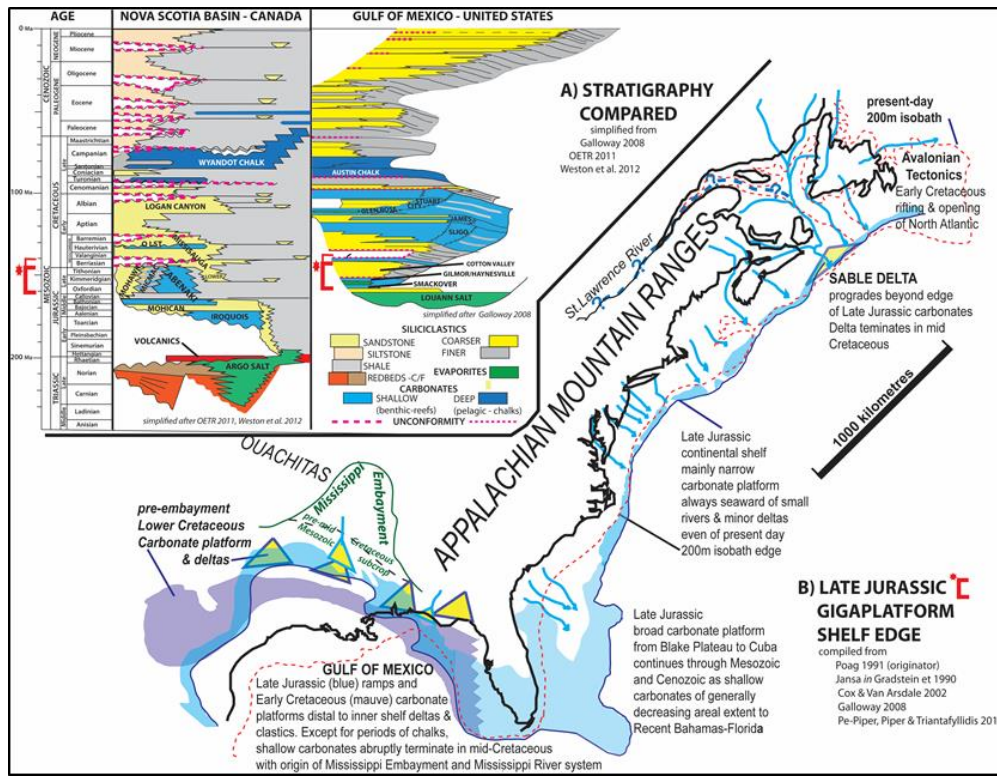


Figure 1. Comparison of two North American continental-scale deltas of different ages and different relationships to major carbonate platforms. A) Comparison of stratigraphic charts for the Scotian Margin (after OETRA, 2011; Weston et al., 2012), and Gulf of Mexico (after Galloway, 2008) and B) paleogeographic sketch (compiled from Poag, 1991; Jansa in Gradstein et al., 1990; Cox and Van Arsdale 2002; Pe-Piper et al. 2013). See Appendix Figure A1.32 in Eliuk (2016) for an enlarged and more detailed depiction of **Figure 1**.

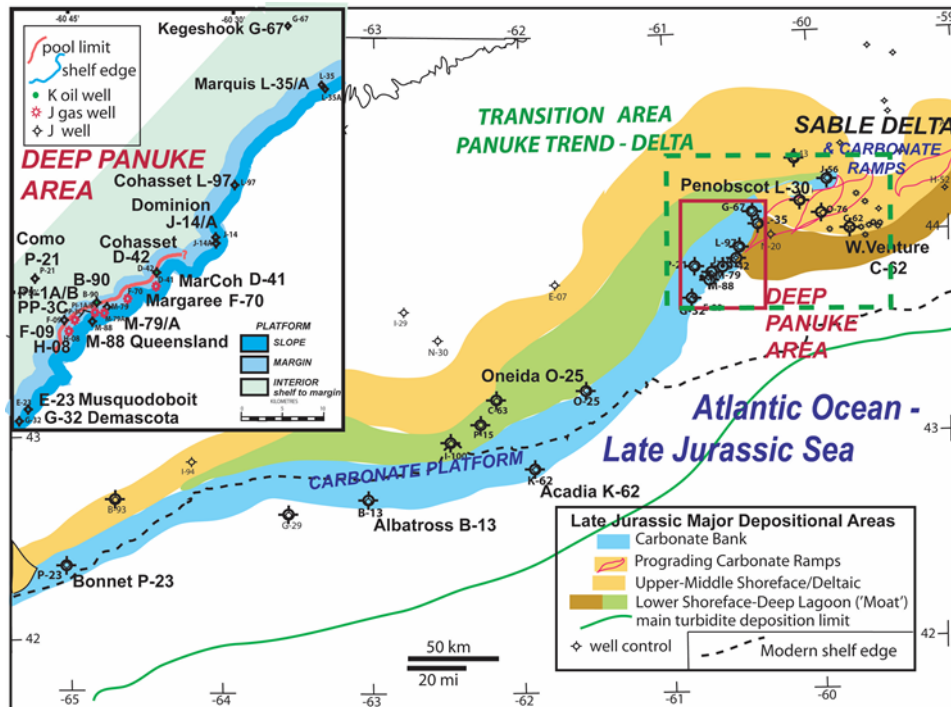


Figure 2. Abenaki Formation paleogeography southwest of Sable Delta and Deep Panuke well locations. Note the juxtaposition of the thick carbonate platform and the contemporaneous large Sable Delta with interbedded carbonate ramps. Main map in part based on data from PanCanadian (John Hogg and David Dolph 1999; unpublished).

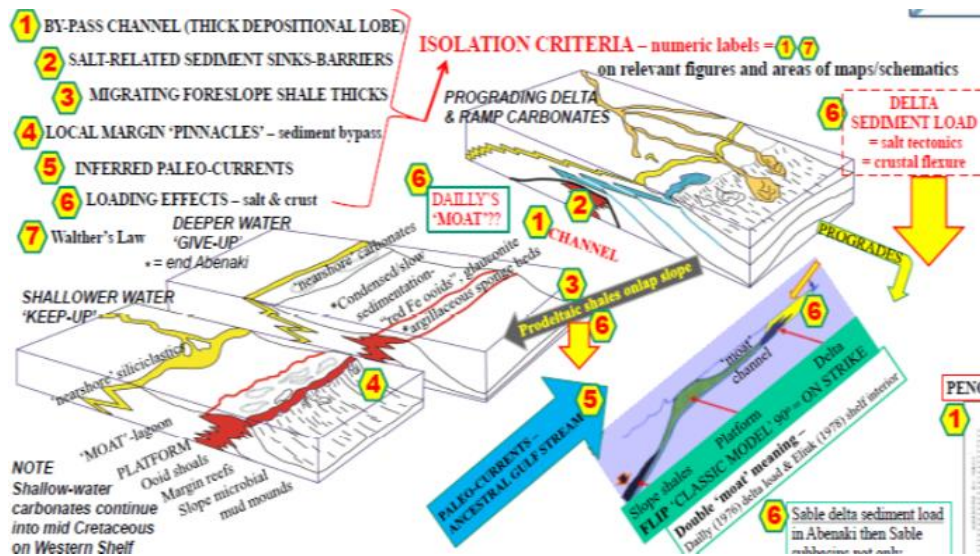


Figure 3. Criteria supporting isolation in the form of a physical gap to explain co-existence of the large delta and thick platform. See Eliuk (2016) for discussion of points and Eliuk (2016) Appendix 2.4 for (5) speculative paleocurrents based on modern current examples in reef-bearing deltas. DAILY'S 'MOAT' refers to the idea of delta load induced unfilled depressions as shown in Eliuk (2016) Figure 5.13, See Eliuk (2016) Appendix A2.2 and Figure A2.1 for 'classic model' mixed carbonate-siliciclastic system discussion. Some ancillary points are also included such as speculative paleocurrents along with some of the fully labelled depositional environment distribution that attempts to show the situation about and just after the time of the NBCU (Near Base Cretaceous Unconformity = latest Jurassic to pre-Valanginian).

3. Deltaic accumulation continued into the mid Cretaceous with periodic oolitic limestone interbeds such as the Oolitic Marker (O-Marker) that subdivides the deltaic accumulation. The Barremian O-Marker marks the base of the formation's Upper Member, with its Middle Member Hauterivian to Berriasian. The delta infill established the modern day continental shelf edge over 50 km seaward of the Middle Jurassic shelf edge whereas the Abenaki platform margin is now under the continental slope off the Western Shelf. The modern shelf edge is in a back-step position relative to the older mid Mesozoic Atlantic continental shelf edge from south of the Sable Island area to Florida. This major progradational relationship of filling a basin-slope of oceanic depths is prime evidence for the continental scale of the Sable-Laurentian delta complex. In contrast, the Late Jurassic gigaplatform shelf edge was always under the modern continental slope or even in drowned plateaus or beneath modern carbonate banks until the younger Mississippi Delta and Texas shelf prograded beyond the Late Jurassic and Early Cretaceous carbonate margin in the Gulf of Mexico.

4. Three intradeltaic carbonate patterns occur within the Sable Delta area of the Abenaki Subbasin and near Sable Island. First, Abenaki limestones are associated with interpreted salt highs or swells, that in the case of Abenaki J-56 became a salt dome, but earlier allowed maintenance of an oolitic shoal with many thin sandstone interbeds. There, carbonate deposition terminated well before that on the Abenaki platform. Second, a more distal salt swell structure in the Penobscot area north of Sable Island may be the locus of possible carbonate atolls. This is evidenced by a marked seismic flexure just shelfward of foreset slope microbialitic limestones within prodeltaic shales in Penobscot L-30. A distally steepened ramp flexure is a possible alternative interpretation. The third type of intradeltaic limestone is in the form of thin marker beds such as in the Late Jurassic #9 Limestone in the Venture field shelf margin delta area. They often are observed as oolitic in cuttings but the West Venture C-62 core has a complex variety of facies over a mere nine metre interval. They extend from depauperate marlstones through pure microbialite mound up to microbial/siliceous sponge/microsolenid coral/red algal reef mound capped by a hardground and prodeltaic shale possibly documenting a forced regression in the delta. These thin marker beds could be considered the thin end member of lateral and distal ramps discussed below.



5. Carbonates ramps and distally steepened ramps inherit their morphology from the underlying prodeltaic basin fill and are dependent on fill of available accommodation space to create shallow enough conditions for carbonate growth and progradation. During transgressive flooding phases on the outer shelf and following delta lobe shifts, carbonates alternate reciprocally with terrigenous deltaic sediments so they flank the active delta(s). A delta lobe switching model recording a complete transgression-regression cycle devised for the Mississippi Delta has been modified with the addition of a capping oolitic shoal on abandoned delta front bars for use in the Sable Delta area.

The delta and ramps developed as a complex response to extra-basinal sediment supply through a continent-draining delta, to salt movement and loading, to listric normal growth faulting, and to relative sea level fluctuations. Thus, correlation and compatibility of sequence subdivision between the deltaic area and the carbonate platform are not obvious and may not be possible. Age dating shows that the top carbonate is diachronous becoming generally older toward the delta in a possible stepwise fashion on the platform margin. Surprisingly, some of the deltaic carbonate ramps are younger than the termination of the Abenaki platform nearest the delta whereas other ramps are older as might be expected.

Ramp lateral facies changes are more gradual than those at the platform margin. A proximal ramp depositional association is seen as topsets on seismic data and consists of mainly quartz sandstone and oolitic limestone in couplets with the amount of thin coral-coraline sponge beds increasing basinward but never plentiful. A distal ramp depositional association is seen as foresets seismically and consists of prodeltaic shale encasing thinner dark limestones of lime peloid mud and microbolite-thrombolitic mounds with only characteristic small encrusters. Correlation of foreset limestones except along depositional strike is highly problematic. Indeed, the ramp carbonates should not be thought of as continuous layer-cake sheets but rather as discontinuous shingles, growing somewhat haphazardly on local highs and at the shelf edge when terrigenous influx is low.

6. A Gap due to bathymetric separation was hypothesized to explain the 15 Ma close juxtaposition of the delta and platform, and to account for the marked differences between the platform margin carbonates and the delta associated ramp carbonates. Initially there also was a separation by distance, even an estuary, as the early Sable Delta prograded south-southwest from the Abenaki Subbasin into the Sable Subbasin. Well control shows that the Sable Delta was active soon after the Abenaki's Callovian Misaine Member shale that must have been supplied by an earlier delta in the Laurentian Channel area (Laurentian Basin). The East Wolverine G-37 well, drilled in the Scotian Basin's eastern extension - South Whale Basin - on the Southern Grand Banks, has continuous marine shale from the Middle Jurassic to the Late Cretaceous (Canada-Newfoundland and Labrador- Offshore Petroleum Board well files, 2010). Seismic can be interpreted to show a bathymetric re-entrant between the Abenaki platform ending a bit northeast of Marquis L-35 and Kegeshook G-67 and southwest of the Penobscot and Abenaki salt-affected areas. In the regional strike directions (southwest-northeast) there appears to be a platform edge slope facing the channel that could have acted as a buttress to focus terrigenous sediment away from the platform and by-pass onto the deeper slope. That this was a long-continued low is supported by published seismic mapping showing a series of isotime thicks basinward that may have been deep sea fans fed through a channel. Unfortunately, just as there is no well deep enough in the postulated gap to more conclusively support its existence there and no 3D seismic available either.

7. At the furthest northeast end of the carbonate platform, the Marquis L-35 well, like many of the terrigenous deltaic wells, had a thickened Abenaki section due to down-to-the-basin listric normal faulting. In fact, it is likely the thickest Abenaki carbonate interval even though it terminates in the Tithonian (late Late Jurassic) before the younger termination in the Panuke Trend wells just to the south. This is also considerably older and prior to the next thickest platform wells on the Western Shelf that continue into the Early Cretaceous. Thus, another influence of the delta on the carbonates was loading by prodelta shales resulting in overall section thickening. The



load of this continental-scale delta may have depressed the lithosphere in addition to contributing to salt tectonism. Application of Dailly's (1975, 1976) delta load pendulum model may explain the gap or unfilled depression on the flanks of the delta that is important in preserving an area that kept the delta and platform separated for much of the 15Ma when they were closely juxtaposed. A salt withdrawal low is also conceivable. Another consequence of the major delta load may be the development of bulge or uplift flexure on the Western Shelf. The Western Shelf has carbonate and overlying siliciclastics with thin intervals interpreted by others as due to unconformities.

Problem #2 Conclusions - Changes within the Platform Margin Carbonates Showing Sable Delta Influence.

8. Closing of the bathymetric Gap occurred in the Tithonian when prodeltaic shales along with ramp oolite and sandstone couplets filled the area. This deposition even occurred on the top of the Abenaki platform in Marquis L-35 and Kegeshook G-67. Marquis L-35 is the only Panuke Trend margin well to not have argillaceous lithistid sponge-rich beds (Artimon Member or similar lithofacies) at the top of the Abenaki. Instead, it is capped by oolite-sandstone couplets similar to and probably correlative with the topset ramp carbonates in Penobscot L-30.

Seismic data shows a slight progradation of ramp sediments into the basin beyond the L-35 platform edge. Age dating shows these ramp style beds are older than the top Abenaki in the Panuke Trend to the south indicating that the platform has a retrograde relationship back stepping away from the advancing deltaic sediments. Further south the Sable Delta prodeltaic shales form a prograding wedge with a slope onlap surface relationship to the distal lower platform slope. Initially, this did not affect the platform lithofacies that was in shallow waters unaffected by the deeper turbid influx. This sediment pile load potentially caused flexuring, fracturing, and faulting of the margin, and with deterioration in surface water conditions aided the change-over from shallow-water coral-stromatopore reefs to sponge reef mounds. This facies change was diachronous, occurring first during the Late Jurassic in the north and progressing southward after.

A few wells in the Panuke Trend do have thick shale interbeds mainly because they were drilled in part on the slope and in the case of Queensland M-88 totally on the slope with only deeper water facies present, particularly microbolite mounds. Platform slope onlap shales are inclined away from the Sable Delta. This wedge-like geometry is revealed by comparing the carbonate facies above and below thick shales encountered along the platform margin and slope. The underlying carbonate is usually replaced by a shallower carbonate facies in the overlying carbonate. Carbonate facies represent a distal slope setting in the Queensland M-88 where influx of shale does not result in shoaling perceptible to the carbonate communities. This illustrates a progression on the slope north of M-88 where first the overlying carbonate is lithistid sponge-rich (Dominion J-14), then coral reefal and oolitic (Penobscot L-30) showing the dip of the prodelta southward.

9. Colour and sedimentological-biological variations within the slope carbonates demonstrate apparent delta proximity changes along with the slope onlap shales with associated carbonates. The most striking thing about the slope sediments and particularly the microbolites is the progression of colour changes starting from very dark grey and brown in the delta to near white with red and pink colour cycles at the furthest well on the southwest edge of the Nova Scotia offshore (Bonnet P-23). Except for West Venture C-62 that is slightly argillaceous to marlstone, the carbonates appear non-argillaceous so the colour change is due to other factors including even burial differences that would still be indirectly attributable to Sable Delta proximity.

The slope carbonates show a variety of microbolite textures including stromatolite mud mound types. The microbolites usually are devoid of large metazoans but have characteristic encrusting microbiota. Several cores show skeletal debris from upslope including bioeroded colonial corals. Only one core far from the delta shows *in situ* delicate branching hexacorals and displacement fabrics and repositioned geopetals within the mound sediment. These Abenaki examples have been plotted on mound classification charts based on European outcrop studies and show the stromatolite and reddened slope beds seem like hold-overs from the mid Paleozoic. With the limited data



control, it is not apparent whether the differences relate to delta proximity or variations in position on the platform slope.

10. The two indicators of shallow water depositional facies - oolite and the slightly deeper coral-stromatoporoid reefal beds - do not show any obvious changes in the platform margin with respect to delta proximity based on cuttings evidence alone. However, the presence of thin sandstone beds and quartz nuclei in ooids do occur in the Panuke Trend but most terrigenous transport occurred mainly as muddy sediment on the distal platform slope and not across the shelf. There is too little core to examine more subtle possible lateral changes, though two sets of shelf margin coral-stromatoporoids reefal cores 40 km apart do show interesting differences – highly bioeroded debris reef with a possible cave or Neptunian dyke versus large *in situ* corals with little evidence of bioerosion and more associated microbolite crusts in separate debris beds. But rather than proximity changes they can just as well be understood as depositional depth differences

The platform carbonate margin in contrast to the ramps has a constricted lateral facies gradient. This is seen in many vertical sections as a ‘catch-up’ or slight progradational or shoaling 2nd order sequence. The succession begins with distal lime muds and microbolite-thrombolitic and mud mounds followed by coral-stromatoporoid reefal intervals and then up to oolite both vertically and laterally. Three shelf margin wells lack oolites and penetrate small pinnacles encased in carbonate. Core from the Margaree F-70 well demonstrates the transition from shallower coral reef-prone facies up to lithistid sponge reef mounding on the inboard grainy slope of the buildup, with many thin reefal intervals as well as a crinoid filled channels or graded debris flows. This is a record of a keep-up to give-up reef being drowned and/or responding to deteriorating conditions due to influx of turbid deltaic waters on the shelf margin.

11. Strangely, with only two exceptions and these both on the Western Shelf, there are always some amount of thin oolite beds at the base of the Abenaki Baccaro Member or sometimes even in the underlying Misaine Member shale that may rarely have sandstone beds capping the shale. This apparent anomaly of going from marine shales up to shallow oolite, even if partly allochthonous, then immediately deeper again to slope carbonates dated as the top Callovian may record a major sea level drop associated with glaciation 24 around the Middle to Late Jurassic age boundary. The morphological profile of the basal Baccaro mimics those of the underlying Misaine shale and dominantly oolitic Scatarie which are distally steepened ramps.

12. Unequivocal delta proximity effects occur at the top of the Abenaki platform with effects continuing into overlying terrigenous sediments. Minor sponge-rich limestones and bioelemental-condensed beds of marine red-coated ironstones are the two key lithologies. The coated ironstones appear to cap nearly all platform wells southwest of the Panuke Trend. Within the Panuke Trend such bioelemental beds are absent but in the uppermost platform margin there is an absence of oolite and a major change in reef community composition from coral-stromatoporoid reefs to siliceous sponge reef mounds. This is interpreted to indicate a drowning of the shallow-marine platform. This may result in part from possible initial subaerial exposure at one or more brief unconformities. This includes the Near Base Cretaceous Unconformity (NBCU; above the Berriasian-Late Jurassic) followed by the deleterious effect of turbid waters associated with the ingress of the Sable Island prodelta clays, and the apparent much slower growth of the lithistid sponge communities as compared to hexacorals and coralline sponges.

The transition is regionally diachronous in front of the expanding Sable prodelta. However, most of the Panuke Trend seemed to have near synchronous termination although the initial onset and mix of lithistid and coral-stromatoporoid communities started at different times. As already mentioned, the downslope loading effects may have aided in the demise of shallow sedimentation in the Panuke Trend. Much further southwest, siliceous sponge-rich beds occur on many of the shelf interior wells in the Mohican Subbasin along with marine red-coated ironstone beds at the top of the main Abenaki Formation and slightly above. That area was the distal limit of the



Sable Delta. Further southwest beyond the presence of prodeltaic beds in the Acadia K-62 and Albatross B-13 wells, sponge beds are also absent although marine redbeds occur at the top of the younger Early Cretaceous age platform.

13. The Abenaki platform continued growing on the far Western Shelf when it had terminated in all wells to the northeast. In Bonnet P-23 slightly interior from the shelf edge, the platform continued growing even into the Aptian and possibly Albian. The topmost shelf limestone was slightly argillaceous with both high amounts of lithistid and stromatoporoid sponges. Finally, the platform was capped by the thickest development of marine red-coated ironstones indicating long-continued sediment-starved conditions beyond the reach of the delta and unfavourable conditions for vigorous carbonate growth. All three near-shelf margin Western Shelf wells are overlain by thin Cretaceous marine sediments including Late Cretaceous (Maastrichtian-Santonian) chalks and marls of the Wyandot Formation. This indicates the likelihood that the platform was drowned and exposed on the seafloor in deep water. Wide near vertical cement-lined fractures occur near the top of the Abenaki platform in Albatross B-13 with asymmetrical red and green geopetal bearing isolated ooids. These are interpreted as Neptunian dykes within cemented oolitic grainstones suggesting that the seafloor exposure started very soon after the end of the Abenaki platform.

14. The final point is a comparison with possible modern analogues. The siliceous sponge mounds in prodeltaic settings may have analogues in the Fraser River prodelta off Vancouver Canada, and in the recently described rhodolith-sponge reef tract at the Brazilian continental shelf edge off the mouth of the Amazon. The cored #9 Limestone facies in West Venture C-62 in front of the Late Jurassic delta shows many similarities. Unfortunately, modern demosponges are generally not calcified, and the Fraser River mounds result from clay baffling by hexactinellid sponges liable to be preserved only as silica spicules leaving a mysterious shale mound as their taphonomic legacy. Reefs within modern deltas often show marked facies variation and distribution relative to oceanic current direction.

Conclusions

There are no modern analogues for the ubiquitous presence of oolite deposits closely associated with delta-derived sandstones in carbonate ramp settings. Similarly, the presence of a thick clean carbonate platform very near a continental-scale delta also lacks modern analogues. This makes the Late Jurassic Abenaki platform and Sable Delta a very strange association in a former world much more hospitable to marine shallow-water carbonates than the seas of the twenty-first century. The long-continued delta-platform relationship is summarized in two diagrams:

First, **Figure 4** is a complementary time series of map views that summarizes the long-continued relationship of carbonate platform and growing delta. The figure caption has additional comments.

Second, **Figure 5** is a time series of schematic strike sections laying out some of the processes and products from older up to younger. These figures show how a gap could have long existed between the platform and the deltaic sediment pile with salt swell highs. The gap was then infilled with periods of ramp carbonate sedimentation over abandoned delta lobes or near the shelf break during transgressions. Loading and associated tectonics affected both delta and carbonate margin during and after the Late Jurassic. On the shelf and margin, siliceous sponge reef mounds grew in turbid waters in front of the prograding delta as it progressively buried the northeastern half of the platform. More distally, the shelf was starved of sediment shown by marine red beds of coated ironstone. Yet further southwest the shallow-water platform continued growing into the mid Cretaceous until it too was drowned but not buried initially.

The Sable Delta and Abenaki carbonate platform interplay generated conditions that resulted in deltaic and reefal shelf margin gas fields by providing linked traps, seals, reservoirs, source rocks and migration paths.



Cuttings, core and seismic data collected over a half century of exploration have been the basis of explaining the delta/platform relationship and the Scotian Shelf geohistory.

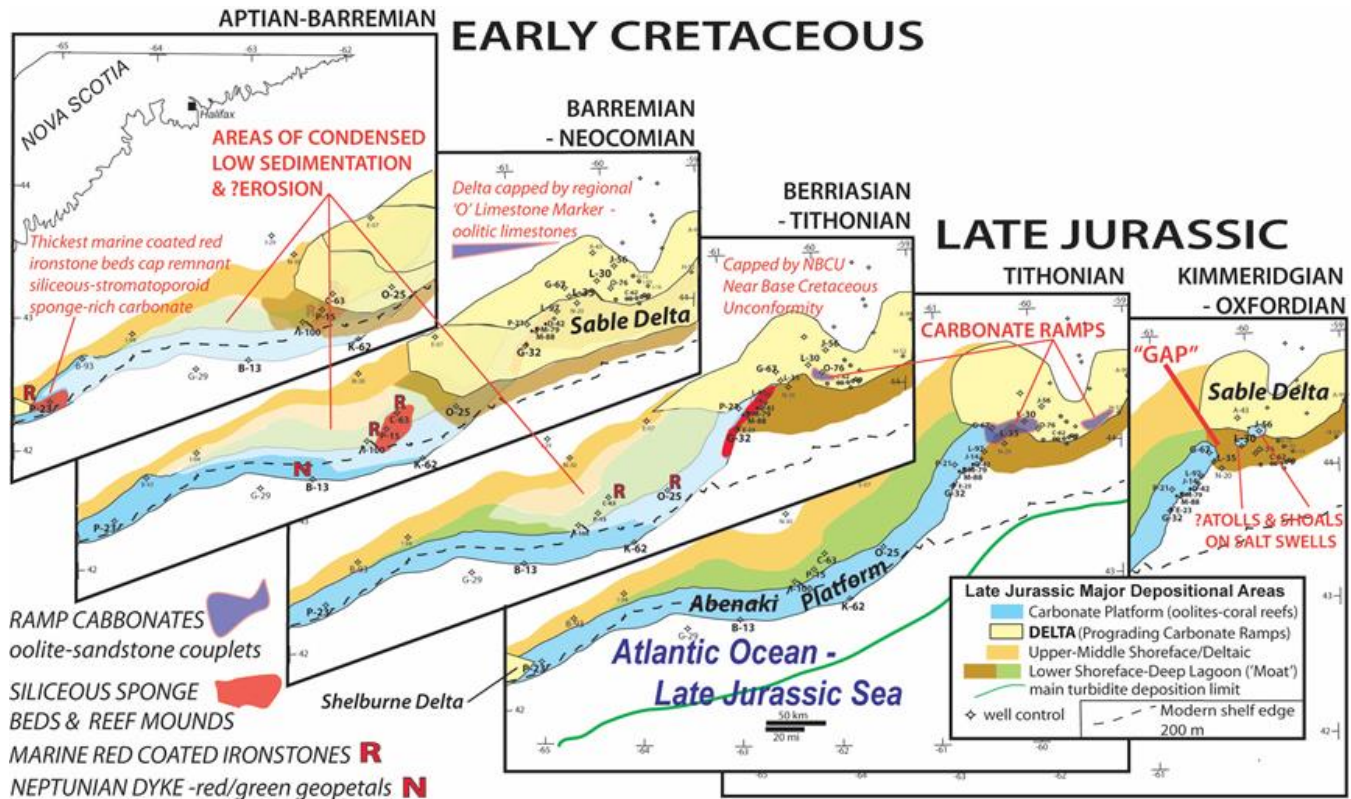


Figure 4. Sketch paleogeographic maps showing key features during expansion of Sable Delta on southwest Scotian Shelf. During the Jurassic-Cretaceous the Sable Delta continuously enlarged to the southwest of the Sable Island area. Initially for millions of years the delta-Abenaki platform (Baccaro Member) co-existed due to separation by a bathymetric 'gap' or channel. After the gap infilled, the platform back stepped and changed to siliceous sponge-rich facies (Artimon Member). It diachronously moved at the prodelta toe with an area of very low sedimentation with thin sponge beds and marine coated ironstone redbeds further southwest. The Cretaceous shallow-water platform reduced in area (Roseway Member) until it too was capped by thick marine red coated ironstones indicating long seafloor exposure and was buried by much younger sediment. Ramp carbonate intervals formed at different times on the abandoned delta lobes or during flooding at the shelf edge. Base map in part after Hogg and Dolph 1999 Encana talk. Delta edges modified from Deptuck and Campbell (2012).

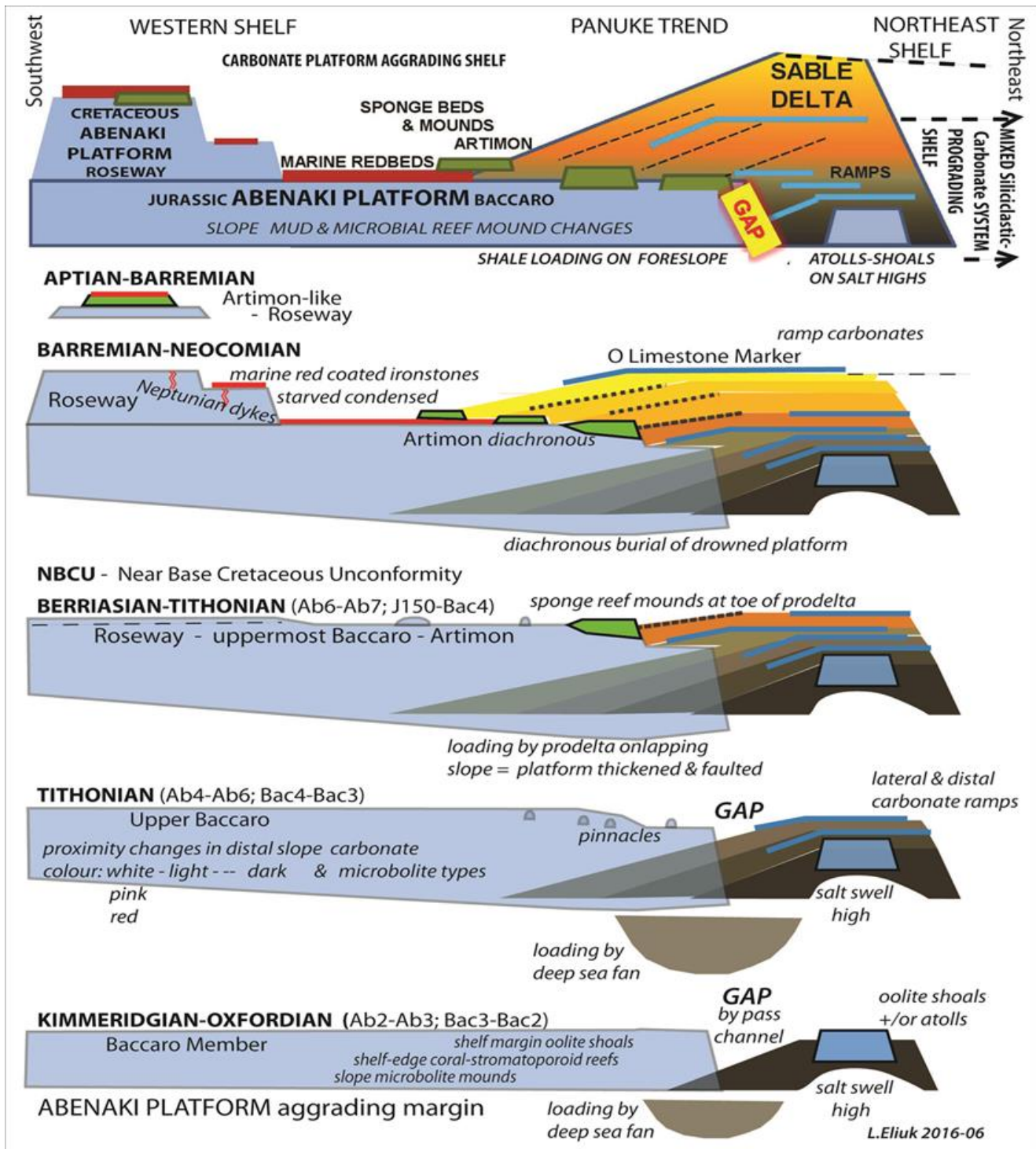


Figure 5. Summary model for Abenaki platform to Sable Delta relationship over time. Schematic strike sections from oldest up to youngest showing the changes as the Sable Delta expanded and eventually buried much of the Abenaki platform southwest of Sable Island. Approximate ages and sequences, lithostratigraphic names, processes and products shown. Neocomian considered to include Berriasian, Valanginian and Hauterivian.



References

- Cox, R.T., and Van Arsdale, R.B., 2002. The Mississippi Embayment, North America: a first order Continental structure generated by the Cretaceous superplume mantle event. *Journal of Geodynamics*, **34**, 163-176.
- Dailly, G.C. 1975. Some remarks on regression and transgression in deltaic sediments. In: C.J. Yorath, E.R. Parker, and D.J. Glas (eds), *Canada's Continental Margins and Offshore Petroleum Exploration*. Canadian Society of Petroleum Geologists Memoir, **4**, 791-820.
- Dailly, G.C. 1976. Pendulum effect and Niger delta prolific belt. *American Association of Petroleum Geologists Bulletin*, **60**(9), 1543-1575.
- Deptuck, M.E., and Campbell, D.C., 2012. Widespread erosion and mass failure from the ~51 Ma Montagnais marine bolide impact off southwestern Nova Scotia, Canada. *Canadian Journal of Earth Sciences*, **49**(12), 1567-1594,
- Eliuk, L.S. 2016. Abenaki Carbonate Platform in Relation to the Jurassic-Cretaceous Sable Island Delta, Offshore Nova Scotia, Canada. Unpublished Ph.D. dissertation, Dalhousie University, 422 p. Complete thesis available at <https://dalspace.library.dal.ca/handle/10222/> with all references and original figures and text used in this summary. Also, all supporting data, results and discussion are available online.
- Galloway, W.E. 2008. Depositional evolution of the Gulf of Mexico sedimentary basin. In: *Sedimentary Basins of the World*, Elsevier, **5**, 505-549.
- Gradstein, F.M., Jansa, L.F., Srivastava, S.P., Williamson, M.A., Bonham Carter, B. and Stam, B., 1990. Aspects of North Atlantic paleo-oceanography, Chapter 8. In: M.J. Keen and G.L. Williams (eds) *Geology of the Continental Margin of Eastern Canada*; Geological Survey of Canada, *Geology of Canada*, No.2, 351-389.
- Moura, R.L., Amado-Filho, G.M., Moraes, F.C., Brasileiro, P.S., Salomon, P.S., Mahiques, M.M., Bastos, A.C., Almeida, M.G., Silva Jr., J.M., Araujo, B.F., Brito, F.P., Rangel, T.P., Oliveira, B.C.V., Bahia, R.G., Paranhos, R.P., Dias, R.J.S., Siegle, E., Figueiredo Jr., A.G., Pereira, R.C, Leal, C.V., Hajdu, E., Asp, N.E., Gregoracci, G.B., Neumann-Leitão, S., Yager, P.L., Francini-Filho, R.B., Fróes, A., Campeão, M., Silva, B.S., Moreira, A.P.B., Oliveira, L., Soares, A.C., Araujo, L., Oliveira, N.L., Teixeira, J.B., Valle, R.A.B., Thompson, C.C., Rezende, C.E., and Thompson, F.L. 2016. An extensive reef system at the Amazon River mouth. *Science Advances*, **2**, e1501252, (<http://advances.science mag.org/>).
- Offshore Energy Technical Research Association (OETRA), 2011. Scotian Basin Play Fairway Analysis Study. <http://www.oera.ca/offshore-energy-research/geoscience/play-fairway-analysis/Play Fairway Analysis-atlas/>
- Pe-Piper, G., Piper, D.J.W., and Triantafyllidis, S. 2013. Detrital monazite geochronology, Upper Jurassic–Lower Cretaceous of the Scotian Basin: significance for tracking first-cycle source. In: R.A. Scott, H.R. Smyth, A.C. Morton, and N. Richardson (eds), *Sediment Provenance Studies in Hydrocarbon Exploration and Production*. Geological Society London Special Publication, **386**, 20 p.
- Poag, C.W., 1991. Rise and demise of the Bahamas-Grand Banks gigaplatform, northern margin of the Jurassic proto-Atlantic seaway. *Marine Geology*, **102**, 63-130.
- Tcherepanov, E.V., Droxler, A.W., Lapointe, P., Dickens, G.R., Bentley, S.J., Beaufort, L., Peterson, L.C., Daniell, J., and Opdyke, B.N. 2008. Neogene evolution of the mixed carbonate-siliciclastic system in the Gulf of Papua, Papua-New Guinea. *Journal of Geophysical Research*, **113**(F1), doi:10.1029/2006JF000684.
- Tcherepanov, E.V., Droxler, A.W., Lapointe, P., Mohn, K., and Larsen, O.A., 2010. Siliciclastics influx and burial of the Cenozoic carbonate system in the Gulf of Papua. *Marine and Petroleum Geology*, **27**, 533-554.
- Weston, J.F., MacRae, R.A., Ascoli, P., Cooper, M.K.E., Fensome, R.A., Shaw, D., and Williams, G.L., 2012. A revised biostratigraphic and well log sequence stratigraphic framework for the Scotian Margin, offshore eastern Canada. *Canadian Journal of Earth Sciences*, **49**(12), 1417-1462.





MULTIPLE JURASSIC SOURCE INTERVALS IN THE SUBSURFACE OF OFFSHORE NOVA SCOTIA

Forkner, Rob¹; Fildani, Andrea¹; Ettinger, Nicholas¹, and Moldowan, John M.²

¹ Equinor Research and Technology, 6300 Bridge Point Parkway, Austin, TX 78730, USA, rfork@equinor.com

² Biomarker Technologies, Inc., 638 Martin Avenue, Rohnert Park, CA 94928, USA

Presence of source rocks is a major risk in petroleum exploration. This may be considered the highest risk to successful hydrocarbon exploration efforts in offshore Nova Scotia, particularly the presence of Jurassic-aged source rocks. To de-risk presence and properly characterize source rocks and their depositional environments, comprehensive organic geochemical analyses of eight oils were performed to better link oils to source rocks. Suspected source intervals were then analyzed geophysically to determine the likelihood of source rock presence.

We interpret the presence of at least two source rocks having contributed to the bulk of the hydrocarbon volumes in our sample set. One source rock deposited in the mid to late Jurassic and likely relates to the oil window component of the liquid volume. An older contributor has a unique diamondoid composition likely related to a carbonate and/or evaporitic depositional setting that we interpret to be early Jurassic in age.

The results of organic geochemical analyses led us to hypothesize the presence of marine source rock facies along the continental margin of Nova Scotia at both Lower and Upper Jurassic levels. High amplitude reflections consistent with the possible occurrence of organic rich mudrocks were identified at interpreted lower and upper Jurassic intervals. The Lower Jurassic source is interpreted to be concentrated in fault-related half grabens slightly inboard of the later Jurassic reef margin. Geophysical analyses of these half graben mini-basins also support source rock presence. Later Jurassic source rock is likely more regional in extent.

Introduction

The majority of successful reservoir targets in Nova Scotia have been within Upper Jurassic carbonates and lower-to-middle Cretaceous clastic intervals (OETRA, 2011). Hydrocarbons in these intervals are believed sourced by Jurassic or Lower Cretaceous-aged source rocks (Weissenberger et al., 2006). However, identifying a consistent time of deposition of source rocks for Scotian Basin hydrocarbons has been challenging, mainly because of over maturity and degradation of age-related biomarkers. Most work points to the Upper Jurassic as a source rock age because of age-related biomarkers, and because reservoirs of Upper Jurassic or younger age must be charged from something stratigraphically older (e.g. summaries and reviews in OETRA, 2011). Older potential source intervals, particularly the Lower Jurassic, are well known in basins around the North Atlantic as intervals of thick black shale accumulation, but remain unproven along the Scotian margin.

In this study, we aim to test the idea that there may be source rock of Lower Jurassic age contributing hydrocarbons to the petroleum system of the Scotian margin. We aim to do this by first determining the plausibility of a working Lower Jurassic petroleum system via analyses of sampled hydrocarbons using cutting-edge organic geochemical analyses. We then use those results that relate to environment and age of source rock deposition to guide us to source intervals that we might high-grade through interrogation of additional geological and geophysical data.



Organic Geochemical Analyses

Sampling

A single oil sample was collected from eight selected wells from the CNSOPB’s Geoscience Research Centre, Dartmouth, Nova Scotia in 2015 (**Table 1** and **Figure 1**). These samples were subject to the following analyses performed at the Biomarkers, Inc. laboratory in Rohnert Park, California:

1. All classical GC-MS and GC-MS-MS analyses for Biomarkers
2. Quantitative Diamondoid Analysis (QDA)
3. Compound Specific Isotopic Analysis of Boimarkers (CSIA-B)
4. Age and taxon-specific Biomarker analyses.

In addition, a subset of four samples (wells 1, 4, 7, and 8) were also analyzed for:

1. Quantitative Extended Diamondoid Analysis (QEDA)
2. Compound Specific Isotopic Analysis of Diamondoids (CSIA-D)
3. Compound Specific Isotopic Analysis of Alkanes (CSIS-A)

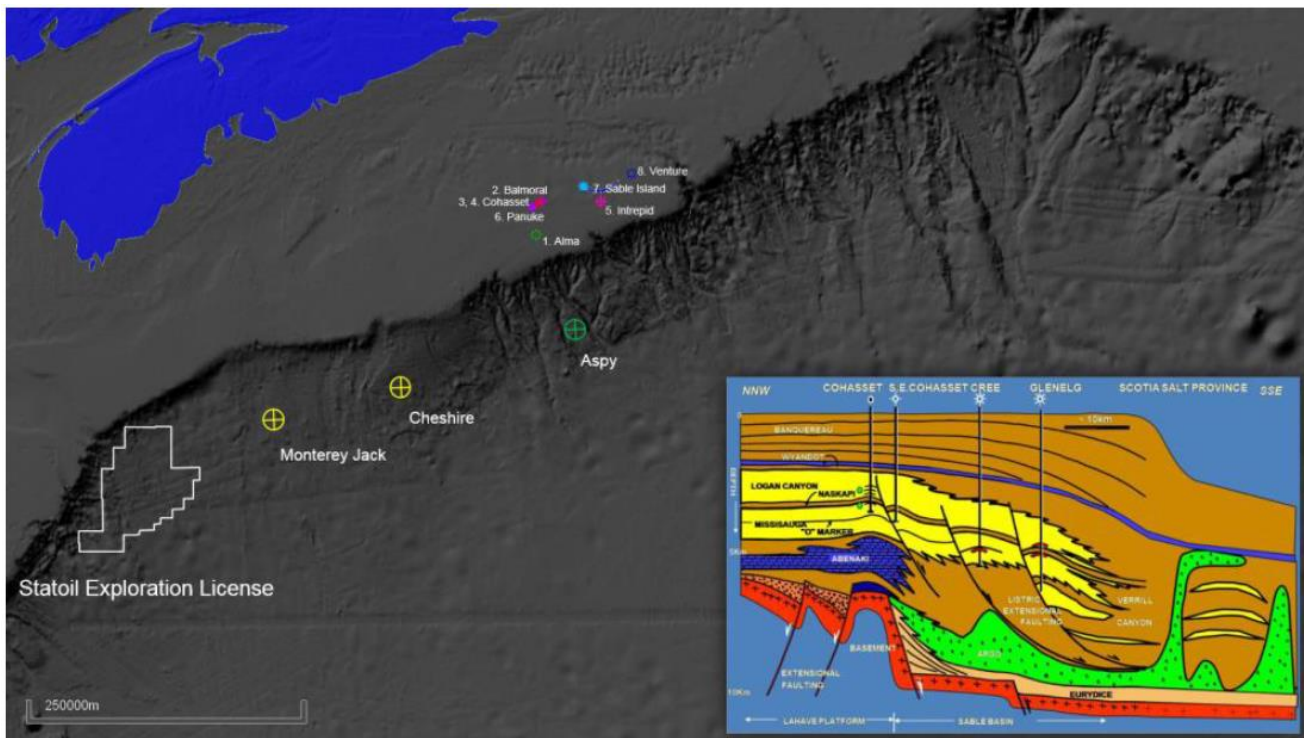


Figure 1. Recent and current exploration efforts are focused on deeper water targets in the salt province with the drilling of the Shell Cheshire L-97/L-97A (2016), Monterey Jack E-43/E-43A (2017), and BP-Hess Aspy D-11/D-11A (2018) wells. While these and other exploration wells tested acreage in deep water, success in the salt province will need to rely on a source that established fields may or may not have tested. Oil samples obtained for analysis in this study are listed above and shown as enumerated well locations on the shelf. Inset schematic profile through the Sable Subbasin sourced from Enachescu et al., (2010).



Well No.	Well Name	Formation	Member / Pool / Zone	DST No.	Interval mMDKB
1*	Alma F-67	Missisauga	Upper Mb., C Sand	2	3026.0-3072.0
2	Balmoral M-32	Logan Canyon	Cree Mb., Sand	1	2065.0-2068.0
3	Cohasset CP3A P-51	Logan Canyon	Cree Mb., C10U Sand	1	2674.0-2681.0
4*	Cohasset A-52	Logan Canyon	Cree Mb., C5 Sand	3	2254.0-2269.5
5	Intrepid L-80	Missisauga	Upper Mb., Zone 7	5	3383.1-3389.2
6	Panuke B-90	Logan Canyon	Naskapi Mb., P2 Sand	1	2293.5-2299.5
7*	Sable Island 2H-58	Logan Canyon	Marmorra Mb.	9	1159.0-1649.2
8*	Venture B-13	Missisauga	Middle Mb., B Sand / Zone 7	6	4572.0-4579.0

Table 1. List of wells and associated oil sample information. As noted on the previous page, four wells were subjected to additional analyses and are identified with an asterisk (*).

Summary of Results of Organic Geochemical Analyses

Rather than sampling for the purposes of grouping oils, our organic geochemical analyses were performed to garner information about the parent source rock. Our intention is to let the geochemical analytical results guide subsequent geological and geophysical work. In summary, the organic geochemical analyses indicate:

1. Maturity: Diamondoid concentrations (QDA) indicate a wide range of oil cracking has occurred in all oil samples analyzed (**Figure 2**). Biomarker maturity parameters indicate that the biomarker-prone component of the fluids is within the early to middle oil window, though this fraction is the minority of the total volume (Figure 3). This portion of the hydrocarbon system was likely sourced from the Verrill Canyon or equivalent later-Jurassic-aged formations. However, overall low biomarker concentrations together with high diamondoid concentrations suggest that the predominant charge to these oils is from a post-mature source. This requires mixing of: 1.) post-mature, and 2.) oil-window sources, and is less likely to indicate a gradation of maturities from one single source.

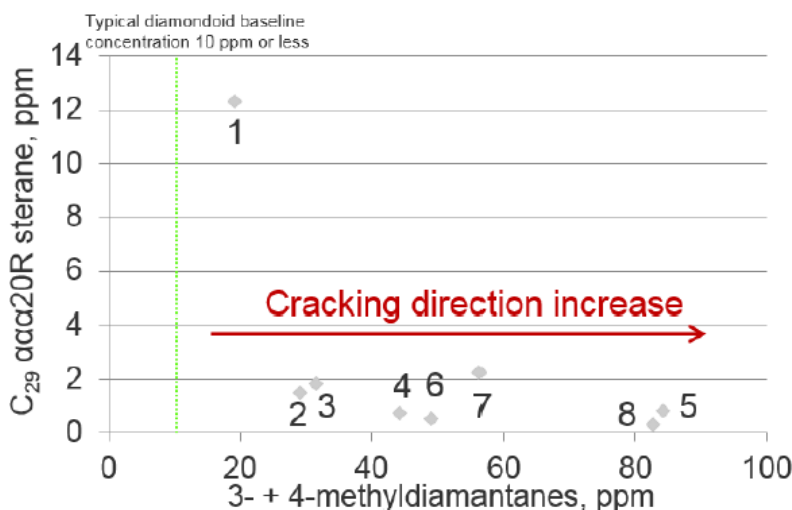


Figure 2. Quantitative diamondoid analysis (QDA) indicates that the oils analyzed in this study are of mixed maturities, including 1. a high-maturity (thermally cracked) component, and 2. a moderate maturity (oil-window) component. The occurrence of biomarkers, indicated by significant (although in some cases quite low) C₂₉-sterane concentrations shows that all the samples have a component that is non-cracked and of maturity in the oil window. Low biomarker concentrations together with high diamondoid concentrations in Samples 2-8 suggest the predominant charge to these oil accumulations is from a post-mature source. Dahl et al., (1999) established a relationship between oil cracking reflected in diminishing biomarker concentration and resultant increase in diamondoid concentration (controlled laboratory experiments with several oils). Diamondoid baseline in most oils is 1-10 ppm, increasing dramatically at ca. 10% oil conversion.



2. *Source Rock age*: All biomarker analyses of age-related components indicate that the most likely age for the oil window fraction of the biomarkers is of Jurassic (probably Upper Jurassic) age (Figure 4). We interpret the diamondoid fraction to be older (probably Lower Jurassic) but cannot quantitatively determine the age of the older fraction.

3. *Environment of source rock deposition*: Biomarker/oil window component: All samples except for sample 8 are mostly terrestrial in biomarker composition, which is to be expected as all samples were recovered from the Sable Island area that is known as a major delta complex in the Mesozoic. By comparison, sample 8 is the most marine in composition, though does also contain terrestrial biomarkers (Figure 5).

4. *Diamondoid component*: All samples are uniform except for sample 8 (Venture B-13), which has evidence for a source from a carbonate or evaporative setting. This most likely places the diamondoid fraction of sample 8 within the Triassic or early Jurassic (Figure 6).

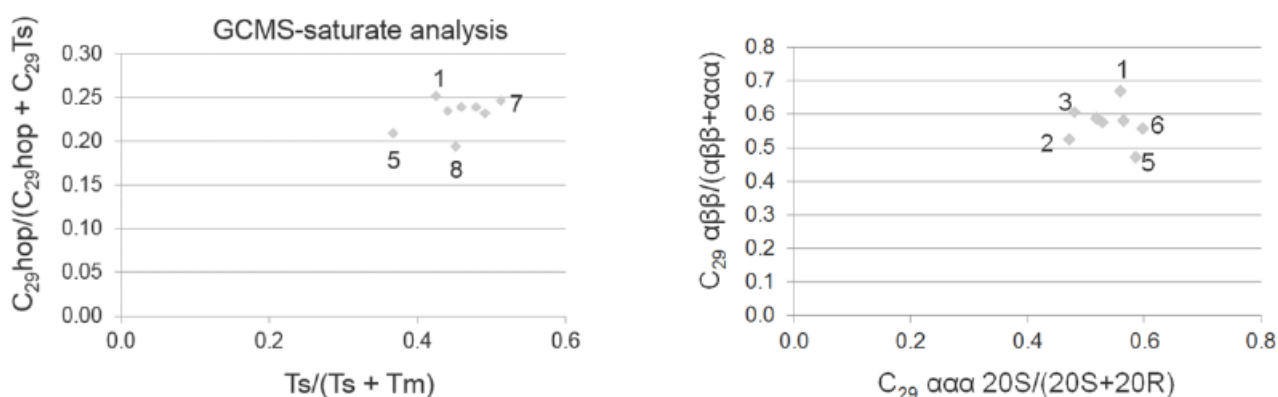


Figure 3. Saturate maturity parameters (left) show a rather similar maturity for the oil-window portion of the oil samples. This maturity based on saturate biomarkers appears to lie slightly before the peak of oil generation (compared to internal standard). This contrasts with the moderate to very high diamondoid concentrations (QDA), which show a very wide range for the extent of oil cracking that would have to occur in the wet gas window and even in the dry gas window. These samples provide further evidence for mixed maturity requiring co-sourcing from a deep source (post-mature) and a shallow source (oil window). Ts/(Ts+Tm) is a thermal parameter based on Tm (C27, 17a-trisnorhopane) being less stable than Ts (C27 18a-trisnorhopane) during thermal maturation (increasing maturity = increasing ratio). This was predicted in molecular mechanics calculations for the formation of various hopanes, and substantiated via laboratory experimentation (Kolaczowska et al., 1990). Ratios of C29hop to C29 hopanes + C29Ts (aka 18a-30 Norneohopane) behave in a similar way, though is more stable than Ts/(Ts+Tm) (Hughes et al., 1985). C29 sterane epimer ratios (right) are consistent with a maturity below the peak of the oil window. Isomerization reactions modeled for steranes indicate conversion from R to S isomers occurs with increasing thermal maturity and has been confirmed with laboratory experiments (MacKenzie and MacKenzie, 1983; Beaumont et al., 1985). Both results indicate that the oil window component of the samples is below peak maturity and suggests that an overmature component would likely be from a different source.

A.

	Triassic			Jurassic		
	Lower	Middle	Upper	Lower	Middle	Upper
No. of Oils	3	8	28	19	26	47
ETR ≥ 2.0	3	8	25	2	0	0
ETR > 1.2	0	0	0	17	4	6

*ETR = (C28 TT + C29 TT) / Ts Peters et al., 2005

B.

Sample #	1	2	3	4	5	6	7	8
ETR	0.45	0.2	0.26	0.18	0.34	0.27	0.26	0.56

Figure 4. The Extended Tricyclic Terpane Ratio (ETR) can be used to distinguish Jurassic from Triassic oil. Tricyclic terpanes are a common component of bacterial and algal membranes. They are predominant in Tasmanites (a prasinophyte alga) common in the Triassic. A) Experimental data from Peters et al., (2005). B) Data from this study. All data indicate that ETR is greater than zero, but smaller than 1.2, which may be indicative of Jurassic age. If so, the low ratios would be more likely Upper Jurassic, at least using the data trends from Peters et al. (2005) as a guide.



Geological Analysis

Very few (8) confirmed well penetrations of the Lower Jurassic exist on the Scotian Margin, which makes interpretation of Lower Jurassic lithologies difficult (Adams, 1986). Data for this study include vintage 2D reflection seismic data from the Nova Scotian offshore margin, as well as a small 3D seismic volume (the EnCana Torbrook survey). Two important themes emerged because of geological and geophysical work in the Jurassic of Nova Scotia: a) evidence for increasingly open marine conditions outboard, and b) high amplitude reflections consistent with the occurrence of organic-rich mudrocks identified in specific Jurassic levels.

Evidence for marine conditions in the Early Jurassic

Previous work in the Lower Jurassic of Nova Scotia indicates that the dominant facies are peritidal marine carbonates and evaporites of the Iroquois Formation, and are not considered viable source or reservoir facies (Adams, 1986). However, studies of both modern and ancient carbonate depositional systems demonstrate that most of the sediment accumulating in peritidal marine carbonate settings was formed in the subtidal realm, and later transported to the marginal marine realm during storms, spring tides, and other energetic events (Demicco and Hardie, 1994). Therefore, an increasingly open marine environment must have existed outboard of tested intervals (**Figure 7**).

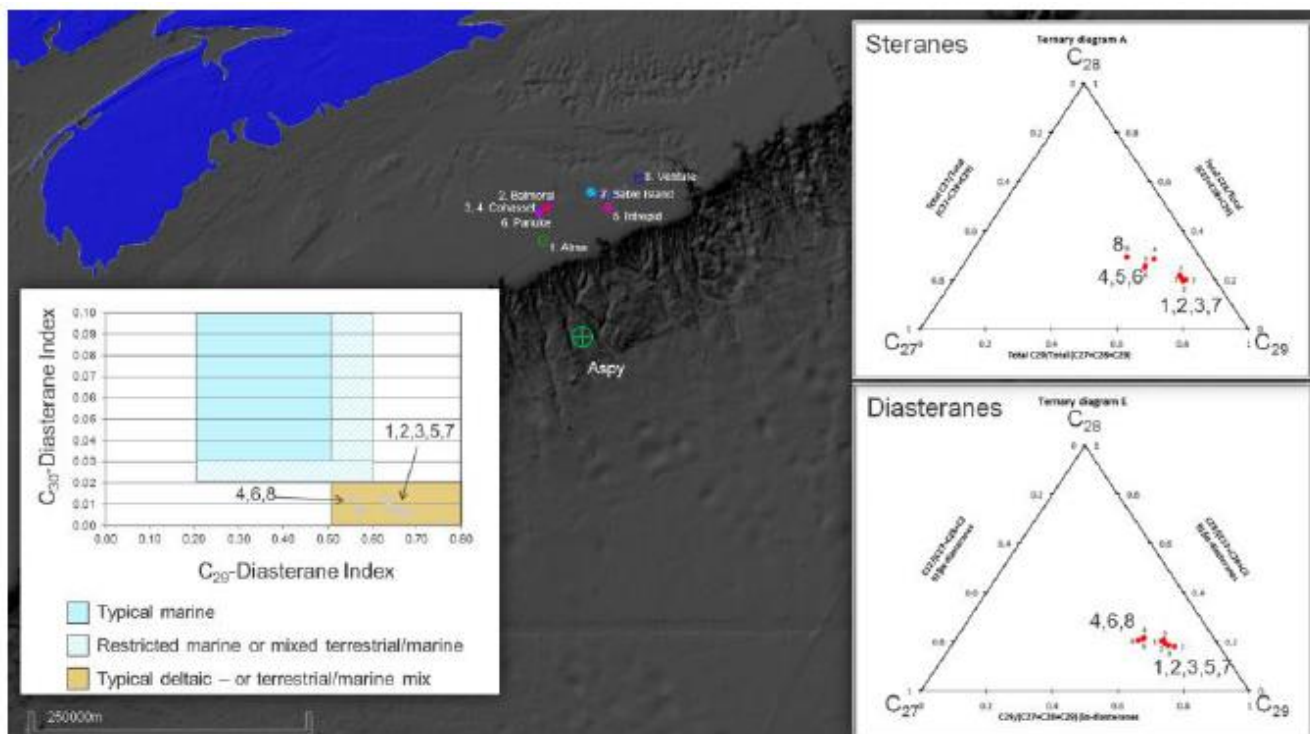


Figure 5. Sterane data of samples from wells in the Cohasset-Panuke oil and Sable Subbasin gas fields / discoveries indicates a mixed marine/non-marine shale typical of a deltaic source. Organic geochemical analysis of selected oils in wells from producing fields and discoveries/shows on the Scotian Margin reveal a locally sourced terrestrial prone Type III kerogen most likely originating from the Upper Jurassic Sable delta system. Predominance of C-29 Sterane and diasterane indicates source facies are likely mixed marine and non-marine shales with a high component of terrestrial input

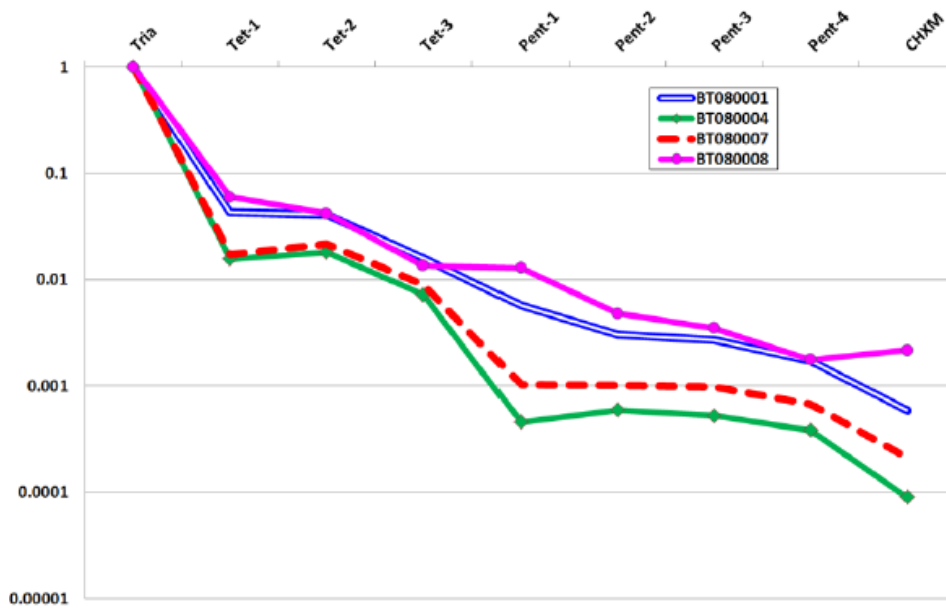


Figure 6. Quantitative Extended Diamondoid Analysis (QEDA) of four (Nos. 1, 4, 7 and 8) of the eight oils sampled in this study. Sample 8 (Venture B-13) is worth particular attention, as Pentamantane-1 higher than Tetremantane-3 and Pentamantane-2 as well as Cyclohexamantane higher than Pentamantane -4 has been observed in oils sourced from carbonate-dominated hypersaline systems (e.g., Smackover GoM) (Dahl et al., 2003; Moldowan et al., 2018).

MacLean and Wade (1993) infer a facies transition occurs from Pliensbachian/Toarcian Iroquois shallow water carbonates present in the Scotian Basin along the Nova Scotia margin to shales in the basin’s extension along the southern of the Grand Banks indicating the possibility that Jurassic source could exist in some areas. Seismic interpretation of these intervals yields evidence for the occurrence of carbonate buildups locally on fault block highs, as well as high amplitude, low impedance reflections in surrounding lows. On the Scotian Basin’s African conjugate, the concept of Lower Jurassic carbonate presence was confirmed by Chariot/ENI’s RD-1 (Rabat Deep) well completed in March 2018 (Reynolds, 2018). While the well was not a commercial success, tight, fractured carbonates were encountered as well as limited hydrocarbon indications. These results confirm both the presence of carbonates outboard, but probably also reflect that any source deposited at the time likely accumulated in geographically restricted areas.

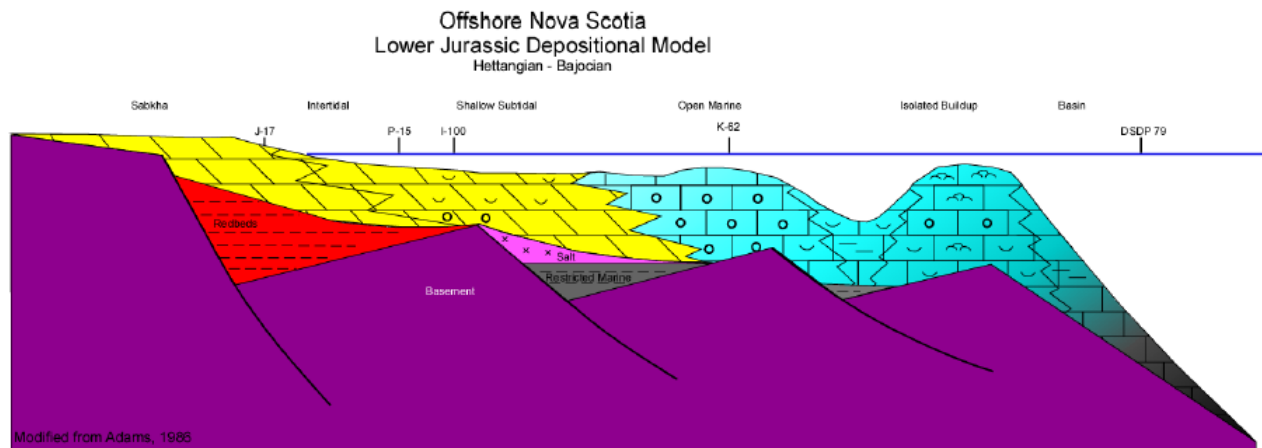


Figure 7. Block model of the Scotian lower-middle Jurassic depositional system modified after Adams (1986) to include both outboard open marine carbonates and restricted Subbasins housing source facies.



Evidence for Early Jurassic source presence

As organic geochemical evidence from produced oils indicated that the older component of the hydrocarbons were carbonate and/or evaporite-prone deposits, we turned our attention to these stratigraphic intervals. Several half grabens were identified and mapped just inboard of the Abenaki margin (**Figure 8**). These half grabens were suspected of being evaporite-prone (Weissenberger et al., 2006), but have until now not been investigated for source potential. Examination of seismic reflections from these half graben basins indicates high amplitude reflections are present that have AVO class IV response, like those identified for other source facies by Loseth et al., (2011). Genetic seismic inversion of the interval also indicates that half graben fill is likely mixed carbonate and mudrock (**Figure 9**) (Campbell, 2018). Finally, sulfur isotopic composition of evaporites sampled from the Upper Triassic Eurydice Formation in the Mohican I-100 well match those analyzed from H₂S produced from the Deep Panuke gas field (Weissenberger et al., 2006). The authors suggest charge to the field's Late Jurassic Abenaki Formation carbonate reservoirs may have migrated up faults from half grabens inboard of the shelf margin.

Conclusions

The results of organic geochemical analyses as well as evidence compiled from seismic mapping and facies analysis had led us to conclude that marine source rock facies along the continental margin of Nova Scotia are present at Lower and Upper Jurassic levels. Structural topography is a fundamental control on the distribution of interpreted lower Jurassic source rock facies, as the most likely location for viable source are in restricted half grabens inboard of the present-day shelf break. Later Jurassic source facies are more widespread, and likely represent higher-TOC members of the Verrill Canyon or equivalent formations.

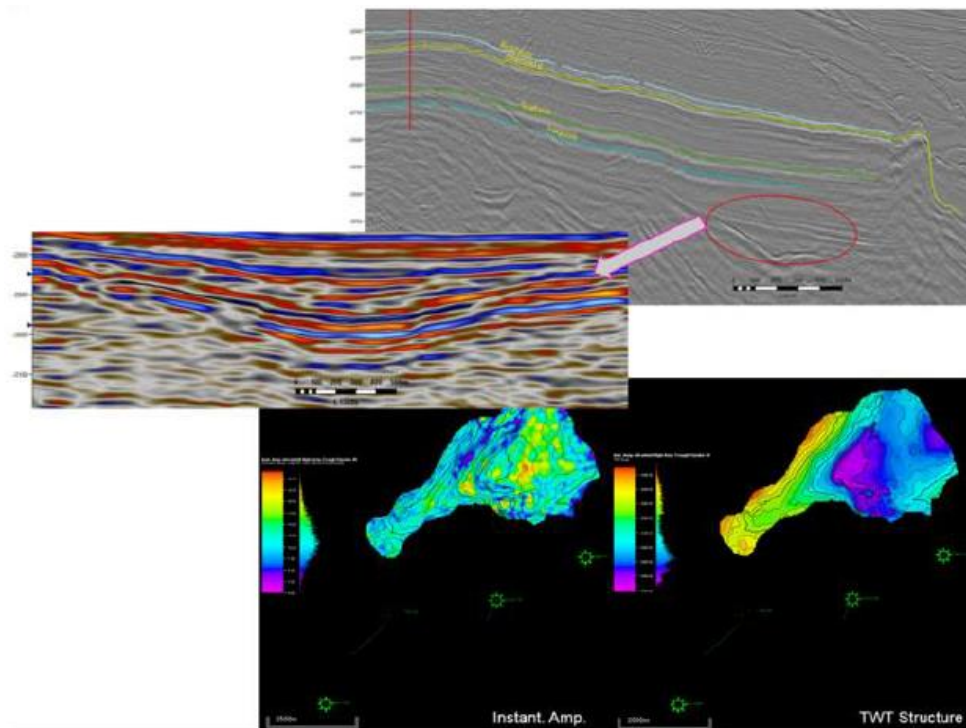


Figure 8. Seismic section from offshore Nova Scotia highlighting the half grabens occurring inboard of the Abenaki carbonate margins. These Late Triassic half grabens contain high amplitude reflections consistent with an AVO class IV response, which is often associated with source rock presence (Loseth et al., 2011). In addition, the highest amplitude reflections occur in the central portion of the half graben, suggesting a genetic link between the elements causing the high amplitude reflection and the structure itself.

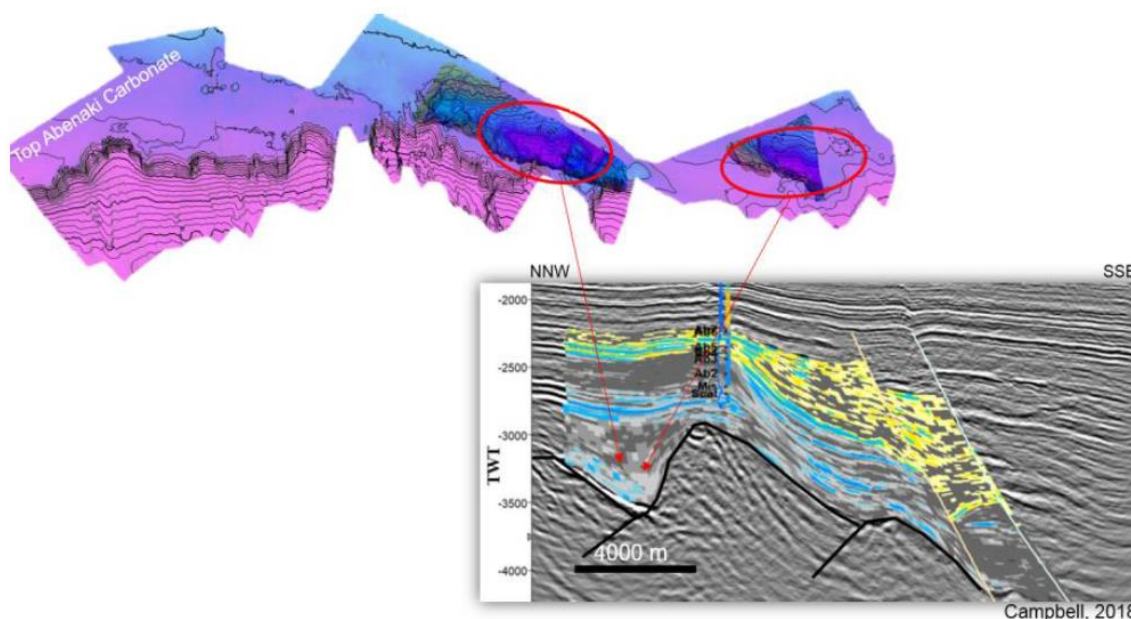


Figure 9. Mapped top Abenaki Formation (ca. Top Jurassic) showing the presence of half grabens interior to the margin system. Genetic seismic inversion within a geocellular model (inversion based on reflection amplitude and lithology log), bottom right, from Campbell (2018). These results closely match numerous soft events mapped within extensional half-grabens.

Acknowledgements

We want to thank Lorena Moscardelli, Jesus Ochoa, Laura Zahm, John Cody, and Ian Lunt (Equinor); David E. Brown and Mark Deptuck (CNSOPB); and Jeremy Dahl (Stanford University/Biomarkers, Inc.) for thoughtful contributions to this work.

References

- Adams, P.J., 1986. A Depositional and Diagenetic Model for a carbonate Ramp: the Iroquois Formation (early Jurassic), Scotian Shelf, Canada. Unpublished M.Sc. thesis, Dalhousie University, Halifax, Nova Scotia, Canada, 172p.
- Beaumont, C., Boutlier, R., MacKenzie, A.S., and Rullkotter, J., 1985. Isomerization and aromatization of hydrocarbons and the paleothermometry and burial history of the Alberta Foreland Basin. *American Association of Petroleum Geologists Bulletin*, **69**(4), 546-566.
- Campbell, T.J., 2018. Seismic Stratigraphy and Architecture of the Jurassic Abenaki Margin at Cohasset-Migrant and potential for distal organic-rich facies. Unpublished M.Sc. thesis, Dalhousie University, Halifax, Nova Scotia, Canada, 187p.
- Dahl, J.E., Moldowan, J.M., Peters, K.E., Claypool, G.E., Rooney, M.A., Michael, G.E., Mello, M.R., and Kohnen, M.L., 1999. Diamondoid hydrocarbons as indicators of natural oil cracking. *Nature*, **399**, 54-57.
- DeMicco, R.V., and Hardie, L.A., 1994. Sedimentary Structures and Early Diagenetic Features of Shallow Marine Carbonate Deposits. *SEPM Atlas Series No. 1*, 265p.
- Enachescu, M.E., Hogg, J.R., Fowler, M., Brown, D.E., and Atkinson, I., 2010. Late Jurassic Source Rock Super-Highway on Conjugate Margins of the North and Central Atlantic (offshore East Coast Canada, Ireland, Portugal, Spain and Morocco). II Central and North Atlantic Conjugate Margins Conference, Lisbon, 2010, Vol. II, Keynotes, 49-80.



- Hughes, W.B., Holba, A.G., Mueller, D.E., and Richardson, J.S., 1985. Geochemistry of greater Ekofisk crude oils. In: B.M. Thomas (ed) *Geochemistry in Exploration of the Norwegian Shelf*. Graham and Trotman, London, 75-92.
- Kolaczowska, E., Slougui, N.E., Watt, D.S., Marcura, R.E., and Moldowan, J.M., 1990. Thermodynamic stability of various alkylated, dealkylated, and rearranged 17a and 17b hopane isomers using molecular mechanics calculations. *Organic Geochemistry*, **16**(4-6), 1033-1038.
- Loseth, H., Wensaas, L., Gading, M., Duffaut, K., and Springer, M., 2011. Can Hydrocarbon Source Rocks be Identified on Seismic Data? *Geology*, **9**(12), 1167-1170.
- MacLean, B.C., and Wade, J.A., 1993, *Seismic Markers and Stratigraphic Picks in the Scotian Basin Wells*. East Coast Basin Atlas Series, Geological Survey of Canada, 276p.
- MacKenzie, A.S., and MacKenzie, D., 1983. Isomerization and aromatization of hydrocarbons in sedimentary basins formed by extension. *Geology Magazine*, **120**, 417-470.
- Moldowan, J.M., Dahl, J.E., Jarvie, D.M., Walker, D.D., Akbar, H., and Yurchenko, I., 2018. Application of Diamondoids for Correlation of very Mature Oil and Oil-Mixtures. American Association of Petroleum Geologists Annual Convention and Exhibition, July 23-25, 2018, Salt Lake City Utah, AAPG Search and Discovery Article No.90323 / Abstract No. 2833822.
- Offshore Energy Technical Research Association (OETRA), 2011. Nova Scotia Play Fairway Atlas. <http://www.oera.ca/offshore-energy-research/geoscience/play-fairway-analysis/pfa-atlas/>
- Peters, K.E., Walters, C.C., and Moldowan, J.M., 2005. *The Biomarker Guide*, Volumes 1 and 2. Cambridge University Press, 1155 p.
- Reynolds, E., 2018, Implications of Rabat Deep 1 Results. Edison Investment Research. <https://www.edisoninvestmentresearch.com/oils-blog/entry/implications-of-rabat-deep-1-results>
- Weissenberger, J.A.W., Wierzbicki, R.A., and Harland, N.J., 2006, Carbonate Sequence Stratigraphy and Petroleum Geology of the Jurassic Deep Panuke Field, Offshore Nova Scotia, Canada. In: P.M. Harris and L.J. Weber (eds), *Giant Hydrocarbon reservoirs of the World: From rocks to reservoir characterization and modeling*. American Association of Petroleum Geologists Memoir, **88**, 395-431.
-





THE RESULTS OF A MAJOR SOURCE ROCKS AND OILS STUDY OF THE NORTH ATLANTIC CONJUGATE MARGIN WITH A FOCUS ON OFFSHORE IRELAND

Hanrahan, Michael¹, English, Kara¹, Armstrong, James P.², and Atkinson, Ian³

¹ Petroleum Affairs Division (PAD), Department of Communications, Climate Action and Environment, 29-31 Adelaide Road, Dublin 2, D02 X285, Ireland, michael.hanrahan@dccae.gov.ie

² Petroleum Systems Limited, 30 Linden Walk, Prestatyn LL19 9EB, Wales, United Kingdom

³ Nalcor Energy Limited, 45 Hebron Way, St. John's, NL A1A 0P9, Canada

A comprehensive review of source rocks and oils from basins offshore Ireland was carried out as part of a major study to further understand the development and distribution of source rock facies and their resultant hydrocarbon products between basins, and, across the conjugate margin with Canada. The study included well data from all offshore Irish basins. The database from offshore Ireland includes source rock geochemical analyses from 153 wells and analyses of 38 oil samples supplemented by source rock extract analyses.

The interpretation of these data indicates that some 15 different source rock horizons exist in the Irish basins within Mesozoic and Early Cenozoic sediments. Oils in the Rockall Basin demonstrate a close affinity to oils in the North Sea and West Shetland due to the presence of 28,30 bisnorhopane sourced from the Upper Jurassic Kimmeridge Clay Formation, suggesting a possible palaeoenvironmental link at this time. Additionally, the Jurassic is an important proven source rock in the Slyne Basin where the Lower Jurassic is in the oil window. The Middle and Upper Jurassic were identified as the primary source of the oils found in the Porcupine Basin and all these oils display also a typical character of gammacerane that suggests a long-standing stratification of the water column within the basin. The Celtic Sea basins demonstrate Jurassic and Lower Cretaceous source rocks ranging from marine to lacustrine organofacies resulting in two main families.

The Irish oil samples were compared to oil samples from the Flemish Pass and Jeanne d'Arc Basins of Newfoundland-Labrador, and demonstrated that various source rock facies across the conjugate margin can be related to one another and grouped into families. We propose several "Super Families" of oils, including the regionally significant Upper Jurassic, highlighting numerous geochemical similarities attributed to analogous source facies across these basins.

This study is underpinned by possibly the most comprehensive oil and source rock dataset accumulated for the Canadian-Irish conjugate North Atlantic basins. From this, it is possible to directly compare the oils and the parent source rock facies within and between each basin. This is especially important in the under-explored portions of some basins (e.g. the southern Porcupine Basin) where there is a lack of well data. In conclusion, the results of the study have positive implications for petroleum prospectivity in basins offshore Ireland as well as other basins within the greater study area.

Introduction

This project involved a comprehensive review of source rocks and oils from basins offshore Ireland and was undertaken as part of a major study to further understand the development and distribution of source rock facies and their resultant hydrocarbon products between basins, and across the conjugate margin with Canada.

In the past, exploration in emerging frontier basins such as in eastern Canada and Ireland has been challenging due to water depth and remote conditions. However, the discoveries of major offshore fields in the Jeanne d'Arc and Flemish Pass Basins offshore Newfoundland have led to a substantial increase in interest and exploration effort. Ireland's Atlantic offshore basins (Porcupine, Goban Spur, and Rockall) are considered



generally the conjugate of Newfoundland-Labrador prior to the breakup of the North Atlantic Ocean in the Middle-Upper Jurassic. However, the significant volumes of oil discovered offshore Canada have not yet been found offshore Ireland despite a similar tectonic history and stratigraphy, and offshore Ireland remains underexplored.

This project is the compilation of a two-year study between the Irish Shelf Petroleum Studies Group (ISPSG) of Ireland's joint Government-Industry Petroleum Infrastructure Programme (PIP), and Nalcor Energy (on behalf of the Offshore Geoscience Data Program with the Government of Newfoundland and Labrador) as part of the North Atlantic Petroleum Systems Assessment (NAPSA) programme. The database and analyses were compiled by Beicip-Franlab. This study aimed to address a number of key questions, including:

- What are the important source rocks?
- Is there mixing of hydrocarbons?
- Can known oils be grouped into families?
- What similarities and differences in oil families and source rocks exist across the conjugate margin?

Tectonic History

The Irish Atlantic basins have a complex history involving rift tectonics, thermal subsidence and igneous activity. The Porcupine and Rockall basins both overlie thin continental crust due to major rift episodes in the Permo-Triassic, Upper Jurassic and Lower Cretaceous. A number of regional unconformities, controlled by both basin tectonics and regional processes, can be mapped and correlated throughout the Porcupine and Rockall basins using modern seismic datasets.

Objectives

The pre-break-up connectivity between Ireland and Newfoundland-Labrador and the correlation between source rock facies between basins is generally poorly constrained. In order to address this, the objectives of this study include:

- A comprehensive review of all available geochemistry data in Mesozoic basins offshore Ireland and Newfoundland-Labrador and the compilation into a single database.
- An extensive programme of new geochemical analyses and biostratigraphic data to further enhance interpretation and understanding.
- The characterisation of organo-facies on both margins and associated depositional environments, and classification of source rocks according to these organo-facies.
- The grouping of oils, per basin, into families and their corresponding organo-facies and source rocks.
- A comparison of the data within basins and across the conjugate margin in order to determine if correlations of oils and source rock facies can be established.

Methodology

An extensive database of all available non-confidential legacy source rock geochemical data was compiled (143 wells from offshore Newfoundland-Labrador and 93 wells from offshore Ireland). The Irish oil database contains 38 oil samples from 27 wells (**Figure 1**) and the Newfoundland-Labrador database 89 oil samples from 38 wells. Following a data gap analysis, a new analytical programme was undertaken:

- Source Rock: Including source rock kinetics and Rock-Eval pyrolysis, and log-derived TOC analysis.
- Oil samples and source rock extracts: Including SARA analysis, carbon isotopes, whole oil High Resolution Gas Chromatography (HRGC), GC-MS plus Kerogen Elemental Analysis, GC-MS/MS and CSIA on selected samples.
- Biostratigraphy to clarify the ages of identified organic rich intervals.

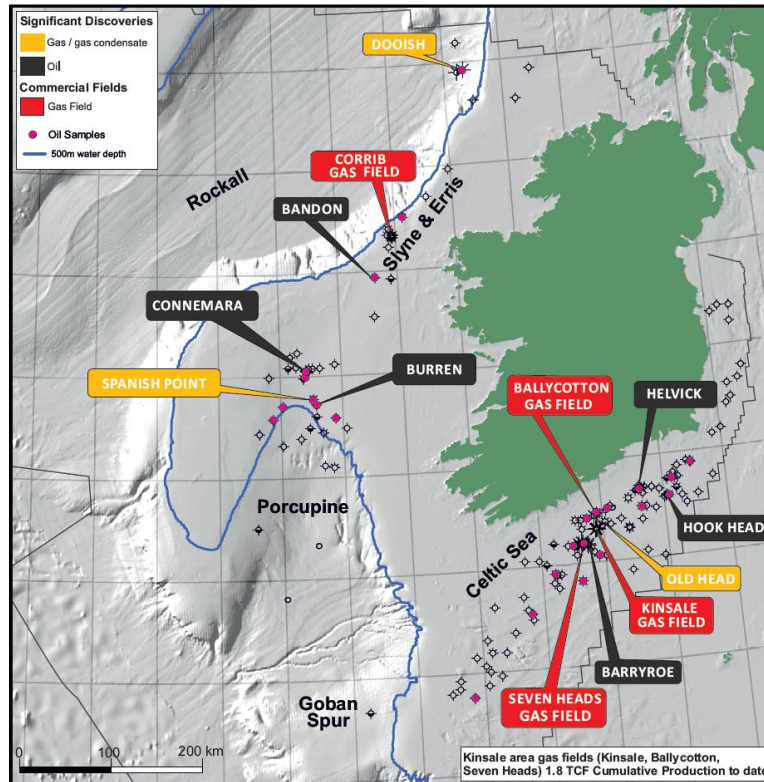


Figure 1: Map of Ireland's offshore showing well locations, commercial gas fields and significant discoveries. The 27 wells with oil samples used in the study are highlighted in pink.

Results

The interpretation of the data indicates that 15 different source rock horizons exist in the Irish basins within Mesozoic and Lower Cenozoic sediments. The Jurassic is demonstrated to contain the most regionally important source rocks in Ireland, with additional potential also identified in the Cretaceous (and the Carboniferous). In the Slyne Basin, the Lower Jurassic is an important proven source rock. Oils in the Rockall Basin demonstrate a close affinity to oils in the North Sea and West of Shetland due to the presence of 28,30 Bisnorhopane sourced from the Upper Jurassic Kimmeridge Clay Formation, suggesting a possible palaeoenvironmental link at this time. In the Porcupine Basin, the Upper Jurassic is identified as the primary source of the oils that all display a common character of gammacerane, suggesting a long standing stratification of the water column within the basin. The biomarker 28,30 Bisnorhopane found in the Rockall Basin oils however is not found in the Porcupine Basin oils (**Figure 2**) indicating the Rockall was separate from the Porcupine during the deposition of the Upper Jurassic (Kimmeridgian) source rock.

More recent biostratigraphic work in the Porcupine Basin has resulted in the re-dating of the previously interpreted Middle Jurassic source rock intervals, which are now interpreted to be Upper Jurassic (Mid-Upper Oxfordian) in age. However, the potential remains for the occurrence of Middle and Lower Jurassic source rocks in the basin. Oils in the Porcupine Basin have been grouped into three families, all interpreted as sourced from the Upper Jurassic (**Figure 3**). The Celtic Sea basins demonstrate Jurassic and Lower Cretaceous source rocks ranging from marine to lacustrine organo-facies resulting in two main families.

The Irish oil samples were compared to oil samples from the Flemish Pass and Jeanne D'Arc Basins of Newfoundland-Labrador, which demonstrated that various source rock facies across the conjugate margin can be



related to one another, and grouped into families. We propose several conjugate margins “Super Families” of oils, including the regionally significant Upper Jurassic, highlighting numerous geochemical similarities attributed to analogous source facies across these basins.

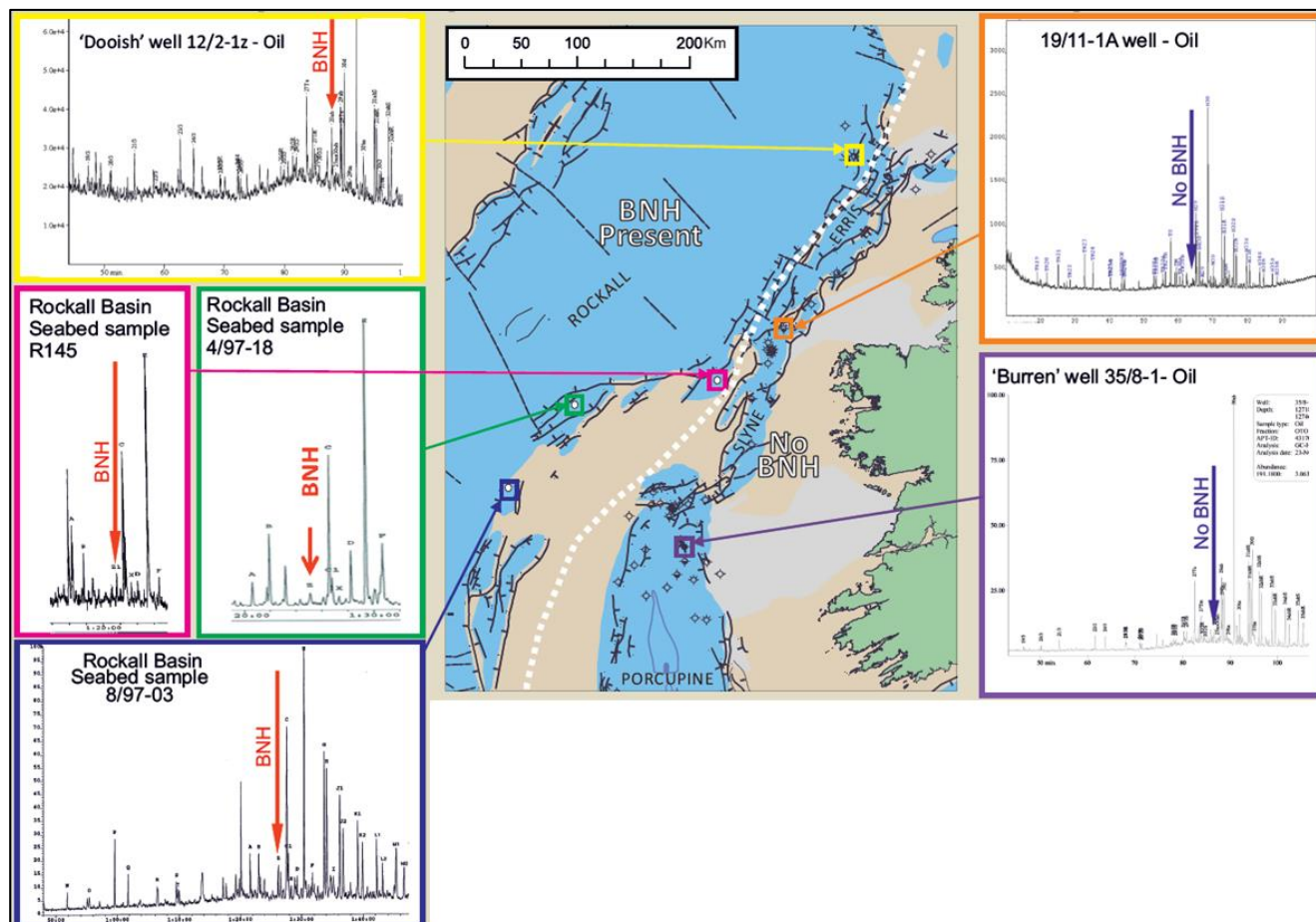
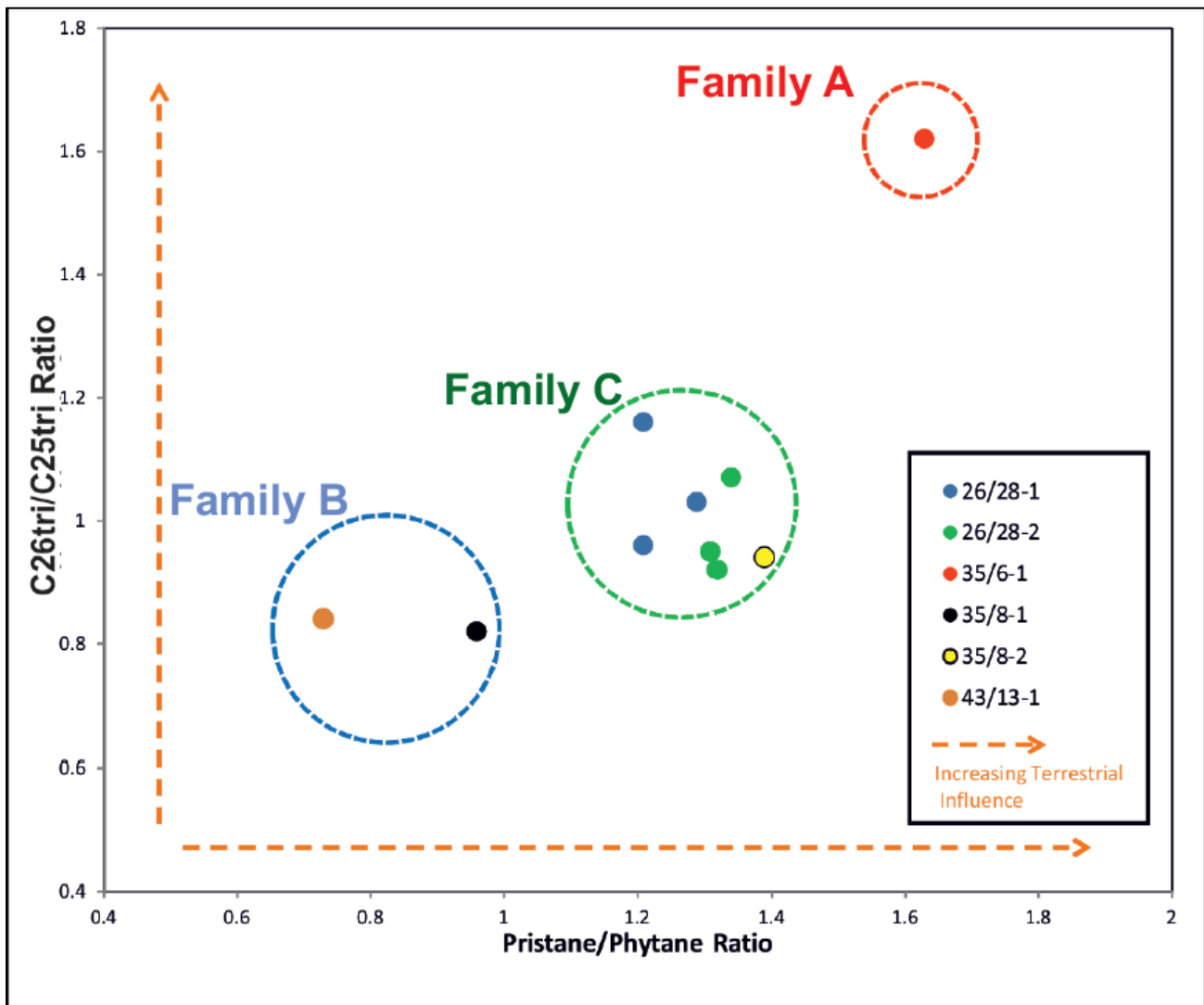


Figure 2: Oils in the Rockall Basin demonstrate a close affinity to oils in both East and West Shetland basins due to the presence of 28,30 Bisnorhopane sourced from the Upper Jurassic Kimmeridge Clay Formation Equivalent, suggesting a possible palaeoenvironmental link at this time. The Slyne, Erris, and Porcupine oils lack Bisnorhopane indicating the Rockall was separate from the Porcupine during the time of deposition of the Upper Jurassic source rock.

This study is underpinned by possibly the most comprehensive oil and source rock dataset accumulated for the Canadian-Irish conjugate North Atlantic basins. From this database, it is possible to directly compare the oils and the parent source rock facies within and between each basin. This regional compilation and assessment of the conjugate margin is especially important for source rock presence in the under-explored portions of some basins (e.g. the southern Porcupine Basin) where there is a lack of well data. In conclusion, the results of the study have positive implications for petroleum prospectivity in basins offshore Ireland as well as other basins within the greater study area.



	Pr/Ph	CPI	Gammacerane / Hopane	C355 / C34S homohopanes	Sterane / Hopane	Sterane distribution	C30 ββS sterane index	C26/C25 tricyclic terpene
Family Porcupine A	> 1	> 1.1	0,15 - 0,2	< 1	very low	High C29	< 4	> 1
Family Porcupine B	< 1 to 1	1 to 1,1	0,2 - 0,3	~ or > 1	> 1	C27/C29 ~ 1	> 7	< 1
Family Porcupine C	> 1	1 to 1,1	0,1 - 0,2	< 1	< 1	C27/C29 ~ 1	~ 5	~ 1

Figure 3: Pr/Ph ratio vs C26 tricyclic terpanes / C25 tricyclic terpanes diagram of Porcupine oil families and a summary table of oil families in the Porcupine Basin. Families represent different organo-facies of the Upper Jurassic.

Conclusions

- This study identified 15 source rocks across the area.
- Upper Jurassic sediments are the primary source rocks for the oils discovered in these basins to date.
- Locally other source rocks are important and mixing of oils from differing source rock organo-facies types is apparent.



- A number of organo-facies have been identified within the Porcupine Basin leading to the distinction of three oil families.
- Bisnorhopane is found in the Rockall Basin and is similar to West of Shetland and North Sea type Kimmeridge Clay equivalent indicating a Boreal influence. Bisnorhopane is not found in the Porcupine Basin.
- The establishment of a single database has allowed for a number of Trans-Atlantic source rock relationships to be recognised.
- This geochemical study provides a broad understanding of the petroleum geology of this transform margin and is key to wider exploration success especially in the under-explored parts of some basins.
- The results of the study have positive implications for the petroleum prospectivity in offshore basins on both sides of the conjugate margin.

Acknowledgements

This paper is derived from the Trans-Atlantic Geochemistry Project IS16/01 funded jointly by the Irish Shelf Petroleum Studies Group of Ireland's Petroleum Infrastructure Programme (PIP) and Nalcor Energy (on behalf of the Offshore Geoscience Data Program with the Government of Newfoundland and Labrador). The database and analysis was compiled by Beicip-Franlab with significant interpretation and project management from Jean-Marie Laigle, Samuel Piriou and Alain-Yves Huc. The project also greatly benefitted from the contribution of Steering Group members including James Carter (Nalcor Energy), Iain Scotchman (Statoil), Annemarie Smyth and Myles Watson (Providence Resources), Ranald Kelly, Andrew McCarthy and Gareth Parry (Woodside Energy), and Ramzi Ghenima, Paul Gannon and Martin Dashwood (Cairn Energy). Additional thanks to Martin Davies, Nick O'Neill, Charlie Carlisle and Alice Mitchinson (PIP), Oonagh O'Loughlin (PAD), Kim Welford (Memorial University), and Shane Tyrrell (NUI Galway).

References

Beicip-Franlab, 2017. Atlas of Source Rocks in Mesozoic Basins of the North Atlantic Conjugate Margin, Offshore Newfoundland-Labrador and Offshore Ireland. Proprietary report for Nalcor Energy (Newfoundland and Labrador) and Petroleum Infrastructure Program (Ireland).



3D SEISMIC GEOMORPHOLOGY OF PARALIC CHANNEL COMPLEXES, SABLE SUBBASIN, OFFSHORE NOVA SCOTIA

Kelly, Trevor, B.¹, and Wach, Grant, D.¹

¹Department of Earth Sciences, Dalhousie University, Life Sciences Centre, 1355 Oxford Street, Halifax, NS B3H 4R2, Canada, tbkelly@dal.ca

Extensive fluvial systems drained expansive areas of present-day Canada throughout the Late Jurassic to Late Cretaceous and deposited several kilometers of sediment within the Scotian Basin, offshore Nova Scotia. In the Logan Canyon Formation, and to a lesser extent the older Missisauga Formation, these fluvial complexes are prominent and can be imaged in the 3D seismic cube known as the Sable Megamerge. The fundamental objective of this research is to observe the temporal and spatial fluvial system architectural variations, with an appraisal of the controlling features that are affecting this variability. This will be achieved by integrating sequence stratigraphy and seismic geomorphology within the 3,000 km² study area.

The seismic cube was flattened on the surface representing the top of the Dawson Canyon Formation's Petrel Member (chalk, Turonian), and designated as the datum. The flattening process converts the seismic time slices into seismic horizon slices, showing sedimentary features in the depositional system. Seismic attributes are applied to allow the fluvial systems and their associated architectural elements to become more distinct on the horizon slice images. These horizon slices are combined with quantitative seismic geomorphology to obtain fluvial architecture parameters (channel width, meander-belt width, radius of curvature, meander wavelength, channel length, channel depth, and sinuosity). Well logs and conventional core 'ground truth' the seismic data. A qualitative analysis of fluvial systems in the study intervals defines the fluvial styles and the lateral spacing between channels. Characterizing these fluvial systems demonstrates the: 1) controlling factors and processes that lead to their formation, 2) reservoir-seal pairs, 3) reservoir heterogeneity within the Sable Subbasin, 4) relative times for deposition of each stratigraphic sequence, and 5), provides a catalogue of geometries and dimensions for the fluvial channel bodies in the study area within an overall deltaic depositional setting. These are applicable to reservoir modelling and simulation studies within the study area, or applied to similar reservoirs in other areas of the world.

Introduction

The ExxonMobil Sable Megamerge 3D seismic data set provides remarkable imaging of paralic channel systems throughout an estimated 1,000 m section of the Aptian to Cenomanian Logan Canyon Formation (Figure 1 and Figure 2). These channel systems are imaged precisely in the volumetrically flattened 3D seismic cube on seismic cross-sections and plan-view sections. From the interpretation of reflection geometries, amplitudes and other seismic attributes observed on the horizon slices, a variety of paralic depositional environments can be inferred spanning terrestrial and marine settings. In contrast, the underlying late Kimmeridgian to Aptian Missisauga Formation lacks the precisely defined channel systems and channel margins, which do not appear as frequently on horizon slices. The two formations were deposited in lower coastal plain and shallow marine environments (Wade and MacLean, 1990). The differences in seismic reflection geometries of the two formations is most likely the result of one or a combination of: 1) the Missisauga Formation being more proximally located in this area, 2) a higher influx of coarser clastic sediments/material during Missisauga Formation deposition, and/or 3), local differences in structural control on sedimentation. This study aims to examine the fluvial-related reservoir rocks within the Sable Subbasin, using 3D seismic geomorphic and seismic stratigraphic analysis, to study the



temporal and spatial fluvial system distribution within the two formations and their associated architectural complexities. Core and well logs were used to ‘ground truth’ the seismic data. This research will contribute to the understanding of fluvial systems within the Sable Delta; specifically, those within the Sable Megamerge 3D seismic dataset.

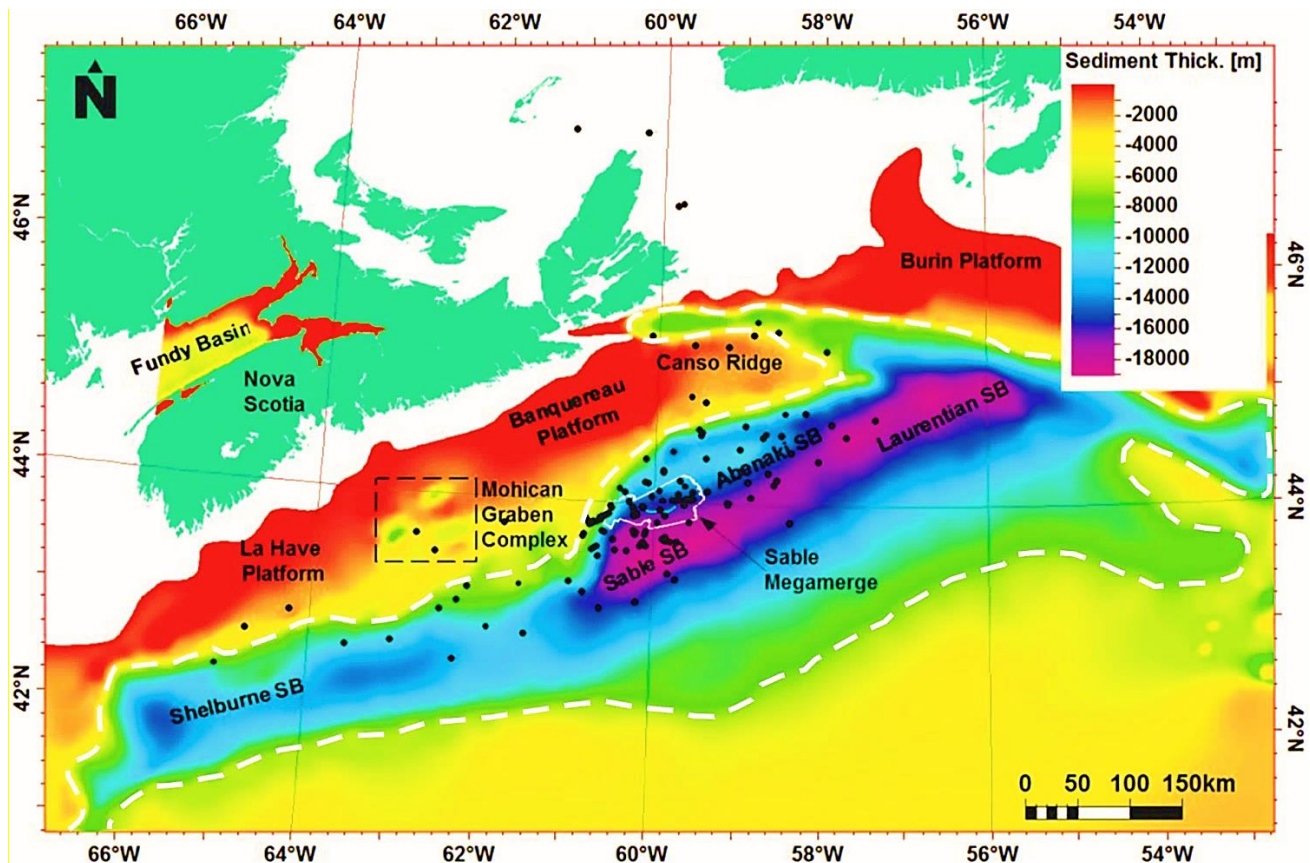


Figure 1: Map of the Sable Megamerge seismic survey area, shown with the solid white line. The Scotian Basin is outlined with the dashed white line. The colours represent sediment thickness (modified from Wade and MacLean 1990).

Study Area

The study area, located offshore Nova Scotia, Eastern Canada, is 300 km southeast of Halifax and 175 km southeast from the nearest point of mainland Nova Scotia. The area is part of the Sable Subbasin (ca. 63,000 km²) of the much larger Scotian Basin (ca. 300,000 km²; **Figure 1**). The Scotian Basin extends for approximately 1,200 km from the Yarmouth Arch (west of the Shelburne Subbasin) in the southwest to the Avalon Uplift (Burin Platform) of the Grand Banks in the northeast and contains 226 wells (MacLean and Wade, 1993; CNSOPB, 2019). Approximately half of the basinal area resides on the continental shelf in less than 200 m of water, while the remaining half resides on the continental slope in water depths extending to 4,000 m. The Sable Subbasin is a northeast-southwest trending rifted basin bounded in the north, southwest and northeast by the Missisauga Ridge, LaHave Platform, and Banquereau Syn-kinematic Wedge respectively. It is the main hydrocarbon-producing region in the Scotian Basin and within it is the 3,000 km² Sable Megamerge study area. The study area lies approximately 30 km from the edge of the continental shelf/continental slope transition within which are over 40 wells. A long, narrow slice of sand approximately 33 km long and at most 1 km wide, known as Sable Island resides within the study area.

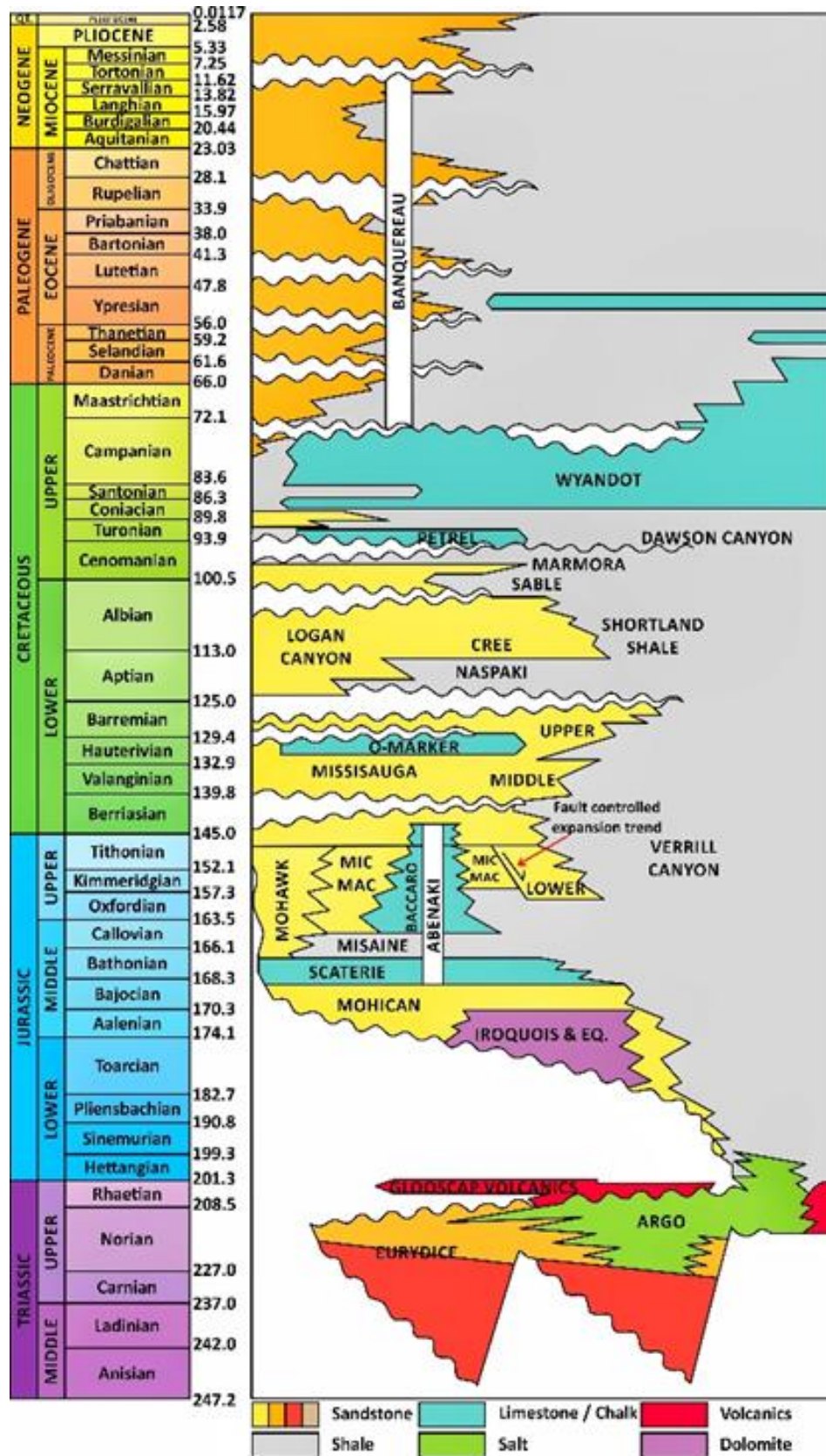


Figure 2: Stratigraphic column for the Scotian Basin. Formations are capitalized. The formations of interest are the Logan Canyon and Mississauga (modified after Wade and MacLean, 1990, and Campbell, 2017).



Dataset

The Sable Megamerge 3D seismic dataset was provided to the Dalhousie University Basin and Reservoir Laboratory in 2002 by ExxonMobil Canada Limited, and Sable Offshore Energy Project (SOEP) partners Shell Canada Limited, Imperial Oil Resources Limited, Pengrowth Corporation, and Mosbacher Operating Limited. The dataset is a post-stack merge of seven smaller, overlapping, varying vintage and operator 3D seismic surveys acquired in the Sable Subbasin near Sable Island. The surveys led to the higher definition and delineation of eleven existing significant gas discoveries made in the 1970s and 1980s. It has a high signal-to-noise ratio, stable zero phase, and a bandwidth of approximately ca. 10-60 Hz. These surveys were re-processed by ExxonMobil to normalize the data and allow for the merging of the separate volumes into one single seismic cube. This seismic volume was donated post-processing; therefore, the raw/original data was not available for analysis, nor were any notes provided regarding the processing parameters or methods of the raw data. No descriptions are available of the processing stream or pre-stack or pre-migration data. This exceptional dataset contains 2,640 inlines and 1,444 crosslines, both with spacing intervals of 37.5 m and a time slice range of 0 to -7,500 ms in 4 ms intervals for a total of 1,875 time-slices. Inline lengths are up to 54,114.30 m with crossline lengths being up to 98,962.87 m. There are 41 exploration/delineation and 17 development wells in the Megamerge survey area. The digital wireline data for the wells was donated by Divestco, and well and seismic data, technical papers, and reports available from the Canada- Nova Scotia Offshore Petroleum Board (CNSOPB) Data Management Centre.

Background

Geology

The Scotian Basin developed on a passive continental margin during the break-up of Pangaea as the North American plate detached from the African plate (Wade and MacLean 1990). Through Middle Triassic rifting, the Scotian Basin and several interconnected rift basins formed (Jansa and Wade 1975; Wade and MacLean, 1990). Within the Scotian Basin (**Figure 2**), the Logan Canyon Formation (125-94 Ma; ca. 1,100 m thick) represents deposition in a broad coastal plain and shallow shelf environment, comprising thick paralic facies (interfingered marine and continental sediments) and sequences of alternating, fining upward sandstone and shale (Jansa and Wade 1975; Wade and MacLean, 1990). The Missisauga Formation (145-125 Ma; ca. 1,100 m thick) is composed of slightly argillaceous, massive sandstone, separated by thin siltstone/shale beds with rare thin limestone layers, and was probably deposited by a major river system during the Early Cretaceous (Wade and MacLean 1990). These form the reservoir seal pairs.

Reservoir Rocks and Distribution

A reservoir rock is a critical component of a petroleum system and defined as a subsurface rock formation having a discrete and separate natural accumulation of moveable hydrocarbons restricted by impermeable rock or water barriers and having a single-pressure system (Society of Petroleum Engineers (SPE), 2005). Porosity and permeability are essential components, with typical porosity values ranging from 5 – 30 % and permeability values ranging from 1–1,000⁺ millidarcys (Tissot and Welte 1984). They fall under three types: siliciclastic (most abundant), carbonate, and igneous/metamorphic (very rare). The thick sands of the Mic Mac (~ 1,300 m thick), Missisauga (ca. 1,100 m thick) and Logan Canyon (ca. 1,100 m thick) formations are common on the Scotian Shelf, and depending on their location have very high sand-to-shale ratios making them good reservoir rock candidates (Wach et al., 2014).



Fluvial Morphometric Parameters

3D seismic reflection data can allow for quantitative data extraction of fluvial system architecture, which is commonly used in reservoir models to constrain fluvial sand body geometry (e.g. Posamentier, 2001; Miall, 2002; Carter, 2003). This technique was termed ‘quantitative seismic geomorphology’ by Wood (2003). Typical parameters include meander length (ML), meander-belt width (MBW), channel length (CL), channel width (CW), radius of curvature (RC), channel depth (CD) and sinuosity (SI) (**Figure 3**). The CL is determined from the length along the channel centerline between the lower- and upper-most inflection points (Alqahtani, 2010). Empirical equations have been developed over the years to predict quantitative values for subsurface channel bodies (e.g. Leopold and Wolman, 1960; Leeder, 1973; Collinson, 1977; Lorenz et al., 1985; Fielding and Crane, 1987). Leeder (1973) plotted 104 measures of published empirical data on CD and CW to develop a relationship for channels with SI and an empirical relationship for modern fluvial channels between CW and MBW. Collinson (1977) used data collected by Carlston (1966) to establish a relationship between MBW and CD. Fielding and Crane (1987) completed a study predicting MBW from basic sandstone thickness data. They compiled published data from 45 sources relating modern/ancient fluvial MBW to CD and demonstrated broad positive relationships between CD and MBW, governed by different channel types.

Five empirical relationships were observed. Leopold and Wolman (1960) developed an empirical equation between ML and CW for modern channels with high SI. Leopold and Wolman (1960) also established a relationship between ML and RC using data from meandering fluvial systems. Collinson (1977) also developed a mathematical relationship between ML and CD. A comprehensive study by Gibling (2006) presented a channel-body geometry terminology review and assembled a data set of more than 1,500 bedrock/Quaternary fluvial bodies of which CW and CD were known. A dozen channel body and valley fill types were classified based on geometry, geomorphic setting, internal structure and CW vs CD log-log plots (Gibling, 2006).

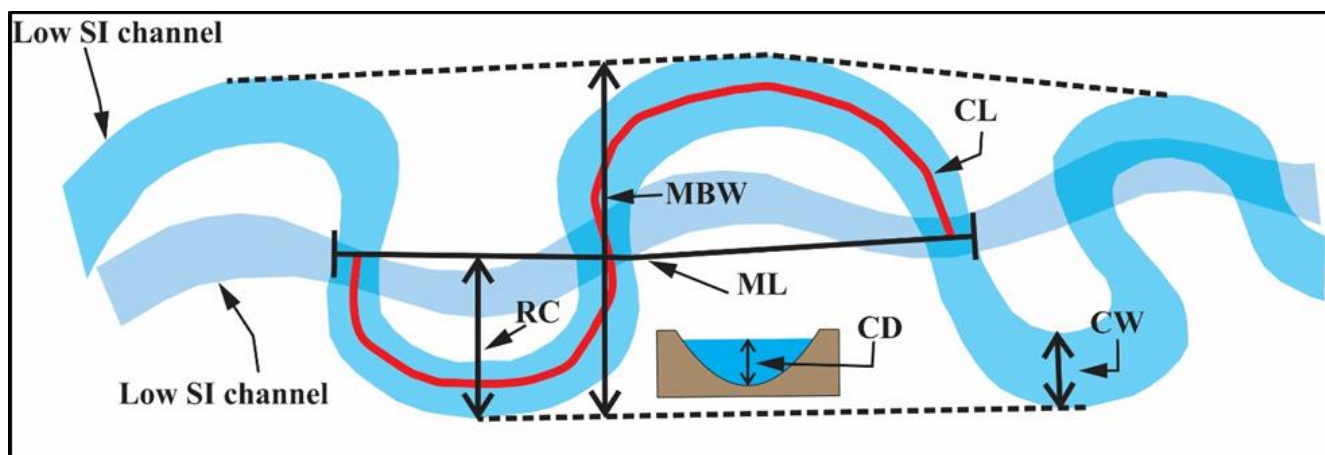


Figure 3: Illustration showing the typical parameters measured from channel bodies for quantitative data collection.

Quantitative Seismic Geomorphology

Geoscientists recognize the benefits of quantitative data extraction of geomorphological parameters from seismic data of precisely-imaged depositional systems in a variety of settings (e.g. Wood 2007; Darmadi et al., 2007; El-Mowafy and Marfurt, 2016; Alqahtani et al., 2017). Wood (2007) applied quantitative seismic geomorphology to a 900 km² area of the northern Gulf of Mexico. Pliocene and Miocene depositional environments, namely fluvial, deltaic, shallow marine, shelf-edge, slope and fan settings, were examined using a 3D seismic and well logs. SI, ML, CW, and meander-belt width were measured and paired with lithologic data from well logs and core to predict the spatial distribution of fluvial elements in the reservoir (Wood, 2007).



Darmadi et al. (2007) used a 680 km² seismic data set from the west Natuna Basin, offshore Malaysia to delineate vertical changes in fluvial architecture within the Pleistocene to Holocene Muda Formation. CD, CW and SI were plotted against stratigraphic position and a global sea-level curve. Results indicated channel parameters changing vertically from wide low-sinuosity channels to smaller highly sinuous channels during lowstand and transgression respectively, within each identified sequence (Darmadi et al., 2007). Channel pattern variability was controlled less by sea level changes and more by discharge variations (sediment load) during aggradation. El-Mowafy and Marfurt (2016) applied seismic geomorphology techniques to the Oligocene middle Frio Formation fluvial systems of south Texas for constructing predictive models of fluvial reservoirs. Results indicated a substantial downstream decrease in channel belt widths along channel belt lengths. This provided valuable information for future exploration and development within the remaining Texas Gulf Coast Basin and other similar reservoirs. Recently, Alqahtani et al. (2017) used a time-migrated 3D seismic data set covering 11,500 km² of the Pleistocene to Recent offshore Malay Basin, Sunda Shelf, southeast Asia to evaluate geometry, distribution, evolution and dimensions of “humid-tropical fluvial channel systems”. The seismic expression and variations in channel depth and sinuosity indicated six fluvial channel types within eight seismic units from 18–145 m thick.

Methods

Seismic Interpretation

Petrel™ software was employed to determine fluvial system types and map their lateral extent within the Logan Canyon and Missisauga formations. Formation tops defined by Wade and MacLean (1990) for the Scotian Basin correspond to lithological variations, identified by sharp changes in seismic characteristics. These correspond to acoustic impedance contrasts between lithological units. The rock type can be estimated with seismic attribute analysis, core and well logs, allowing fluvial channel bodies to be distinguished.

Volumetric Flattening

Volumetric flattening is a process whereby 3D seismic volumes are automatically flattened/converted into horizon slice volumes (Lomask and Guitton, 2007). As reported by Parks (2010), the method attempts to reverse geologic processes by removing the geologic structure present in a seismic image and transforming the image into layers as they were deposited. To flatten the seismic volume, the local dips (step-outs) for the entire seismic volume are calculated using a dip estimation technique, where the dips are resolved into time-shifts or depth-shifts by way of an efficient non-linear least-squared solution (Lomask and Guitton, 2007). The seismic volume data are shifted vertically, either in the positive or negative sense, according to the summed time-shifts, to output a flattened seismic volume. This results in portions of the original image being squeezed and stretched in areas to flatten the features (Lomask and Guitton, 2007; Parks, 2010). The seismic data will be flattened on the expansive, carbonate-dominated Petrel Member (Turonian) flooding surface (datum), attempting to revert the features in the Logan Canyon and Missisauga formations back to the time of their deposition. This will be helpful in showing whether major channel positions persist in nearly the same location through time, or move variably across the area. Channel positions through time can be used to determine if channel clustering (e.g. Hajek et al., 2010; Hofmann et al., 2011) is present, which concentrates sand in certain areas, influencing reservoir distribution, net-to-gross ratio and heterogeneity.

One Dimensional Stochastic Inversion (ODiSI)

A One-Dimensional Stochastic Inversion was performed on the Sable Megamerge to delineate, quantify, and qualify the reservoir sands of the Logan Canyon Formation. This inversion method was initially developed by British Petroleum (BP) and works by creating a large set of pseudo-wells (1,000-20,000) for each seismic trace



position using well log data (P/S-wave velocity, density, total porosity, shale volume, water/hydrocarbon saturation, and lithology) populated from actual wells (Casteleyn et al., 2017). Synthetic seismic traces created from each pseudo well are statistically matched to the seismic trace (Casteleyn et al., 2017). Normally, the properties associated with the 30 best matching pseudo wells are averaged to obtain different outputs, such as the average net reservoir fraction, porosity, and hydrocarbon pore volume, along with their corresponding uncertainties (standard deviation), and lithofacies probabilities at each trace location (Casteleyn et al., 2017). The results will present a delineation of reservoir quality sands, provide new definition of zone bounding surfaces and alternative structural interpretations (e.g. faults) (Casteleyn et al., 2017).

Qualitative Seismic Geomorphology

This method requires the integration of volumetric flattening, the application of seismic attributes and seismic interpretation to perform a comprehensive examination of the Logan Canyon and Missisauga intervals to develop a qualitative description and database of channel bodies from seismic horizon slices and cross-sections. This requires classifying the fluvial channel bodies in the study area based on their dimensions, architecture and geomorphic setting for the analysis of the 3D form, internal architecture and geometry of channel bodies.

Quantitative Seismic Geomorphology

This involves the measurement and calculation of the typical morphometric parameters. The measurement of fluvial morphometric parameters will be applied using the ArcGIS Software Platform (hereinafter referred to as ArcGIS); a specialized geographic information system software platform that is used extensively for working with maps and geographic information. New empirical equations will be developed for the study area using the measured and calculated parameters, followed by a comparison to published standard equations.

Well Logs and Core

Well log data and core will help ‘ground truth’ lithology and are useful where wells penetrate channel bodies. A detailed suite of well logs is also available, including sonic, density, resistivity and gamma ray logs. Physical core is available for many wells drilled within the study area and is stored at the Canada-Nova Scotia Offshore Petroleum Board (CNSOPB) Geoscience Research Centre.

Results and Significance

This research contributes to the understanding of fluvial systems within the Sable Delta; specifically, those within the Sable Megamerge 3D seismic data set. The measured/calculated morphometric parameters could be used for the development of detailed reservoir analogs (models) for the poorly-imaged areas of offshore Nova Scotia. Through the application of volumetric flattening and seismic attribute analysis, valuable insight pertaining to the modes of deposition are determined and it provides information on the space and time characteristics of the fluvial systems observed, leading to inferences on the length of stratigraphic cycles (1st, 2nd, 3rd, or 4th order). This study will help to confirm the dimensions of fluvial systems for the benefit of petroleum exploration and development within the Subbasin and may be beneficial for similar reservoirs worldwide.

References

Alqahtani, F.A., 2010. 3D Seismic Geomorphology of Fluvial Systems. Unpublished Ph.D. thesis, Department of Earth Science and Engineering, Imperial College, London, England, 317 p., doi: 10044/1/6180.



- Alqahtani, F.A., Jackson, A.-L., Johnson, H.D., and Som, M.R.B., 2017. Controls on the geometry of humid-tropical fluvial systems: Insights from 3D seismic geomorphological analysis of the Malay Basin, Sunda Shelf, southeast Asia: *Journal of Sedimentary Research*, **87**, 17-40, doi: 10.2110/jsr.2016.88.
- Campbell, T., 2017. Seismic Stratigraphy and Architecture of the Jurassic Abenaki Margin, at Cohasset-Migrant, and Potential for Distal Organic-Rich Facies. Unpublished M.Sc. thesis, Department of Earth Sciences, Dalhousie University, Halifax, Nova Scotia, Canada, 187p.
- Canada-Nova Scotia Offshore Petroleum Board (CNSOPB), 2019. Directory of Offshore Wells – January 2019. https://www.cnsopb.ns.ca/sites/default/files/pdfs/DOW_Jan_2019.pdf Accessed January 4, 2019.
- Casteleyn, L., Ashton, P., D'Alessandria, A., Connolly, P., and Sayer, J., 2017. Central North Sea, Upper Jurassic Fulmar Inversion Case Study. *Cegal*, 1-15.
- Carlston, C.W., 1966. The effect of climate on drainage density and streamflow: *International Association of Scientific Hydrology Bulletin*, **11**, 62-69, doi: 10.1080/02626666609493481.
- Carter, D.C., 2003. 3-D seismic geomorphology: Insights into fluvial reservoir deposition and performance, Widuri field, Java Sea. *American Association of Petroleum Geologists Bulletin*, **87**(6), 909-934, doi: 10.1306/01300300183.
- Collinson, J.D., 1977. Vertical sequence and sand body shape in alluvial sequences. In: A.D. Miall (ed), *Fluvial Sedimentology*. Canadian Society of Petroleum Geologists Memoir, **5**, 577-586.
- Darmadi, Y., Willis, B.J., and Dorobek, S.L., 2007. Three-dimensional seismic architecture of fluvial sequences on the low-gradient Sunda Shelf, offshore Indonesia. *Journal of Sedimentary Research*, **77**, 225-238, doi: 10.2110/jsr.2007.024.
- El-Mowafy, H.Z., and Marfurt, K.J., 2016. Quantitative seismic geomorphology of the middle Frio fluvial systems, south Texas, United States. *American Association of Petroleum Geologists Bulletin*, **100**(4), 537-564, doi: 10.1306/02011615136.
- Fielding, C.R., and Crane, R.C., 1987. An application of statistical modeling to the prediction of hydrocarbon recovery factors in fluvial reservoir sequences: *The Society of Economic Paleontologists and Mineralogists, Special Publication*, **39**, 321–327, doi: 10.2110/pec.87.39.0321.
- Gibling, M.R., 2006. Width and thickness of fluvial channel bodies and valley fills in the geological record: A literature compilation and classification. *Journal of Sedimentary Research*, **76**, 731-770, doi: 10.2110/jsr.2006.060.
- Jansa, L.F., and Wade J.A., 1975. Geology of the Continental Margin off Nova Scotia and Newfoundland. In: W.J.M. Van Der Linden and J.A. Wade (eds) *Offshore Geology of Eastern Canada*. Geological Survey of Canada Paper 74-30, Volume 2, 51-105., doi: 10.4095/123963.
- Leeder, M.R., 1973. Fluvial fining-upward cycles and the magnitude of palaeochannels. *Geological Magazine*, **110**, 265-276, doi: 10.1017/S0016756800036098.
- Leopold, L.B., and Wolman, M.G., 1960. River Meanders. *Geological Society of America Bulletin*, **71**(6), 769-794, doi: 10.1130/0016-7606(1960)71[769:RM]2.0.CO;2.
- Lomask, J., and Guitton, A., 2007. Volumetric flattening: an interpretation tool. *The Leading Edge*, **26**, 888-897, doi: 10.1190/1.2756869.
- Lorenz, J.C., Heinze, D.M., Clark, J.A., and Searls, C.A., 1985. Determination of Widths of Meander-Belt Sandstone Reservoirs from Vertical Downhole Data, Mesaverde Group, Piceance Creek Basin, Colorado. *American Association of Petroleum Geologists Bulletin*, **69**(5), 710-721.
- MacLean, B.C., and Wade, J.A., 1993. Seismic Markers and Stratigraphic Picks in the Scotian Basin Wells. *East Coast Basin Atlas Series*, Geological Survey of Canada, 276p.



- Miall, A.D., 2002. Architecture and sequence stratigraphy of Pleistocene fluvial systems in the Malay Basin, based on seismic time-slice analysis. *American Association of Petroleum Geologists Bulletin*, **86**(7), 1201-1216, doi: 10.1306/61EEDC56-17E-11D7-8645000102C1865D.
- Parks, D., 2010. Seismic image flattening as a linear inverse problem. Unpublished M.Sc. thesis, Mathematical and Computer Sciences, Colorado School of Mines, Golden, Colorado, USA, 4p.
- Posamentier, H.W., 2001. Lowstand alluvial bypass systems: Incised vs. unincised. *American Association of Petroleum Geologists Bulletin*, **85**(10), 1771-1793, doi: 10.1306/8626D06D-173B-11D7-8645000102C1865D.
- Society of Petroleum Engineers, 2005. Glossary of Terms Used in Petroleum Reserves/ Resources, Definitions. http://www.spe.org/industry/docs/GlossaryPetroleumReserves-ResourcesDefinitions_2005.pdf, Accessed June 14, 2018.
- Tissot, B., and Welte, D.H., 1984. *Petroleum formation and occurrence*. Second Edition, Springer Verlag, Heidelberg.
- Wach, G., Pimentel, N., and Pena dos Reis, R., 2014. Petroleum systems of the Central Atlantic margins, from outcrop and subsurface data. In: J. Pindell, B. Horn, N. Rosen, P. Weimer, M. Dinkeleman, A. Lowrie, R. Fillon, J. Granath, and L. Kennan (eds), *Sedimentary Basins: Origin, Depositional Histories, and Petroleum systems of Continental Margins of the World*. Proceedings of the 33rd Annual Gulf Coast Section SEPM Foundation Bob F. Perkins Conference, 26-28 January, 2014, Houston, Texas, TX, CD, 1-20.
- Wade, J.A. and MacLean, B.C., 1990. Chapter 5 - The geology of the southeastern margin of Canada, Part 2: Aspects of the geology of the Scotian Basin from recent seismic and well data. In: M.J. Keen and G.L. Williams (eds), *Geology of Canada No.2 - Geology of the continental margin of eastern Canada*. Geological Survey of Canada, 190-238.
- Wood, L.J., 2003. Quantitative seismic geomorphology and reservoir architecture of clastic depositional systems; the future of uncertainty analysis in exploration and production. Annual Meeting Expanded Abstracts - American Association of Petroleum Geologists, United States, AAPG and SEPM: Tulsa, OK, 182.
- Wood, L.J., 2007. Quantitative seismic geomorphology of Pliocene and Miocene fluvial systems in the northern Gulf of Mexico, U.S.A. *Journal of Sedimentary Research*, **77**, 713-730, doi: 10.2110/jsr.2007.068.
-





INVESTIGATING THE PRESENCE OF BOUDINAGE STRUCTURES OFFSHORE NEWFOUNDLAND USING GEOPHYSICAL DATA

MacDougall, Malcolm, D.J.¹, Braun, Alexander¹, and Fotopoulos, Georgia¹

¹Department of Geological Sciences and Geological Engineering, Queen's University, Kingston, ON K7L 3N6, Canada, malcolm.macdougall@queensu.ca

The evolution of the passive margin off the coast of Eastern Canada is characterized by a series of rifting episodes resulting in widespread extension of the crust and associated structural anomalies, some with the potential to be classified as boudinage structures. These features are segments within the subsurface formed during lithospheric stretching and rifting, which begin as pinch-and-swell structures among structurally competent layers of strata bound by incompetent layers, and later separate into discrete boudins. Crustal thinning of competent layers is often apparent in seismic sections or appears as repeating elongated anomalies in gravity and magnetic surveys.

In general, boudinage at the lithospheric scale develops undulation wavelengths approximately four times the competent layer thickness. Additionally, the presence of listric faults and Moho undulations are thought to be related to these regimes and have been identified in gravity, magnetic and seismic surveys. By comparing the evolution of the Grand Banks to other examples of passive margins where boudinage has been suggested as a driving mechanism, it is reasonable to explore the potential of the same structures being present in the Newfoundland margin. Some useful analogues include the Greenland-Norway and Brazil-West Africa conjugate margins, the South China Sea and the Basin and Range province in the western United States.

This investigation will supplement our knowledge of the aforementioned examples with a thorough investigation of seismic, gravity and magnetic signatures, in order to determine if boudinage structures are evident in the context of the Grand Banks. The identification of boudinage in geophysical data here is challenging because it is a more complex passive margin segment. However, the application of these methods to the Grand Banks is valuable due to the economic prospects, the potential for increasing geological knowledge of the area, as well as validating existing model results of extensional margin evolution.

Introduction

The mechanism, “boudinage” (from the French, meaning blood sausage) refers to the creation of pinch-and-swell structures within a body of varying competencies (Ramberg, 1955; Smith, 1977; Ricard and Froidevaux, 1986; Goscombe et al., 2004). When there are layers of differing rheologies – some more structurally competent than others – an extensional stress field is applied to stretch them apart, the competent layers are transformed into ellipsoidal structures, which eventually split into discrete segments also known as *boudins*. They are typically more recognizable in sections parallel to the long axis of the boudins and may appear as a series of repeated elongate structures in gravity anomaly maps. In general, the competent layers will split by faulting or fracturing, exhibiting brittle deformation, and the surrounding incompetent layers behave with ductile deformation, resulting in plastic flowage to occupy the space generated from the brittle deformation (Fossen, 2010). From Ramberg (1955), the terms competent and incompetent are relative and generally correspond to materials which are either brittle and do not deform by plastic flow or are ductile and do deform by plastic flow, respectively.

According to Ribeiro (2002), the ratio of dominant wavelength to layer thickness is approximately four (also from Smith, 1975, 1977). For the wavelengths observed in this study, the boudinage mechanism would correspond to intervals within the lithosphere, such as the upper crust or upper mantle. In some cases, there may



be two separate layers of boudinage within the lithosphere, as discussed by Froidevaux (1986). Supporting this is the fact that the strength of the lithosphere varies with depth, as the lower crust is ductile relative to the upper crust, and the upper mantle is relatively brittle compared to the lower crust (Kearey et al., 2009).

The Grand Banks evolved as successive rifting episodes gradually opened up the North Atlantic Ocean, separating North America from northern Africa and Eurasia. The first rift episode to impact eastern Canada was the *Tethys Phase* approximately 200 million years ago between the Late Triassic and Early Jurassic periods. During this time, the conjugate Scotian and Moroccan margins split apart and coevally basins began to form in the Grand Banks as half grabens slipping down large detachment faults (Enachescu, 1987; Sinclair, 1994; Husky Oil Operations Ltd., 2001; and Enachescu and Fagan, 2004).

During the late Jurassic-early Cretaceous (ca. 160 Ma), rifting in the North Atlantic Phase split the southern Grand Banks away from the conjugate Iberian margin, and introduced oceanic crust as far north as the Newfoundland Transform Fault Zone, which currently bounds the southern edge of the Grand Banks (Sinclair, 1994; Husky Oil Operations Ltd., 2001; Enachescu and Fagan, 2004). This was also the first instance the Grand Banks experienced extension at an angle oblique to the rotated fault blocks from the first rifting episode.

Finally, during the mid-Cretaceous approximately 120 million years ago, the *Labrador Phase* caused rifting towards the northwest, separating the rest of the Grand Banks from the British Isles and eventually Greenland. During this time, the basins experienced intense fragmentation because of their relatively sub-perpendicular orientation compared to the initial rifting phase (Enachescu, 1987; Sinclair, 1994).

In the case of the Grand Banks, it is likely that multiple phases of extensional rifting have led to more than one instance of boudinage, which are observable as successively amplified and overprinting structures in the seismic, gravity and magnetic data.

Data Analysis

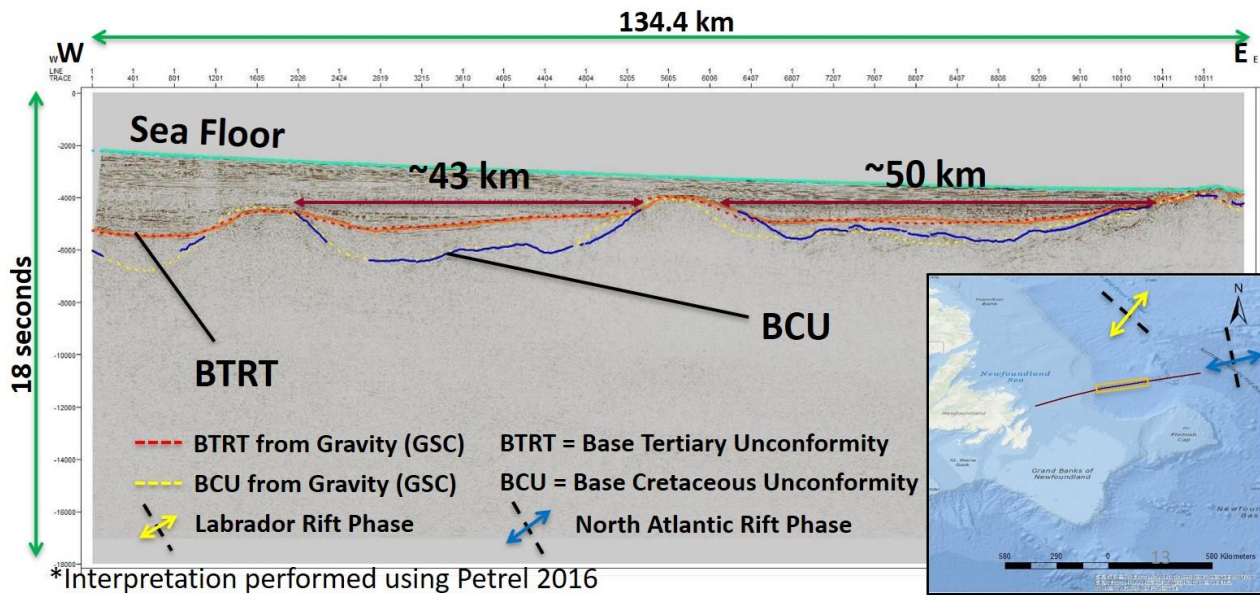
The datasets used in the analysis of Grand Banks structures includes 2D seismic lines, gravity anomaly and magnetic anomaly maps. The 2D seismic lines consist of the deep crustal surveys from the Lithoprobe Project in the 1980's, and traverse distances ranging from approximately 90 km to over 600 km offshore Newfoundland in order to image entire pinch-and-swell structure wavelengths. This data was obtained from public government repositories. The gravity and magnetic anomaly maps were accessed via the University of California at San Diego (UCSD, Sandwell et al., 2014) and the Geological Survey of Canada (GSC, 2010), respectively.

Seismic Data

Within the seismic data, it is evident that pinch-and-swell structures exist even in the 2D perspective, as they traverse in directions roughly perpendicular to the orientations of rifting episodes, and thus sub-parallel to extension. **Figure 1** displays the interpretation of Lithoprobe line segment 84-3b, suggesting wavelengths of approximately 50 km. This would imply that the competent layer being deformed has a thickness of around 12 km or one quarter of the wavelength. It seems that in general, the wavelength has some correlation with the orientation of the seismic line. For lines with NW-SE transects, wavelengths appear to be around 20 km. In contrast, lines oriented in more west-east trends display longer wavelength features, indicating thicker competent layers of deformation. This is addressed further in the discussion.

Gravity and Magnetic Data Observations

Magnetic and gravity anomaly data seem to complement the undulations seen in the seismic sections quite well. **Figure 2** displays the gravity field along the same seismic line segment (84-3b), as well as magnetic anomaly data along the line.



* Interpretation performed using Petrel 2016

Figure 5. Interpretation of Lithoprobe line segment 84-3b, with boudinage wavelengths and some horizons labelled. Inset: location of line segment within the Grand Banks region.

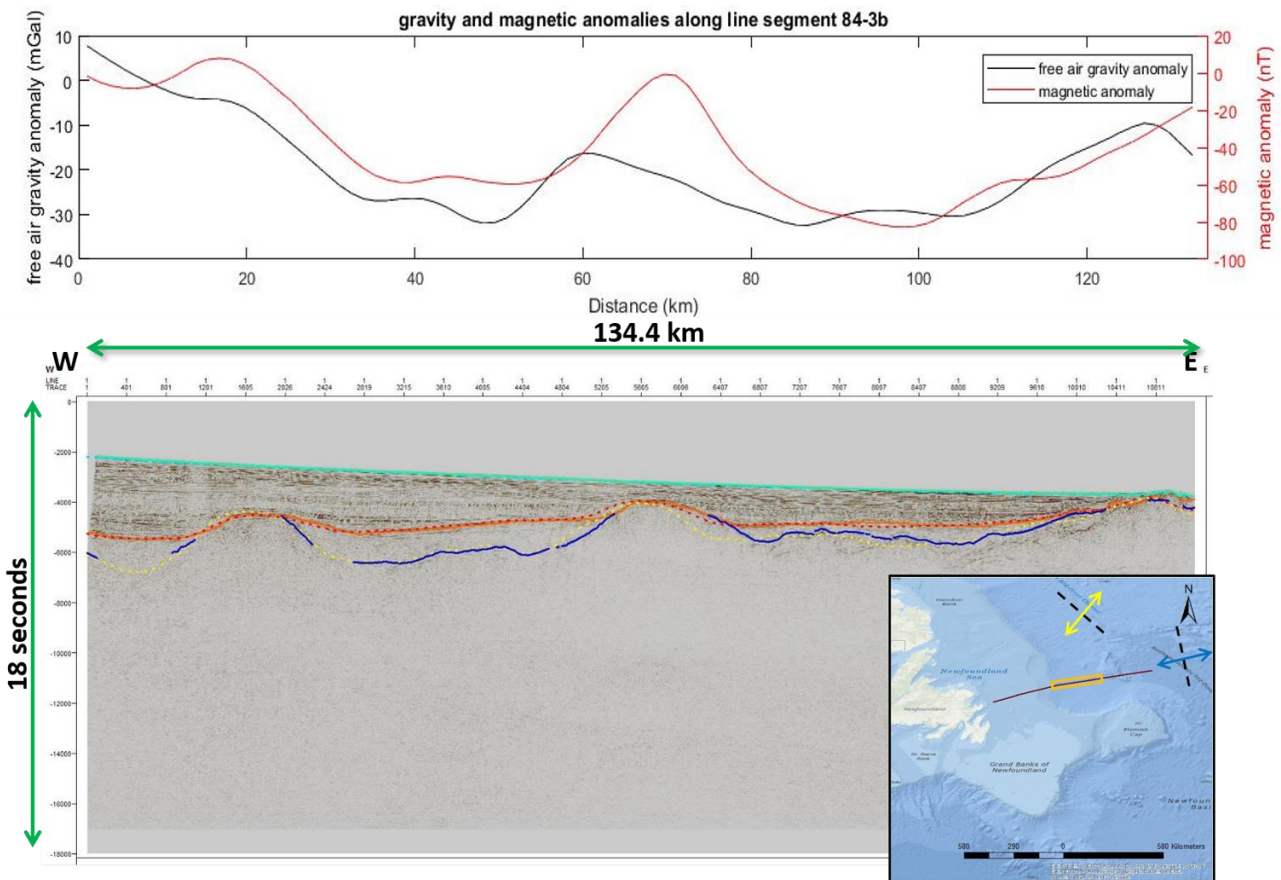


Figure 6. Interpretation of Lithoprobe line segment 84-3b, with corresponding free air gravity field and magnetic anomaly data along profile. Inset: location of line segment within the Grand Banks region.



Figure 2 shows undulations in the gravity field of a similar length to those seen purely based on the seismic interpretation, approximately 40 km. There is some uncertainty mainly within the seismic interpretation due to the age of the data and the processing that went into this dataset. More recent acquisition and processing or even reprocessing of the original data might yield a more accurate interpretation of the structures.

Wavelengths seen in the magnetic data seem to follow the gravity field undulations closely, however they exhibit a longer wavelength of around 50 km. These effects are interesting due to their similar periodic nature to the subsurface pinches and swells present in the seismic interpretation - and combined with a relatively flat although tilted bathymetric profile – support the presence of structures directly impacted by boudinage mechanisms.

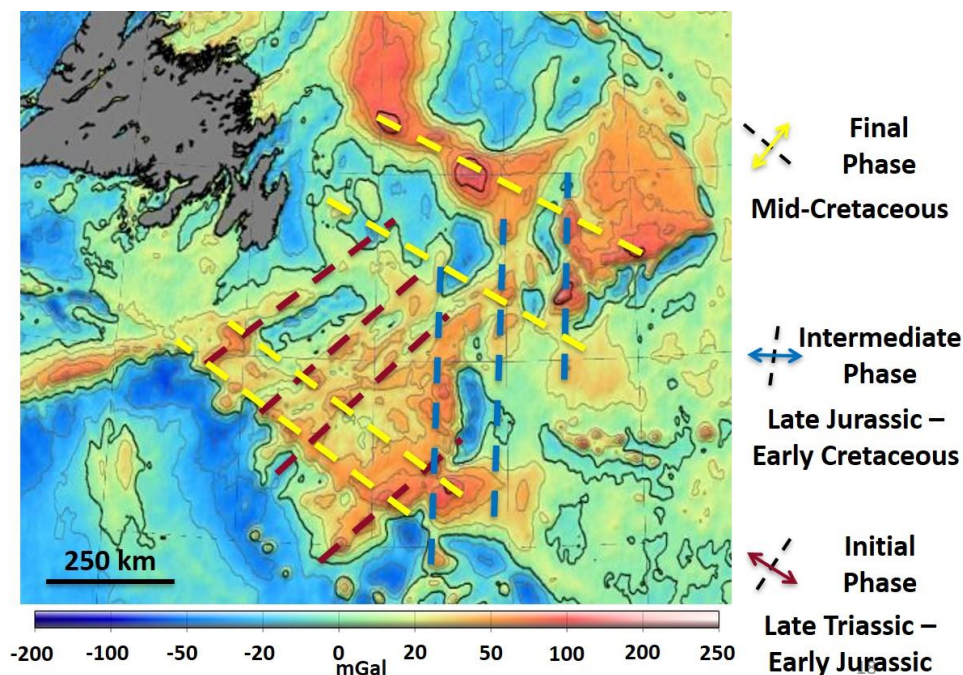


Figure 3: One arc-minute resolution gravity anomaly map of the Grand Banks with elongate structures highlighted with dashed lines. Colours of lines correspond to rifting episodes indicated on the right. Modified portion of global gravity anomaly map from UCSD (2015).

Finally, the gravity anomaly map is perhaps one of the best examples of the periodic nature of boudinage on the regional scale. **Figure 3** shows a portion of the global gravity anomaly map generated by Sandwell et al. (2014), zoomed to the Grand Banks, and each elongated anomalous structure is highlighted, with colour-coding to relate them to each rifting episode. Since it is assumed that boudinage features would appear somewhat parallel to rifting (sub-perpendicular to extension direction), the colours were assigned based on which phase they most nearly correlated with. The wavelengths on this figure are notably much larger than the seismic section, which is potentially due to a coarser resolution than is needed to resolve the smaller wavelength structures.

Discussion

Due to the tectonic evolution of the Grand Banks, it is anticipated that most features typically associated with extensional regimes would be present. However, the complexity of multiple rifting phases oriented at varying degrees of obliquity to each other raises some interesting questions about the observed structures. The rifting history is quite well known (e.g. Enachescu, 1987; Sinclair, 1994; Driscoll et al., 1995; Husky Oil Operations Ltd., 2001; Enachescu and Fagan, 2004; Crosby et al., 2008). Boudinage mechanisms are studied in detail in other



analogous settings (Froidevaux, 1986; Wernicke and Tilke, 1989; Gueguen et al., 1997; Braun and Marquart, 2004; Pubellier et al., 2015; Brune et al., 2017; Clerc et al., 2018), so the suggestion of boudinage mechanisms contributing to the evolution of the Grand Banks is not unreasonable. In fact, boudinage as a factor in forming some of these structures may help explain the periodicity of anomalies found in gravity and magnetic data, as well as the pinch-and-swell structures observed in seismic data.

Figure 1 shows a basic seismic interpretation that likely represents boudinage of a later rifting phase. This is due to both the orientation of the seismic line and the wavelength of the pinch-and-swell structures observed. Since the line segment is striking roughly west-east (entire line approaching southwest-northeast strike), the boudinage structures defined would correspond to the latter two rifting phases, according to the extensional regime geometry. Wavelengths here are much greater than earlier-phase boudinage wavelengths, which can be explained in a couple of different ways:

1. Longer wavelength features in the latter phases are due to successive extension over multiple rift phases, compounding on one another.
2. As extension occurs repeatedly at oblique angles, the crust (upper competent layer) is thinned such that the deeper Moho wavelengths become dominant and the inferred competent layer thickness is that of the upper mantle (lower competent layer)

As another option, there is the possibility that these two results are not entirely independent of each other and there is likely some combination of these contributing to the longer wavelength features.

The results from **Figure 2** indicate that the potential fields align well with the seismic interpretation, with some degree of uncertainty that may originate in the complexity of the subsurface rocks and their geophysical signatures density, magnetic susceptibility and seismic velocity. **Figure 3** confirms the periodicity of the structures and coupled with a relatively flat bathymetry (van der Linden and Wade, 1975), implies that the anomalies must certainly be within the subsurface.

We propose that the boudinage mechanism in the Grand Banks is most similar to the Norwegian Margin example (Braun and Marquart, 2004) in that there are likely two layers of boudinage. The upper crust layer and the upper mantle layer, with entirely separate thicknesses derived from different wavelengths. Towards the later rifting phases, due to a combination of the reasons listed above, the deeper features become more visible, which would explain the longer wavelengths.

Summary and/or Conclusions

It is clear after analysis of various geophysical data that boudinage mechanisms have likely contributed to the evolution of the Grand Banks and in addition may explain the periodic nature of many structures found in this region. Basic seismic interpretation indicates that pinch-and-swell structures exist in orientations that would be expected from classic definitions of lithospheric boudinage, and the wavelength seems to increase as orientation rotates counter-clockwise from the NW-SE to the SW-NE directions.

The gravity and magnetic potential field data seem to complement the seismic interpretation well, with slightly longer wavelengths. Combined with the well-known relatively flat bathymetry of the Grand Banks, this data reinforces that these anomalous structures are located within the subsurface and are not simply bathymetric undulations.

Wavelength differences are proposed to be due to either a compounded successive extension of the crust, or a system containing two separate boudinage mechanisms with the upper competent layer consisting of the upper crust and the lower competent layer consisting of the upper mantle. This would explain why longer wavelengths are observed from later rifting events, once the upper crust is thinned successively and the deeper features become more dominant.



Acknowledgements

Husky Energy Inc., MITACS, and NSERC CREATE are thanked for funding. Husky is also acknowledged for software and public data access. The Geological Survey of Canada is thanked for access to public data. Additionally, the authors wish to express deep gratitude to David Emery for many thought-provoking discussions on boudinage mechanisms.

References

- Braun, A., and Marquart, G., 2004. Evolution of the Lofoten-Vesterålen margin inferred from gravity and crustal modeling. *Journal of Geophysical Research*, **109**(B06404), 15 p. doi: 10.1029/2004JB003063
- Brune, S., Heine, C., Clift, P.D., and Pérez-Gussinyé, M., 2017. Rifted margin architecture and crustal rheology: Reviewing Iberia-Newfoundland, Central South Atlantic, and South China Sea. *Marine and Petroleum Geology*, **79**, p. 257-281, doi: 10.1016/j.marpetgeo.2016.10.018
- Clerc, C., Ringenbach, J.-C., Jolivet, L., and Ballard, J.-F., 2018. Rifted margins: Ductile deformation, boudinage, continentward-dipping normal faults and the role of the weak lower crust. *Gondwana Research*, **53**, 20-40, doi: 10.1016/j.gr.2017.04.030
- Crosby, A., White, N., Edwards, G., and Shillington, D., 2008. Evolution of the Newfoundland-Iberia conjugate rifted margins. *Earth and Planetary Science Letters*, **273**, 213-226, doi: 10.1016/j.epsl.2008.06.039
- Driscoll, N.W., Hogg, J.R., Christie-Blick, N., and Karner, G.D., 1995. Extensional tectonics in the Jeanne d'Arc Basin, offshore Newfoundland: implications for the timing of break-up between Grand Banks and Iberia. In: R.A. Scrutton, M.S. Stoker, G.B. Shimmiel, and A.W. Tudhope (eds), *The Tectonics, Sedimentation and Palaeoceanography of the North Atlantic Region*. Geological Society, London, Special Publications, **90**, 1-28, doi: 10.1144/GSL.SP.1995.090.01.01
- Enachescu, M.E., 1987. Tectonic and structural framework of the northeast Newfoundland continental margin. In: C. Beaumont and A.J. Tankard (eds), *Sedimentary Basins and Basin-Forming Mechanisms*. Canadian Society of Petroleum Geologists, Memoir **12**, 117-146
- Enachescu, M.E., and Fagan, P., 2004. Newfoundland and Labrador Call for Bids NF04-01. Government of Newfoundland and Labrador, Department of Natural Resources, 35p. (Also available at http://www.gov.nl.ca/minesanden/oil/call_for_bids_nf04_01.stm)
- Fossen, H., 2010, Chapter 14 – Boudinage. In: *Structural Geology*, Cambridge University Press, 271-284, doi: 10.1017/CBO9780511777806.016
- Froidevaux, C., 1986. Basin and Range large-scale tectonics: constraints from gravity and reflection seismology. *Journal of Geophysical Research*, **91**(B3), 3625-3632, doi: 10.1029/JB091iB03p03625
- Goscombe, B.D., Passchier, C.W., and Hand, M., 2004. Boudinage classification: end-member boudin types and modified boudin structures. *Journal of Structural Geology*, **26**, 739-763, doi: 10.1016/j.jsg.2003.08.015
- Government of Canada, 2010. Aeromagnetic - Residual Total Field Map, Natural Resources Canada; Earth Sciences Sector; Central and Northern Canada Branch - Geological Survey of Canada, Airborne Geophysics Section, Grid Spacing 200m. <https://open.canada.ca/data/en/dataset/feb31a68-580d-594b-863a-73e5c8132e9b>
- Gueguen, E., Doglioni, C., and Fernandez, M., 1997. Lithospheric boudinage in the Western Mediterranean back-arc basin. *Terra Nova*, **9**(4), 184-187, doi: 10.1046/j.1365-3121.1997.d01-28.x
- Husky Oil Operations Ltd., 2001. White Rose Oilfield Development Application. Rep. **Volume 2**, 18-73
- Kearey, P., Klepeis, K.A., and Vine, F.J., 2009. *Global Tectonics – 3rd Edition*. Oxford, Wiley-Blackwell, 482p.
- Pubellier, M., Delescluse, M., Savva, M., Franke, D., Meresse, F., Auxietre, J.-L., Aurelio, M., Chamot-Rooke, N., Nanni, U., and Chan, L.S., 2015. Collapse and rifting in the South China Sea. Adapted from oral



- presentation, as well as the extended abstract prepared for the presentation, at American Association of Petroleum Geologists Asia Pacific Region Geosciences Technology Workshop, “Tectonic Evolution and Sedimentation of South China Sea Region,” Kota Kinabalu, Sabah, Malaysia, May 26-27, 2015, Search and Discovery Article #30406 (2015)
- Ramberg, H., 1955. Natural and Experimental Boudinage and Pinch-and-Swell Structures. *The Journal of Geology*, **63**(6), 512-526, doi: 10.1086/626293
- Ribeiro, A., 2002. Global Tectonics with Deformable Plates. In: *Soft Plate and Impact Tectonics*. Springer-Verlag Berlin Heidelberg, 51-173, doi: 10.1007/978-3-642-56396-6
- Ricard, Y., and Froidevaux, C., 1986. Stretching instabilities and lithospheric boudinage. *Journal of Geophysical Research*, **91**(B8), 8314-8324, doi: 10.1029/JB091iB08p08314
- Sandwell, D.T., Müller, R.D., Smith, W.H.F., Garcia, E., and Francis, R., 2014. New global marine gravity model from CryoSat-2 and Jason-1 reveals buried tectonic structure. *Science*, **346**(6205), 65-67, doi: 10.1126/science.1258213
- Sinclair, I.K., 1994. Tectonism and sedimentation in the Jeanne d’Arc Basin, Grand Banks of Newfoundland. Unpublished Ph.D. thesis, University of Aberdeen, Aberdeen, Scotland, 260p.
- Smith, R.B., 1975. Unified theory of the onset of folding, boudinage, and mullion structure. *Geological Society of America Bulletin*, **86**(11), 1601-1609, doi: 10.1130/0016-7606(1975)86<1601:UTOTOO>2.0.CO;2
- Smith, R.B., 1977. Formation of folds, boudinage, and mullions in non-Newtonian materials. *Geological Society of America Bulletin*, **88**(2), 312-320, doi: 10.1130/0016-7606(1977)88<312:FOFBAM>2.0.CO;2
- Van Der Linden, W.J.M., and Wade, J.A., 1975. Offshore Geology of eastern Canada, **Volume 2 – Regional Geology**. Geological Survey of Canada, Paper 74-30, 258p., doi: 10.4095/119752
- Wernicke, B., and Tilke, P.G., 1989. Extensional Tectonic Framework of the U.S. Central Atlantic Passive Margin. In: A.J.Tankard, and H.R. Balkwill (eds), *Extensional tectonics and stratigraphy of the North Atlantic margins*, American Association of Petroleum Geologists and Canadian Geological Foundation, American Association of Petroleum Geologists Memoir, **46**, 7-21
-





INVESTIGATING THE ROLE OF CRESTAL FAULTING ON HYDROCARBON ACCUMULATION AND MIGRATION IN ROLLOVER ANTICLINAL TRAPS OF THE ANCIENT SABLE DELTA OFFSHORE NOVA SCOTIA - INSIGHTS FROM THE MIGRANT STRUCTURE AND IMPLICATION FOR ROLLOVER STRUCTURES IN THE SABLE-SUBBASIN

Martyns-Yellowe, Kenneth T.¹, Richards, Frank W.¹, Wach, Grant D.¹, and Watson, Neil²

¹Dalhousie University, Basin and Reservoir Lab, Department of Earth Sciences, Life Sciences Centre, 1355 Oxford Street, Halifax, NS B3H 4R2, Canada, Ken.Martyns-Yellowe@dal.ca

²Atlantic Petrophysics Limited, Nova Scotia

Located in the Sable Subbasin, the Migrant structure is a fault controlled, four-way dip anticlinal closure, which formed as one of a series of related structures during sediment loading and salt mobilization in the Cretaceous. The Migrant N-20 well was drilled to test for hydrocarbons presumed trapped in Late Jurassic to Early Cretaceous deltaic and fluvial-deltaic reservoirs in the structure. Results from a drill stem test (DST) indicates the well tested gas from a deep sand reservoir with a reported flow rate of 10 million standard cubic feet per day (MMscf/d) to the surface, with associated decline over the duration of the test. The operator considered this declining flow rate indicative of a non-commercial accumulation. Further geologic analysis showed diminishing net porous sand with little evidence of extensional crestal faulting deep in the core of the Migrant rollover anticline.

Through the integration of 3D seismic with well data, we investigate the characteristics of the Migrant structure as a potential hydrocarbon trap. Through a combination of well pressure data and 3D geocellular models populated with input parameters such as shale volume, porosity, water saturation and permeability calculated in Petrel from key wireline logs, we show fault distribution and seal versus reservoir properties offset in an Allan diagram. Our models demonstrate the inferred mechanism for leakage at Migrant (the crestal fault) with varying fault displacements, seal thicknesses/net to gross ratios, and reservoir permeabilities.

Our analyses of the Migrant structure show diminishing net to gross with depth. The intervals that tested hydrocarbons are distally located and potentially stratigraphically or diagenetically isolated. Additionally, the rapidly depleting, non-commercial test rates, are attributed to the juxtaposition of sand against sand across the main crestal fault in the structure, just above seismic resolution but with sufficient offset to allow cross-fault leakage between reservoirs.

Introduction

Globally, shelf margin deltas like the Mississippi, Amazon, Niger, and ancient Sable Delta host some of the world's largest gas accumulations. These prolific hydrocarbon reservoirs are impacted by gravity-driven extension, syntectonic sedimentation, and movement of salt in the subsurface (Cummings and Arnott, 2005; Adam et al., 2006). Their interaction impacts syndepositional fault evolution and the formation of structures typically comprised of a reservoir rock with porosity and a seal rock (Vendeville, 1991; Adam et al., 2006) with the capacity to store hydrocarbons.

The Scotian Basin is an extensional rift basin comprising four subbasins covering an area of ca. 300,000 km² (**Figure 1**). Hydrocarbon resources have been explored for offshore Nova Scotia since 1959 (Enachescu and Wach, 2005). A report of hydrocarbon well failure analysis by the Canada Nova Scotia Offshore Petroleum Board (Smith et al., 2014) highlights the absence of effective seal against faults to be the reason most wells targeting rollover structures offshore Nova Scotia fail to find producible quantities of hydrocarbons. Rollover anticlines are



syn-depositional structures that develop on the downthrown side of deltaic growth faults. They are prolific for trapping significant and commercial volumes of hydrocarbon with approximately 75% of the significant/commercial discoveries offshore Nova Scotia related to this type of structure.

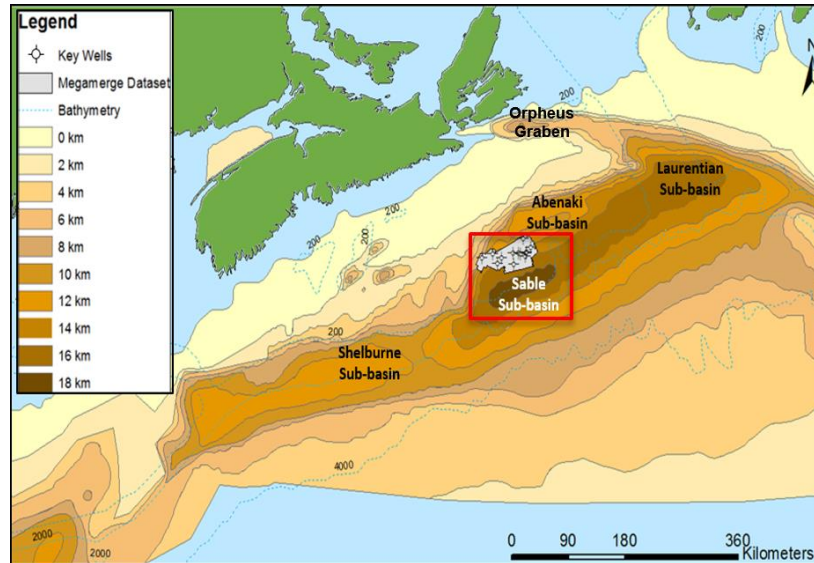


Figure 1. A sediment thickness map of the Scotian Basin (after Wade 2000). The Sable Subbasin (Red Box) is one of the Subbasins in the Scotia Basin. The area shaded in grey represents the extent of the 3D Sable Megamerge seismic volume used for this study.

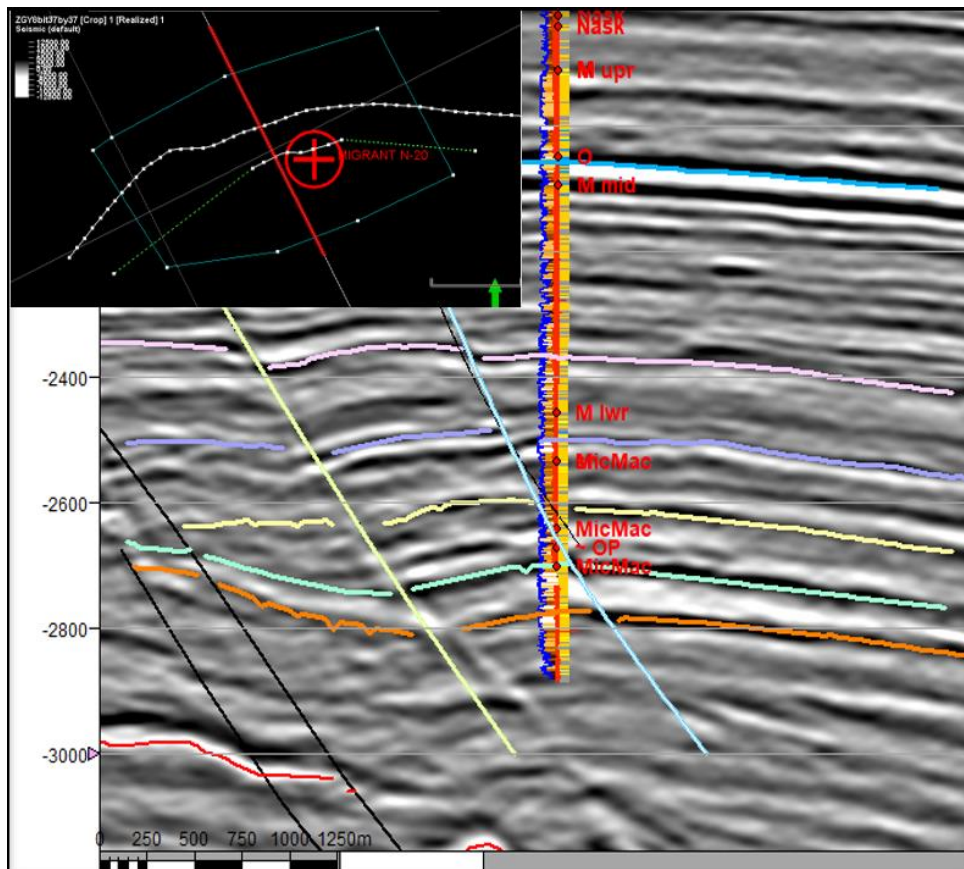


Figure 2. A Seismic profile showing the Migrant rollover with the N-20 well that penetrates the structure with interpreted horizons.



Located in the Sable Subbasin, the Migrant structure (**Figure 2**) is a four-way dip closure formed above the low side of listric fault within a basin having an active petroleum system, and, an abundance of reservoir. However, the Migrant N-30 well, drilled to test for hydrocarbons trapped in Late Jurassic to Early Cretaceous deltaic and fluvial-deltaic reservoirs, revealed reservoir rocks were almost entirely wet. Drillstem testing indicated the well flowed gas only from a single deep sand reservoir with a reported rate of 10 million standard cubic feet per day to the surface, with rate decline over the duration of the test. The operator concluded that the declining flow rate indicated limited gas reserves in this reservoir sand and thus was non-commercial.

Based on seismic interpretation (**Figure 2**), petrophysics, construction of a geocellular model, a reservoir simulation model, and associated Allan diagrams together support the interpretation that a small crestal fault, just above seismic resolution, has sufficient offset to allow cross-fault leakage between reservoirs. As a result, hydrocarbons migrated cross-fault, up-section into levels that are not within four-way dip closure. Hence, reservoirs under structural closure were almost all wet.

Data and Method

The data and methods are outlined in **Figure 3**.

Results and Observations

Integration of logs and 3D seismic allowed seismic interpretation from time to true depth, correlated across the seismic section on a well-to-well basis. At Migrant, the reservoirs near the base of the well are tight, resulting in limited, localized trapping. The composite section in **Figure 4** shows residual gas saturation is as high as 40% in some of the reservoirs including those reported to contain water from the DST report. Apart from an anomalous sand interval at the bottom of the well that forms the base of a fining upward sequence, most of the reservoirs leak across the major crestal fault in the Migrant structure.

As the extensional response of a rollover, crestal faulting may impact intra-field fluid migration and hydrocarbon distribution. In a high net-to-gross system with no crestal faulting, unless there is top seal failure (from a mechanical breach or capillary leak), a shale sequence over a reservoir will be impermeable to the flow of gas until down to the bounding fault, or the saddle spill point (Richards et al., 2008).

In the pressure elevation plot in **Figure 3B**, the mud weight appeared to mimic the hydrostatic curve. At about 4000 m depth, a rightward shift in gradient to higher pressure points to the onset of overpressure. Of the three DST test intervals the only hydrocarbon-bearing one is at the base of the well at depths where reservoir quality is poor due to fluid related (water) diagenesis. The tested reservoir is relatively distal facies and potentially both stratigraphically and diagenetically isolated as indicated by a rapidly depleting, obviously non-commercial, test rates.

Despite being distal, discontinuous and heavily cemented, the bottom test interval in the final 1000 m of the Migrant Structure within four-way dip closure flowed gas regardless of well summary report indicating that the top two tested reservoirs above were tight and unable to deliver any flow. Considering the isolation and increased pressure regime, an enhancement in permeability thickness product (Kh) in the bottom-tested reservoir attests to a possible fracturing of the zone where the crestal fault soles out.

Conclusions

The Migrant structure is one of many northeast-trending rollover features that result from the interaction between gravity driven extension, synsedimentary deposition and the movement of a mobile substrate. It is a four-way dip closure formed above the low side of listric fault in a subbasin that has an active petroleum system, and an abundance of reservoirs. Yet, the trap's reservoirs are almost entirely wet. An alternative hypothesis that the



Migrant structure is in a migration shadow is discounted as there are hydrocarbons at the base. Hence, hydrocarbons are known to have migrated into the structure, yet the issue remains why they are not trapped there.

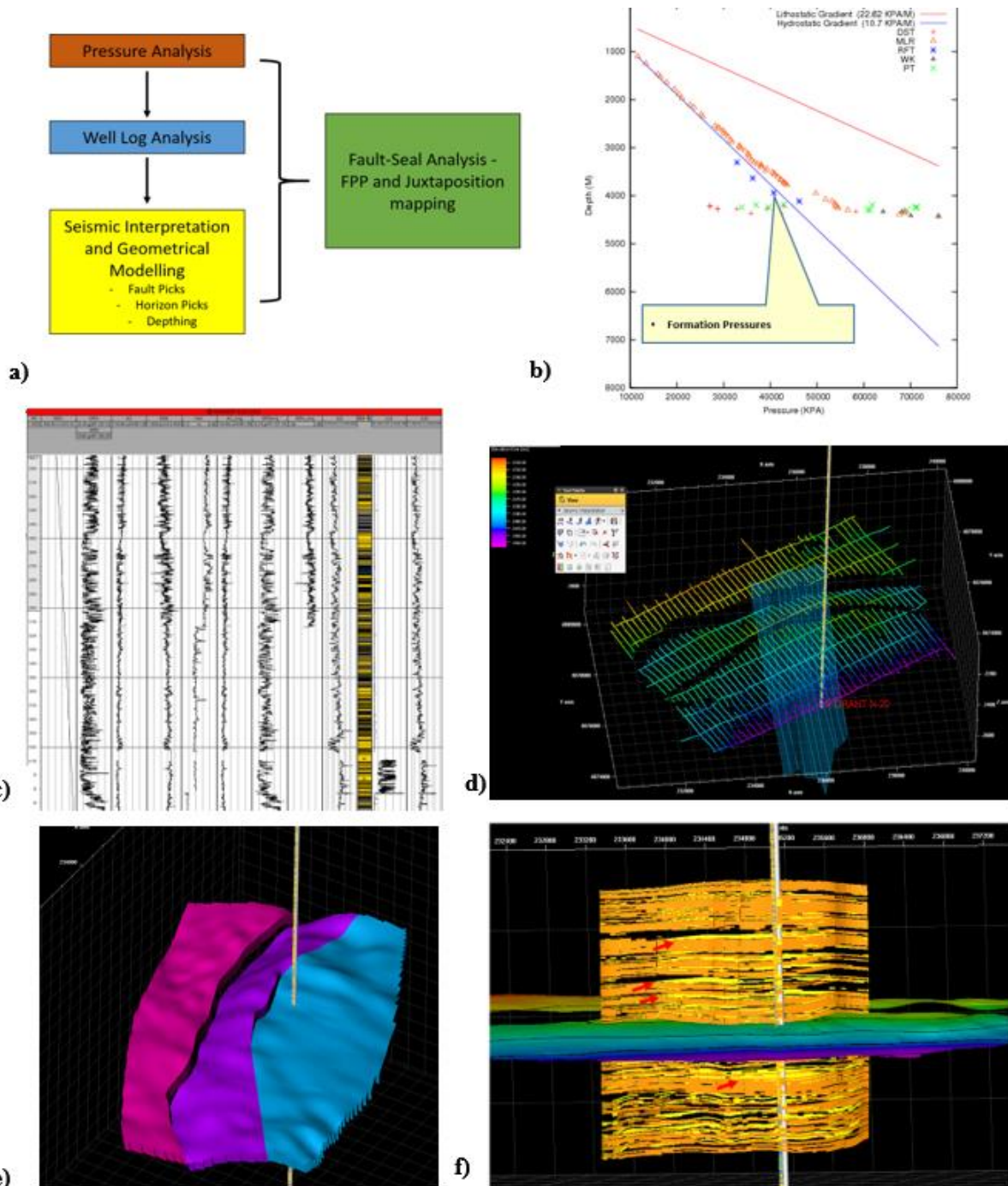


Figure 3. A) Study workflow. B) Pressure elevation information to determine the connectivity between zones from formation pressure plots. Also, useful for the potentially modelling of gas water contacts. C) Petrophysical well logs used for generating and projecting fault rock petrophysical properties in our models. D) Location of fault with an unidentified top of reservoir horizon. E) Geometric modelling of reservoir and seal thickness displacement at the fault F) A modelled fault plane profile showing potential leakage pathways indicated by the red arrows. It is a useful tool for quick initial examination of fault seal capacity. In the profile, sands from the footwall (yellow) can be seen juxtaposed against sands in the hanging wall (orange) as depicted by (Knipe, 1997). The holes filled with black are supposed to represent shale distribution.



Based on careful seismic interpretation, petrophysical analysis, construction of a geocellular model, reservoir simulation model, and associated Allan diagrams, a small crestal fault, just above seismic resolution, has sufficient offset to allow cross-fault leakage between reservoirs. As a result, hydrocarbons have migrated across-fault, up-section, to levels that are not within four-way dip closure. This forms the underlying reason why the Migrant structure's reservoirs are wet (**Figure 5**).

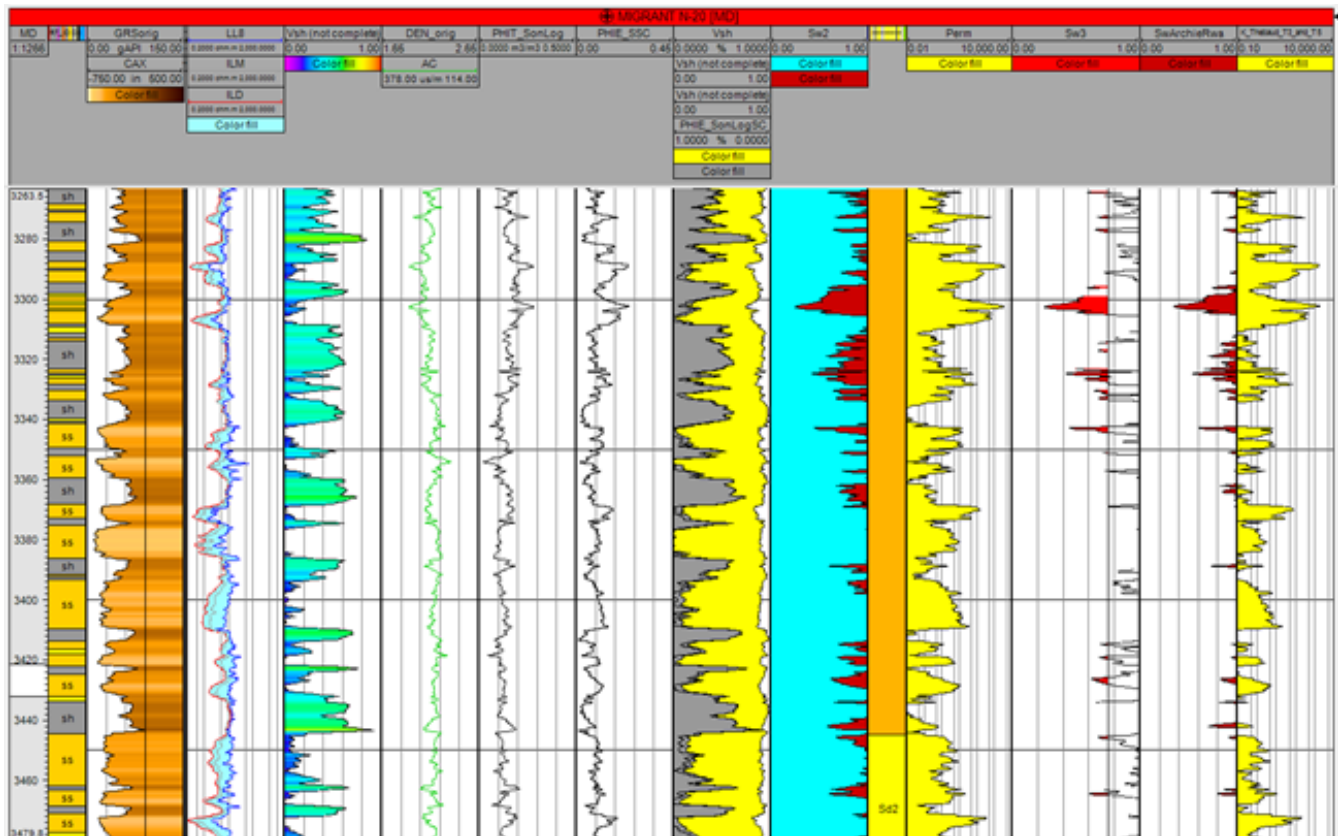


Figure 4. Petrophysical analysis of the Migrant N-20 well. Log characteristics typical of a deltaic sequence followed by a transgressive system is observed in gamma ray logs at the bottom of the well around depths of 3450 m (11,319 ft). Interpreted gas saturations in porous intervals with corresponding change in resistivity from a few ohms to 10 to 20 ohms. Gas is trapped in poor quality reservoirs in the bottom sections at the Migrant Structure.

In the Sable Subbasin, the issue of leakage associated with small extensional faults on the crest of lowside rollovers is pervasive. In zones up shallow, faults with larger throws in a high net to gross section results in leakage. At the intermediate to deeper sections, the fault throw decreases as the fault soles out in lower net to gross intervals. This is the commercial sweet spot in the structure since the best traps begin to form as the fault offset diminishes into the core of the structures. At even greater depths, the reservoirs get tight and discontinuous with some high-pressure gas zones that are not commercial. These comprise the stratigraphic/diagenetically controlled traps.

For this study, literature review, well data with 3D seismic is used to demonstrate the fault sealing mechanism in the Migrant Structure. New interpretations and results from this work combined with predictive models adds to the new insights to our understanding of hydrocarbon spill/leakage scenarios and fault sealing in rollover structures offshore Nova Scotia and may be useful for de-risking untested geologically related targets on the Scotian Margin.

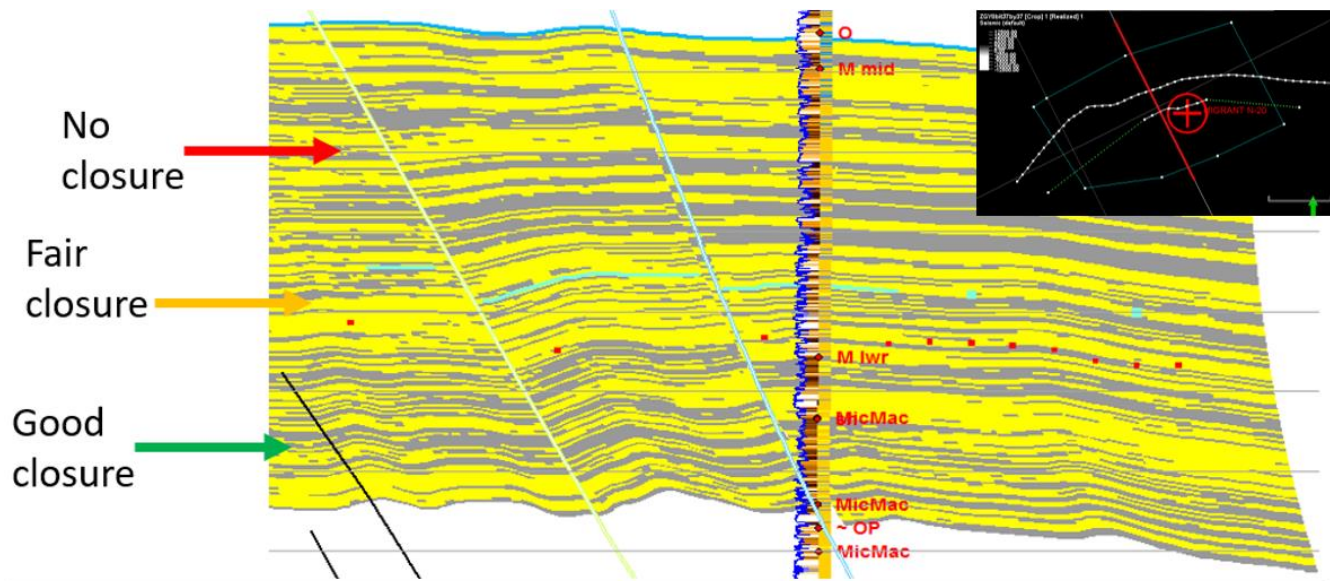


Figure 5. A modelled cross section of the migrant structure populated with sand and shale properties from well estimates reveals the magnitude of crestal faulting through the offset of sand-shale pairs. In zones up shallow, faults with larger throws in a high net to gross section results in leakage. At the intermediate to deeper sections, the fault throws decreases as the fault soles out in lower net to gross intervals. This is the goldilocks zone since the best traps begin to form as the fault offset diminishes into the core of rollover structures. At even greater depths, the reservoirs get tight and discontinuous with some high-pressure gas zones that are not commercial.

Acknowledgements

This research is sponsored by a Petroleum Geoscience Grant from the Sable Project operator to Professor Grant Wach of Dalhousie University's Basin and Reservoir Lab. I extend my thanks to my supervisors Dr. Grant Wach, Mr. Bill Richards and Mr. Neil Watson for their guidance and support. Additional thanks to Carl Makrides and Shawn Rhyno of Canada-Nova Scotia Offshore Petroleum Board, and the rest of my team at the Dalhousie University Basin and Reservoir Lab.

References

- Adam, J., Krezsek, C., and Grujic, D., 2006. Thin-skinned extension, salt dynamics and deformation in dynamic depositional systems at passive margins. Proceedings of the 8th SEGJ International Symposium, Kyoto, Japan, 26-28 November 2006, 1-6.
- Cummings, D.I., and Arnott, R.W.C., 2005. Growth-faulted shelf-margin deltas: a new (but old) play type, offshore Nova Scotia. Bulletin of Canadian Petroleum Geology, **53**(3), 211-236.
- Enachescu, M.E., Hogg, J.R., and Wach, G.D., 2005. Exploration lessons; a decade of drilling in Atlantic Canada. In: Program with Abstracts, Geological Association of Canada-Mineralogical Association of Canada, Joint Annual Meeting. Geological Association of Canada, Waterloo, ON.
- Knipe, R.J., 1997. Juxtaposition and seal diagrams to help analyse fault seals in hydrocarbon reservoirs. American Association of Petroleum Geologists, **81**(2), 187-195.
- Richards, B., Fairchild, L., Vrolijk, P., and Hippler, S., 2008. Reservoir Connectivity Analysis, Hydrocarbon Distribution, Resource Potential, and production Performance in the Clastic Plays of the Sable Subbasin, Scotian Shelf. In: D.E. Brown (ed), Program and Extended Abstracts, Central Atlantic Conjugate Margins Conference, 13-15 August 2008, Halifax, Nova Scotia, Canada, 165-185.



- Smith, B.M., Makrides, C., Altheim, B. and Kendell, K., 2014. Resource Assessment of Undeveloped Significant Discoveries on the Scotian Shelf. Canada Nova Scotia Offshore Petroleum Board, 182p. http://www.cnsopb.ns.ca/sites/default/files/pdfs/sda_report_-_finalhighquality_april_3_2014.pdf
- Vendeville, B., 1991. Mechanisms generating normal fault curvature: a review illustrated by physical models. In: A.M. Roberts, G. Yielding, and B. Freeman (eds), *The Geometry of Normal Faults*. Geological Society, London, Special Publications, **56**, 241-249.
- Wade, J.A. (with contributions by Brown, D.E., Durling, P., MacLean, B.C. and Marillier, F.), 2000. Depth to Pre-Mesozoic and Pre-Carboniferous Basements. Geological Survey of Canada, Open File Report No.3842 (1:1,250,000 map of Scotian Shelf and Adjacent Areas).
-





SEISMIC INVERSION AND SOURCE ROCK EVALUATION ON JURASSIC ORGANIC RICH INTERVALS IN THE SCOTIAN BASIN, NOVA SCOTIA

Morrison, Natasha M.¹, Silva, Ricardo L.¹, Richards, F.W. (Bill)¹, and Wach, Grant D.¹

¹Basin and Reservoir Lab, Department of Earth Sciences, Dalhousie University, Life Sciences Centre, 1355 Oxford Street, Halifax, NS B3H 4R2, Canada, natasha.morrison@dal.ca

Source rocks are a key element of a petroleum system and have been identified as a risk in the exploration of the Scotian Margin, offshore Nova Scotia, Canada. Twenty-six significant hydrocarbon discoveries were made since 1967 in the Sable Subbasin of the Scotian Basin. Although there are proven hydrocarbon accumulations (some commercial) in both Jurassic and Cretaceous reservoirs, identification of their source is problematic due to the low organic matter content of the studied interval, ‘turbo’ drilling practices, and drilling mud contamination.

This project investigated the extent and geochemical properties of known and presumed Middle to Upper Jurassic source rocks in the Scotian Basin. It tested the hypothesis that source rocks, (if present in a 2120 km² area surrounding Sable Island), can be identified using petrophysical techniques and then mapped using seismic inversion.

This investigation was completed using a combination of petrophysical and seismic techniques. Wireline log estimation of total organic carbon (TOC) using the Passey method. Seismic inversion was achieved via a 3D constrained sparse spike inversion, to highlight the presence of low impedance source rocks using the Løseth et al. (2011) “Source Rock from Seismic” method.

The petrophysical methods did not identify intervals of source rock in the studied wells. This is consistent with the publicly available geochemical data showing measured TOC values of generally <2%. Seismic inversion was effective in mapping low acoustic impedance intervals, especially in calcareous shales. However, without evidence of high TOC content (>2%), low acoustic impedance cannot be interpreted as source rock.

Introduction

Source rocks are a fundamental element of any petroleum system and a key uncertainty in the exploration of the Scotian Basin, offshore Nova Scotia, Atlantic Canada (e.g. OERA 2013). The Scotian Basin (**Figure 1**), surrounding and underlying Sable Island, has had 24 significant hydrocarbon discoveries, including two oil fields and six gas fields all of which have ceased production (Enachescu and Wach, 2005; Smith et al., 2014). Though there are proven hydrocarbon accumulations in both Jurassic and Cretaceous reservoirs, identifying their definitive source(s) is difficult (Fowler et al., 2016). The accumulations are currently assumed to be predominantly sourced by pro-deltaic and basinal shales within the Upper Jurassic to Upper Cretaceous Verrill Canyon Formation (e.g. Mukhopadhyay and Wade, 1990; Mukhopadhyay, 2006). Beicip-Franlab (2011) interpret Aptian and Valanginian pro-deltaic and paralic sediments, Tithonian and Callovian shales deposited during maximum flooding events, and potentially Early Jurassic shales as key source rocks in the Scotian Basin.

The Scotian Basin stretches 1200 km from the Grand Banks in the northeast past the Shelburne Subbasin in the southwest (**Figure 1**), covering approximately 300,000 km². Offshore Nova Scotia has had 210 wells drilled and approximately 100 penetrate the Jurassic. These include 129 exploratory, 53 development, 27 delineation, and 1 service relief well (CNSOPB, 2018). Despite extensive research efforts over the last 30 years (e.g. Mukhopadhyay and Wade, 1990; Mukhopadhyay 1991, 1995) source rock intervals are still poorly characterized. This is due to the quality of the geochemical data collected from prospective source rock intervals, the effect of



oil based muds and lignite additives (which both add external hydrocarbons into the sample), and turbo-drilling (which causes the mixing of contaminants and pulverizing of the sample) (e.g. Mukhopadhyay 1990a). As such, the Scotian Margin is recognized as having low content of organic matter, yielding low or “lean and disseminated” average total organic carbon (TOC) content (Williamson and Desroches, 1992, 1993). The main source rock intervals in the Scotian Basin and Sable Subbasin are thought to have been deposited during the Jurassic (Mukhopadhyay, 1990a; Beicip-Franlab, 2011). The Jurassic is a known time for significant source rock deposition globally (e.g. Huc and Schneidermann, 1995; Duarte et al., 2012; Silva et al., in prep.), commonly in restricted basins related to the break-up of the supercontinent Pangea (e.g. Jeanne d’Arc Basin, offshore Newfoundland, and Essaouira Basin, Morocco).

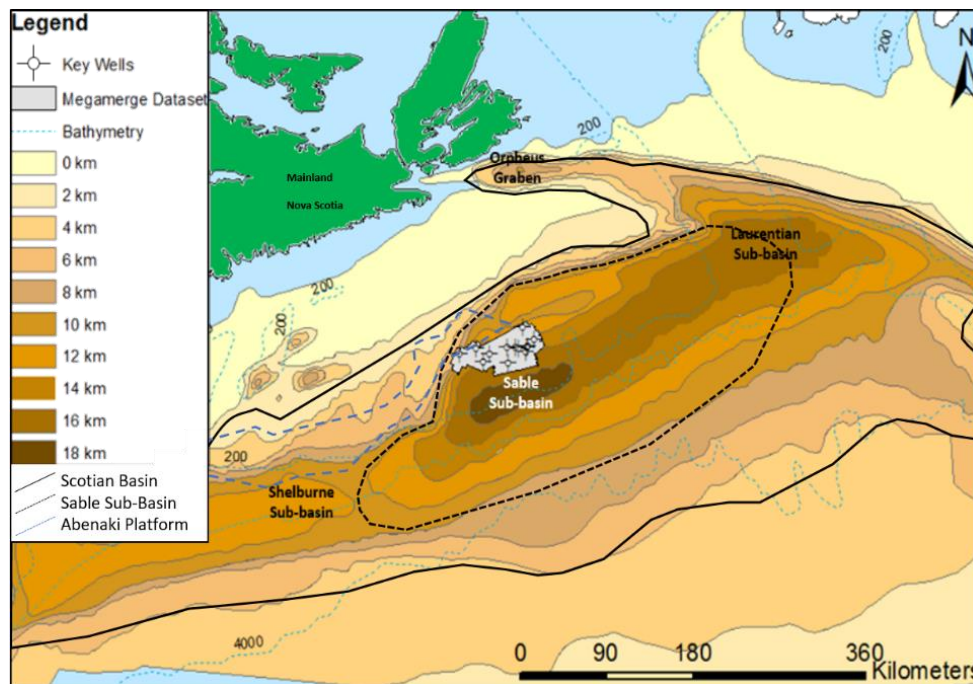


Figure 7. Map of the Scotian Basin with total Mesozoic and Cenozoic sediment thickness; the Sable Subbasin and the MegaMerge Dataset (modified from Wade, 2000); outlines of the Scotian Basin and Sable Subbasin based on Williams et al. (1990).

There has been success in the use of seismic techniques to study source rocks. Løseth et al. (2011) suggested that source rocks can be identified using a combination of petrophysical and seismic techniques, specifically the Passey Method (Passey et al., 1990) and acoustic impedance seismic inversion. These authors observed that acoustic impedance (AI) decreases non-linearly with increasing TOC content. They also noted that the AI of a shale source rock (>3% TOC) will be significantly lower than the AI in a non-organic shale. This relationship was observed through the study of significant source rocks such as the Kimmeridge Clay in southern England (Morgans-Bell et al. 2001) and the Hekkingen Formation in the Barents Sea (Langrock, 2004).

The Sable Subbasin contains one of the most extensive 3D seismic data sets on the shelf area of the Scotian Margin (**Figure 2**). The Sable MegaMerge dataset was made available to Dalhousie University by ExxonMobil, operators of the Sable Offshore Energy Project. This survey consists of a post-stack merge of six 3D seismic surveys acquired in the Scotian Basin from 1996 to 1999; three using marine streamers and three using ocean bottom cables (CNSOPB, 2014) (Figure 2). With a good signal to noise ratio, stable zero phase, reasonable bandwidth (approximately 10-60 Hz), and resolution (peak frequency ca. 15-30 Hz depending on depth and tuning at between 15-35 m), this merged seismic cube provides extensive coverage of part of the Sable Subbasin. This



includes Middle Jurassic to Lower Cretaceous deposition, such as the Abenaki carbonate bank, the proximal siliciclastics of the MicMac Formation, and the distal finer grained siliciclastics of the Verrill Canyon Formation (Wade and MacLean, 1990) (**Figures 1 and 2**).

Understanding the extent and geochemical properties of known and presumed source rocks, as well as identifying new organic-rich intervals, is critical for future petroleum exploration offshore Nova Scotia. The possibility of using indirect methods (i.e. wireline and seismic) to improve upon the current limitations in identifying source rock intervals from drill cuttings, such as contamination, open new possibilities of research in the Sable Subbasin and the Scotian Margin.

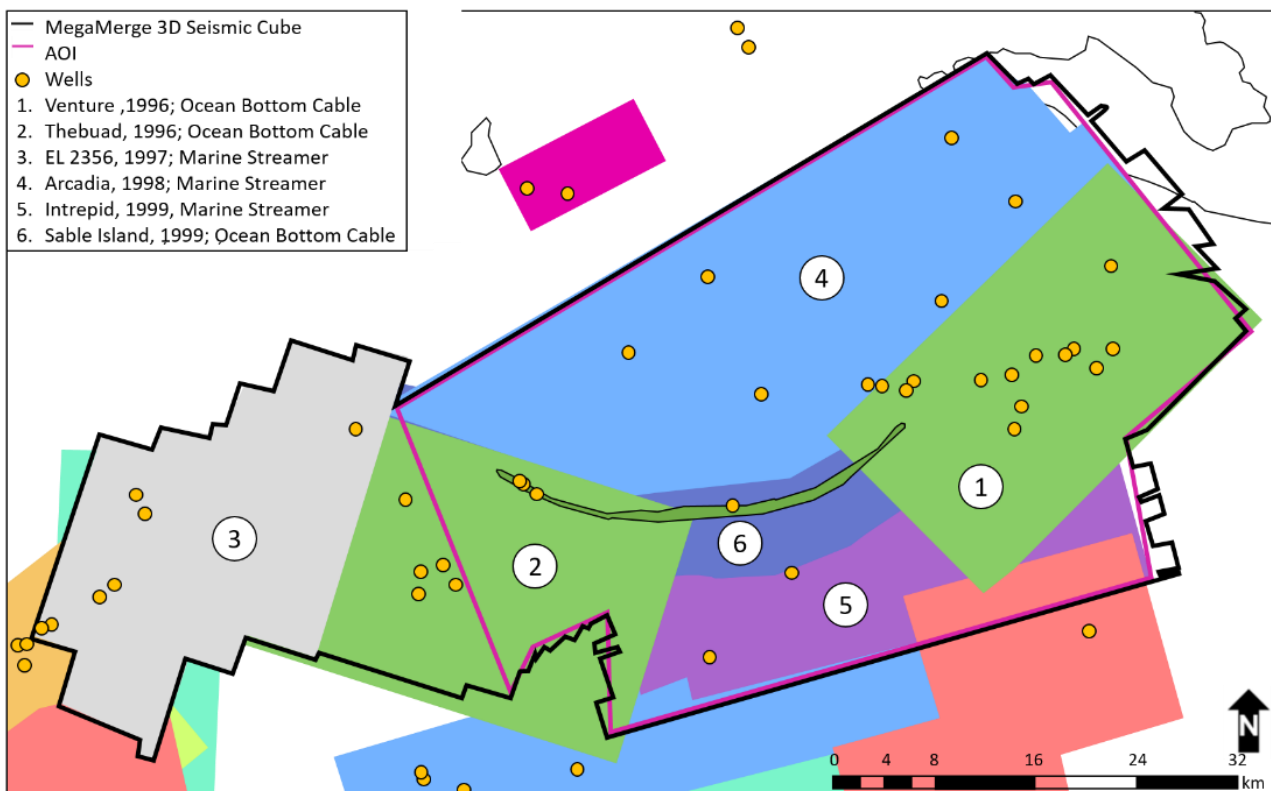


Figure 2. The six 3D seismic surveys included in the Sable MegaMerge survey and other surveys surrounding the area.

Objectives

This study hypothesized that source rocks in the Sable Subbasin, if present, can be identified using petrophysical and seismic techniques when applied to the Sable MegaMerge dataset. To test this hypothesis, we undertook the following: i) TOC was estimated from available wireline data using the Passey Method (Passey et al., 1990) in selected stratigraphic intervals and was examined for potential as source rock; ii) a seismic inversion was completed on the available seismic data within the study area, via a 3D constrained sparse spike inversion (CSSI, CGG Jason InverTrace^{PLUS}); and iii) the estimated TOC was correlated with the AI of selected intervals to identify source rock intervals (with high TOC and low AI) (Løseth et al. 2011). This was completed to investigate known and presumed Middle to Upper Jurassic source rocks within the Sable Subbasin using indirect petrophysical and seismic methods. The study area excluded the proximal Abenaki carbonate bank, focusing on the area with higher potential for the occurrence of source rock in the distal, eastern portion of the dataset (**Figure 2**).



Scotian Margin Results

Wireline TOC determination methods, such as the Passey Method, are proven to work best in thick organic-rich shale intervals (e.g. Passey et al., 1990). Within the Sable Subbasin, extensive and high TOC shales are not common, which meant there were issues in applying the method. For instance, difficulty in establishing a baseline was a problem encountered for a portion of the wells, including Venture B-52. This was likely due to extensive overpressure, and possible carbonate intervals, creating anomalous separation in the ΔLogR response in the non-organic shale intervals. When a baseline was unable to be established, the baseline from the closest well, in this case the neighboring Venture B-43 well (approximately 2500 m away) was used. This adds uncertainty when estimating the TOC values. Furthermore, the stratigraphic and structural variability made calibration between distant wells difficult.

Secondly, the limited thickness of the shales in the study area altered the effectiveness of this method. Typically, the Passey Method is completed on areally extensive, thick shales. Within the Sable Subbasin, there are many thin, interbedded shales less than a few meters thick. Petrophysically, intervals with thicknesses less than the combined resolution of the resistivity and sonic logs, approximately 1 m, cannot be reliably quantified (Passey et al., 1990). A strong shale signal from a thin bed may be masked by surrounding geology, giving an incorrect TOC estimate. Though it is possible source rocks as thin as 0.33 m can be identified using this method, results are not accurate (Passey et al., 1990). Many of the shales within the study area are only approximately 0.5 m thick and could fall below log resolution. Though shales this thick would not be considered viable source rocks, they could mask high TOC intervals.

Finally, this method was calibrated using TOC measurements. It is accepted that drilling practices have introduced contaminants to many samples tested in the basin and many high TOC values measured are likely a result of contamination (Mukhopadhyay, 1990a; Fowler et al., 2016). Overall, the Passey method's accuracy and success in the Sable Subbasin was variable. The method did not identify new intervals of high TOC values. Nevertheless, it did help identify possible contaminated intervals within the geochemical data. Within a single well interval, adequate estimations were achieved, especially when tested on thicker shale intervals outside the studied area (i.e. the Lower Cretaceous Logan Canyon Formation Shortland (Shale) Member in the Louisbourg J-47 well). However, both baselines and scale factors change from well to well, even with RockEval calibration. This level of uncertainty, as well as needing the comparison of the measured data, has deemed the method inapplicable on a basin wide scale in the study area.

The results of the source rocks from seismic method were inconclusive and varied from the examples presented in Løseth et al. (2011), (see also Ouadfeul and Ouadfeul, 2016). Attempting to plot acoustic impedance values versus TOC of the shales within the entire studied interval yielded no discernible relationship (**Figure 3**). Attempting this correlation at an individual well level yielded similar results in the majority of the wells. Some wells, such as South Venture O-59, visually illustrated a more meaningful correlation (**Figure 4**), however clusters of low impedance/ low TOC values were present which created a low R^2 value of the trendline.

The method was then attempted at a 150 m interval on the South Venture O-59 well. Though it yielded a trendline with a relatively low R^2 value of 0.4786, a profile was still created to test the method. The profile created from the AI relationship seemed to overestimate the TOC values in shales outside the tested 150 m. There is an additional uncertainty in this section, where a coal is identified by the Canadian Stratigraphic (CanStrat) logs, that could be the overlying cause of the low impedance values.

With no discernible correlation between AI and TOC, coupled with the uncertainties surrounding the geochemical analysis and the Passey Method, it was concluded that the TOC profiling would not work on a basin wide or seismic cube (ca. 2100 km²) scale.



An alternative explanation for the anomalous low acoustic impedance in some shale intervals is overpressure. Pennebaker (1968) described the change in bulk elastic properties of a rock due to the relationship between the expansion of the rock from overpressured fluids and the reduction in bulk density and velocity. Dutta et al. (2002a) highlights the observation that seismic velocity, thus acoustic impedance, in overpressured zones appears to be lower than in normally pressured intervals at equal depths.

In this study, low impedance calcareous shales, highlighted in the seismic inversion can be correlated via well calibration to overpressured zones (Figure 5). This means it is possible, as outlined by Dutta et al. (2002b), to image overpressured zones using the obtained seismic inversion. It was suggested that late stage hydrocarbon generation and migration in the Scotian Basin (see Wong et al., 2015; and Skinner, 2016) is the cause of the overpressured intervals in certain areas of the Sable Subbasin. We suggest that the low acoustic impedance shales highlighted in this study result from overpressure. If this assumption is true and overpressure results from hydrocarbon generation processes, then it provides indirect evidence of source rock presence outside the study area. Since overpressure is a key risk factor in the Scotian Basin (Skinner, 2016), this would be an excellent topic for future work.

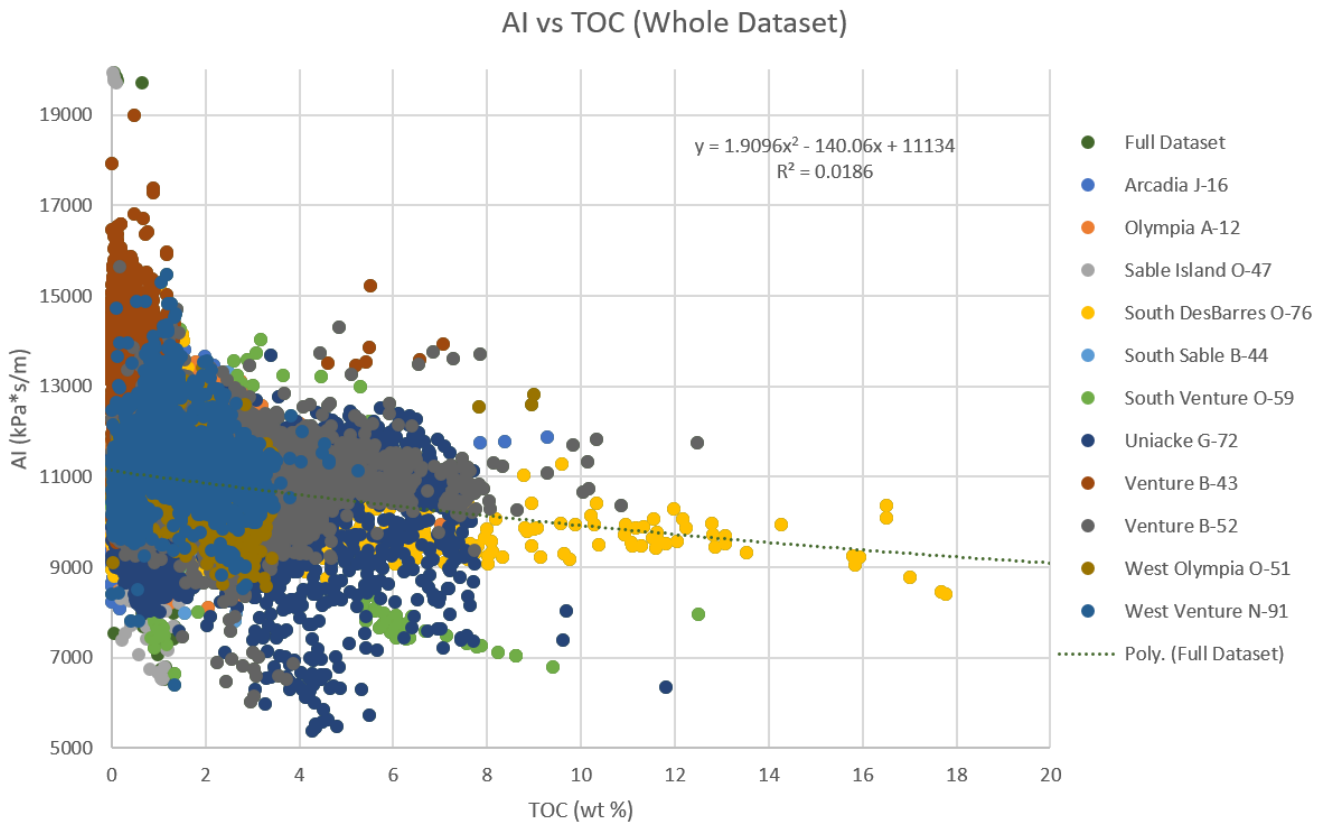


Figure 3. Acoustic impedance versus estimated TOC cross-plot for the shales over the entire inverted interval using all wells with TOC calculations completed.



South Venture O-59

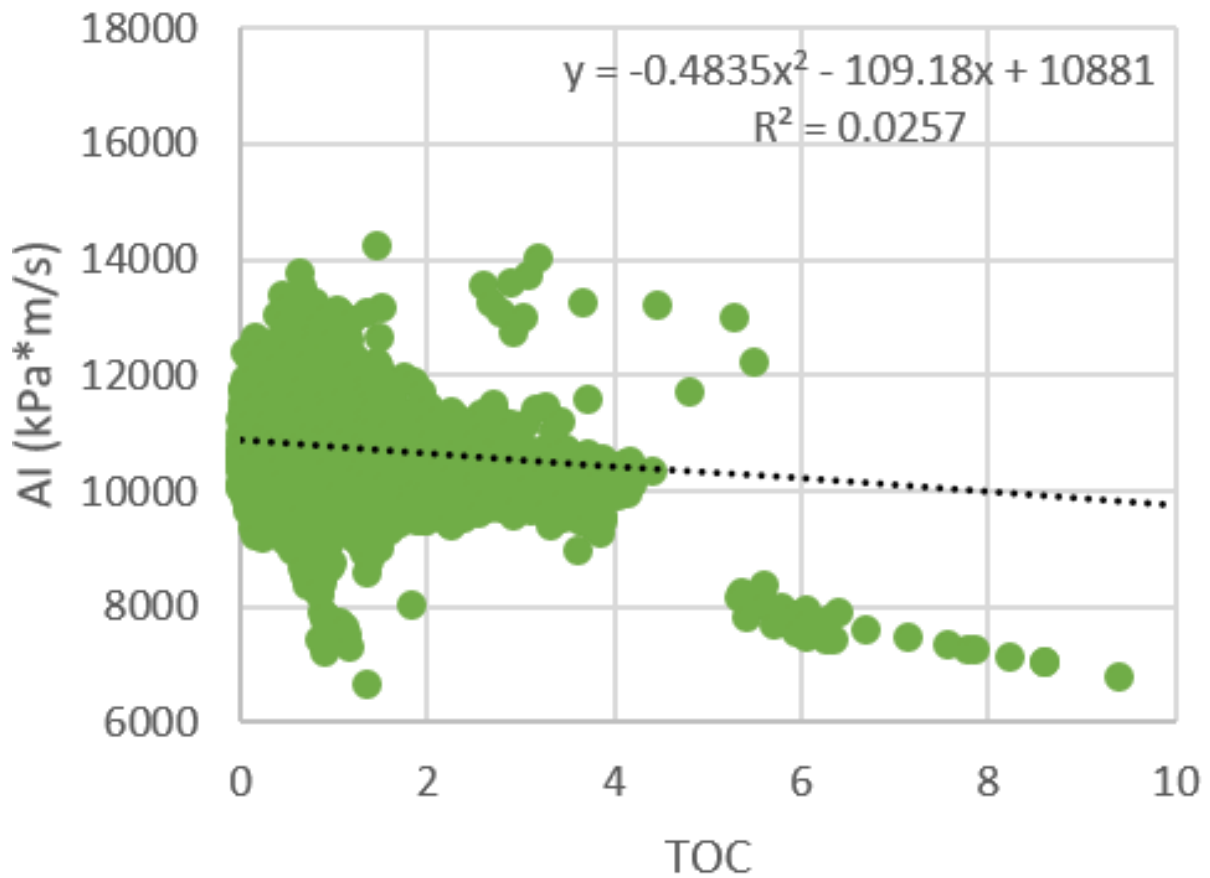


Figure 4. Acoustic impedance versus TOC cross-plots for the shales in the South Venture O-59 well.

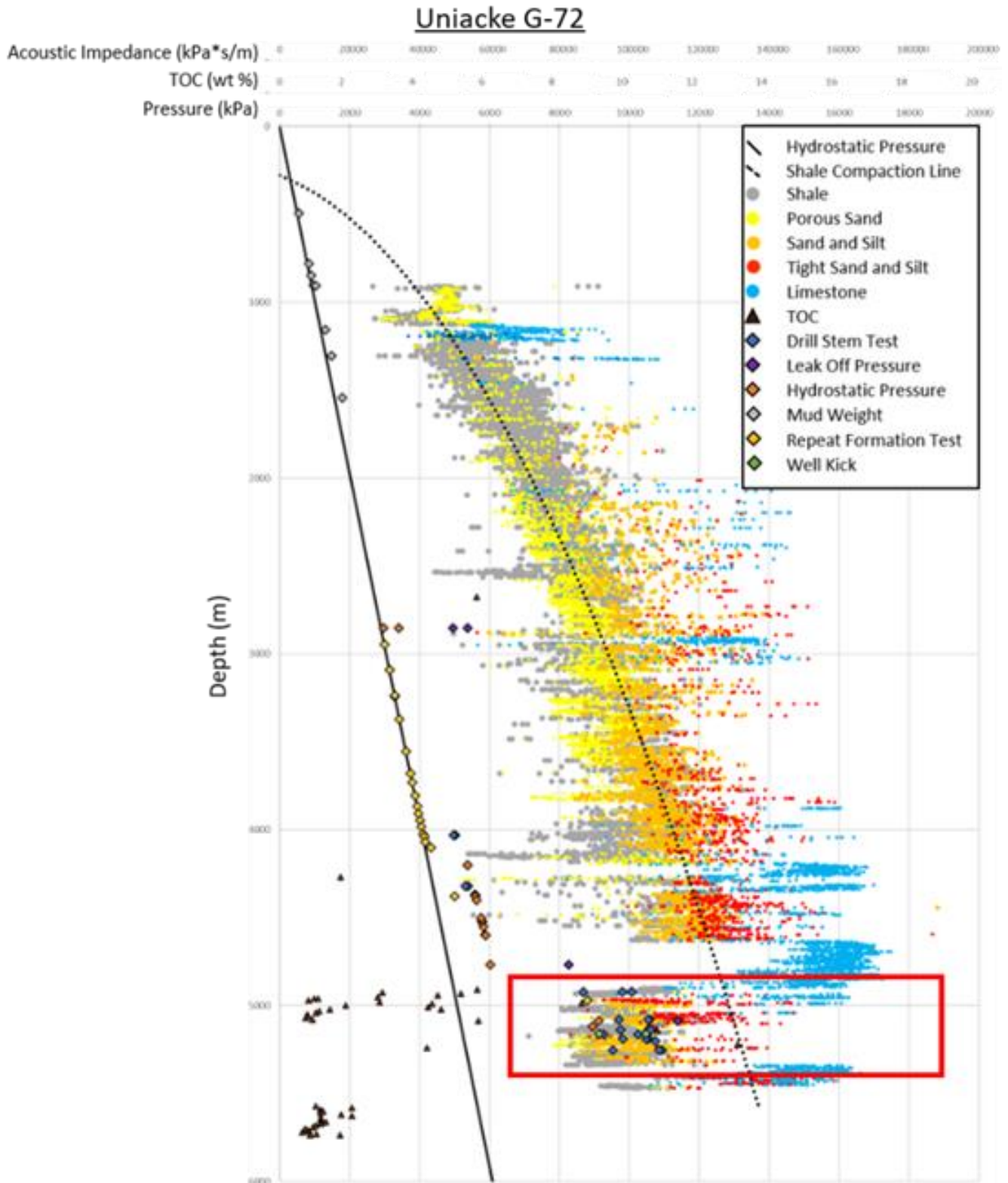


Figure 5. Cross-plot of AI, TOC and pressure measurements versus depth. The red box shows the interval of low AI that corresponds with excess pressure values



Summary and Conclusions

Though there are proven hydrocarbon accumulations in both Jurassic and Cretaceous reservoirs, as well as several studies and analysis done on shales in the Sable Subbasin, there have been difficulties identifying a definitive source of the hydrocarbons in what is an effective petroleum system (Fowler et al., 2016). The published TOC and RockEval pyrolysis data are often unreliable due to extensive use of oil-based muds, lignite additives and turbo-drilling practices (Mukhopadhyay, 1990a). The Scotian Margin is considered to have lean or low organic matter content, yielding low average TOC values, with a basinal average of approximately 0 to 2% (Mukhopadhyay 1989, 1990a, 1990b, 1991). Well penetrations of Jurassic sediments, a known time of prolific source generation along the Atlantic Margin, are very limited in this area.

The objective of this project was to investigate known and presumed Middle to Upper Jurassic source rocks within the Sable Subbasin using indirect methods, hypothesizing that source rocks intervals could be identified by petrophysical and seismic techniques. Results of this hypothesis were negative; though lean organic matter is present throughout the study area (Mukhopadhyay 1989, 1990a, 1991), prevalent source rocks could not be imaged using seismic inversion. The petrophysical methods did not identify specific intervals of source rock in the eleven wells studied, even when the TOC values calculated were compared to the measured TOC values from studies published (Mukhopadhyay et al., 1990a, 1995). TOC and RockEval data in these studies, and data from the Geological Survey of Canada's BASIN online database, show similar low TOC values and identify contaminants that can skew results to over 4% TOC (Mukhopadhyay, 1990a; NRCan, 2016). The seismic inversion was effective in mapping low acoustic impedance intervals, especially calcareous shales; however, a strong relationship between AI and TOC was not found. This was the result of the low TOC contents of the thin shales that were investigated. The studied shale intervals have insufficient thickness and organic richness to be considered viable source rocks.

The conclusion of this research is that the petrophysical and seismic techniques used in this project do not identify presumed or potential source rocks within the study area of the Sable Subbasin. This is the first time that these approaches to source rock presence and distribution have been documented in offshore Nova Scotia. Though the results were not promising for source rock identification in the study area and stratigraphic interval, the method should not be ruled out for use on other parts of the Margin and did identify a link between low AI sections mapped via seismic inversion and overpressure.

References

- Bicep-Franlab (Nova Scotia Department of Energy), 2011. Play Fairway Analysis (PFA) offshore Nova Scotia Canada. Published report [online]. Available from <http://www.oera.ca/offshore-energy-research/geoscience/play-fairway-analysis/> [cited September 30, 2014].
- Bicep-Franlab (Nova Scotia Department of Energy), 2016. Central Scotian Slope Atlas. Published Report [online]. Available at <http://www.oera.ca/offshore-energy-research/geoscience/central-scotian-slope-atlas-2016/> [cited March 1 2016].
- CNSOPB. Information on Well Data, Geological Data, and Geophysical Data [online]. Available http://www.cnsopb.ns.ca/sites/default/files/pdfs/information_on_well_data_geological_data_and_geophysical_data_april_2014.pdf [cited 23 March 2017].
- Dutta, N., Mukerji, T., Prasad, M., and Dvorkin, J., 2002a. Seismic Detection and Estimation of Overpressures Part I: the Rock Physics Basis. CSEG Recorder, **27**(7).
- Dutta, N., Mukerji, T., Prasad, M., and Dvorkin, J., 2002b. Seismic Detection and Estimation of Overpressures Part II: Field Applications. CSEG Recorder, **27**(7).



- Dutta, N.C. 2012. Geopressure prediction using seismic data: Current status and the road ahead. *Geophysics*, **67**(6), 2012-2041.
- Enachescu, M. and Wach, G.D. 2005. Exploration Offshore Nova Scotia: Quo Vadis? (Where do we go from here?). *Ocean-Resources*, 23-35.
- Fowler, M., Webb, J., Obermajer, M., Monnier, F., Mort, A., Kuheshi, M., and MacDonald, A., 2016. Petroleum Systems of the Scotian Basin. Adapted from oral presentation given at American Association of Petroleum Geologists 2016 Annual Convention and Exhibition, Calgary, Alberta, Canada, June 19-22, 2016, AAPG Search and Discovery Article #90259.
- Huc, A.-Y. (ed) 1995. Paleogeography, Paleoclimate, and Source Rocks. American Association of Petroleum Geologists, *Studies in Geology*, **40**, 347.
- Jason – a CGG Company. 2013. Introduction to Acoustic Impedance Inversion. Fugro Jason.
- Langrock, U. 2004. Late Jurassic to Early Cretaceous: black shale formation and paleoenvironment in high northern latitudes. *Ber. Polarforsch. Meeresforsch.*, 472.
- Løseth, H., Wensaas, L., Gading, M., Duffaut, K., and Springer, M. 2011. Can hydrocarbon source rocks be identified on seismic data? *Geology*, **39**, 1167–1170.
- Morgans-Bell, H.S., Coe, A.L., Hesselbo, S.P., Jenkyns, H. C., Weedon, G.P., Marshall, J.E.A., Tyson, R.V., and Williams, C.J. 2001. Integrated stratigraphy of the Kimmeridge Clay Formation (Upper Jurassic) based on exposures and boreholes in south Dorset, UK. *Geologic Magazine*, **138**(5), 511-539.
- Mukhopadhyay, P.K. 1995. Organic petrography and kinetics of Jurassic/Cretaceous shales and geochemistry of selected liquid hydrocarbons, Scotian Basin. Geological Survey of Canada, Open File Report 3284, 101 p.
- Mukhopadhyay, P.K. 1994. Organic petrography and kinetics of limestone and shale source rocks in wells adjacent to Sable Island, Nova Scotia and the interpretation on oil-oil or oil-source rock correlation and basin modeling. Geological Survey of Canada, Open File Report 3167, 100p.
- Mukhopadhyay, P.K. 1993. Analyses and interpretation of geochemical and source rock data from Scotian Shelf wells. Geological Survey of Canada, Open File Report 2804, 232p.
- Mukhopadhyay, P.K. 1991. Evaluation of Organic Facies of the Verrill Canyon Formation Sable Subbasin, Scotian Shelf. Geological Survey of Canada, Open File Report 2435, 37p.
- Mukhopadhyay, P.K. and Wade, J. A. 1990. Organic facies and maturation of sediments from three Scotian Shelf wells. *Bulletin of Canadian Petroleum Geology*, **38**(4), 407-425.
- Mukhopadhyay, P.K. 1990a. Mesozoic Organic Facies Isotopes. For Atlantic Geoscience Centre, Geological Survey of Canada.
- Mukhopadhyay, P.K. 1990b. Characterization and maturation of selected Cretaceous and Jurassic source rocks and crude oil, Scotian Shelf. Geological Survey of Canada, Open File Report 2621, 99p.
- Mukhopadhyay, P.K. 1989. Organic Facies in the Sable Subbasin, Scotian Shelf. For Scientific Authority, D. McAlpine. Atlantic Geoscience Center, Bedford Institute of Oceanography, and Geological Survey of Canada.
- Natural Resources Canada (NRCAN), 2016. BASIN Database. http://basin.gdr.nrcan.gc.ca/index_e.php
- Ouadfuel, S.-I., and Ouadfeul, L. 2016. Total organic carbon estimation in shale-gas reservoirs using seismic genetic inversion with an example from the Barnett Shale. *The Leading Edge*, **35**(9): 790-794.
- Offshore Energy Research Association of Nova Scotia (OERA). 2013. Chapter 4: Petroleum Geology. Written for the OERA [online]. Available from <http://www.oera.ca/wp-content/uploads/2013/04/Chapter-4-Final.pdf> [cited 10 January 2015].



- Offshore Energy Research Association of Nova Scotia (OERA). 2013. OERA Recommended Research Programs; 2013 to 2016 [online]. Available from <http://www.oera.ca/wp-content/uploads/2013/07/OERA-Geoscience-Programs-11-April-2013.pdf> [cited 8 December 2014].
- Passey, Q.R., Creaney, S., Kulla, J.B., Moretti, F.J., and Stroud, J.D., 1990. A practical model for organic richness from porosity and resistivity logs. *AAPG Bulletin*, **74**: 1777-1794.
- Pennebaker, E.S., 1968. Seismic data indicate depth, magnitude of abnormal pressure. *World Oil*, **166**: 73-78.
- Skinner, C.H., 2016. Excess Pressure and Reservoir Compartmentalization in the Sable SubBasin, Offshore Nova Scotia. Unpublished M.Sc. thesis, Department of Earth Sciences, Dalhousie University, Halifax, Nova Scotia, Canada, 220p.
- Wade, J.A. and MacLean, B.C. 1990. Chapter 5 - The geology of the southeastern margin of Canada, Part 2: Aspects of the geology of the Scotian Basin from recent seismic and well data. In: M.J. Keen and G.L. Williams (eds), *Geology of Canada No.2 - Geology of the continental margin of eastern Canada*. Geological Survey of Canada, 190-238.
- Wade, J.A., MacLean, B.C., and Williams, G.L., 1995. Mesozoic and Cenozoic stratigraphy, eastern Scotian Shelf: new interpretations. *Canadian Journal of Earth Science*, **32**(9), 1462-1473.
- Wade, J.A. (with contributions by Brown, D.E., Durling, P., MacLean, B.C. and Marillier, F.), 2000. Depth to Pre-Mesozoic and Pre-Carboniferous Basements. Geological Survey of Canada, Open File Report No.3842 (1:1,250,000 map of Scotian Shelf & Adjacent Areas).
- Weston, J.F., MacRae, R.A., Ascoli, P., Cooper, M.K., Fensome, R.A., Shaw, D., and Williams, G.L. 2012. A revised biostratigraphic and well-log sequence-stratigraphic framework from the Scotian Margin, offshore Eastern Canada. *Canadian Journal of Earth Sciences*, **49**(12), 1417-1462.
- Williams, H., and Grant, A.C. 1998. Tectonic assemblages, Atlantic Region, Canada. 1:3 000 000 map. Geological Survey of Canada, Open File 3657.
- Williamson, M.A., and Desroches, K., 1993. A Maturation Framework for Jurassic Sediments in the Sable Sub-basin, Offshore Nova Scotia. *Bulletin of Canadian Petroleum Geology*, **41**(2), 244-257.
- Williamson, M. A., and Desroches, K., 1992. Source Rock Maturity Modeling: Sable and Jeanne D'Arc Basins Offshore Eastern Canada. Abstract, American Association of Petroleum Geologists Annual Meeting, Calgary, Alberta, Canada, June 22-25, 1992, AAPG Search and Discovery Article #91012.
- Wong, J. C., Skinner, C. H., Richards, F. W., Silva, R. L., Morrison, N., and Wach, G.D., 2016. 1D thermal model of South Venture O-59, Sable Subbasin (Scotian Basin, Nova Scotia). In: Proceedings of the 42nd Colloquium and Annual Meeting of the Atlantic Geoscience Society, Truro, Nova Scotia.
-



NEWFOUNDLAND ORPHAN BASIN: STRUCTURAL KEY ELEMENTS FOR THE NORTHEAST ATLANTIC OPENING

Pichot, Thibaud¹, Le Guerroué, Erwan¹, Filleaudeau, Pierre-Yves¹, and Micarelli, Luca¹

¹Beicip-Franlab, 232 avenue Napoléon Bonaparte, Rueil-Malmaison 92500, France, thibaud.pichot@beicip.com

The Newfoundland margin has a high hydrocarbon potential confirmed with discoveries and production in the Jeanne d'Arc Basin, and most recently discoveries in the Flemish Pass Basin. Both basins share a common structural evolution within the Orphan Basin. The recent acquisition of a large high quality 2D-3D seismic dataset sheds new light on the hydrocarbon prospectivity of the margin, and provides constraints to a new structural model for the early stage of Northeast Atlantic rift. (Nalcor Energy invested in a TGS/PGS multi-client 2D broadband long offset seismic program offshore Newfoundland.)

The newly imaged 400 km wide Orphan Basin, at the junction between Newfoundland-Iberia and Newfoundland-Irish rift systems, records the long-lasting rifting processes active in the Northeast Atlantic region during the Mesozoic.

The NW-SE Upper Jurassic-Lower Cretaceous (Neocomian) tectonic extension related to Newfoundland-Iberia rift system explains most of the structural evolution of the Orphan Basin and implies that up to 800 km of stretched continental lithosphere must be considered when studying the continental rifting processes between these margins.

The Northeast Atlantic region is characterized by the Late Jurassic-Neocomian intracontinental rift system with two main branches: a western branch passing through the Jeanne d'Arc, Orphan, Porcupine and Rockall basins that experienced several hyper-extensions episodes without achieving a continental break-up, and an eastern branch reaching rupture through rift propagation between Newfoundland and Iberia during the Late Aptian. Before extension, the Orphan Knoll, Porcupine High, Galicia Bank, Goban Spur, and Flemish Cap continental fragments formed a large, unstretched continental block that may have played a role in the rifting process as partially locked zones.

The tectonic stress drastically changes from NW-SE to NE-SW at the end of the Lower Cretaceous with only minor impact in the Orphan Basin (i.e. local tectonic inversion). This stage led to continental stretching between Newfoundland and Northwest Europe and reached continental breakup in the Late Albian. The study of the Orphan Basin demonstrates the influence of inherited structural features (i.e. orogenic sutures) and continental blocks on the spatial and temporal dynamics of the Northeast Atlantic rifting.

Introduction

North Atlantic passive margins are studied actively with detailed geophysical investigations and drilling programs especially around Newfoundland-Iberia conjugate margins that are usually considered as the classical end-member of magma-poor rifted margin. Most of recent improvements are concentrated in distal margins and help better understand the final stage of rifting (Tucholke et al., 2007; Péron-Pinvidic and Manatschal, 2009; 2010). On the other hand, proximal domains and failed rift systems provide key elements about the earliest stages of rift formation and its propagation.

The Orphan Basin forms part of a series of Mesozoic rift basins east of Newfoundland, off Canada's east coast (**Figure 1**) with active hydrocarbon production and exploration. This margin experienced successive rift episodes associated with the opening of the North Atlantic Ocean. Continental extension started between the North American and Northwest African plates in the Upper Triassic and ended with seafloor spreading in the Lower Jurassic. After relative tectonic quiescence during the Middle Jurassic, the dislocation of the supercontinent Pangea



continued further north between North America (Newfoundland) and Iberia (Galicia) plates during the Upper Jurassic to Lower Cretaceous. As the rift propagated, continental breakup was achieved between the North American and Western Eurasian plates at the end of Lower Cretaceous. Continental extension migrated toward the northern sector of the North Atlantic during the Upper Cretaceous and seafloor spreading initiated in the Eocene between Greenland and Northwest Europe.

The Orphan Basin (including the Flemish Pass Basin) is 400 km long and 350 km wide. The Charlie-Gibbs fracture zone and the Orphan Knoll, just west of the Continent Ocean Transition (COT), mark its northern limit (**Figure 1**). The Flemish Cap and the Bonavista Platform, two shallow marine highs, bound respectively its eastern and western basin flanks. Defining the Orphan Basin’s southern limit is a strong positive free-air gravimetric anomaly called the Cumberland Transfer Zone that isolates it from the Jeanne d’Arc Basin.

A limited number of wells have been drilled in the marginal basins of Newfoundland. The first significant oil discovery was made in 1979 by the Hibernia P-15 well in the Jean d’Arc Basin, and demonstrated the high hydrocarbon prospectivity of the region. Recent discoveries in the Flemish Pass Basin have considerably revived the regional interest and provided new perspectives along not only the Newfoundland margin but also the Irish marginal basins. In order to better understand and define the prospectivity of the offshore Newfoundland and Labrador margin, since 2010 Nalcor Energy has invested in an extensive high quality 2D-3D seismic data acquisition initiative, with TGS/PGS undertaking a multi-client 2D broadband long offset seismic program. In this study, we use these newly acquired seismic data to define key elements for the early stages of rifting and to bring a new perspective on the Orphan Basin prospectivity.

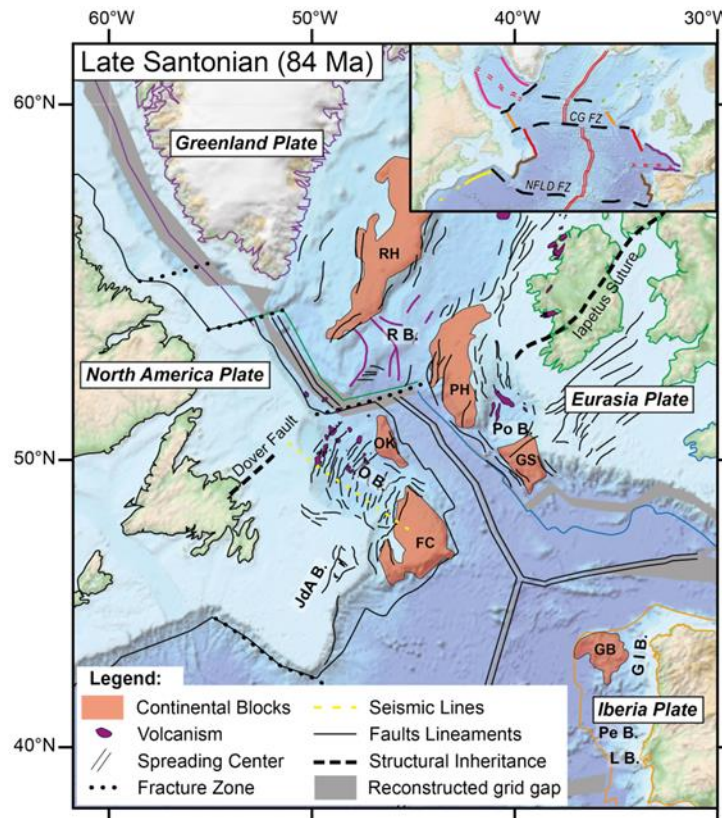


Figure 1. Plate reconstruction at 84 Ma (Seton et al., 2012), the main structural elements and the main Mesozoic Basins are indicated – G I B. Galicia Interior Basin; JdA B. Jeanne d’Arc Basin; L B. Lusitania Basin; O B., Orphan Basin; Pe B. Peniche Basin; Po B. Porcupine Basin. Inset: Regional map of the North Atlantic showing the conjugate segments of margins (colored lines) and Fracture Zones: CGFZ Charlie Gibbs fracture zone; NFLDFZ, Newfoundland fracture zone.



Results

Seismic interpretation is calibrated on several key wells available in the region including the Hare Bay E-21, Blue H-28, Great Barasway F-66, and Lona O-55 wells. Major seismic horizons are mapped and the represent stratigraphic sequence base and/or top, and regional unconformities. Because most of the wells are located on shallow structures (i.e. shelf, horsts, and top of tilted fault blocks), the base of the sedimentary cover is commonly not well constrained. The Paleozoic metasediments are recorded at wells in the central part of the Orphan Basin (referred later as Central Orphan High). Carboniferous anthracitic sediments have been cored in the Orphan Knoll (Laughton et al., 1973). Fault interpretation was performed in order to reveal the regional fault patterns and the spatial distribution of the deformation.

The oldest sedimentary sequence recorded in wells in the Eastern and Central parts of the Orphan Basin is Kimmeridgian in age representing the climax of the synrift sequence. Change in the sedimentary fill geometry occurs at the Kimmeridgian-Tithonian transition. The extent of Tithonian interval is more widespread (**Figure 2**).

Affecting the Upper Jurassic sedimentary cover are numerous NNE-SSW-trending normal faults. These are generally sealed by the top Tithonian, and root down into the continental crust (**Figure 2**). Major faults' dip decreases with depth somewhere in the continental crust. Their geometries suggest these faults root in a ductile shear level, presumably in the middle or lower continental crust. The hanging wall blocks rotate along the fault plane and define half-graben crustal fault blocks with variable vergence. This thick-skin tectonic style affects most of the Orphan Basin. The NNE-SSW crustal faults are bounded often by short N120° structural lineaments. This latter structural trend may be linked to relay ramps within an overlapping faults zone, to transfer zones, or, to inherited heterogeneities.

In the eastern part of the basin, a continuous seismic reflector with strong amplitude is observed below the acoustic basement and interpreted as the Moho discontinuity. Refraction seismic study and forward gravimetric modelling (Watermez et al., 2015; Lau et al., 2015) confirm this interpretation and show that the continental thickness thins to less than 5 km. This domain of localized hyperextension is defined along a narrow corridor where the normal crustal faults root at the crust-mantle boundary, and can be compared to the S-reflector (Reston et al., 1996). This failed rift axis is offset locally in a right-lateral sense.

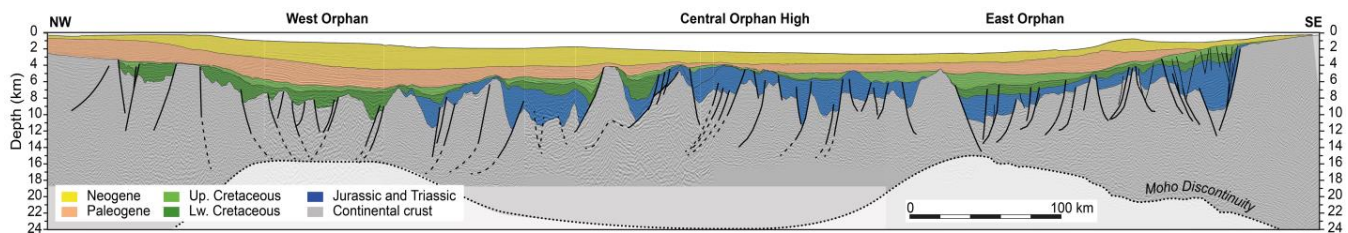


Figure 2. Seismic interpretation along the whole Orphan Basin. Moho depth deduced from seismic reflection data and Lau et al. (2015). See **Figure 1** for location.

Further west the Central Orphan High that corresponds to the southwestern extension of the Orphan Knoll, is characterized by a shallower Paleozoic basement (**Figure 2**), and a deeper Moho (20-25 km depth) (Chian et al., 2001; Watremez et al., 2015). Here, large northwest-dipping normal crustal faults define half-graben structures. Top Tithonian lies within the synrift sequence, confirming the widespread lateral extent of the Upper Jurassic rifting.

A second phase of deformation occurs in the Neocomian (Lower Cretaceous) and consists mainly in fault reactivation sealed by the top Valanginian horizon. Some other faults do not show clear downdip continuity at depth and may sole out in Early Cretaceous or Late Jurassic sediments (**Figure 2**). This stage marks the second



major extensional phase that shaped the Orphan Basin. While this stage is less intense than the previous one in the eastern and central parts of the Orphan Basin, important subsidence is recorded at the western edge of the Flemish Cap area. The Neocomian fault pattern shows a similar direction. The central rift valley described in the eastern part of the basin subsided progressively without major fault activity.

As proposed by Doré et al. (1999), the Upper Jurassic and Lower Cretaceous stage must be viewed as two consecutive extensional stages. While the maximum horizontal stress remained unchanged, the tectonic style (and the intensity of the deformation) is different. These two phases are separated generally by a strong unconformity at the base of Lower Cretaceous.

In the western part of the Orphan Basin, the Lower Cretaceous interval is affected by normal faulting. Growth strata in Neocomian synrift sediments confirm Lower Cretaceous extension in this region. Conjugate crustal normal faults geometry suggests the presence of a rift valley. The refraction seismic results of the Lithoprobe 86-6/86-8 seismic line (Chian et al., 2001) agree with extreme continental thinning at the same location. The western part of the Orphan Basin experienced hyperextension in the Lower Cretaceous (**Figure 2**) associated with local volcanic intrusions in the center of the rift valley. However, due to the lack of deep wells in this area, uncertainties remain about the age of the extension initiation. The possible influence of Upper Jurassic extension as far as the western part of the Orphan Basin cannot be excluded.

In some places, fault activity is recorded in the late Lower Cretaceous interval, and sealed by the top Aptian horizon. This stage contrasts from those previously described, and the intensity of the deformation is less important than the previous ones. Local inversion features are described along NNE-SSW Upper Jurassic crustal faults. Here, transpressional deformation induces local uplift of the hanging-wall blocks. The NW-SE (N120°E) transfer zones present extensional faults reactivation. Normal faults develop at the edge of the N120°E Cumberland Transfer Zone, south of the Orphan Basin.

These observations are in agreement with the drastic change of the regional tectonic stress regime in the late Lower Cretaceous passing from NW-SE to NE-SW. The N125° normal faults formed at the northern edge of the Flemish Cap and similar faults trend are presents south of the Goban Spur on the Irish conjugate margin.

The late Lower Cretaceous rift described in the Orphan Basin arises from the continental separation between Newfoundland and Irish conjugate margins.

Overall, the Upper Cretaceous (including Albian) sedimentary fill presents a well-developed depocentre in the eastern part of the Orphan Basin with the sequence thinner throughout the western part of the basin. The initiation of the depocentre occurs later within the Paleogene interval, suggesting a distinct subsidence history. This supports the hypothesis of two consecutive stages of rifting; one focusing in the eastern part of the basin during the Upper Jurassic, and one more localized in the western part during the Lower Cretaceous.

The base of the Tertiary sequence is regionally well defined across the Orphan Basin. In the Central Orphan High, it represents an erosional surface on top of the tilted fault blocks. This suggests that the Central Orphan High region records differential subsidence. Progressive downlaps overlaying the base of the Tertiary illustrate a regional thermal subsidence of the basin in Lower Tertiary time (**Figure 2**).

Discussion

In a classical rifted margin model, the crustal extension occurs orthogonally to the continental margin. In the Orphan Basin, the major NNE-SSW crustal fault trend is perpendicular to the Newfoundland-Irish continental margins (**Figure 1**). This fault trend matches perfectly the flow lines describing the relative motions between the Newfoundland and Iberia plates. Also, the timing and style of deformation described in the Orphan Basin fit perfectly with those described at the distal domains of the Newfoundland and Galicia conjugate



margins. This implies that the Orphan Basin shares more genetic links with the Newfoundland-Iberia rift rather than the Newfoundland-Irish rift.

Refraction seismic acquisition along the marginal basins offshore Ireland reveals that the South Porcupine and Rockall basins show hyper-extension domains comparable to those found in the Orphan Basin (Lau et al., 2015). The thickness of the crust does not exceed 5 km (Watremez et al., 2016) in South Porcupine Basin and ca. 6 km (O'Reilly et al., 1995) in Rockall Basin. The Upper Jurassic deformation in the South Porcupine Basin is very similar to the eastern Orphan Basin.

The drastic change in the tectonostratigraphic evolution between north and south Porcupine Basin is likely due to the presence of lithospheric anisotropy represented by the inherited Caledonian Iapetus sutures separating the Laurentia and Avalonia cratons (Domeier and Trorsvik, 2014). The presence of the Iapetus suture would explain why the Upper Jurassic-Neocomian extension is less intense in the north Porcupine Basin than in the south.

This feature extends the Irish margin on to the Newfoundland margin as the Dover Fault and corresponds to the Charlie-Gibbs fracture zone in the oceanic domain. The Upper Jurassic half-graben structures described in the Central Orphan Basin likely can be compared to the perched marginal basins of the Rockall Basin (Bróna, Pádraig, and Macdara basins). The Lower Cretaceous tectonic subsidence associated with volcanic intrusion and the hyperextension found in the Rockall Basin is comparable to the western part of the Orphan Basin at the same period. The points mentioned above suggest that these basins have shared the same tectonic evolution during the Upper Jurassic to Neocomian times (Pichot et al., 2016).

The Newfoundland, Iberia, and Irish margins share similar shallow marine highs at their outer proximal margin domains (**Figure 1**). They are the Flemish Cap and Orphan Knoll (Newfoundland), Galicia Bank (Iberia), and Porcupine and Rockall Highs (Ireland). Refraction profiles and gravimetric modelling (Pérez-Gussinyé et al., 2013; Watremez et al., 2015; Lau et al., 2015) indicate a total crust thickness of 32 km beneath Flemish Cap and 20 km beneath Galicia Bank. Along the Irish continental margin, the Porcupine and Rockall Highs have the same characteristics with a total crust thickness of ca. 30 km (Morewood et al., 2005; O'Reilly et al., 2006). The hyperextension mentioned above took place systematically between each of the continental blocks.

Plate reconstructions presented in **Figure 3** show that the Flemish Cap and Galicia Bank present similar positions relative to the continental margin. They can be interpreted as originating from a unique single block. Similarly, the Orphan Knoll and Porcupine High must have formed one single block before continental breakup (**Figure 3**). During rifting, these continental blocks must have kept stronger crustal cohesion compared to the surrounding area thus creating locked zones.

The Newfoundland-Iberia rifted margins present a diachronous locus of continental rift migrating progressively northward (**Figure 3**). The M0 magnetic anomaly is identified 200 km from the continental margins' COT just north of the Newfoundland fracture zone and gets closer further north until disappearing completely toward the continental margin of Flemish Cap and Galicia Bank. The rifting process in place at the Newfoundland-Iberia conjugate margins can be viewed as rift propagation as described by Courtillot (1982), and Van Wijk and Blackman (2005). During the initial rifting stage, tensional forces lead to rifting initiation between locked zones. The rift propagates towards the locked zones along thinned lithosphere and slows down as it approaches one with higher strength. The amount of stretched continental lithosphere is much higher at the vicinity of locked zones where the deformation is distributed over a larger area. Finally, the strength decreases during the thinning of the lithosphere, and the tensional forces lead to break apart of the locked zone and allow the rift to propagate toward the next locked zone.

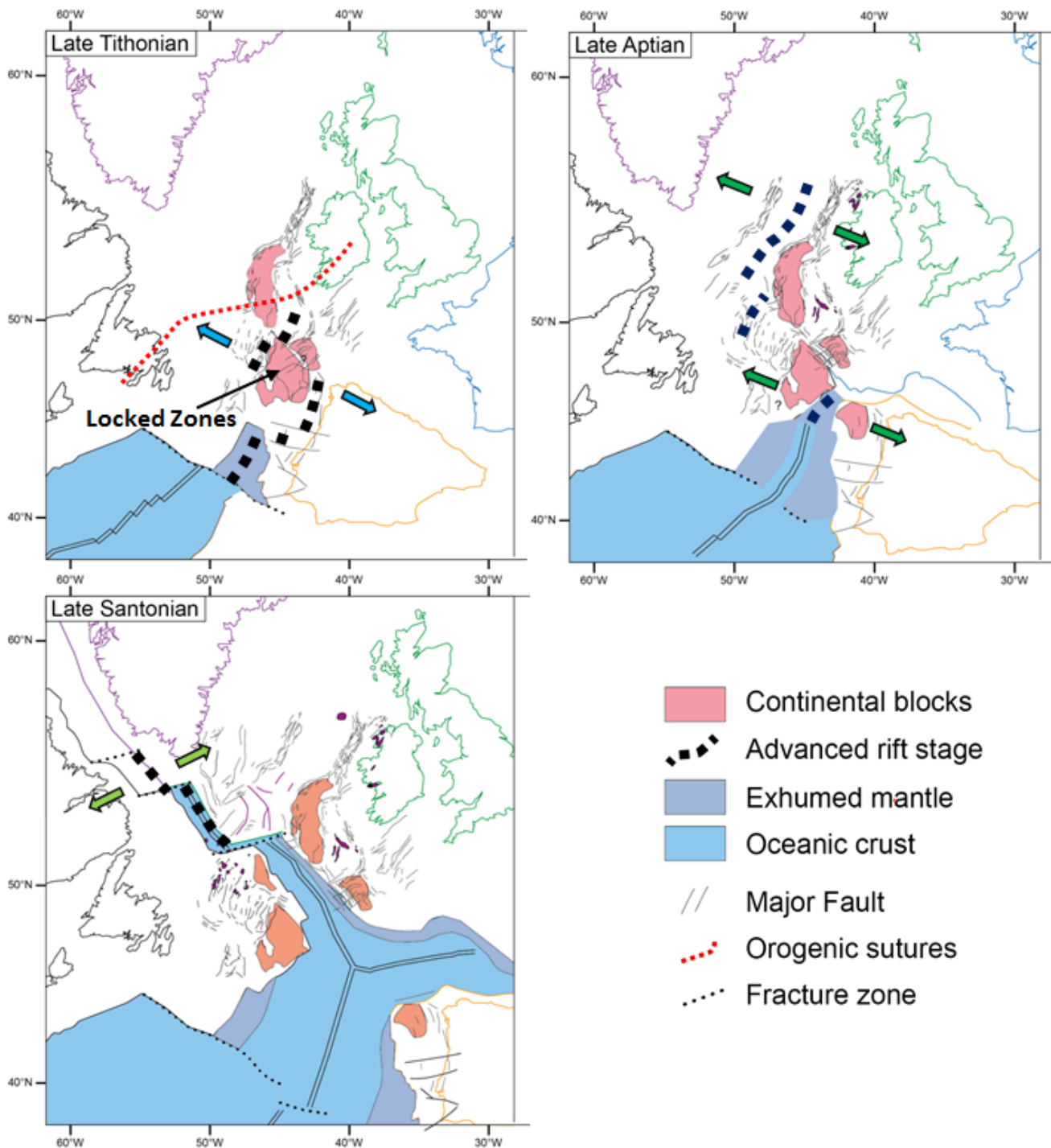


Figure 8. Plate reconstructions during the early stage of rifting showing the continental blocks and the main continental rifting area (adapted from Seton et al., 2012).

The South China Sea (SCS) is a good example of a “V-shape” propagation rift system and shares common characteristics with Newfoundland-Iberia conjugate margins (Huchon et al., 2001). Macclesfield Bank and Reed Bank are two unstretched granitic plutons located on each side of the conjugate margins (Savva et al., 2014). A failed rift system and extinct seafloor-spreading centre is present north of the Macclesfield Bank. The presence of



these continental blocks seems to have an impact on the propagation of the rift toward the southwest. Moreover, the southwestern margin of the SCS exhibits more than 500 km of extended continental crust (Pichot et al., 2014).

Within the framework of a consistent and global tectonic framework over the North Atlantic margin, the tectonostratigraphic analysis of the Orphan Basin presented in this study, with a critical review of the evolution of the surrounding marginal basins, allow us to propose a model for the early stage of rifting in the southern Northeast Atlantic region.

The Hettangian (earliest Jurassic) evaporite succession deposited in the Lusitanian-Peniche Basin (Iberian Plate) has the same age as the one deposited in the Jeanne d'Arc basin (North American margin). This implies a connection and similar depositional environments between these two basins until the late Middle Jurassic. This is confirmed by the presence of hydrocarbon source rock intervals throughout the Lower and Middle Jurassic described in both margins (McAlpine, 1990; Alves et al., 2009; Welsink and Tankard, 2012). The Jeanne d'Arc Basin and the Lusitanian and Peniche basins record an earlier rifting phase in the Upper Callovian. The major phase of deformation took place between the latest Kimmeridgian and the Lower Berriasian (in the Lusitania-Peniche Basin) or Lower Valanginian (in the Jeanne d'Arc Basin) (**Figure 3**).

During Upper Jurassic time, the Flemish Cap and Galicia Bank were still aggregated together forming a large locked zone. According to Lundin and Doré (2011), the Cumberland Transfer Zone may have acted as a potential decoupling zone between the Orphan and Jeanne d'Arc basins during the rifting.

Upper Jurassic extension focused at the eastern and western rims of this large locked zone (**Figures 3 and 4**). In the Galicia interior basin (east of the Galicia Bank), a major extension stage initiates in the Kimmeridgian and culminates in the Valanginian (Murillas et al., 1990). Concurrently, the eastern and central parts of the Orphan Basin underwent widespread crustal extension and local hyperextension from the Kimmeridgian to Upper Tithonian (Figure 4). This rift branch extends farther north up to the south Porcupine Basin where the intensity of the deformation decreases in the Lower Cretaceous (**Figure 3**). The rift stops at the approach of the lithospheric Iapetus suture. With decreasing strength during the thinning of the lithosphere, the tensional forces lead to a break apart of the Flemish Cap-Galicia Bank locked zone thus allowing the rift to propagate between them during the Neocomian.

Across the Iberian Margin, the deformation shifted oceanward within the Galicia Bank and Deep Galicia Margin after the Valanginian (Boillot and Winterer, 1988; **Figures 3 and 4**). At the same time, the Newfoundland margin experienced two distinct locus of deformation (**Figures 3 and 4**). While crustal hyperextension occurred in the western Orphan Basin, active faulting has been described in the western edge of the Flemish Cap area. Moreover, continental extension propagated east of the Flemish Cap and continental breakup was achieved during the Hauterivian (Tucholke et al., 2007). Finally, subcontinental mantle exhumation occurred from the Barremian to Upper Aptian (Tucholke et al., 2007; **Figures 3 and 4**). The Upper Aptian marks a regional unconformity that correlates with the final separation of subcontinental mantle lithosphere and initiates sea-floor spreading between North American and Iberian Plates.

After Upper Jurassic transtensional deformation (from the Oxfordian to Tithonian, Montadert et al., 1979; Jammes et al., 2009) the climax of rifting in the Bay of Biscay occurred in the Lower Cretaceous (from the Berriasian to Hauterivian). The drastic change of regional maximum horizontal stress from NW-SE to NE-SW implies that continental rifting propagated now toward the northwest and led to the continental breakup between North America and Northwest Europe in the late Lower Cretaceous (Aptian-Albian).

The Flemish Cap-Goban Spur, which may still have been attached and forming a locked zone, started to dislocate (**Figure 3**). Generalized rifting occurred in the Lower Barremian (128-126 Ma; de Graciansky et al., 1985) and postrift sediments indicate final breakup in the Upper Albian. Further north, the Orphan Knoll and Porcupine High must have rifted slightly later.

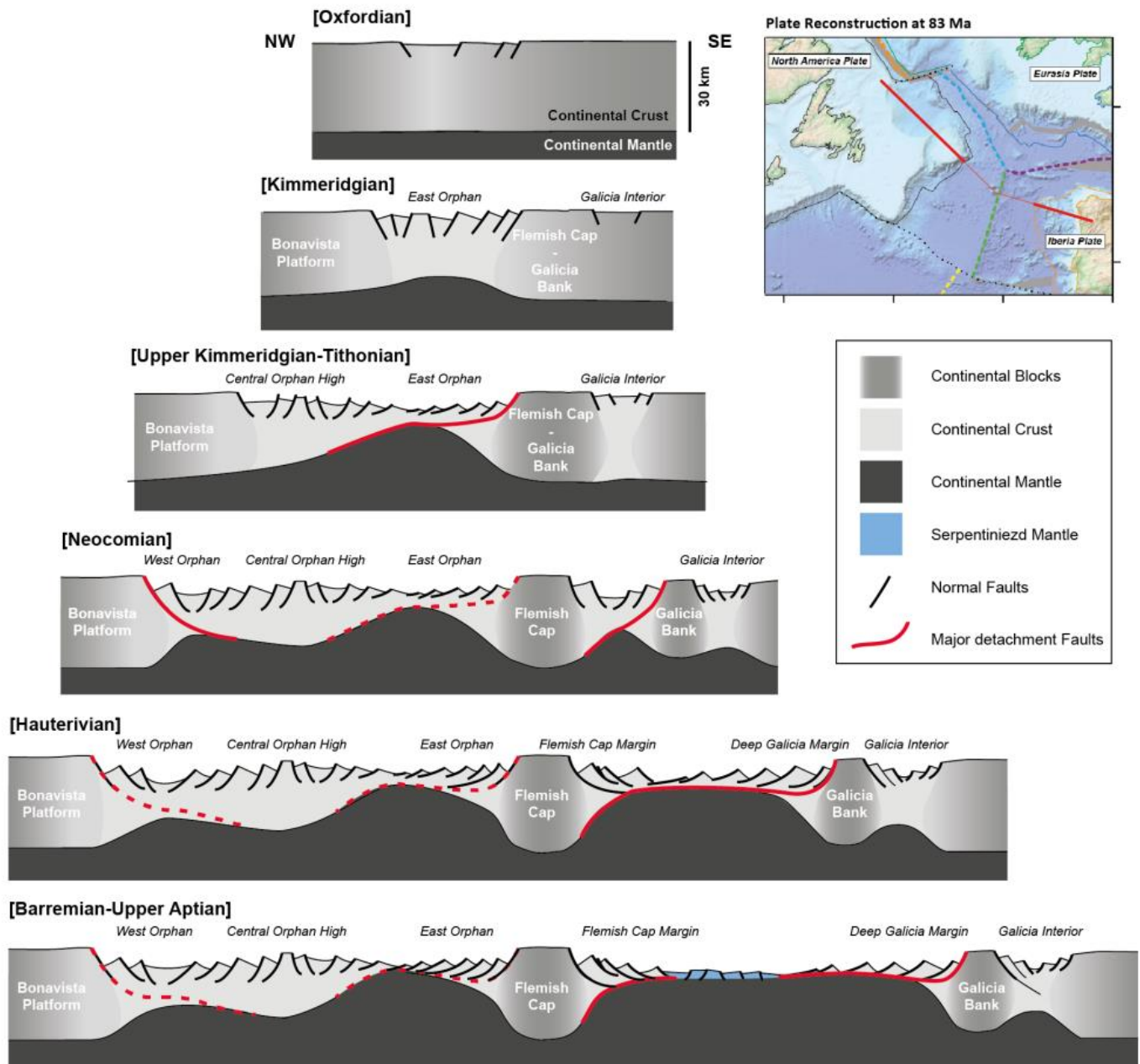


Figure 9. Conceptual cross section from Orphan Basin to Galicia Interior Basin according to main rifting stages discussed in the text.

Summary and Conclusions

The tectonostratigraphic analysis of the Orphan Basin presented in this study allow the following conclusions:

- The Orphan Basin records a long-lasting rifting process of more than 65 Ma in the Northeast Atlantic region during the Mesozoic.
- Most of the tectonic evolution of the Orphan Basin is related to the Newfoundland-Iberia rift system.
- The Northeast Atlantic region is characterized by Late Jurassic-Neocomian intracontinental rift system having two main branches: a western branch passing through Jeanne d'Arc, Orphan and Porcupine basins that experienced several hyper-extensional episodes without achieving a continental breakup, and



an eastern branch reaching rupture through rift propagation between the Newfoundland and Iberia conjugate margins at late Aptian.

- Locked zones (continental blocks and the Iapetus suture) have a major impact on rift propagation.

Acknowledgements

We are grateful to Nalcor Energy for granting access to the seismic dataset and allowing us to publish them. T.P. thanks Matthias Delescluse for fruitful discussions, and Bernard Colletta and Amandine Prélat for their valuable comments that helped to improve the quality of the manuscript.

References

- Alves, T. M., Moita, C., Cunha, T., Ullnaess, M., Myklebust, R., Monteiro, J. H., and Manuppella, G., 2009. Diachronous evolution of Late Jurassic–Cretaceous continental rifting in the northeast Atlantic (west Iberian margin), *Tectonics*, **28**, TC4003.
- Boillot, G., and Winterer, E., 1988. Drilling on the Galicia margin: Retrospect and prospect. In: G. Boillot, E.L. Winterer et al. (eds), *Proceedings of the Ocean Drilling Project Science Results*, College Station, TX, **103**: 809-828.
- Chian, D., Reid, I.D., and Jackson, H.R., 2001. Crustal structure beneath Orphan Basin and implications for nonvolcanic continental rifting. *Journal of Geophysical Research*, **106**, 923–940.
- Courtilot, V., 1982. Propagating rift and continental break up. *Tectonics*, **1**(3), 239-250.
- de Graciansky, P.C., Poag, C.W., Cunningham Jr., R., Loubere, P., Masson, D.G., Mazzullo, J. M., Montadert, L., Müller, C., Otsuka, K., Reynolds, L.A., Sigal, J., Snyder, S.W., Townsend, H.A., Vaos, S.P., and Waples, D., 1985. The Goban Spur transect: Geologic evolution of a sedimentary-starved passive continental margin: *Geological Society of America Bulletin*, **96**, 58-76.
- Domeier, M., and Torsvik, T.H., 2014. Plate tectonics in the late Paleozoic. *Geoscience Frontiers*, **5**(3): 1-48.
- Doré, A., Lundin, E., Jensen, L.N., Birkeland, Ø., Eliassen, P. and Fichler, C. 1999. Principal tectonic events in the evolution of the northwest European Atlantic margin. In: A.J. Fleet and S.A.R. Boldy (eds), *Petroleum Geology of Northwest Europe: Proceedings of the 5th Petroleum Geology Conference*. Geological Society of London and Petroleum Exploration Society of Great Britain, 26-29 October 1997, London, UK, 41-61.
- Huchon, P., Nguyen, T., and Chamot-Rooke, N., 2001. Propagation of continental breakup in the southwestern South China Sea. In: R. Wilson, R. Whitmarsh, B. Taylor, and N. Froitzheim (eds), *Non-Volcanic Rifting of Continental Margins: A Comparison of Evidence from Land and Sea*. Geological Society of London Special Publications, **187**, 31-50.
- Jammes, S., Manatschal, G., Lavier, L., and Masini, E., 2009. Tectonosedimentary evolution related to extreme crustal thinning ahead of a propagating ocean: Example of the western Pyrenees, *Tectonics*, **28**, TC4012.
- Lau, K.W.H., Watremez, L., Loudon, K.E., and Nedimović, M.R., 2015. Structure of thinned continental crust across the Orphan Basin from a dense wide-angle seismic profile and gravity data. *Geophysical Journal International*, **202**, 1969-1992.
- Laughton, A.S., Berggren, W.A., Benson, R., Davies, T.A., Franz, U., Musich, L., Perch-Nielson, K., Ruffman, Al., van Hinte, J.E., Whitmarsh, R.B., Nelson, H., Hacquebard, P.A., Bloam, T.W., Kelling, G., James, N.P., Hopkins, J.C., Pocock, S.A.J., Jeletzky, J.A., Pessagno Jr., E.A., Longoria, T.J.F., and Bukry, D., 1972. Site 111. In: *Deep Sea Drilling Project Volume II: Shipboard Site Reports*, 127p.
- Lundin, E.R., and Dore, A.G., 2011. Hyperextension, serpentinitization, and weakening: A new paradigm for rifted margin compressional deformation. *Geology*, **39**, 347–350. <https://doi.org/10.1130/G31499.1>



- McAlpine, K.D., 1990. Mesozoic stratigraphy, sedimentary evolution, and petroleum potential of the Jeanne d'Arc Basin, Grand Banks of Newfoundland. In: Geological Survey of Canada, Paper 89-17, 1-56.
- Montadert, L., De Charpal, O., Roberts, D.G., Guennoc, P., and Sibuet, J.-C., 1979. Northeast Atlantic passive margins: Rifting and subsidence processes, In: M. Talwani, W. Hay, and W.B.H. Ryan (eds), *Deep Drilling Results in the Atlantic Ocean: Continental Margins and Paleoenvironment*, Maurice Ewing Series, vol. 3, American Geophysical Union, Washington, D.C., 154-186.
- Morewood, N.C., Mackenzie, G.D., Shannon, P.M., O'Reilly, B.M., Readman, P.W., and Makris, J., 2005. The crustal structure and regional development of the Irish Atlantic margin region. In: A.G. Doré and B.A. Vining (eds), *Petroleum Geology: North-West Europe and Global Perspectives – Volume 1*, Proceedings from the 6th Petroleum Geology Conference, Geological Society of London and Petroleum Exploration Society of Great Britain, 6-9 October 2003, London, UK, 1023-1033, doi:10.1144/0061023
- Murillas, J., Mougnot, D., Boillot, G., Comas, M.C., Banda, E., and Mauffret, A., 1990. Structure and evolution of the Galicia Interior Basin (Atlantic western Iberian continental margin), *Tectonophysics*, **184**, 297–319.
- O'Reilly, B.M., Hauser, F., Jacob, A.W.B., and Shannon, P.M., 1996. The lithosphere below the Rockall Trough: wide-angle seismic evidence for extensive serpentinisation. *Tectonophysics*, **255**, 1–23.
- O'Reilly, B.M., Hauser, F., Ravaut, C., et al., 2006. Crustal thinning, mantle exhumation and serpentinization in the Porcupine Basin, offshore Ireland: evidence from wide-angle seismic data. *Journal of the Geological Society of London*, **163**, 775-787. doi: 10.1144/0016-76492005-079
- Pérez-Gussinyé, M., Ranero, C.R., Reston, T.J., and Sawyer, D., 2003. Mechanisms of extension at nonvolcanic margins: Evidence from the Galicia Interior Basin, west of Iberia. *Journal of Geophysical Research*, **108**, 6-19.
- Péron-Pinvidic, G., and Manatschal, G., 2009. The final rifting evolution at deep magma-poor passive margins from Iberia-Newfoundland: a new point of view. *International Journal of Earth Sciences*, **98**, 1581-1597.
- Péron-Pinvidic, G., and Manatschal, G., 2010. From microcontinents to extensional allochthons: witnesses of how continents rift and break apart? *Petroleum Geoscience*, **16**, 189-197.
- Pichot, T., Delescluse, M., Chamot-Rooke, N., Pubellier, M., Qiu, Y., Meresse, F., Sun, G., Savva, D., Wong, K.P., Watremez, L., and Auietre, J.L., 2014. Deep crustal structures of the conjugate margins of the SW South China Sea from wide-angle refraction seismic data. *Marine and Petroleum Geology*. In: M. Pubellier, D. Franke, K. McIntosh, D. Menier, and L. Chun-Feng, *Evolution, Structure, and Sedimentary Record of the South China Sea and Adjacent Basins*, *Marine and Petroleum Geology Special Publication*, **58(B)**: 627-643.
- Pichot, T., Piriou, S., Pitz, J., Mouchot, N., and Laigle, J.-M. 2016. Tectono-stratigraphic study across Mesozoic basins of Newfoundland and Irish conjugate margins, geodynamical implications. *Atlantic-Ireland Conference 2016, Program and Abstracts*: 112-113.
- Reston, T.J., Krawczyk, C.M., and Klaeschen, D., 1996, The S reflector west of Galicia (Spain): Evidence from prestack depth migration for detachment faulting during continental breakup: *Journal of Geophysical Research*, **101**, 8075-8091, doi: 10.1029/95JB03466.
- Savva, D., Pubellier, M., Franke, D., Chamot-Rooke, N., Meresse, F., Steuer, S. and Auietre, J.L., 2014. Different expressions of rifting on the South China Sea margins. *Marine and Petroleum Geology*, **58**, 579-598.
- Seton, M., Müller, R.D., Zahirovic, S., Gaina, C., Torsvik, T., Shephard, G., Talsma, A., Gurnis, M., Turner, M., Maus, S., and Chandler, M., 2012. Global continental and ocean basin reconstructions since 200 Ma. *Earth-Science Reviews*, **113**, 3-4.



- Tucholke, B.E., Sawyer, D.S., and Sibuet, J.-C., 2007. Breakup of the Newfoundland–Iberia rift. In: G.D. Karner, G. Manatschal, and L.M. Pinheiro (eds), *Imaging Mapping and Modelling Continental Lithosphere Extension and Breakup*. Geological Society, London, Special Publications, **282**, 9-45.
- Van Wijk J.W., and Blackman, D.K., 2005. Dynamics of continental rift propagation: the end-member modes. *Earth and Planetary Science Letters*, **229**, 247-258.
- Watremez, L., Helen Lau, K.W., Nedimović, M.R., and Loudon, K.E., 2015. Traveltime tomography of a dense wide-angle profile across Orphan Basin. *Geophysics*, **80**, B69-B82.
- Watremez, L., Prada, M., Minshull, T., O'Reilly, B., Chen, C., Reston, T., Shannon, P., Wagner, G., Gaw, V., Klaeschen, D., Edwards, R., and Lebedev, S., 2016. Deep structure of the Porcupine Basin from wide-angle seismic data. Geological Society of London, *Petroleum Geology Conference series 2016*, **8**, 1-30. doi:10.1144/PGC8.26
- Welsink, H., and Tankard, A., 2012. Extensional tectonics and stratigraphy of the Mesozoic Jeanne d'Arc basin, Grand Banks of Newfoundland. In: D.G. Roberts and A.W. Bally (eds) *Regional Geology and Tectonics: Phanerozoic Rift Systems and Sedimentary Basins*, Elsevier, Amsterdam, 336-381.
-





ENIGMATIC ASPECTS OF THE EARLY HISTORY OF THE SOUTHERN GULF OF MEXICO MARGIN

Rowan, Mark G.¹

¹ Rowan Consulting, Inc., 850 8th Street, Boulder, CO 80302, USA, mgrowan@frii.com

Several aspects of the early history of the southern Gulf of Mexico are enigmatic. First, the amount of Upper Jurassic thin-skinned extension is much greater to the northeast. Second, early allochthonous flow of salt over oceanic crust is less extensive to the southwest. Third, although an outer marginal trough is apparent to the northeast, its presence to the southwest is questionable and the level of salt is higher than the oceanic crust. These observations have led to an interpretation in which the Campeche and Yucatan segments of the margin are subbasins separated by a basement high, with the Campeche salt confined at its distal end by uplifted basement just landward of oceanic crust.

A revised explanation based on the opening history of the Gulf of Mexico nicely explains the observations. Oceanic crust was generated by the counter-clockwise rotation of Yucatan about a pole near western Cuba, with the geometry of the basin requiring a higher proportion of transform margin segments in the west and more ridge segments in the east. Three scenarios are compatible with this: 1) the onset of spreading was coeval everywhere but the amount of spreading decreased to the east; 2) the onset of spreading was diachronous, getting gradually younger eastward; or 3) the onset was diachronous but shifted abruptly across one or more transform faults.

The last option best accounts for the differences between the Campeche and Yucatan segments. First, excess thin-skinned Upper Jurassic extension in the Yucatan subbasin is balanced by crustal hyperextension and/or mantle exhumation prior to oceanic spreading, whereas coeval extension in the Campeche area was accommodated by spreading. Second, the relatively minor early movement of salt over oceanic crust in the southwest is due to the dominance of transform segments and thus initially small areas of oceanic crust. Finally, outer marginal troughs are not absent in the Campeche subbasin but are generally small and local, separated by longer transform faults. For two reasons, seismic lines across these faults show the salt higher than oceanic crust as opposed to the outer marginal troughs: first, the juxtaposed oceanic crust is relatively older and thus deeper; and second, continental crust along transform segments is often elevated along marginal ridges.

Introduction

The Gulf of Mexico (GoM), which formed in conjunction with the Central Atlantic rift system (Kneller and Johnson, 2011), comprises conjugate salt-bearing margins separated by oceanic crust. The evaporites were deposited late in the rift history, just prior to the onset of oceanic spreading. They subsequently were separated by counter-clockwise rotation of the Yucatan block into the Louann salt of the northern GoM and the Campeche salt of the southern GoM (Pindell and Kennan, 2007; Kneller and Johnson, 2011; Hudec et al., 2013; Pindell et al., 2014, 2016; Rowan, 2014, 2018; Pascoe et al., 2016). Although some interpretations invoke magma-rich margins with seaward-dipping reflectors (e.g. Imbert and Philippe, 2005; Mickus et al., 2009), most suggest that the margins are magma-poor (e.g. Kneller and Johnson, 2011; Hudec et al., 2013; Pindell et al., 2014, 2018; Rowan, 2014, 2018).

The relationship between salt and underlying strata and crust varies (Rowan, 2014, 2018). In the proximal, necking, and distal domains (Péron-Pinvidic et al., 2013), the salt overlies extended continental crust and associated growth strata, but has a largely unfaulted base and is thus locally postrift. In the outer domain, however,



the base salt is faulted and the salt is thus synrift. There, it forms part of the outer marginal trough, a zone possibly characterized by exhumed mantle, with the base salt below the level of oceanic crust (Pindell et al., 2014, 2018; Rowan, 2018). Finally, in the oceanic domain, salt was emplaced allochthonously out over oceanic crust and abyssal strata as salt nappes (Hudec et al., 2013; Rowan, 2018). Above the salt, strata form basin-scale linked systems of proximal extension and distal contraction.

There are several enigmatic aspects of the southern GoM, which are divided informally into the Campeche (southwestern) and Yucatan (northeastern) segments (**Figure 1**). First, there is a much larger amount of suprasalt Upper Jurassic extension in the Yucatan segment, in fact much more than can be balanced by distal contraction (Imbert and Philippe, 2005; Hudec et al., 2013). Second, the outer marginal trough, although present in the Yucatan segment, is apparently missing in the Campeche segment, where the base salt is actually above the level of oceanic crust (Hudec, 2017). Third, although there is generally a greater volume of salt in the Campeche segment, salt nappes have limited extent compared to in the Yucatan segment (Hudec et al., 2013). These observations have led to a model in which the Yucatan and Campeche segments are separated by a basement high, and another basement high separates the Campeche salt from oceanic crust (Hudec, 2017).

Here I present a simple model of along-strike variations in the opening history of the GoM that can explain these observations. The implications of this model apply also to the northern GoM, where at least some of the same features are present. Moreover, elements of the model may be applicable to some aspects of the South Atlantic salt basins.

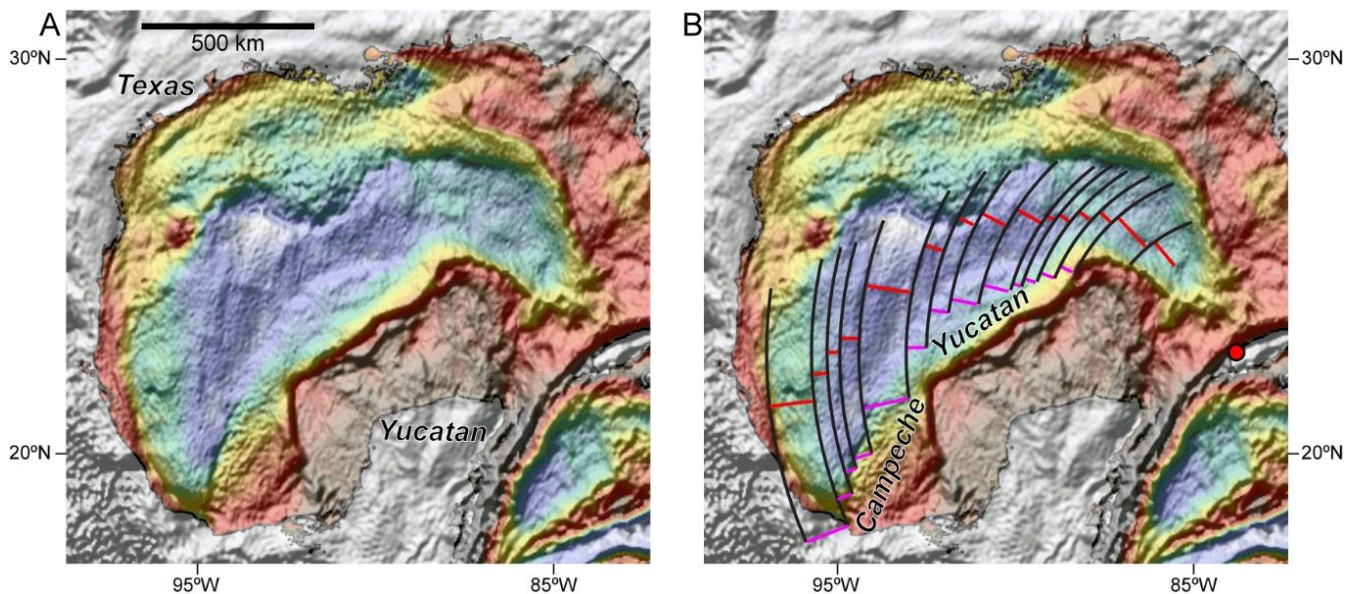


Figure 1. Image of the Gulf of Mexico combining shaded free-air gravity and calculated crustal thickness (courtesy of N. Kusznir). A) uninterpreted; B) interpreted in the southern Gulf of Mexico to show spreading centers (red lines), transform faults (black lines), the limit of oceanic crust and breakup edge of salt (pink lines), approximate pole of rotation (red dot), and the Campeche and Yucatan margin segments.

Opening Model

The Gulf of Mexico oceanic crust is wedge-shaped, having formed during counter-clockwise rotation about a nearby pole located close to western Cuba (Pindell, 1985; Pindell et al., 2016). Thus, it is widest (700 km) in the west, where it is bounded by a major wrench-fault margin off the east coast of Mexico, and narrows to the east until it is no longer present west of southern Florida (**Figure 1**).



Three simple models are compatible with this geometry. First, the onset of spreading may have been synchronous everywhere (**Figure 2A**). In this case, spreading would have been at a faster rate to the west, which is not compatible with the abnormally thin oceanic crust in this area (Pascoe et al., 2016). Second, spreading might have started earlier in the west and progressively propagated to the east (**Figure 2B**), the model preferred by Pindell et al. (2014) and Pascoe et al. (2016). Third, the onset of spreading might have propagated to the east, but shifting abruptly across transform faults instead of gradually (**Figure 2C**).

One consequence of the rotational opening about a pole near the southeastern limit of oceanic crust is that the western portion of the oceanic crust is dominated by transform segments with short ridges, whereas the eastern half is characterized by ridges and only short transform offsets (**Figure 1**). As a result, the original breakup edge of salt (limit of oceanic crust) is mostly along transform segments in the west (Campeche) and ridge segments in the east (Yucatan).

The differences between the Campeche and Yucatan margin segments cited above can be explained easily by the model of eastward propagation, probably with abrupt shifts across transform faults (**Figure 2C**), combined with the different character of the edge of salt in the west versus the east. In the sections below, I discuss five consequences of this model.

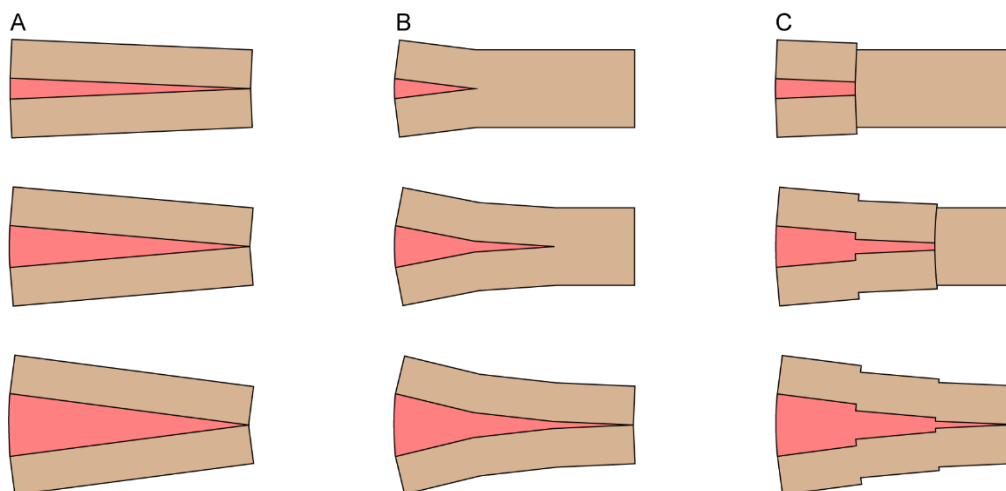


Figure 2. Simple opening models for the wedge-shaped oceanic crust (pale red) of the Gulf of Mexico: A) synchronous onset of spreading, with spreading rates increasing to the west (left); B) progressive eastward propagation of the onset of spreading; and C) eastward propagation, but with abrupt shifts in timing across transform faults.

Strike-Parallel Variations

Original salt thickness

In both the northern and southern Gulf of Mexico, there is generally less salt to the east and more to the west. Accommodation for evaporite deposition was generated by crustal thinning and associated subsidence (Rowan, 2018), so an earlier onset and longer history of rifting in the west resulted in a deeper basin and thus thicker salt.

Timing of evaporite deposition relative to the onset of spreading

If evaporite deposition was controlled by climate, it is reasonable to assume that the timing was the same from west to east in the center of the salt basin (proximal areas may have ceased evaporite deposition earlier due to exposure above a lowering brine level). But if the onset of spreading was younger to the east, the relative timing between it and salt deposition would have varied along strike. If, for example, the onset of spreading in the west



occurred immediately after evaporite deposition ceased, there would have been a period of time between that cessation and the onset of spreading to the east, a time of ongoing crustal extension and/or mantle exhumation in the outer marginal trough postdating salt deposition (**Figure 3**).

This simple model explains the excess suprasalt Upper Jurassic extension in the Yucatan segment. Because the onset of spreading occurred after burial of the salt by Upper Jurassic strata, ongoing crustal extension in the outer marginal trough had to be balanced by equivalent suprasalt extension. This was decoupled by the salt however, so that suprasalt deformation was accommodated by thin-skinned faulting in more proximal positions (**Figure 3F**, inset). The along-strike transition to this style from relatively minor suprasalt Upper Jurassic extension appears to be abrupt, suggesting a significant change in timing of the onset of spreading across a transform fault basinward of the northwestern corner of the Yucatan platform.

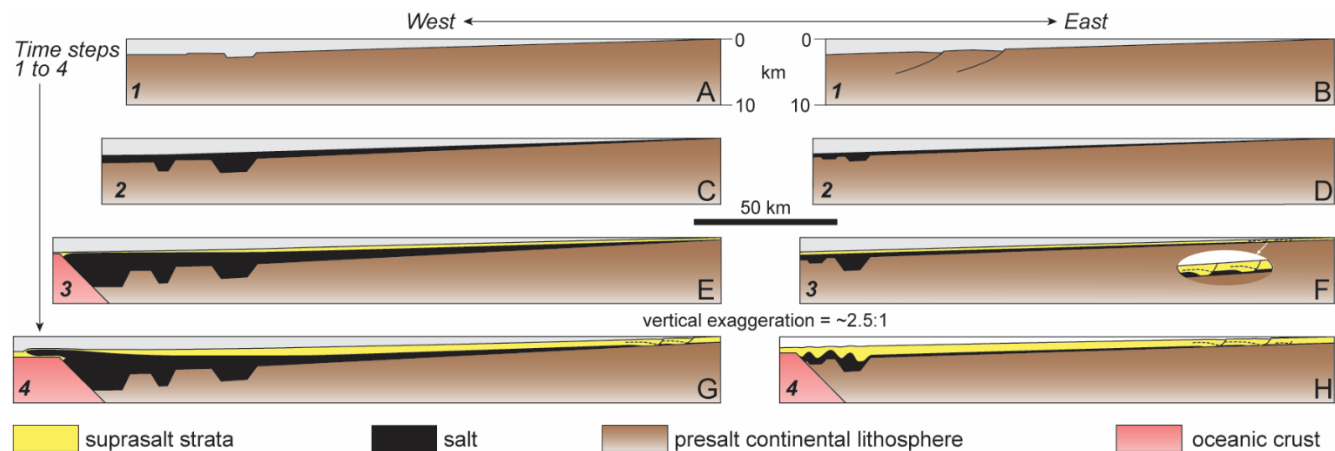


Figure 3. Schematic west to east variations in late-stage opening of the Gulf of Mexico (after Rowan, 2018), with each time step (1 to 4) coeval in the west and east. Presalt crustal faults and syntectonic strata are not shown. Time step 1: initiation of outer marginal trough in west (A), ongoing hyperextension in east (B). Time step 2: evaporite deposition, with extension in outer marginal trough ongoing in west (C) but only just initiated in east (D). Time step 3: burial of salt after onset of oceanic spreading in west (E), continued extension in outer marginal trough balanced by suprasalt extension (inset) in more proximal positions in east (F). Time step 4: linked gravity-driven deformation above salt in both west (G) and, after onset of oceanic spreading, in east (H).

Distribution of outer marginal trough

Outer marginal troughs develop only along ridge segments of the margin; transform segments have no such features (**Figure 4**). This readily explains the mostly continuous outer marginal trough along the Yucatan segment and the relative lack of troughs along the Campeche segment. Moreover, this sets up dramatically different relationships between the level of the base salt and that of oceanic crust. Where there is an outer marginal trough, the base salt is below the top of oceanic crust (**Figure 4B**). Transform segments of passive margins, however, are often characterized by basement highs such as the Ghana Ridge in the Equatorial Atlantic or the Coromondal transform along eastern India (e.g. Nemčok et al., 2016). Thus, the base of salt might be higher than the level of oceanic crust, with the highest parts of any such ridges possibly bald of salt (**Figure 4C**). The elevation of such ridges is expected to vary along their length due to juxtaposition of different-aged oceanic crust and variably extended (and thus subsided) continental crust. The relationship between the levels of salt and oceanic crust can thus differ considerably along the margin.

Emplacement of allochthonous salt nappes

Edges of the salt basin dominated by ridge segments (e.g. Yucatan segment) develop large, continuous areas of new oceanic crust over which allochthonous salt can be emplaced. However, those dominated by transform



segments (Campeche) generate only small, local areas of oceanic crust early in the spreading history (**Figure 5**). In addition, the transform-related basement highs (**Figure 4C**) may impede basinward salt flow. Thus, even though there was more salt and more gravity-driven deformation in the Campeche segment, the extent of salt nappes is smaller there than along the Yucatan segment.

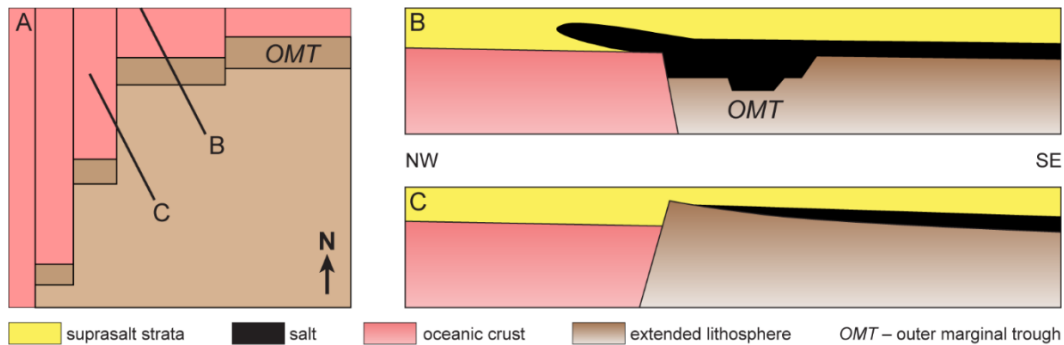


Figure 4. Simplified illustration of the difference between ridge and transform margin segments: A) plan view showing margin dominated by ridge segments in the east and transform segments in the west; B) cross section across ridge segment, with outer marginal trough and allochthonous salt nappe emplaced over oceanic crust; C) cross section across transform segment with basement high.

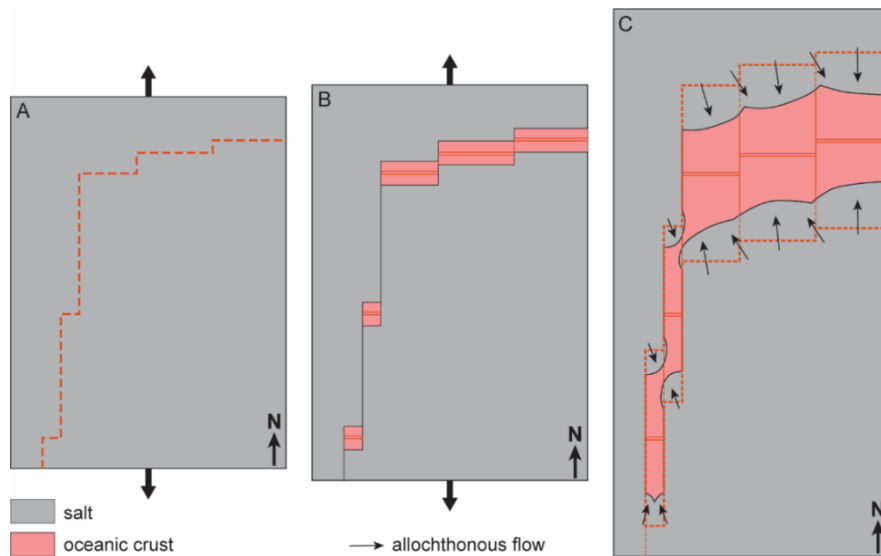


Figure 5. Allochthonous salt flow over oceanic crust (after Rowan, 2018). A) plan view of originally contiguous salt basin (grey) that will be split by spreading (red dashed line); B) early stage of oceanic crust (pale red) with large area generated along ridge-dominated margin (east) but only local areas along transform-dominated margin (west); C) extent of salt nappes (grey lobes with arrows) after further spreading.

Presalt and intrasalt stratigraphy

The GoM evaporite sequence is thought to be relatively pure, dominated by halite and with effectively no non-evaporite interbeds. However, modern proprietary seismic data in the southwestern GoM show intrasalt reflectivity at the autochthonous level, which suggests a larger percentage of non-halite material. A purely speculative model (**Figure 6**) shows that siliciclastic sediment shed off the footwall of the western transform margin might interfinger with the evaporites, introducing siliciclastic layers into the salt (yellow dashed line). Moreover, presalt facies might change laterally, dominated by siliciclastics in the west but possibly transitioning to lacustrine carbonate facies in the east. There are no presalt well penetrations in the offshore to test this conceptual model.

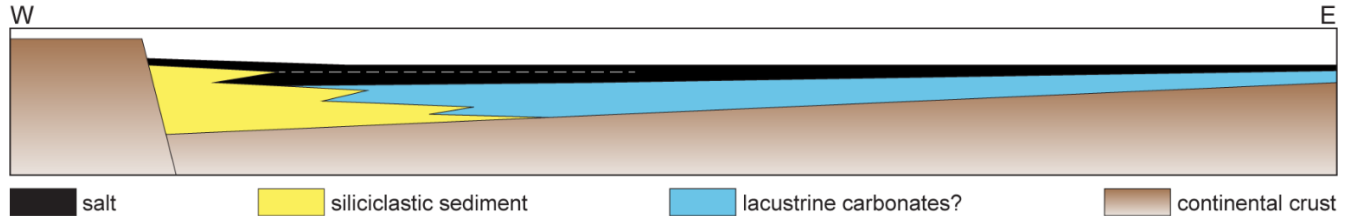


Figure 6. Speculative strike section along southern Gulf of Mexico salt basin. Salt and presalt section thicken to west, where they are bounded by a basement high at the wrench margin of the basin. Siliciclastic sediment shed off the high interfinger with the salt and possible presalt carbonates.

Summary

Two aspects of the early opening history of the Gulf of Mexico combine to explain features that are observed to vary along the strike of the southern GoM. First, the wedge-shaped area of oceanic crust is inferred to have been generated by eastward propagation of the onset of spreading, likely with abrupt shifts across transform faults. Second, the western GoM is dominated by transform faults, with short ridges, whereas the eastern GoM is characterized by ridges with shorter transform faults.

The geometry and history of late-stage rifting and early oceanic spreading led to: 1) original depositional salt than thinned to the east; 2) ongoing crustal extension, after salt deposition, in the outer marginal trough along the Yucatan segment that was balanced by decoupled suprasalt extension in more proximal positions; 3) development of extensive outer marginal troughs with the base salt below the top oceanic crust in the Yucatan segment, but mostly basement highs with the base salt at or above the level of oceanic crust along the Campeche segment; 4) more extensive early allochthonous salt flow along the Yucatan segment compared to in the Campeche area; and 5) possible increased siliciclastic components in both the presalt and salt sequences to the west.

Most, if not all, of these concepts also apply to the northern GoM. For example, salt nappes are less extensive in the Perdido area of the northwestern GoM, and there is increased suprasalt Upper Jurassic extension in the northeastern GoM. The concepts outlined here may also apply to some degree to the South and Central Atlantic salt basins. For example, the relationship between the base salt and the level of the top oceanic crust varies considerably along strike along the Angola to Gabon margin. In addition, presalt strata are dominated by carbonates in the Kwanza Basin but by siliciclastics farther north in Gabon. Although this has been attributed to climate (e.g. Lentini et al., 2010), another possible contributing factor is siliciclastics shed along strike from the relative basement high on the northern side of the Ascension fracture zone at the northern edge of the salt basin.

Acknowledgements

I thank N. Kusznir for providing the free-air gravity image of Figure 1. In addition, a conversation with G. Manatschal and P. Ball spurred me to crystallize my thoughts on some of the material presented here.

References

- Hudec, M.R., 2017, Basement structure and Jurassic evolution of the southern Gulf of Mexico salt province: AAPG Search and Discovery Article 90291.
- Hudec, M.R., Norton, I.O., Jackson, M.P.A., and Peel, F.J., 2013. Jurassic evolution of the Gulf of Mexico salt basin: American Association of Petroleum Geologists Bulletin, **97**(10), 1683-1710, doi:10.1306/04011312073.
- Imbert, P., and Y. Philippe, 2005, The Mesozoic opening of the Gulf of Mexico: Part 2. Integrating seismic and magnetic data into a general opening model. In: P.J. Post, N.C. Rosen, D.L. Olson, S.L. Palmes, K.T. Lyons,



- and G.B. Newton (eds), Petroleum systems of divergent continental margin basins. 25th Annual Gulf Coast Section SEPM Foundation Bob F. Perkins Research Conference, December 4-7, 2005, Houston, Texas, 1151-1190, doi:10.5724/gcs.05.25.1151.
- Kneller, E.A., and Johnson, C.A., 2011. Plate kinematics of the Gulf of Mexico based on integrated observations from the Central and South Atlantic: *Gulf Coast Association of Geological Societies Transactions*, **61**, 283-299.
- Lentini, M.R., Fraser, S.I., Sumner, H.S., and Davies, R.J., 2010. Geodynamics of the central South Atlantic conjugate margins: implications for hydrocarbon potential. *Petroleum Geoscience*, **16**, 217–229, doi:10.1144/1354-079309-909.
- Mickus, K., Stern, R.J., Keller, G.R., and Anthony, E.Y., 2009, Potential field evidence for a volcanic rifted margin along the Texas Gulf Coast: *Geology*, **37**, 387-390, doi:10.1130/G25465A.1.
- Nemčok, M., Rybár, S., Sinha, S.T., Hermeston, S.A., and Ledvényiová, L., 2016. Transform margins: development, controls and petroleum systems – an introduction. In: M. Nemčok, M., S. Rybár, S.T. Sinha, S.A. Hermeston, and L. Ledvényiová (eds), *Transform margins: development, controls and petroleum systems*: Geological Society, London, Special Publications, **431**, 1-38, doi:10.1144/SP431.15.
- Pascoe, R., Nuttall, P., Dunbar, D., and Bird, D., 2016. Constraints on the timing of continental rifting and oceanic spreading for the Mesozoic Gulf of Mexico basin. In: C.M. Lowery, J.W. Snedden, and N.C. Rosen (eds), *Mesozoic of the Gulf rim and beyond: new progress in science and exploration of the Gulf of Mexico basin*. 35th Annual Gulf Coast Section SEPM Foundation Perkins-Rosen Research Conference, December 8-9, 2016, Houston, Texas, 81-122.
- Péron-Pinvidic, G., G. Manatschal, and P. T. Osmundsen, 2013, Structural comparison of archetypal Atlantic rifted margins: a review of observations and concepts: *Marine and Petroleum Geology*, **43**, 21-47, doi: 10.1016/j.marpetgeo.2013.02.002.
- Pindell, J. 1985. Plate tectonic evolution of the Gulf of Mexico and Caribbean region. Unpublished Ph.D. thesis, University of Durham, UK, 302p., <http://etheses.dur.ac.uk/7042/>
- Pindell, J., and Kennan, L., 2007. Rift models and the salt-cored marginal wedge in the northern Gulf of Mexico: implications for deep-water Paleogene Wilcox deposition and basinwide maturation. In: L. Kennan, J. Pindell, and N.C. Rosen (eds), *The Paleogene of the Gulf of Mexico and Caribbean basins: processes, events, and petroleum systems*, 27th Annual Gulf Coast Section SEPM Foundation Bob F. Perkins Research Conference, December 2-5, 2007, Houston, Texas, 146-186, doi:10.5724/gcs.07.27.0146.
- Pindell, J., Graham, R., Horn, B., 2014. Rapid outer marginal collapse at the rift to drift transition of passive margin evolution, with a Gulf of Mexico case study. *Basin Research*, **26**, 701-725, doi:10.1111/bre.12059.
- Pindell, J., Miranda, C.E., Cerón, A., and Hernandez, L., 2016. Aeromagnetic map constrains Jurassic–Early Cretaceous synrift, break up, and rotational seafloor spreading history in the Gulf of Mexico. In: C.M. Lowery, J.W. Snedden, and N.C. Rosen (eds), *Mesozoic of the Gulf rim and beyond: new progress in science and exploration of the Gulf of Mexico basin*. 35th Annual Gulf Coast Section SEPM Foundation Perkins-Rosen Research Conference, December 8-9, 2016, Houston, Texas, 123-153.
- Rowan, M.G., 2014. Passive-margin salt basins: hyperextension, evaporite deposition, and salt tectonics: *Basin Research*, **26**, 154-182, doi:10.1111/bre.12043.
- Rowan, M.G., 2018. The South Atlantic and Gulf of Mexico salt basins: crustal thinning, subsidence and accommodation for salt and presalt strata. In: K.R. McClay and J.A. Hammerstein (eds), *Passive margins: tectonics, sedimentation and magmatism*. Geological Society, London, Special Publications. **476**, doi:10/1144/SP476.6.





LATE JURASSIC TO EARLY CRETACEOUS DEPOSITIONAL SYSTEMS AND SEQUENCES, FLEMISH PASS EXTENSIONAL BASIN, OFFSHORE NEWFOUNDLAND, CANADA

Scott, Anthony¹, Schwartz, Stephen¹, van Lanen, Xavier M.T.¹, Martinius, Allard W.², and MacEachern, James A.³

¹ Equinor ASA Canada Ltd., 2 Steers Cove, St. John's, NL A1C 6J5, Canada, ajsc@equinaor.com

² Equinor ASA Norway Ltd., Trondheim 4035, Norway

³ ARISE, Department of Earth Sciences, Simon Fraser University, Burnaby, BC V5A 1S6, Canada

The Flemish Pass is a Mesozoic extensional basin located 500 km offshore of Newfoundland containing oil discoveries in multiple stacked reservoirs. Recent wells (2013-2017) drilled into structures at Bay du Nord and Baccalieu resulted in significant oil discoveries. Retrieved conventional cores were logged sedimentologically and ichnologically to understand Late Tithonian to Early Berriasian depositional systems and to build a sequence stratigraphic framework. Micropaleontological and petrological data were also utilized to refine these interpretations.

Late Tithonian reservoirs at Bay du Nord are interpreted as fifth- to sixth-order composite sequences. Fluvial channel sandstone complexes with erosional bases represent broad, shallow lowstand incised fluvial valley fills (5–7 km wide and 15–40 m thick) overlying subaerial unconformities. Sandstones are sublitharenites to feldspathic litharenites with siliciclastic metasedimentary and reworked carbonate rock fragments. Lower delta plain deposits are overlain by delta-front heterolithic intervals, recording transgression in a hypoxic, inner neritic environment. By contrast, outer shelf mudstones, consisting of coccolithophoroids, with quartz grains and minor illite and mica, pass upwards into prodeltaic heterolithic intervals, correspond to highstand system tracts in an oxic, inner neritic environment. The sandstones were sourced from sediments and metasediments with a significant proportion of limestone lithic fragments lying to the south and west of Bay du Nord, which were fed into a low gradient basin with minor topographic relief.

The Early Berriasian reservoirs in the Baccalieu F-89 well consist of progradational cycles 15-50 m thick. Outer shelf calcareous mudstones, overlain by prodeltaic silty mudstones and delta-front structureless sandstones, were deposited in an oxygenated inner to middle neritic environment, largely by hyperpycnal flows, and represent a late lowstand/early transgressive sequence set. Early Berriasian sandstones are litharenitic with metamorphic rock fragments. Mudstones are illite-mica with minor intercalated quartz grains. The sediments represent localised lowstand shelf-type deltas (~10 km wide fans) with hyperpycnal flows building out onto a steeper, narrow basin with sediment sourced from the east. The changes in paleoenvironment, depositional systems, and provenance during the Early Berriasian are linked to fault movement and generation of localized accommodation space along the margins of the Flemish Cap.

Introduction

The Grand Banks region of offshore Newfoundland and Labrador contains sedimentary basins within national and international waters (**Figure 1A**). During 2013, the Bay du Nord C-78/C-78Z discovery was made in the frontier deep-water Flemish Pass Basin within Late Tithonian sandstones. Between 2014 and 2015, the Bay du Nord discovery was appraised with the Bay de Verde F-67/F-67Z and the Bay du Nord L-76/L-76Z wells. In 2016, the Baccalieu F-89 discovered light oil in Early Berriasian sandstones to the east of the Bay du Nord discovery (**Figure 1B**).



The Flemish Pass Basin is a NE-SW oriented basin and encompasses an area more than 10,000 km² (3,861 mi²), with Mesozoic and Cenozoic sedimentary packages up to 10 km (6.2 mi) in thickness. Large-scale transgressive-regressive (probably 3rd order) regionally developed cycles have been identified within the Late Tithonian to Early Berrisian. Late Tithonian deposition in the Flemish Pass Basin resulted in a series of fluvio-deltaic successions (i.e., Bodhran Formation). The latest Tithonian to base Middle Berriasian interval is dominated regressive-transgressive deltaic shelf deposition, whereas the Middle Berriasian to Earliest Valanginian reflects a regressive deltaic cycle.

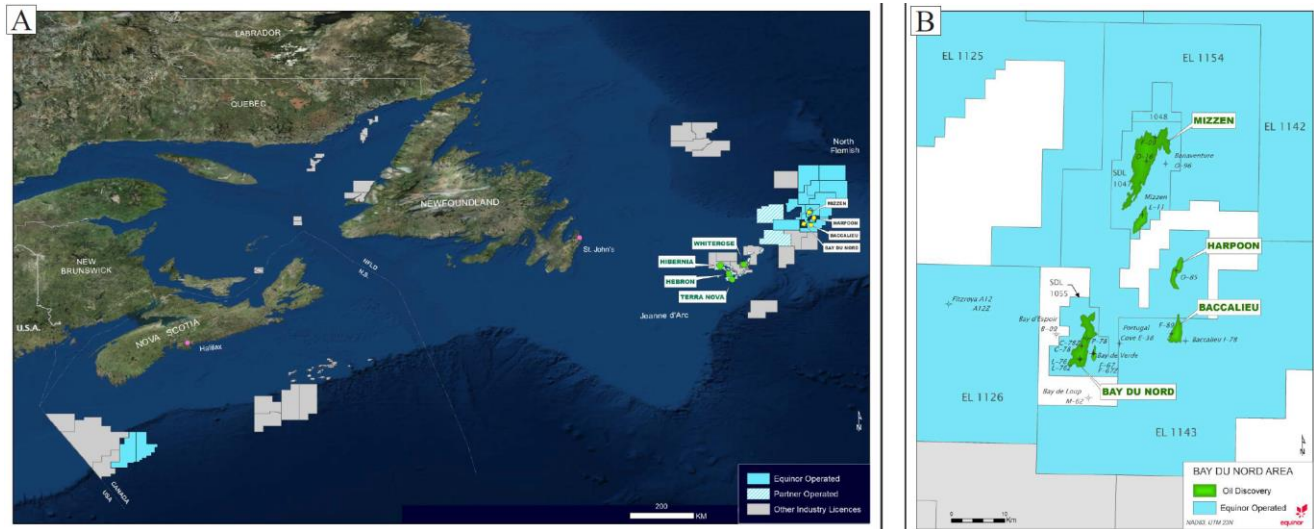


Figure 1. A) Offshore Newfoundland, Eastern Canada, has three producing fields (Hibernia, Terra Nova, and Hebron) located in the Jeanne d’Arc Basin. B) Discoveries in the Flemish Pass.

We document how a sequence stratigraphic approach to evaluating these recent wells has elucidated stratigraphic controls on the distribution of major oil-bearing fluvial and deltaic sandbodies encased within marginal-marine and marine strata, enabling more confident prediction of reservoir architecture and distribution, STOIP, and forecasting of fluid flow during production. The purpose of this extended abstract is to: 1) present the facies associations and depositional environments encountered in recent exploration and appraisal wells; and 2) propose a sequence stratigraphic model and list key uncertainties for the Late Tithonian to Early Berrisian succession.

Facies Analysis

A stepwise workflow was followed in the development of a sequence stratigraphic framework. Conventional cores were analyzed from wells Bay du Nord L-76Z and C-78, Bay de Verde F-67Z, Mizzen F-09, and Baccalieu F-89. A facies scheme has been developed that characterizes the stratigraphic interval using twenty discrete lithofacies, which are vertically arranged into twelve facies associations occurring within six depositional environments (**Figure 2**).

Alluvial Plain

The alluvial plain consists of multistory, multilateral fluvial channel fills (*FA1*) and channel abandonment (*FA2*). *FA1* is characterized by bedload-dominated traction deposition built of lower flow regime bedforms and lesser upper flow regime sheet flow deposits. The successions broadly fine upward and show a bioturbation index (BI) of 0. This channel-fill style implies that deposition occurred in downstream accreting bedforms. Abundant



internal scour surfaces suggest multiple phases of cut and fill, pointing towards a confined (straight) style of river system. Where sampled for microfossils, the coarse-grained sandstones yield dinocysts, prasinophytes, lesser acritarchs, and agglutinated and calcareous foraminifers, suggesting deposition in the presence of marine or brackish water or due to erosion and reworking of material by fluvial channels from the underlying prodelta mudstones.

Subaqueous Lower Delta Plain and Interdistributary Bay

The lower delta plain is characterized by deposits reflecting both fluvial and marine processes. Depositional environments include wave-influenced bay-fills (FA3), distributary channels (FA4), and distributary mouthbars (FA5). It is closely associated with the position of the channel complexes, and typically caps FA1. The lower delta plain complexes are dominated by thin, sandstone-dominated heterolithic cycles reflecting subaqueous deposition. Wave-generated structures are associated with current-generated features, locally strongly aggradational. Syneresis cracks are locally present. Burrowing is generally more abundant in these cycles. Samples show abundant dinocyst, prasinophyte, acritarch, and foraminiferal suites, attesting to marine or brackish-water deposition.

Mixed River- and Wave-influenced Delta Front

The mixed river- and wave-influenced delta front is characterized by sediments deposited landward of fair-weather wave-base. Facies associations include proximal (FA6), medial (FA7), and distal (FA8) delta front subenvironments. Deposits show abundant wave, combined flow, and current-generated, small-scale bedforms, variable storm-generated wavy parallel lamination, abundant soft-sediment deformation structures and rare graded beds. Many mudstones are laminated and unburrowed, reflecting dynamic (fluid) mud accumulation, generated by bedload transport or by rapid settling from buoyant (hypopycnal) mud plumes. Microfossil and palynological data show abundant and persistent dinocysts, prasinophytes, and acritarchs, as well as foraminiferal and (more rarely) radiolarian suites, indicating deltaic accumulation into a marine basin.

Density Flow Delta Front

The density flow-dominated delta front in the Early Berriasian of the Baccalieu area is characterized by sediments deposited below storm-weather wave-base. Facies associations are heterolithic, and correspond to proximal (FA6), medial (FA7), and distal (FA8) delta-front subenvironments. Sandstones are mainly fine- to medium-grained and structureless, and display cryptic bioturbation (BI 0-1). Intercalated mudstones are laminated and locally burrowed (BI 2-4). Micropaleontology and palynology indicate oxygenated conditions in a middle neritic environment, which is supported by high counts of benthic agglutinated foraminifera, dinocysts, and miospores. Sand-rich lithofacies are consistent with subaqueous density-dominated sedimentation away from most wave energy.

River-Dominated Subaqueous Prodelta

The river-dominated prodelta (FA9) deposits comprise sediments deposited below fair-weather wave-base, but above storm wave-base. These deposits are characterized by oscillation-generated structures such as wave ripples and wavy parallel lamination (micro-HCS), locally with superimposed currents to produce combined flow ripples. Facies demonstrate that most of the mudstone layers required physical energy in their accumulation and show evidence of rapid deposition, which could readily be accommodated by hyperpycnal discharge (e.g., Bhattacharya and MacEachern, 2009), rapid sediment settling from buoyant mud plumes, and/or by longshore mobilization of bedload mud as part of an active mud belt. Dinocyst and (where present) benthic foraminiferal concentrations attest to fully marine deposition.



Alluvial plain deposits		Lower delta plain deposits		Delta-front deposits		Prodelta deposits		Outer Shelf (anoxic)		Outer Shelf (oxic)		
Depositional Environment	FA1 FA2 Incised Fluvial Valleys and Channel Abandonment	FA3 FA4 Subaqueous Lower Delta Plain and Interdistributary Bay	FA4 FA5 Mixed River- and Wave-influenced Delta Complex	FA9 River-dominated Prodelta	FA10 Shelf Turbidite	FA11 Shelf Mudstone (anoxic)	FA12 Shelf Mudstone (oxic)					
Facies Association Description	FA1 Channel belt, Multistorey, Multilateral FA2 Channel abandonment FA3 Wave-influenced bayfill; Distributary channel fill FA4 Distributary channel fill FA5 Distributary Mouthbar	FA3 Wave-influenced bayfill; Distributary channel fill FA4 Distributary channel fill FA5 Distributary Mouthbar	FA6-FA7 Proximal - Medial Delta Front: Distal Delta Front FA8 Distal Delta Front	FA9 Prodelta	FA10 Shelf Turbidite FA11 Shelf Mudstone (anoxic) FA12 Shelf Mudstone (oxic)	FA10 Shelf Turbidite FA11 Shelf Mudstone (anoxic) FA12 Shelf Mudstone (oxic)	FA10 Shelf Turbidite FA11 Shelf Mudstone (anoxic) FA12 Shelf Mudstone (oxic)	FA10 Shelf Turbidite FA11 Shelf Mudstone (anoxic) FA12 Shelf Mudstone (oxic)				
Interpretation	Bypass and minor cut-and-fill processes by turbulent current flows. Traction deposition with abundant sand-sized suspension in ponded water (in a column) of lower flow regime conditions. 2D and 3D dunes.	Bypass and minor cut-and-fill processes by turbulent current flows. Traction deposition with abundant sand-sized suspension in ponded water (in a column) of lower flow regime conditions. 2D and 3D dunes.	Sand-dominated dune fallout, reworked by low-energy wave orbits. Redposition as tractive bedload layers (lower flow regime in turbidite deposit) from sustained decelerating turbulent currents with asymmetric 2D and 3D bedforms of dune scale.	Sand-dominated dune fallout, reworked by low-energy wave orbits. Redposition as tractive bedload layers (lower flow regime in turbidite deposit) from sustained decelerating turbulent currents with asymmetric 2D and 3D bedforms of dune scale.	Deposition from low-density sediment gravity (turbulent) flow; likely sandy and muddy turbidites below storm weather wave base.	Deposition from low-density sediment gravity (turbulent) flow; likely sandy and muddy turbidites below storm weather wave base.	Deposition mainly from suspension (hemipelagic) fallout below storm wave base within a mixed, oxic water column. Minor deposition from dynamic processes; very low-density currents.	Deposition mainly from suspension (hemipelagic) fallout below storm wave base within a mixed, oxic water column. Minor deposition from dynamic processes; very low-density currents.				
Geometry (inferred)	Erosional Channel, 100-600 m wide, > km long	Sheet-like channel, < 200 m wide, intra-channel spacing 200-500 m	Sheet-like > km-long and wide	Sheet-like < km-long and wide	Sheet-like < km-long and wide	Sheet-like < km-long and wide	Sheet-like < km-long and wide	Sheet-like < km-long and wide	Sheet-like < km-long and wide	Sheet-like < km-long and wide	Draping Sheet-like > km-long and wide	

Figure 2. Summary of facies associations encountered in the Late Tithonian to Early Berriasian of the Bay du Nord and Baccalieu discoveries. Description and interpretation of depositional environments and facies associations are shown with inferred geometries.



Outer Shelf

The hypoxic outer shelf comprises sediments deposited basinward of storm-weather wave-base. Typical facies associations include Shelf Turbidite (*FA10*) linked to low-density sediment gravity flows, geostrophic currents, and/or hyperpycnal discharge and Shelf Mudstone (*FA11*), generated by hemipelagic deposition interspersed with periods of rapid mud emplacement linked to a mobile mudbelt. Units are unburrowed and show modest microfossil and marine palynomorph abundances. The outer shelf setting is interpreted to have been subject to poor circulation, leading to periods of slightly reduced dissolved oxygen. Generally rapid mud emplacement led to a mobile mudbelt that inhibited infaunal activity and locally reduced microfossil populations. The oxic outer shelf (*FA12*) represents the most "distal" part of the succession. Mudstones show zones of pervasive bioturbation (BI of 5) and contain considerable interstitial silt and sand. Trace fossil suites are diverse, abundant and are dominated by specialized ichnogenera attributable to the *Cruziana* Ichnofacies, consistent with fully marine, well-oxygenated quiet water environments with slow rates of deposition.

Proposed Sequence Stratigraphic Model

Candidate sequence stratigraphic surfaces and depositional sequences (after Catuneanu et al. 2009, 2010, 2011) together with tectonic events (after Bernal et al. 2018) have been identified within the 3rd order transgressive-regressive cycles based on the relative magnitude of base-level change combined with shifts in paleo-environment (**Figure 3**).

Late Tithonian Depositional Sequences

Four depositional sequences (5th to 6th order), each bounded by a subaerial unconformity or a correlative conformity and displaying a recurring stacking pattern have been identified. The paleogeographic setting during the lowstand systems tract was either a low-lying alluvial plain with fluvial channel systems incising previous highstand deposits, or a low-lying lower delta plain, interdistributary bay, and delta-front environment characterized by the interaction of fluvial and wave processes. Facies and paleocurrent analysis suggest a southwestern source, with a depositional direction toward the northeast. The transgressive systems tracts correspond to an important shift from lower delta plain and delta front to prodelta and outer shelf environments. This would have dramatically changed the coastal morphology with progressive backstepping of distributaries towards the southwestern margins of the basin. The highstand systems tracts demonstrate the re-establishment of a laterally extensive prodeltaic mobile mudbelt linked to the progradation of distributary channel and delta plain complexes.

Early Berrisian Depositional Sequences

Three depositional sequences (5th to 6th order) have been identified. The sequences are bounded by sequence boundaries or correlative conformities. The lowstand systems tract in the Baccalieu area is dominated by density-flow processes on a delta front in a middle neritic environment. Facies, seismic, and mineralogical analyses point toward an eastern source, with a depositional direction towards the west. The sediments represent localized falling stage and lowstand shelf-type deltas (~10 km [6 mi] wide lobes), with density flows building out onto a steeper, narrow basin. The change in drainage pattern is linked to fault movement and generation of localized accommodation space along the margins of the Flemish Cap. The transgressive system tracts correspond to a shift from lower delta plain and delta front environments to prodelta and outer shelf settings.



Sedimentological and Stratigraphic Uncertainties

Four key uncertainties are recognized: 1) the *chronostratigraphic* significance of marker horizons remains uncertain, due to limited biostratigraphic resolution; 2) the degree to which *marine processes* influenced the fluvial lowstand systems tract; 3) the role *autogenic processes* may have played in the development of the marginal marine facies; and 4) the applicability of *sequence stratigraphic models* - such as the T-R model (e.g., Embry, 1993) or the depositional sequence model (e.g., Van Wagoner et al., 1988, 1990; Catuneanu et al., 2010, 2011) - to a tectonically active basin.

Acknowledgements

We thank Doug Stewart for his sedimentological work and contribution to important discussions early in the project. We also thank colleagues Asdrubal Bernal, James Carter, Andrew Churchill, Stephen Kearsley, Irene Kelly, Lew Manuel, Tania Roenitz, and Rainer Tonn. We would also like to thank Equinor and Husky Energy Inc. For their permission to publish this abstract.

References

- Bernal, A.J., Tonn, R., Novoa, E., and S oderstr om, B., 2018. Structural Style and Fault Evolution in the Greater Bay du Nord Area, Flemish Pass Basin, Offshore Newfoundland. Program and Short Abstracts: 6th Conjugate Margins Conference, Halifax, Nova Scotia, Canada, 19-22 August 2018 "Celebrating 10 Years of the CMC: Pushing the Boundaries of Knowledge", 103.
- Bhattacharya, J.P., and MacEachern, J.A., 2009. Hyperpycnal rivers and prodeltaic shelves in the Cretaceous seaway of North America: *Journal of Sedimentary Research*, **79**, 184-209.
- Catuneanu, O., Abreu, V., Bhattacharya, J.P., Blum, M.D., Dalrymple, R.W., Eriksson, P.G., Fielding, C.R., Fisher, W.L., Galloway, W.E., Gibling, M.R., Giles, K.A., Holbrook, J.M., Jordan, R., Kendall, C.G.St.C., Macurda, B., Martinsen, O.J., Miall, A.D., Neal, J.E., Nummedal, D., Pomar, L., Posamentier, H.W., Pratt, B.R., Sarg, J.F., Shanley, K.W., Steel, R.J., Strasser, A., Tucker, M.E., and Winker, C., 2009. Towards the standardization of sequence stratigraphy. *Earth-Science Reviews*, **92**, 1-33.
- Catuneanu, O., Bhattacharya, J.P., Blum, M.D., Dalrymple, R.W., Eriksson, P.G., Fielding, C.R., Fisher, W.L., Galloway, W.E., Gianolla, P., Gibling, M.R., Giles, K.A., Holbrook, J.M., Jordan, R., Kendall, C.G.St.C., Macurda, B., Martinsen, O.J., Miall, A.D., Nummedal, D., Posamentier, H.W., Pratt, B.R., Shanley, K.W., Steel, R.J., Strasser, A., and Tucker, M.E., 2010. Sequence stratigraphy: common ground after three decades of development: *First Break*, **28**, 21-34.
- Catuneanu, O., William, E.G., Kendall, C.G.St.C., Miall, A.D., Posamentier, H.W., Strasser, A., and Tucker, M.E., 2011. Sequence Stratigraphy: Methodology and Nomenclature. *Newsletters on Stratigraphy*, **44**, 173-245.
- Embry, A.F., 1993. Transgressive-regressive (T-R) sequence analysis of the Jurassic succession of the Sverdrup Basin, Canadian Arctic Archipelago. *Canadian Journal of Earth Sciences*, **30**, 301-329.
- Sharp, I.R., Higgins, S., Scott, M., Freitag, U., Allsop, Catherine., Kane, K., Sultan, A., Doubleday, P., Leppard, C., Bloomfield, J., Cody, J., Rait, G., Haynes, S., Torudbakken, B.O., Hansen, T., Fossl , V., and Adam, C., 2018. Rift to drift evolution and hyper- extension in the North Atlantic – insights from a super- regional approach. Program and Short Abstracts: 6th Conjugate Margins Conference, Halifax, Nova Scotia, Canada, 19-22 August 2018 "Celebrating 10 Years of the CMC: Pushing the Boundaries of Knowledge", 48-49.
- Van Wagoner, J.C., Posamentier, H.W., Mitchum, R.M., Vail, P.R., Sarg, J.F., Loutit, T.S., and Hardenbol, J., 1988. An overview of sequence stratigraphy and key definitions. In: C.K. Wilgus, B.S. Hastings, C.G.St.C Kendall, H. Posamentier, C.A. Ross and J.C. Van Wagoner (eds), *Sea Level Changes – An Integrated Approach*. SEPM Special Publication, **42**, 39-45.



Van Wagoner, J.C., Mitchum Jr., R.M., Campion, K.M., and Rahmanian, V.D., 1990. Siliciclastic sequence stratigraphy in well logs, core, and outcrops: concepts for high-resolution correlation of time and facies. *American Association of Petroleum Geologists Methods in Exploration Series*, **7**, 55.



A PROVENANCE STUDY OF UPPER JURASSIC HYDROCARBON SOURCE ROCKS OF THE FLEMISH PASS BASIN AND CENTRAL RIDGE, OFFSHORE NEWFOUNDLAND, CANADA

Scott, Matthew W.¹, Sylvester, Paul J.², and Wilton, Derek H.C.¹

¹ Canada-Newfoundland and Labrador Offshore Petroleum Board, 500 - 140 Water Street, St. John's, NL A1C 6H6, Canada, mscott@cnlopb.ca

² Department of Geosciences, Texas Tech University, Lubbock, TX 79409-1053, USA

There are a number of recent hydrocarbon discoveries in the Flemish Pass Basin and Central Ridge, offshore Newfoundland, Canada, but only limited geological information is available. This provenance study is aimed at providing new mineralogy, geochronology, and geochemistry datasets on Upper Jurassic source and reservoir rocks from this area. The primary goal was to determine the provenance and paleodrainage patterns of the Upper and Lower Kimmeridgian source rock members, and Upper and Lower Tempest Member sandstone reservoirs of the Rankin Formation. The provenance results thus help define where thicker sequences of hydrocarbon source rocks and reservoir units are located in the region.

Sixty lithology samples from conventional core and cuttings of both mudstones and sandstones were acquired, processed, and analyzed from four wells: Baccalieu I-78, Panther P-52, South Tempest G-88, and Lancaster G-70. A combination of detrital zircon U-Pb geochronology, whole-rock geochemistry, and SEM-MLA analysis of heavy mineral concentrates were used to decipher provenance. Based on these data, the Upper and Lower Kimmeridgian source rocks are composed of detritus from the Avalon Zone and Central Mobile Belt, along with the underlying basement. These source regions are not overly indicative of a drainage orientation, as they exist both northeast and west of the study area. Therefore, it is possible that detritus would have been derived from both areas, and thicker sequences of these units are likely to be present in either the western, or, northeastern portions of the Flemish Pass Basin and Central Ridge. The Upper and Lower Tempest Member sandstones are characterized by material from the Avalon Zone; however, some of the detritus in these units is interpreted to be derived from Iberia to the east. Thus, the Tempest Member sandstones were likely derived at least in part from the east, which infers thicker sequences of this unit are likely present towards the eastern edges of the Central Ridge and Flemish Pass Basin.

Knowledge of where these units are thickest should be an important consideration for petroleum exploration in the region. In addition, the Upper Tempest sandstone contains Mesozoic age zircons, which constrain the depositional age of this unit, and not found in samples from the other units.

Introduction

The prolific Kimmeridgian source rocks of the Grand Banks of Newfoundland have received considerable attention as they are the primary oil source rock for this significant petroleum district. The Egret Member, the Kimmeridgian source rock for the four producing fields in the Jeanne d'Arc Basin, has been studied in detail there but only to limited degrees in proximal basins. The Flemish Pass Basin, in particular, has had significant hydrocarbon discoveries at the Mizzen area (2009), and the Harpoon and Bay du Nord areas (2013), spurring current industry exploration (Enachescu, 2014). The region has been the focus for academic research as well (Lowe et al., 2011). The Flemish Pass Basin is separated from the Jeanne d'Arc Basin by a topographic high called the Central Ridge, in which hydrocarbon discoveries have also been made. Tithonian-aged sandstone, consisting of four siliciclastic intervals interbedded with shale, is the primary oil reservoir at Mizzen (Cody et al., 2012). The primary source for the oil is considered to be Kimmeridgian organic-rich shale, likely equivalent to the Egret



Member in the Jeanne d'Arc Basin (Fowler et al., 2007). Unlike the Jeanne d'Arc Basin however, the source rock here is present as two distinct intervals, designated as the Upper and Lower Kimmeridgian source rock members of the Rankin Formation (C-NLOPB, 2007; 2011). Previous work on the Upper and Lower Kimmeridgian source rocks in the Flemish Pass has focused on organic geochemistry and hydrocarbon source potential of the units (McCracken et al., 2000; Creaney and Allison, 1987). This study presents new mineral data that contribute to the understanding of this important interval within the basin.

The goal of this study is to determine the provenance and paleodrainage patterns that supplied detritus to the Kimmeridgian source rocks as well as to the interbedded Tempest Member sandstones within the Flemish Pass Basin and Central Ridge. Lowe et al. (2011) determined provenance patterns within the coarse-grained reservoir intervals of the basin using detrital zircon geochronology as well as the geochemistry of detrital tourmaline. For this project, detrital zircon geochronology and trace element geochemistry has been applied to help predict where the thickest accumulations of fine-grained, organic-rich source rocks might be located. All of the information gathered will enable a more accurate prediction of prospective areas for hydrocarbon exploration.

Methods

Conventional cores and cuttings samples of Kimmeridgian source rocks were collected from three wells within the Flemish Pass and Central Ridge area. The selected wells - Baccalieu I-78, South Tempest G-88, Panther P-52, and Lancaster G-70 - all intersected Kimmeridgian source rocks in different parts of the basin. The cores and cuttings were logged and sampled at the C-NLOPB's Core Storage and Research Centre in St. John's, Newfoundland. Although samples from conventional cores were preferred for this study, the entire Kimmeridgian source rock interval was not cored, thus cuttings were sampled where cores were unavailable.

Several different analytical methods were employed in this study. Techniques employed for whole rock geochemical analysis include X-Ray Fluorescence, and inductively coupled plasma mass spectroscopy (ICP-MS). Polished thin sections were analyzed on a scanning electron microscope using mineral liberation analysis techniques (hereafter referred to as MLA-SEM) to determine mineralogy. For detrital zircon geochronology, MLA-SEM imaging was the first step, followed by laser-ablation microprobe (LAM) ICP-MS analysis.

Whole Rock Geochemistry – Trace Element Data

Whole rock geochemical analyses were completed on samples of Upper Jurassic source rocks from the Central Ridge and Flemish Pass Basin. Since a significant amount of core was available over the Late Jurassic interval, all samples were of conventional core. Core is preferable for geochemical analysis as cuttings samples may possess contaminants from drill bit shavings, drilling mud, and/or cave-ins from overlying units.

To help ascertain the composition of the source region(s) and determine provenance, trace element plots were examined. Typically, the distribution of trace elements such as Ti, Mn, Zr, Hf, Nb, Sn, Cr, Ni, V, Co, La-Lu, Y, and Sc are sensitive to the nature of their source region (McLennan et al., 2001, 2003). These elements have short residence times in seawater and are less susceptible to mobilization during sedimentary processes (McLennan et al., 2003).

Figure 1 indicates that detritus for these Upper Jurassic units was derived predominantly from an upper crustal or felsic terrane as both the mudstone (**Figure 1A**) and sandstone (**Figure 1B**) samples plot in close proximity to the average composition of the upper continental crust. It is difficult to say precisely where this upper crustal detritus is sourced. However, nearby terranes such as the Avalon Zone and Central Mobile Belt represent likely candidates as they both possess abundant felsic volcanic rocks as well as sedimentary cover sequences.

The sandstone samples plot closer to the passive margin field than the mudstones as hydraulic sorting and sedimentary recycling processes acted to enrich the sand beds in recycled zircon.

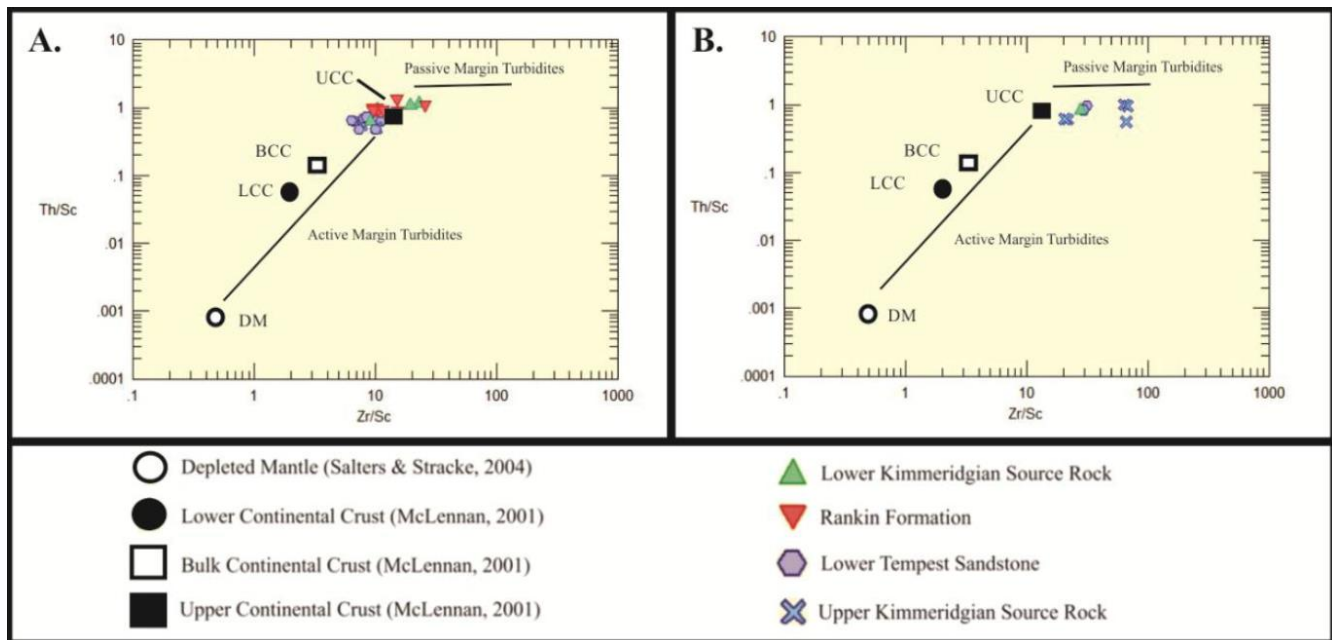


Figure 1. Zr/Sc vs. Th/Sc provenance diagrams for Upper Jurassic (A) mudstone and (B) sandstone samples. Figure adapted from McLennan et al. (1990).

This indicates that the zircon in these beds is likely multi-cycle, and has been through multiple erosional and depositional cycles. However, the sandstones may not necessarily have had a different provenance than the mudstones, because recycling and enrichment of heavy minerals may have been more dominant in the sand-sized fraction of the detritus, which was not well sampled by the mudstones as a result of hydraulic sorting.

Samples from different stratigraphic units appear to have a similar provenance based on these plots. However, the Lower Tempest Sandstone samples plot slightly closer to the average composition of the Bulk Continental Crust, suggesting a slightly more mafic component in, and potentially different provenance for, the Lower Tempest Member sandstone detritus.

Detrital Zircon Geochronology

The geochronological analyses for this study were undertaken to define detrital zircon ages for mudstone and interbedded sandstone beds from the Upper Jurassic units. Four representative samples are discussed in the following section.

Results – Upper Kimmeridgian Source Rock

Several thin sections were prepared from Upper Kimmeridgian Source Rock core sample at 3837.3 m depth in the South Tempest G-88 well. Although within the Upper Kimmeridgian source rock unit, this sample represents an interbedded sandstone bed and is defined as an arkosic wacke. Zircons from three thin sections were imaged using the MLA-SEM and then dated, yielding 56 concordant U-Pb ages (**Figure 2A**) with three major populations. The first is a peak of 11 Cambrian–Devonian aged grains (533–405 Ma); the second group a major peak of 20 late Neoproterozoic-aged grains (626–544 Ma); and the third group is composed of 19 grains > 1 Ga (2740–970 Ma).

Another sample of the Upper Kimmeridgian Source Rock was obtained from the Baccalieu I-78 well. This sample was composed of selected cuttings taken over a 5 m thick interval (4500–4505 m). Based on observations of the cuttings, this interval is composed of fine-grained mudstones with some interbedded siltstone. Grains were



imaged using the MLA-SEM and 27 yielded concordant analyses (**Figure 2B**). The most abundant group of grains is late Neoproterozoic with 10 grains of this age present (552–635 Ma). Eight grains composed a group of Cambrian–Devonian grains (363–507 Ma). A small group of five grains >1 Ga is also present.

Results – Upper and Lower Tempest Sandstone

A 5 m thick cuttings sample from the 3210–3215m interval in the Upper Tempest Member sandstone from the Panther P-52 well contained sufficient detrital zircons for analysis. Observations of the cuttings indicated that the interval was predominantly composed of fine-grained sandstone with some minor interbedded siltstones and mudstones. Grains were imaged using the MLA-SEM and 29 yielded concordant data (**Figure 2C**). Five major groups of zircons are present. The most abundant is the late Neoproterozoic group (545–649 Ma), with eight grains present. The next most abundant group consists of seven Permian–Carboniferous grains (275–345 Ma). Six older grains form a cluster of >1 Ga grains, ranging from 1026–2752 Ma. Another cluster is composed of three grains that are Late Jurassic in age (145–150 Ma). The final group is composed of two grains that are Ordovician and Devonian, respectively.

A sample of the Lower Tempest Member sandstone was obtained from a conventional core at 4195.8 m depth from the South Tempest G-88 well. The sample is a fine-grained sandstone. Zircons were mapped and imaged using the MLA-SEM. Of the imaged grains, 87 yielded concordant results (**Figure 2D**). These grains fall into four major groups. The first is a group of 57 late Neoproterozoic grains (570–682 Ma). The second group is composed of 16 grains >1 Ga (986–2838 Ma) and the third group is a cluster of six Carboniferous–Permian grains (286–298 Ma). A group of five Cambrian–Devonian grains (416–503 Ma) is also present.

Provenance Interpretations – Kimmeridgian Source Rock, and Rankin Formation

Three main groups characterize detrital zircon populations of samples from the Upper Kimmeridgian source rock. The most abundant grains are late Neoproterozoic (ca. 600 Ma), and these zircons are interpreted to have been derived from Avalon Zone rocks. Grains that were dated at >1 Ga are also interpreted to be derived from the Avalon Zone. As shown in **Figure 2A** and **2B**, these grains are interpreted predominantly as multi-cycle based on their morphologies. Therefore, although the grains may have been derived originally from the Avalon Zone, they likely went through numerous erosional and depositional cycles before being deposited in this unit. The youngest significant cluster of grains is a Cambrian–Devonian group, and these zircons are interpreted to be derived from Gander and Dunnage zone rocks in the Central Mobile Belt. The three Middle Neoproterozoic grains dated in the Upper Kimmeridgian source rock of the South Tempest G-88 well are interesting as there are few known correlative sources for grains of this age. A likely source, however, is the Flemish Cap granodiorite, which is considered an offshore extension of the Avalon Zone. With an age in the 750–830 Ma range (King et al., 1985), it is located to the east and northeast of the Flemish Pass Basin.

The combination of whole rock geochemical data and zircon age-dates suggest that the Kimmeridgian source rock and Rankin Formation samples had a provenance from rocks of the Avalon Zone and Central Mobile Belt. It is difficult to determine conclusively whether these grains were derived from the west or the east, as both Avalon Zone and Central Mobile Belt rocks exist west and east of the study area. The presence of detritus interpreted to be from the Flemish Cap granodiorite or correlative sequences, however, suggests that sediment input was in part from the northeast. It is likely that basin entry points existed to the northeast, as interpreted by Cody et al. (2012) for Upper Jurassic reservoir units of the Flemish Pass Basin. **Figure 3A** shows the interpreted large-scale drainage routes and **Figure 3B** shows the interpreted basin-scale entry points and areas of abundant and restricted sediment supply. In addition, it is noteworthy that the majority of zircon grains in this unit are likely



multi-cycle (**Figure 2A, 2B**). This is consistent with the trace element plot (**Figure 1**), which suggests sedimentary recycling was an important process in the deposition of these units.

If sediment was derived from the northeast, this implies sediment supply would have been much more abundant in the northern regions of the basin, with a likely thicker source rock sequence. This is an important consideration for the petroleum potential of the source rock. If the source rock is indeed more proximal to sediment supply in the north, then it is likely that the source rock has a more terrestrial component in this region.

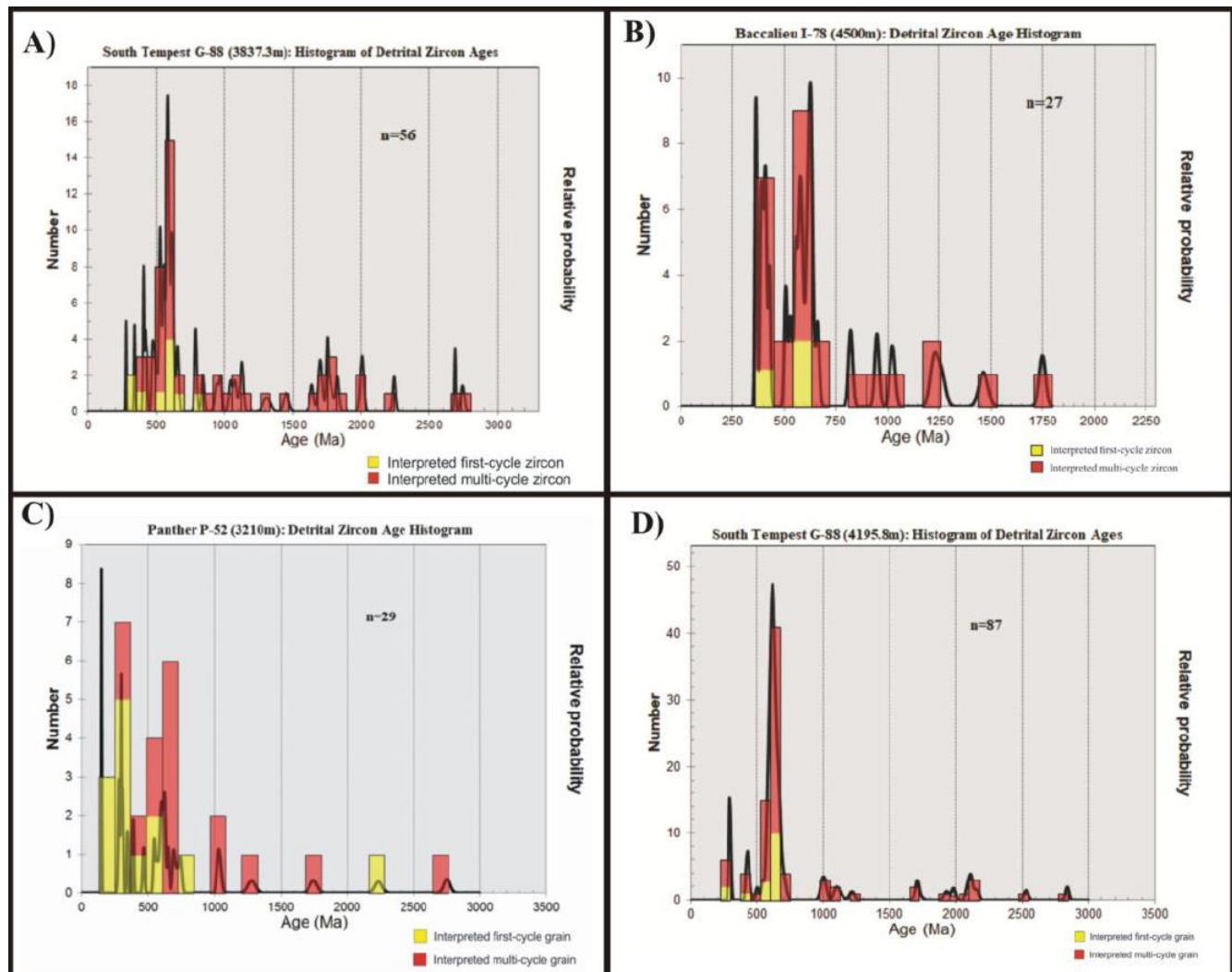


Figure 2. Detrital zircon age histograms for four samples. (A) Sandstone from South Tempest G-88 (3837.3 m). (B) Mudstone from Baccaieu I-78 (4500 m). (C) Sandstone from Panther P-52 (3210 m). (D) Sandstone from South Tempest G-88 (4195.8 m). First or multi-cycle zircon grains identified based on grain morphology.

Provenance Interpretations – Upper and Lower Tempest Sandstone

In addition to previously described zircon groups (Late Neoproterozoic group, >1 Ga group, and Cambrian–Devonian Group), two new zircon populations were observed in the Tempest Member sandstone samples. These include Permian–Carboniferous grains, as well as a group of Upper Jurassic grains. Permian–Carboniferous grains are noteworthy as there are few known correlative sources from Newfoundland or the Newfoundland offshore. Our preferred interpretation for the presence of Carboniferous zircons in these Tempest



Sandstone samples is that they were derived directly from Iberia. Permian–Carboniferous granitic intrusions are abundant on the Iberian Peninsula, and therefore, detritus of this age would be abundant if the Iberian Peninsula represented a significant source.

The provenance of the Upper Jurassic grains is difficult to identify as they have few known correlatives. Some potential Mesozoic sources exist offshore Newfoundland, as well as on the island of Newfoundland. However, it is also possible that they are from a currently unknown source of contemporaneous magmatism.

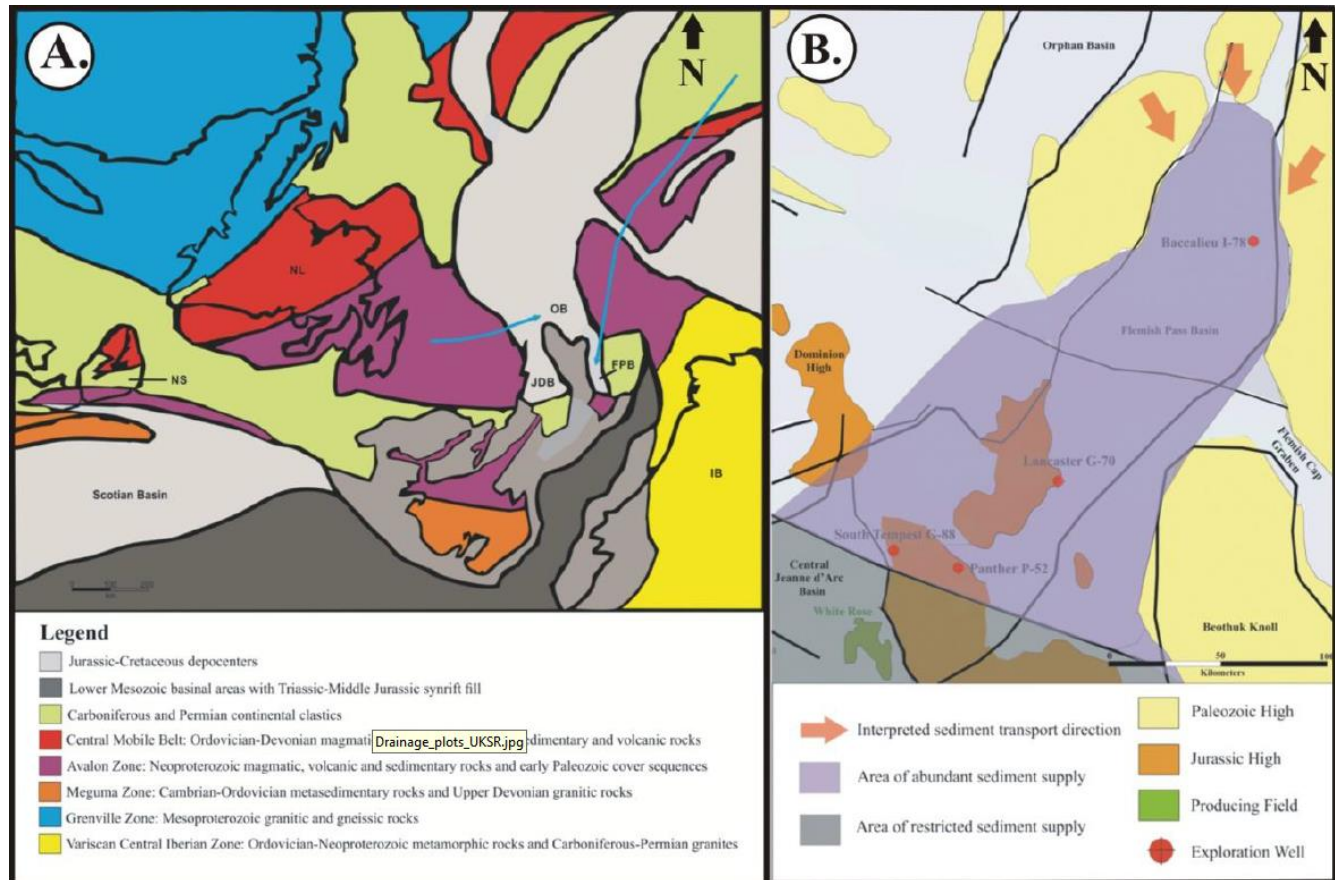
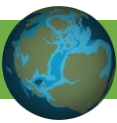


Figure 3. (A) Interpreted large-scale drainage routes during deposition of the Upper and Lower Kimmeridgian Source Rock, and the Rankin Formation. Figure modified from Lowe et al. (2011). (B) Interpreted basin entry points and areas of abundant and restricted sediment supply during deposition of the Upper and Lower Kimmeridgian Source Rock, and the Rankin Formation. Figure modified from Cody et al. (2012).

Major zircon groups, particularly the Permian–Carboniferous grains indicate an easterly provenance (**Figure 4A**) as the ages of these grains closely match those of intrusions of Iberia. A provenance from the east can also account for the late Neoproterozoic and >1 Ga grains that are linked to the Avalon terrane as Avalonian basement is present to the east of the Grand Banks. An easterly provenance can also explain the unique trace element geochemical signature of the Tempest Member sandstone samples. Minor Cambrian–Devonian grains, as well as Jurassic grains, however, may indicate minor input from the west. It is also possible late Neoproterozoic and >1 Ga grains are derived from the west as Avalonian basement is present to the west as well.

As the Tempest Member sandstone units are important reservoir intervals on the Grand Banks (e.g. flowed 1250 barrels of oil per day in the South Tempest G-88 well), the drainage orientations and basin entry points have important implications for reservoir quality during this time. Presumably, accumulations of coarse-grained, high quality reservoir rocks are more likely to occur in close proximity to sediment supply and basin entry points



whereas finer-grained shales would be deposited basinward. If this is applied to the current interpretation for the Tempest Member sandstones, it is likely that thicker, higher reservoir quality rocks would be deposited in the east, with decreasing reservoir grade to the west (**Figure 4B**). This may be an important consideration for further exploration and drilling in this area.

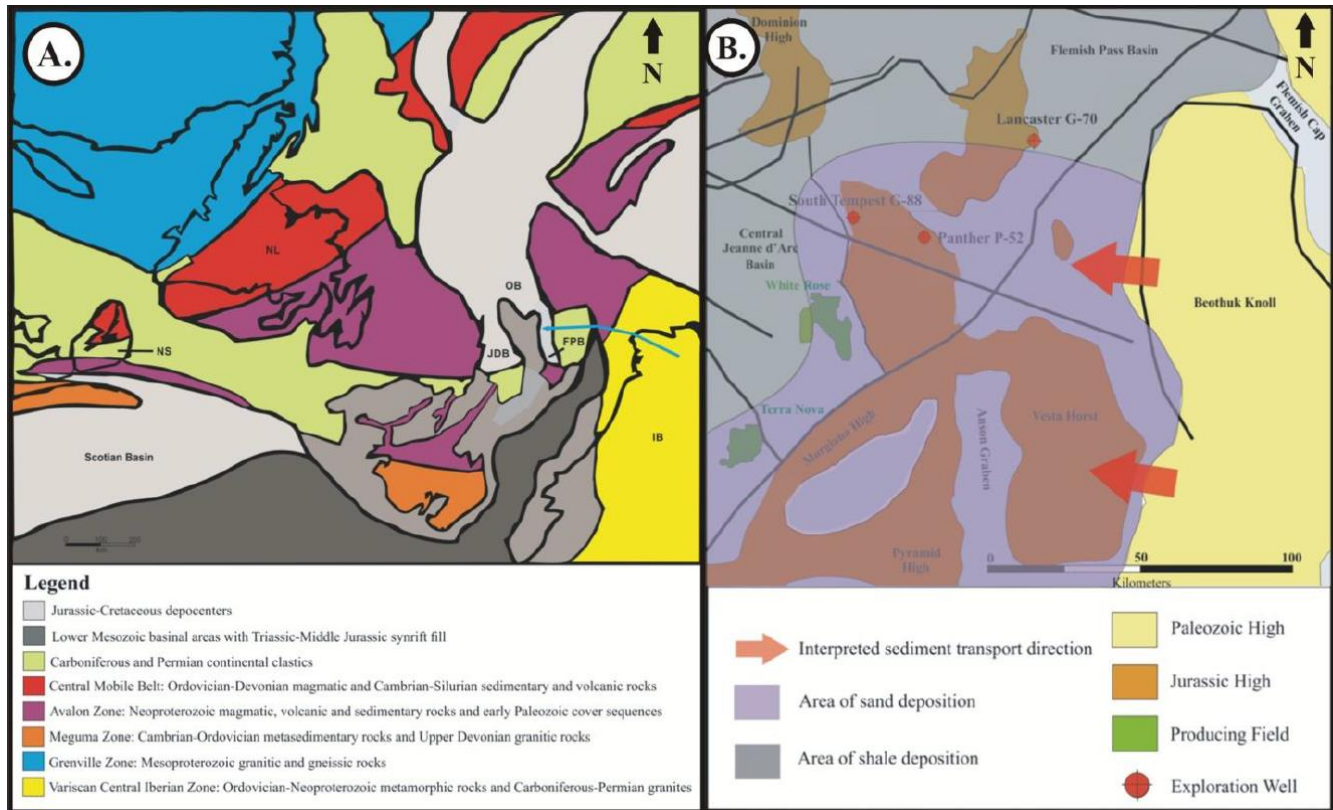


Figure 4. (A) Interpreted large-scale drainage routes during deposition of the Upper and Lower Tempest Sandstone. Figure modified from Lowe et al. (2011). (B) Interpreted basin entry points and areas of abundant and restricted sediment supply during deposition of the Upper and Lower Tempest Sandstone. Figure modified from Cody et al. (2012).

Constraints on Depositional Ages

The three Jurassic zircon grains (145 ± 5 Ma, 148 ± 4 Ma, and 150 ± 6 Ma) from the Upper Tempest Member sandstone sample (Panther P-52 at 3210 m) can help refine the depositional age of this unit. In this sample, the weighted average of age dates from these three grains is 147.5 ± 2.8 Ma (MSWD = 0.85), which may be taken as the maximum depositional age (Dickinson and Gehrels, 2009). If the age of the youngest single grain is accepted, the maximum depositional age would be reduced to 144.9 ± 5.6 Ma. Whether the youngest single grain or the weighted average of the three grains is used, a Late Tithonian depositional age for the Upper Tempest Sandstone is suggested, as the Tithonian Stage ranges from 152.1 ± 0.9 to ~ 145 Ma (ICS, 2013). When compared to biostratigraphic interpretations for this interval, a Late Tithonian age is consistent with findings from Robertson Research (2004), but conflicts with interpretations from the Bujak Davies Group (1987) who interpreted this interval to be Early Kimmeridgian in age. Based on the detrital zircon age results, and the Robertson Research (2004) report, the Upper Tempest Member sandstone from the Panther P-52 well is considered to have a Late Tithonian depositional age.



Summary

Detailed analysis of Upper Jurassic rocks from the Flemish Pass Basin and Central Ridge through a combination of detrital zircon geochronology and whole rock geochemistry highlights important provenance characteristics of these units. Whole rock geochemistry was employed on both Upper Jurassic sandstones and mudstones to identify sediment provenance. The whole rock geochemistry indicates that the units were derived from sources with upper crustal compositions, commonly seen in passive margins. In addition, detrital zircon geochronology revealed information and for generating provenance and paleodrainage models. Samples from the Upper Kimmeridgian source rock, Upper Tempest Member sandstone, and Lower Tempest Member sandstone were analyzed. Zircon populations from within the Upper Kimmeridgian source rock indicate grains were likely derived from the Avalon Zone, Central Mobile Belt, and underlying basement. Samples from the Upper and Lower Tempest Member sandstones had overall similar detrital zircon populations. A significant population of Permian–Carboniferous grains, however, are present in these Tempest sandstone samples suggesting derivation from Iberian intrusive rocks. This change in provenance within the Tempest sandstones was also noted in the whole rock geochemical data from the Lower Tempest Member sandstone samples.

In addition to important provenance information, Upper Jurassic detrital zircons constrain the age of the Upper Tempest Member sandstone to Late Tithonian or younger. This is a particularly useful result as conflicting ages exist in the published biostratigraphic interpretations for this unit.

Acknowledgements

Financial support for this project was provided by the Research and Development Corporation of Newfoundland and Labrador in the form of an Ocean Industries Student Research Award and is gratefully acknowledged. The MITACS Accelerate program also contributed to this project financially.

There are many others who have helped and contributed to the completion of this project in some way. Dylan Goudie, David Grant, Sarah Jantzi, and Pam King of the CREAT Network at Memorial University were extremely helpful to MWS with guidance and timely analyses for the various methods undertaken. Kate Souders and Angela Norman helped significantly by teaching MWS sample preparation methods as well as aiding with analytical techniques.

MWS would also like to thank the C-NLOPB, particularly David Mills and Jason Newell, for access to the core and sample materials, and Kelly Batten Hender and Jeff O’Keefe for the freedom to continue his research while working under their supervision.

References

- Bujak Davies Group, 1987. Palynological biostratigraphy of the interval 395–4203 m, Panther P-52, Grand Banks. Geological Survey of Canada Open File Report 1876, 16p.
- C-NLOPB, 2007. Schedule of Wells – Newfoundland and Labrador offshore area, South Tempest G-88, Panther P-52 and Lancaster G-70. Accessed June 15, 2018, <http://www.cnlopb.ca/wells/>
- C-NLOPB, 2011. Schedule of Wells – Newfoundland and Labrador offshore area, Baccalieu I-78. Accessed June 15, 2018, <http://www.cnlopb.ca/wells/>
- Cody, J., Hunter, D., Schwartz, S., Marshall, J., Haynes, S., Gruschwitz, K., and McDonough, M., 2012. A Late Jurassic play fairway beyond the Jeanne d’Arc Basin: new insights for a petroleum system in the Northern Flemish Pass Basin. In: N.C. Rosen, P. Weimer, S.M.C. dos Anjos, S. Henrickson, E. Marques, M. Mayall, R. Fillon, T. D’Agostino, A. Saller, K. Campion, T. Huang, R. Sarg, F. Schroeder (eds), *New understanding of the petroleum systems of continental margins of the world*. 32nd Annual GCS-SEPM Foundation Bob F. Prekins Research Conference, December 2-5, 2012, Houston, Texas, 599-608.



- Cohen, K.M., Finney, S.C., Gibbard, P.L., and Fan, J.-X., 2013. The ICS International Chronostratigraphic Chart. *Episodes*, **36**, 199-204.
- Creaney, S., and Allison, B.H., 1987. An organic geochemical model of oil generation in the Avalon/Flemish Pass Subbasins, East Coast Canada. *Bulletin of Canadian Petroleum Geology*, **35**(1), 12-23.
- Dickinson, W.R., and Gehrels, G.E., 2009. Use of U-Pb ages of detrital zircons to infer maximum depositional ages of strata: A test against a Colorado Plateau Mesozoic database. *Earth and Planetary Science Letters*, **288**, 115-125, doi:10.1016/j.espl.2009.09.013
- Enachescu, M.E., 2014. Petroleum exploration opportunities in the Flemish Pass Basin, Newfoundland and Labrador offshore area; Call for Bids NL13-01, Area "C" – Flemish Pass Basin, Parcel 1. Government of Newfoundland and Labrador Department of Natural Resources, <https://www.nr.gov.nl.ca/nr/invest/PetExOpCarsonNL1302.pdf>.
- Fowler, M.G., Obermajer, M., Achal, S., and Milovic, M., 2007, Results of geochemical analyses of an oil sample from Mizzen L-11 well, Flemish Pass, offshore Eastern Canada. Geological Survey of Canada, Open File 5342, 3p.
- King, L.H., Fader, G.B., Poole, W.H., and Wanless, R.K., 1985. Geological setting and age of the Flemish Cap granodiorite, east of the grand banks of Newfoundland. *Canadian Journal of Earth Sciences*, **22**(9), 1286-1298.
- Lowe, D.G., Sylvester, P.J., and Enachescu, M.E., 2011. Provenance and paleodrainage patterns of Upper Jurassic and Lower Cretaceous synrift sandstones in the Flemish Pass Basin, offshore Newfoundland, east coast of Canada. *American Association of Petroleum Geologists Bulletin*, **95**(8), 1295-1320, doi:10.1306/12081010005
- McCracken, J.N., Haager, A., Saunders, K.I., and Veilleux, B.W., 2000. Late Jurassic source rocks in the northern Flemish Pass Basin, Grand Banks of Newfoundland. Proceedings of GeoCanada 2000 - The Millennium Geoscience Summit, May 29 - June 2, 2000, Calgary, Alberta, GAC-MAC 2000 Program with Abstracts Volume **25**: GeoCanada 2000 Conference CD, Geological Association of Canada.
- McLennan, S.M., 2001, Relationships between the trace element composition of sedimentary rocks and upper continental crust. *Geochemistry, Geophysics, Geosystems*, **2**(2000GC000109).
- McLennan, S.M., Taylor, S.R., McCulloch, M.T., and Maynard, J.B., 1990. Geochemical and Nd-Sr isotopic composition of deep-sea turbidites: crustal evolution of and plate tectonic associations. *Geochemica et Cosmochimica Acta*, **59**, 1153-1177.
- McLennan, S.M., Bock, B., Hemming, S.R., Hurowitz, J.A., Lev, S.M., and McDaniel, D.K., 2003. The roles of provenance and sedimentary processes in the geochemistry of sedimentary rocks. In: D.R. Lentz (ed), *Geochemistry of Sediments and Sedimentary Rocks: Evolutionary Considerations to Mineral Deposit-Forming Environments*. Geological Association of Canada, *GeoText* **4**, 7-38.
- Robertson Research International Ltd., 2004. Palynology (2650-4205 m) and micropaleontology (2635–4210 m), Panther P-52 biostratigraphy report. Available from the C-NLOPB, File Number 8632-R005-001P.
- Salters, V.J.M., and A. Stracke, 2004, Composition of the Depleted Mantle, *Geochemistry, Geophysics, Geosystems*, **5**, 27p., doi:10.1029/2003GC000597
-





MLA-SEM ANALYSIS OF WELL CUTTINGS FROM NEWFOUNDLAND AND LABRADOR OFFSHORE BASINS

Wilton, D.H.C.¹, Feely, M.², Costanzo, A.², Hunt, J.², and Norris, D.³

¹ Department of Earth Sciences, Memorial University of Newfoundland, St. John's, NL A1B 3X5 Canada
dwilton@mun.ca

² Earth and Ocean Sciences, School of Natural Sciences, National University of Ireland, University Road, Galway
LL32 8FA, Ireland

³ Nalcor Energy Limited, 500 Columbus Drive, St. John's, NL A1B 0C9, Canada

Mineral Liberation Analysis-Scanning Electron Microscope (MLA-SEM) of well cuttings were undertaken to ascertain whether quantifiable data on their mineralogy and physical characteristics could provide insight into potential stratigraphic breaks within the sample set analysed. These insights can be utilized to evaluate stratigraphic relationships within the wells analysed and potentially establish a framework to build a mineralogical database for Newfoundland and Labrador's offshore region. A total of 236 well cuttings samples were analyzed with 176 from seven legacy wells offshore Labrador and 60 samples from three offshore Newfoundland wells. Sandstone lithologies were sampled preferentially, due to the multi-phase analysis with a National University of Ireland, Galway (NUIG) fluid inclusions study.

The MLA-SEM data defined mineralogy, sorting, and angularity of grains within each sample. Mineralogical Associations (MAs) were established for sample subgroups within each well to define intervals with discernible mineralogical attributes that might provide inter-well stratigraphic insights. These MAs can be further assessed for their physical characteristics such as grain size, sorting, and angularity in defining stratigraphic packages within each well. Also mapped were diagenetic cement types and amounts that provide insight into the dynamic fluid system affecting the areas from where the samples were taken. Results from this study, paired with fluid inclusion analysis completed by NUIG, suggest that hydrocarbon-bearing fluid inclusion samples were derived from well-sorted, mature intervals.

Further advancement of the MLA-SEM cuttings analysis technique could offer stratigraphic insights within frontier exploration regions of Newfoundland and Labrador's offshore. Future analysis could be incorporated with provenance studies to provide insight into sediment input terranes, as well as establish distinct mineralogical differences within stratigraphically complex regions. Further work on broader stratigraphic intervals may lead to mineralogically defined stratigraphic successions that would be of great support to previous work completed within this frontier region.

Introduction

Mineral Liberation Analyser-Scanning Electron Microscope (MLA-SEM) analyses were conducted on 236 cuttings samples from 10 wells in the Newfoundland and Labrador offshore region (**Figure 1**). The maximum number of samples collected from a single well was 50 from Skolp E-07, and the least number collected were 10 samples from the Snorri J-90 well. **Table 1** lists the number of samples collected from each well. Preliminary results from both the MLA-SEM and fluid inclusion research were reported by Wilton et al. (2016), and Feely et al. (2016).

The samples were provided from the Canada-Newfoundland and Labrador Offshore Petroleum Board (C-NLOPB) Core Storage and Research Centre. Sandstone lithologies were sampled because they were necessary for fluid inclusion analysis conducted in a companion study (Costanzo et al., this volume). It is important to note that



consistent sampling of stratigraphy throughout each well was not conducted, in part because of the need for sandstones to complete the fluid inclusion work, but also due to the restricted availability of sample material from some of the Labrador legacy wells.

The fundamental aim of this project was to determine whether groups of samples within a given well have similar mineralogical (and physical) characteristics that allow the defining of Mineralogical Associations (MAs) over a specific interval. An MA is essentially a group of samples with a matrix of common mineral compositions that uniquely define the interval from which they were derived. The ultimate goal is to define mineralogically recognizable layers within the stratigraphy of the sampled intervals. As such, these MAs may essentially form the basis for a mineralogical/geochemical stratigraphy in the cuttings samples.

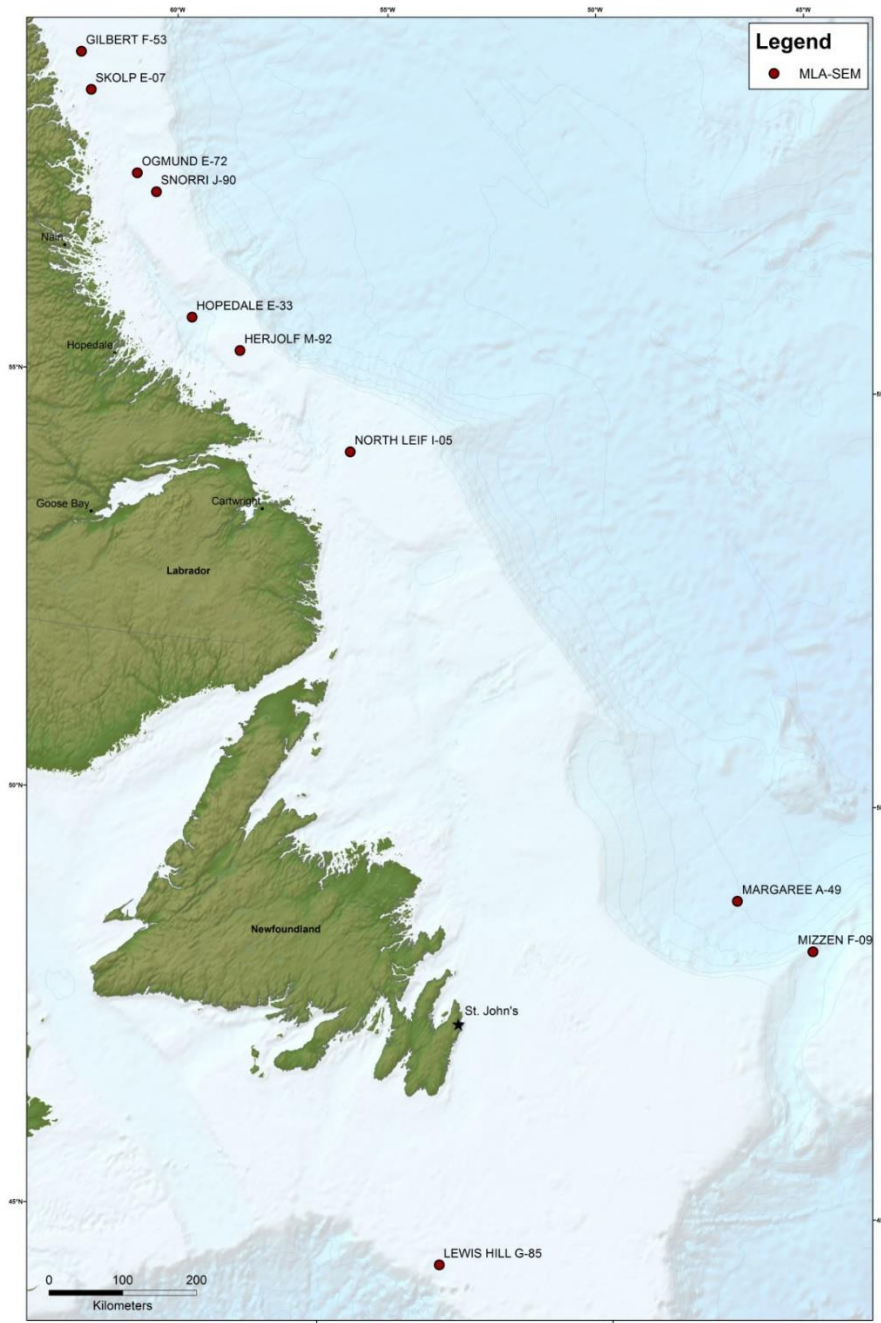


Figure 10. Location of the wells investigated in this study; Source (Nalcor Energy).



MLA-SEM methods and sample preparation

The MLA-SEM facility in the CREAT laboratories, Memorial University, consists of a fast FEI MLA 650 FEG (2011 model) Scanning Electron Microscope (SEM) and associated sophisticated MLA software. Essentially the MLA software allows the Energy Dispersive X-ray (EDX) component of the SEM to define quantitatively the abundance, association, size, and shape of minerals in an automated, systematic fashion (Sylvester, 2012; Wilton et al., 2017; Wilton and Winter, 2012).

Each sample consisted of up to 50 g of cuttings from a pre-selected interval. The coarser grains were split into a portion sent to the Geofluids Research Laboratories, National University of Ireland, Galway, (Costanzo et al., this volume) for fluid inclusion analysis. The remaining material, retained for the MLA work, was lightly crushed with a mortar and pestle and then carefully washed with soap to remove barite drilling mud. The washed sample material was wet sieved into three size fractions: i) < 75 µm in diameter, ii) >75 but <180 µm, and iii) > 180 µm in diameter. The 75-180 µm fraction from each sample was further split until a separate weighing approximately 1 g was derived. This was then mounted in epoxy within a transversal (30 x 17 mm with a height of 10mm) rectangular mould after the method of Grant et al. (2016). The resultant solid epoxy block for each sample was divided in half, and each half polished using an internally developed polishing protocol method.

Prior to analysis on the MLA-SEM, each polished mount was coated with a thin graphite film. A duplicate sample was inserted with every five samples. The SEM is equipped with a Bruker EDS Detector. The SEM electron gun uses a filament at an operating voltage of 25 Kv and a beam current of 10 nA. The working distance between sample and detector is 13.5 mm and spot size is about 5 µm. The imaging scan speed was 16 micro sec, with frame resolution of 800 dpi, and X-ray collection at 12 micro sec.

Table 1: Number of cuttings samples collected from each offshore well

Well	# Samples	Location
Gilbert F-53	11	Labrador
Skolp E-07	50	Labrador
Ogmund E-72	47	Labrador
Snorri J-90	10	Labrador
Hopedale E-33	11	Labrador
Herjolf M-92	24	Labrador
North Leif I-05	23	Labrador
Margaree A-49	21	NE Newfoundland
Mizzen F-09	27	NE Newfoundland
Lewis Hill G-85	12	Grand Banks

The basis for Mineral Liberation Analysis (MLA) studies is the derivation of an energy dispersive spectrum for each mineral. The analysed spectra are matched against the MLA database of stored EDX (energy-dispersive X-ray) spectra, also known as mineral fingerprints or Species Identification Protocols (SIPs). At present, the MLA-SEM analysis of a grain mount with cuttings material can accurately identify up to 99.7% of mineral particles present in the sample; a given individual sample when prepared for analysis can contain up to 20,000 particles, and at least 10,000 particles. A typical analysis time per sample is two to four hours.

The MLA software requires the SEM be configured in back-scatter electron (BSE) image mode wherein minerals containing denser elements produce brighter images. Essentially, the MLA detects mineral particles in the grain mount, based on variations in BSE grey scale and then it analyses each particle.



For each analysis, the grey-scale threshold is set with the epoxy (very low grey scale) as black and metallic copper as white (very high grey scale). The dwell time (i.e., time spent acquiring data) for each X-ray analysis of a particle is 60 microseconds. The image size resolution was set at 800 dpi and the minimum particle diameter detected was about 5 µm.

The MLA maps each grain mount in terms of frames per mount, typically using a horizontal field width (HFW) of 1-2 mm. The frame is the fundamental organizational template for the MLA technology. About 50-70 frames are measured per sample with approximately 100-150 particles per frame. **Figure 2** contains a BSE frame map and the corresponding false coloured MLA map for that frame.

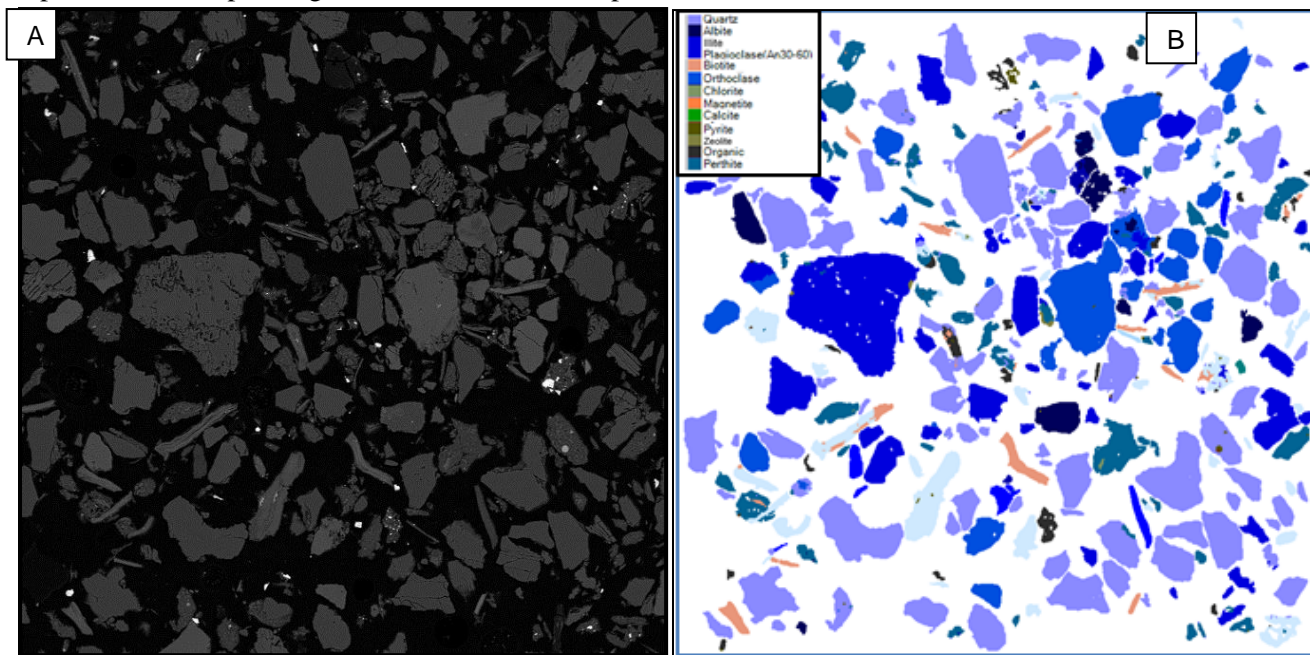


Figure 2. Images of Frame 42, sample 1610 m Skolp E-07 cuttings sample. A: Back Scatter Electron (BSE) map of frame. B: False colour MLA map of the same frame; most minerals are quartz and feldspar (blue), biotite (orange) is also common in this frame (views are about 1.5 mm across).

Results

The MLA data were used to produce downhole strip logs and bar graphs of mineral contents using a ratio of the mapped area of each mineral to the total area of all minerals mapped in the sample (**Figure 3**). From these logs and bar graphs, the Mineralogical Associations (MAs) within each well were determined. The MAs were confirmed by further observations such as determination of Top Ten Minerals (**Figure 4**), downhole logs of Heavy Mineral Ratio Indices (after Morton, 2012; **Figure 5**), and bivariate mineral plots (**Figure 6**).

In a number of the wells studied, the bivariate plots indicate subtle differences in mineral contents between MAs that might reflect slightly different detrital input. In some cases, the plots (e.g. quartz vs. biotite) even suggest greater maturity between units (**Figure 7**).

Carbonate minerals, including calcite, dolomite, ankerite, and siderite, were mapped by the MLA in most cuttings samples as a minor component. Essentially the carbonates are cement to detrital grains in the cuttings. Distinct differences in cement contents could be observed between MAs in different wells (**Figure 8**). Hence, different diagenetic reactions could be suggested for different groups of samples from the MLA data.



Comparison of Snorri Member samples from offshore Labrador wells

As demonstrated above, the MLA-SEM can define Mineralogical Associations (MAs) within individual wells that may provide a mineralogical stratigraphy for that well. And these MAs can compare favourably to the interpreted time breaks from pre-existing biostratigraphic analysis (Wilton, 2018). Some interesting observations arise, however, when the complete data set is queried for a regional unit of a similar age that has been biostratigraphically interpreted throughout a number of wells.

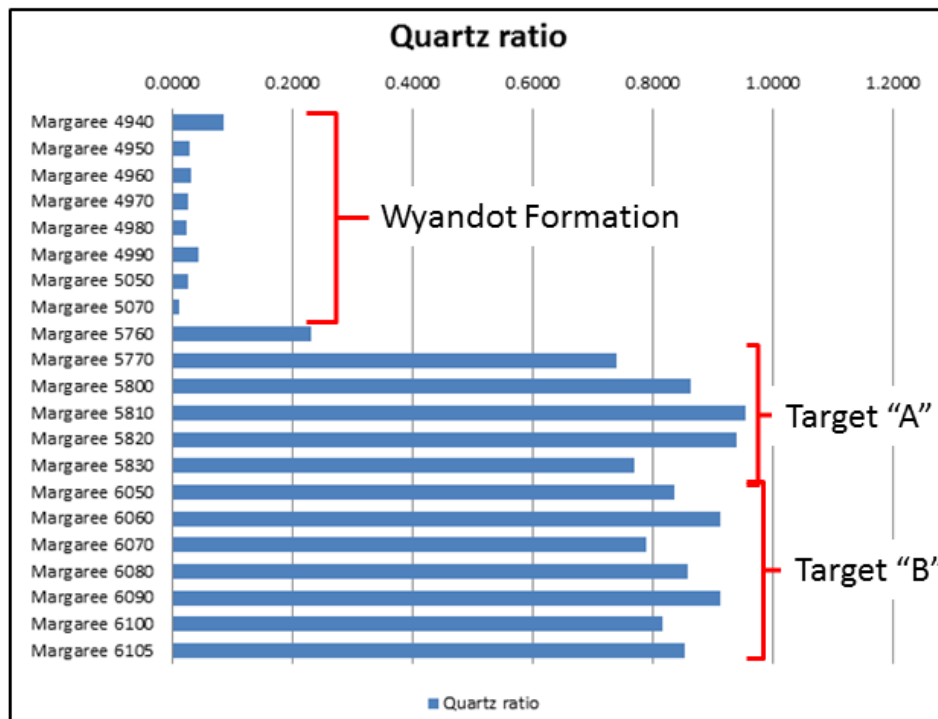


Figure 3. Example of downhole bar graph for quartz in Margaree A-49 cuttings samples. The Wyandot Formation equivalent limestones are readily distinguishable from the deeper sandstones and there are subtle variations in the sandstones, in particular the sample from 5760 m. This sample is also distinctive in many other mineral contents and it has been suggested that this sample may have been deposited directly on the sequence boundary separating the Jurassic and Cretaceous intervals (James Carter, pers. com., 2017).

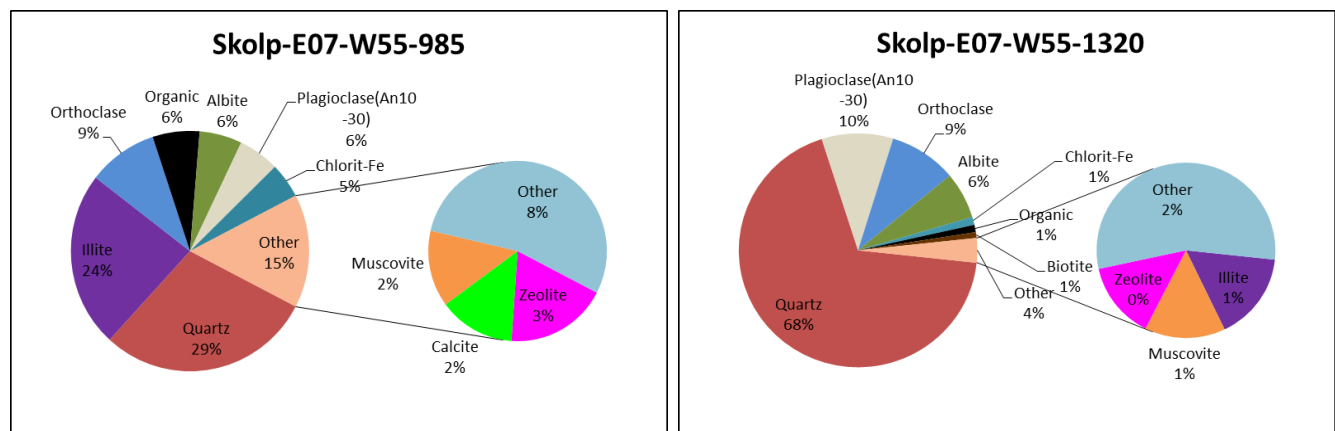


Figure 4. Top Ten minerals in two samples from Skolp E-07, upper from 985 m and part of Mineralogical Association (MA)_A and bottom from 1320 m part of MA_B.

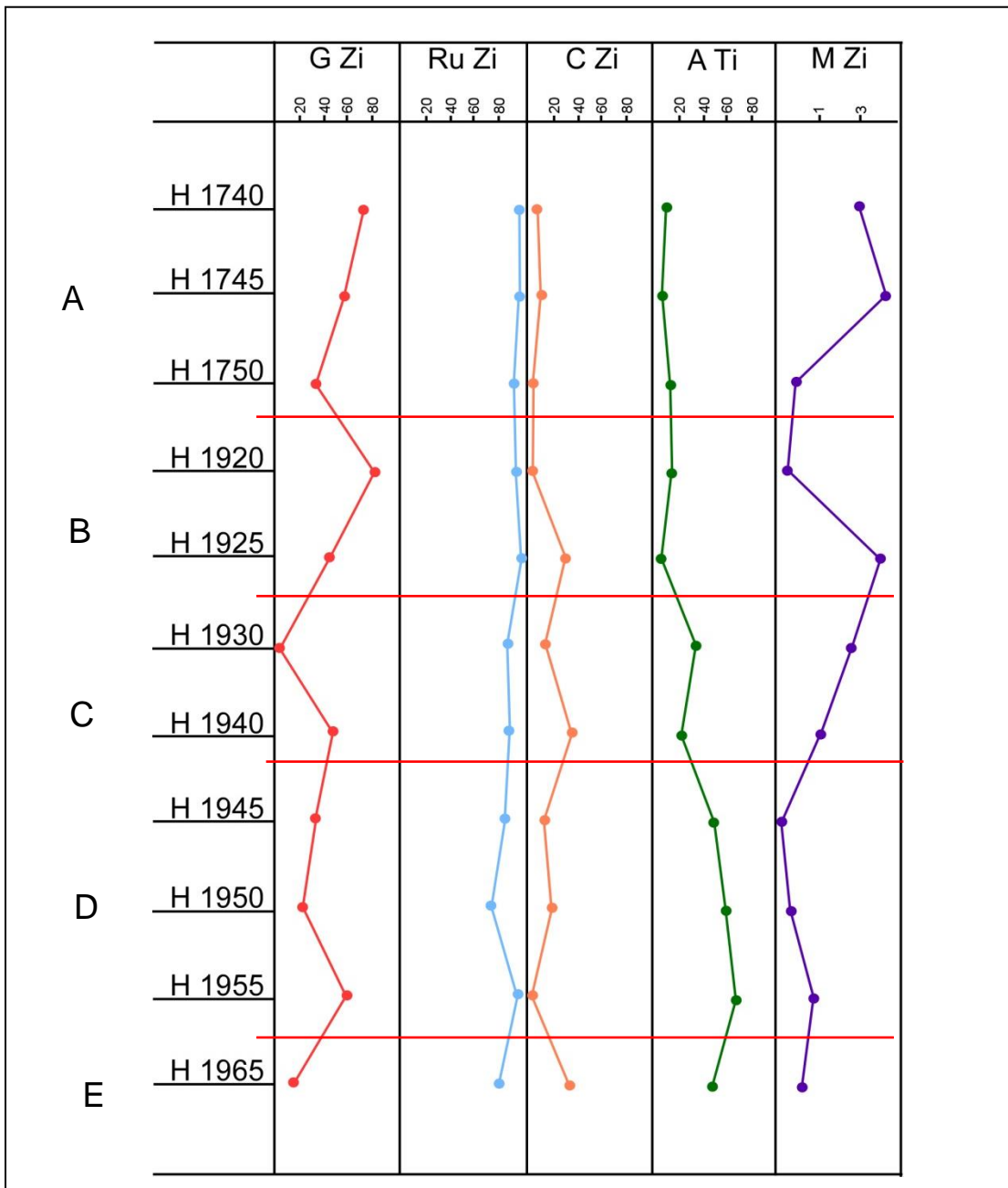


Figure 5. Downhole strip logs from Hopedale E-33 of Morton Heavy Mineral Ratio Indices (after Morton, 2012) as calculated from MLA-SEM mapping; the red lines divide the samples in Mineralogical Associations (A to E) based on MLA-SEM analysis.

Sandstone samples from the biostratigraphically interpreted Snorri Member of the Bjarni Formation (Lower Cretaceous), as logged by previous workers, were collected from all the offshore Labrador wells, except Gilbert F-53. Bivariate mineral plots (**Figure 9**) readily demonstrate that the lithologies mapped as Snorri member in these wells are mineralogically different yet display similar mineralogical characteristics within each well. Feldspar and quartz distributions are different between wells. For instance, Herjolf M-92 samples have the greatest orthoclase content, and Ogmund E-72 the greatest plagioclase content. Micaceous minerals are likewise distinct with demonstrably higher contents in North Leif I-05. Distinctions in these minerals may reflect different source regions for detritus in these wells.

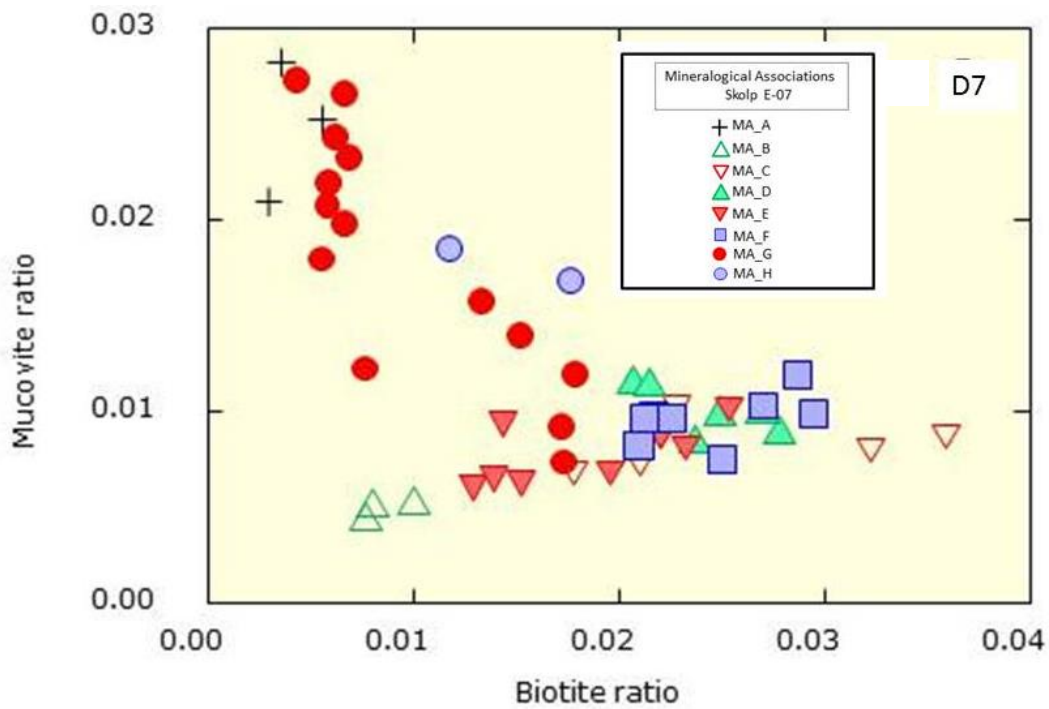


Figure 6. Bivariate plot of muscovite vs. biotite for different MAs in Skolp E-07 sample; these are just two minerals of up to 30 used to define the MAs.

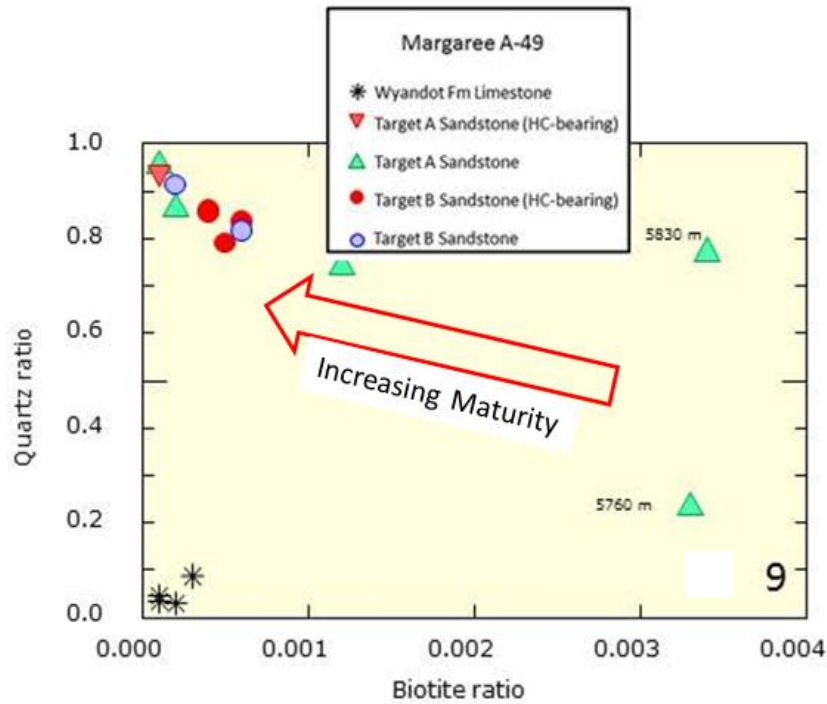


Figure 7. Bivariate plot of quartz vs. biotite contents in Margaree A-49 cuttings samples. The Target B samples have generally lower biotite and higher quartz contents suggesting a more mature nature than the Target A samples (HC-bearing refers to samples in which Hydrocarbon-bearing inclusions were identified after Costanzo et al., this volume).

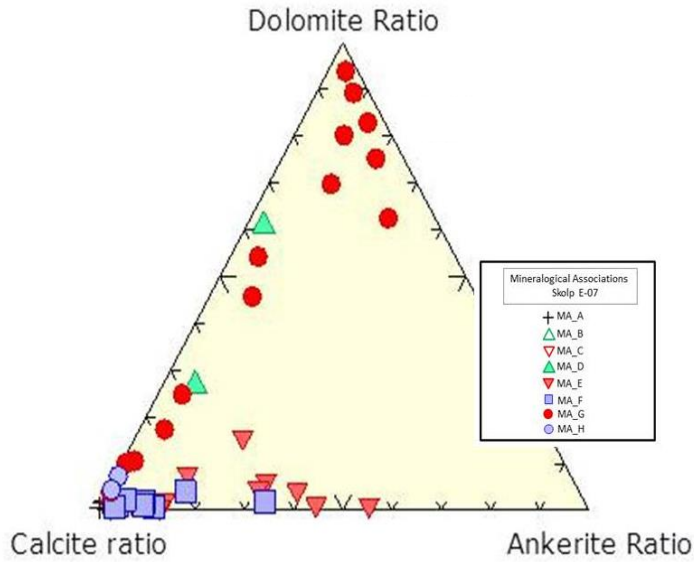


Figure 8. Ternary plot of calcite-dolomite-ankerite for Skolp E-07 samples. The diagram indicates that samples in the different MAs have unique and definable cement compositions.

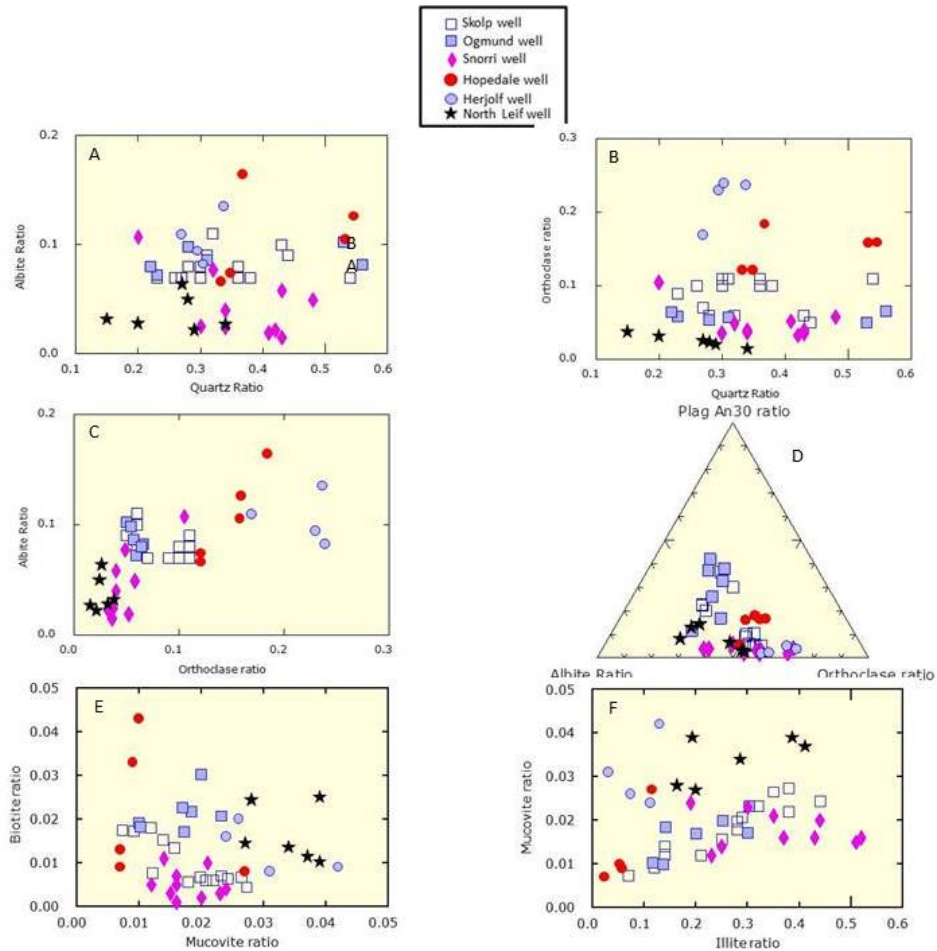


Figure 9. Bivariate plots of minerals identified by MLA-SEM in each of the offshore Labrador wells (excepting Gilbert F-53).



Carbonate minerals are also distinct between these Snorri member samples (not shown). Skolp E-07 samples are enriched in dolomite whereas Hopedale E-33 and some Snorri E-07 samples are enriched in siderite compared to the other cements. The Gilbert F-53 and Skolp E-07 samples also contain significant Mn-calcite (Wilton et al., 2016). Variations in minerals such as pyrite (not shown) may reflect different redox conditions at their depositional site.

Conclusions

The MLA-SEM analyses of cuttings samples in this study provided quantifiable data on the mineralogy and physical characteristics, including sorting, angularity, and sphericity characteristics, of sample grains. The data were primarily used to define Mineralogical Associations (MA) among the samples from each well. These MAs form the basis for a mineralogical/geochemical stratigraphy in the cuttings samples. In some wells, such as Margaree A-49 and Mizzen F-09, the sampled intervals cover a broader stratigraphic coverage than other well within the study. In the Labrador wells, sample coverage was more sporadic, and hence, the full stratigraphic extents of the MAs could not be defined. Based on the presence of diagnostic minerals, the data could also provide insight on depositional environments and provenance sources. Analysis can also define variations in diagenetic cements in each sample.

Whether these MA intervals represent definable lithological units that can be correlated between wells requires much more detailed work. Furthermore, the full extent of each MA in a given well cannot be determined without more extensive sampling. However, we were able to sample broader stratigraphic coverage of sandstone units/MAs in two of the wells: Mizzen F-09 and Margaree A-49. The number of different MA intervals in those wells cannot be determined though, without more complete sampling of the entire well.

The MLA-SEM data also indicated that samples from a unit logged as the Snorri Member, Bjarni Formation, in all offshore Labrador wells (except Gilbert F-53) are mineralogically dissimilar. The groups of samples from each well, however, are generally similar and correlative. The mineralogies are so unlike between the wells, that it appears the sandstones sampled in the wells were either not from the same unit, or there are significant provenance variations across the Labrador basins. With more detailed sampling, cross well correlations might be possible for this unit.

The MLA-SEM mineralogical data derived from the Snorri Member samples also allow comparisons of three important parameters from the sample material in each well. These are: (1) differences in source(s) of the constituent detrital material, (2) variations in depositional environments (e.g., redox conditions), and (3) contrasts in carbonate cement composition which may in part be linked to diagenetic reactions and pore fluid compositions.

The material examined in these and the fluid inclusion studies was cuttings. In contrast with solid drill core, due to their broken, fine-grained disaggregated natures, cuttings material is typically very difficult to use for petrographic and textural studies. The MLA-SEM paired with fluid inclusion analysis offers insight into depositional environments, provenance, and the petroleum system potential.

One final point is that the cuttings provide an aggregate sample, which reflects the nature of the lithologies encountered over several metres. By using the MLA-SEM and fluid inclusion techniques, data over that interval can be generated. In contrast, while thin sections of solid drill core provide the best, most detailed textural-mineralogical data, they do so only for a centimetre of a well and is only available where core has been cut. The MLA-SEM technique, using cuttings data, offers a broader range of analysis within a wellbore and also has fewer limitations in sample availability compared to thin section sampling from core data.

Future studies using the MLA-SEM techniques should include consistent sampling of entire well intervals to assess better the subject mineralogical architecture.



Acknowledgements

The MLA-SEM studies of the Labrador and Newfoundland offshore basins were funded by the Offshore Geoscience Data Program (OGDP) that is jointly administered by Nalcor Energy – Oil and Gas, and the Department of Natural Resources, Government of Newfoundland and Labrador. The MUN CREAT crew of David Grant (Ph.D.) and Brent Myron (Ph.D.), Dylan Goudie, David Sooley, and Elizabeth Baird generated this tremendous data set. The C-NLOPB provided the cuttings material.

References

- Costanzo, A., Hunt, J., Feely, M., Wilton, D.H.C., and Norris, D., this volume. Hydrocarbon and aqueous fluid inclusion signatures in well cuttings from Newfoundland and Labrador Offshore Basins.
- Feely, M., Costanzo, A., Hunt, J., Wilton, D.H., and Carter, J.S., 2016. Oil Exploration and its Relationship to the World of Trapped Micron Scale Fluids: A Review of the Applications of Fluid Inclusion Microscopy to the Study of Aqueous and Hydrocarbon Fluid Dynamics in Sedimentary Basins. Proceedings of the Artic Technology Conference, St. John's, Newfoundland, Canada, 12p., doi:10.4043/27395-MS.
- Grant, D.C., Goudie, D.J., Shaffer, M., and Sylvester, P. 2016. A single-step trans-vertical epoxy preparation method for maximising throughput of iron-ore samples via SEM-MLA analysis. Applied Earth Science: Transactions of the Institutions of Mining and Metallurgy Section B: Applied Earth Science **125**, 57-62.
- Morton, A.C., 2012. Value of heavy minerals in sediments and sedimentary rocks for provenance, transport, and stratigraphic correlation. Mineralogical Association of Canada, Short Course Notes, Volume **42**, 133-166.
- Sylvester, P.J., 2012. Use of the Mineral Liberation Analyzer (MLA) for Mineralogical Studies of Sediments and Sedimentary Rocks. In: Quantitative Mineralogy and Microanalysis of Sediments and Sedimentary Rock, Mineralogical Association of Canada Short Course Series, Volume **42**, 1-16.
- Wilton, D.H.C., 2018. MLA-SEM analysis of well cuttings from offshore Newfoundland and Labrador, Unpublished Report, Nalcor Energy, 28p.
- Wilton, D.H.C., Feely, M., Carter, J.S., Costanzo, A., and Hunt, J., 2016. The Application of Automated SEM-Based Identification of Detrital and Diagenetic Mineral Phases in Offshore Cuttings from the Labrador Sea - Looking for the Source. Proceedings of the Artic Technology Conference, St. John's, Newfoundland, Canada, 12 p., doi:10.4043/27380-MS.
- Wilton, D.H.C., Thompson, G.M., and Grant, D.C., 2017. The use of automated indicator mineral analysis in the search for mineralization – A next generation drift prospecting tool. Explore (Newsletter for the Association of Applied Geochemists), Number 174 – March 2017, 11p.
- Wilton, D.H.C., and Winter, L.S., 2012. SEM-MLA (Scanning Electron Microprobe-Mineral Liberation Analyser) research on indicator minerals in glacial till and stream sediments: An example from the exploration for awaruite in Newfoundland and Labrador. In: Quantitative Mineralogy and Microanalysis of Sediments and Sedimentary Rocks. Mineralogical Association of Canada Short Course Series, Volume **42**, 265-283.



1D AND 2D PETROLEUM SYSTEM MODELLING OF POTENTIAL LOWER JURASSIC SOURCE ROCK ON SCOTIAN MARGIN

Hu, Xinyue¹, Wong, Juan C.¹, Silva, Ricardo L.¹ and Wach, Grant D.¹

¹Basin and Reservoir Lab, Department of Earth Science, Dalhousie University, Life Sciences Centre, 1355 Oxford Street, Halifax, NS B3H 4R2, Canada, emma.hu@dal.ca

The Scotian Basin is a passive margin with an area of approximately 280,000 km². Five potential Mesozoic source rocks intervals (Aptian, Valanginian, Tithonian, Callovian, and Early Jurassic) have been identified in the Scotian Basin. However, the Early Jurassic source interval has never been penetrated by drilling and is inferred from the Moroccan and Portuguese conjugate margins. The characteristics of the Lower Jurassic source rock have a large uncertainty. Building 1D and 2D models can reduce these uncertainties and lower the risk of hydrocarbon exploration.

In this study, 28 1D models and four 2D models were created and analyzed in PetroMod™ (Schlumberger). Compared to previous models of the petroleum systems for the Scotian Margin, our 1D models have greater lithostratigraphic resolution and these results are incorporated into the formulation of the 2D models not previously completed along the margin. The high resolution of lithostratigraphy is based on the extensive well cuttings descriptive database provided by Canadian Stratigraphic Services, and correlated with seismic lines and well data (wireline and lithology logs). The 1D models show the impact of salt structures on thermal maturity. The wells within salt diapiric area of the central Scotian Margin have higher temperature and higher source rock maturity. The 2D models are based on strike lines of the ION-GXT NovaSPAN™ geophysical dataset (NVR1-5100, NVR1-5400, NVR1-5420, and NVR1-5300), and a single dip line (NVR1-1600). Variable source rock properties (TOC, total organic carbon; HI, hydrogen index) were incorporated reflecting the potential range that may be encountered during deposition and subsequent maturation of organic-rich intervals along the Scotian margin. The transformation ratio is related to the HI, with higher numbers giving to a higher transformation ratio, and the potential for the formulation of oil. Source rock properties are based on the data from the High and Middle Atlas basins of Morocco. Our results suggest the potential Lower Jurassic source rocks have different ranges of maturity in the Scotian Basin and are within oil window in the north and transition to the gas window in the south.

Introduction

Petroleum System Modelling (PSM) is widely applied in academia and the petroleum industry. Basin modelling is a dynamic forward modelling of geological processes in sedimentary basins over geological time spans (Hantschel and Kauerauf, 2009; Hermanrud, 1993). Basin modelling has been utilized since the 1980s, progressing to the three-dimensional realm during the late 1990s (Hantschel and Kauerauf, 2009). These models incorporate depositional processes, pore pressure calculation and compaction, heat flow analyses, and temperature determination. Calibration parameters such as Vitrinite Reflectance (VR), temperature, and porosity can be used to refine the model as it calculates the hydrocarbon generation, adsorption and expulsion processes, fluid analysis, and migration pathways (Hantschel and Kauerauf, 2009).

In this study, PSM is completed on five 2D seismic lines from the Scotian margin with emphasis on potential Lower Jurassic source rocks and 28 wells drilled across the margin. No existing wells reach the depth of interest in the Lower Jurassic of the Scotian margin. A strong possibility of Lower Jurassic source rocks in the Scotian margin is based on the occurrence of Lower Jurassic successions of offshore Portugal (OETRA, 2011). PSM is the modern technology we used to test this possibility. A complete understanding of the regional geologic



history, stratigraphy, and paleoenvironments are required for building the PSM. Previous studies from Basin and Reservoir Lab and other institutions are used in the building the PSM models. In this study PetroMod™ by Schlumberger is used for 1D and 2D modelling for the prediction of the Lower Jurassic source rock.

Geological background

The Scotian Basin is located offshore Nova Scotia with an area approximately of 280,000 km² and an estimated maximum thickness of 24 km (OETRA, 2011) (**Figure 1**). The Scotian Basin is a classic passive, mostly non-volcanic, conjugate margin. The margin started to form during the breakup of Pangea in the Late Triassic when North America separated from the Africa continent. The Shelburne Subbasin, LaHave Platform, Sable and Abenaki Subbasins, Banquereau Platform, Huron and Laurentian Subbasin and Orpheus Graben are all part of this basin.

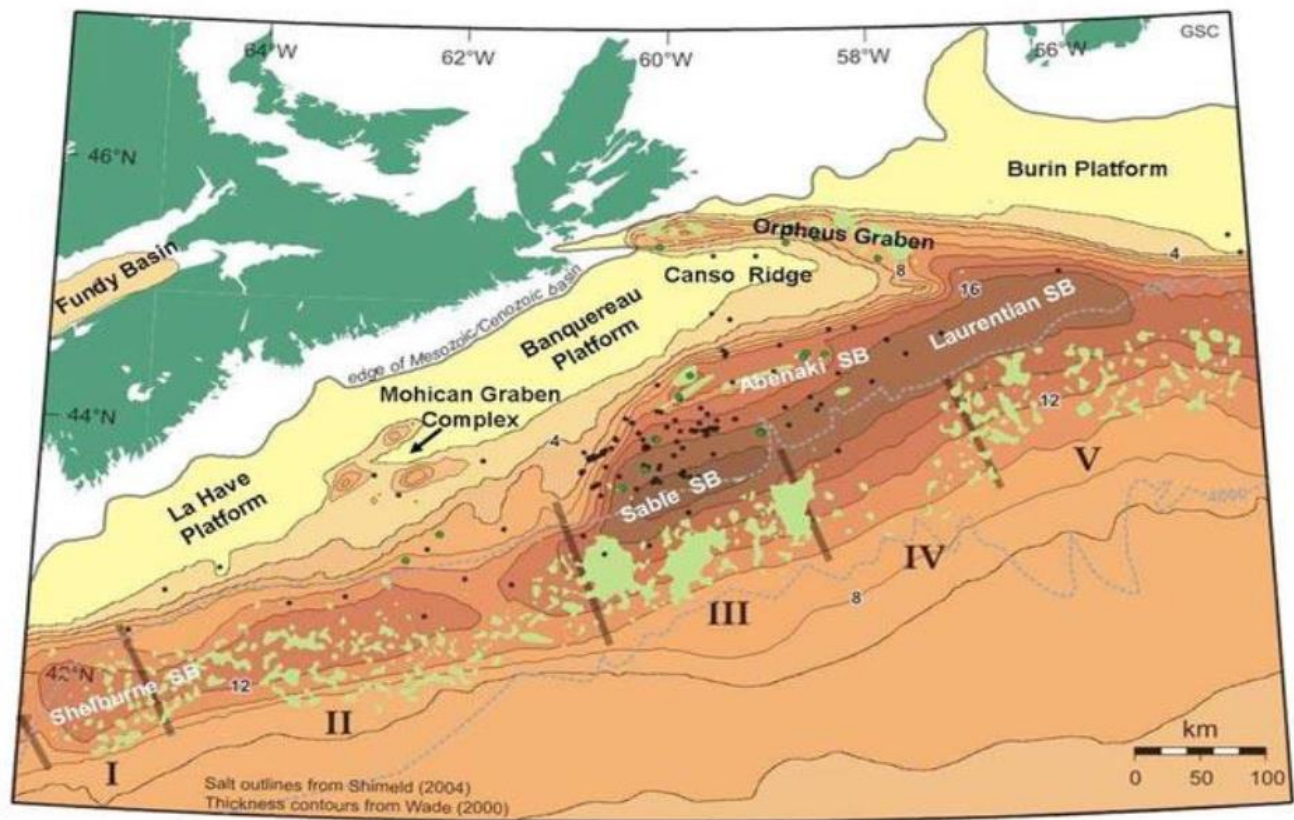


Figure 1. Regional geological map of the Scotian Basin identifying associated depocentres and tectonic elements (CNSOPB, 2009).

Study Methods

The objective of basin modelling is to integrate physical and chemical properties into a time-dependent model. This model is run based on the burial and thermal history, giving outputs of hydrocarbon generation, migration, and accumulation (Hantschel and Kauerauf, 2009). Two regional seismic lines are presented here from the ION-GXT NovaSPAN program (**Figure 2**). Line NVR1-1600 is a dip line extending from the LaHave Platform, through the Sable Subbasin and out into the deepwater salt province (green). Line NVR1-5400 is a strike line that parallels the inboard edge of the LaHave Platform and Late Jurassic Abenaki carbonate bank margin and extends to the northwestern edge of the Sable Subbasin (black).

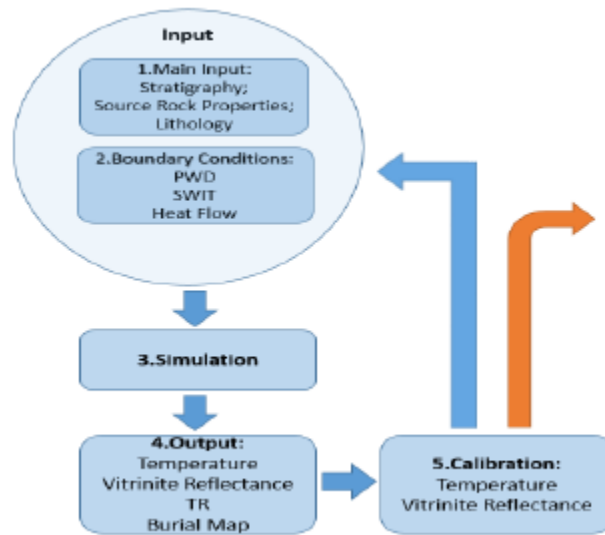


Figure 2. Flow chart of modelling methodology. The model building starts by inputting known geological data in the following categories. 1) Main input with stratigraphy, source rock properties, and lithology properties. 2) Boundary conditions, paleo-water depth (PWD), sediment-water interface temperature (SWIT), and heat flow. Once the model is built it can be simulated (3), each simulation has an output (4) depending on the inputs values (1), and (2). With the output (4), the model has to be validated with measured data from well (5) and if it fails validation, the process has to start over again with the inputs (1) and (2) and repeat the process again. If the validation is within acceptable ranges, then a possible valid solution is created.

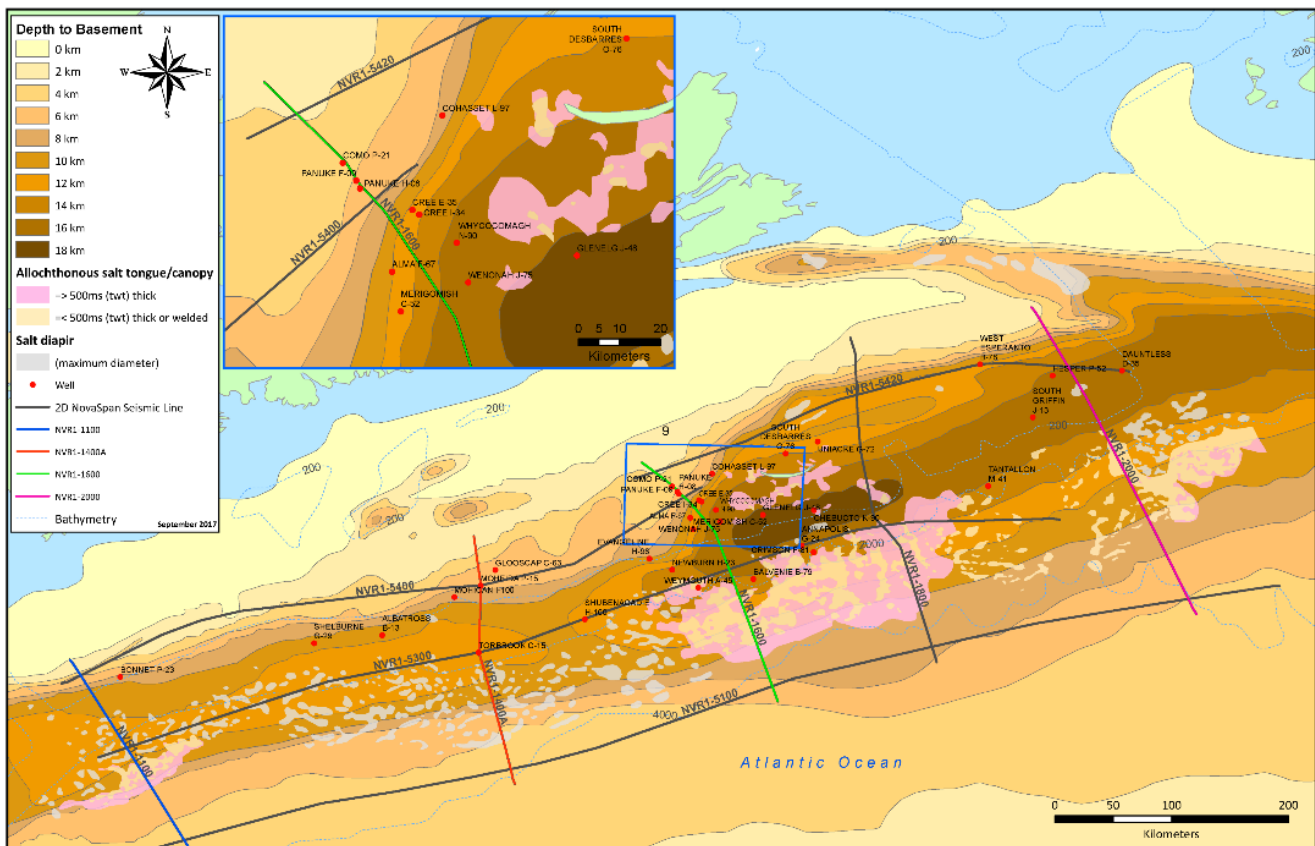


Figure 3. Depth to basement map of the Scotian Basin showing salt structures, distribution, and thicknesses. Key exploration wells are highlighted, and continuous lines are ION-GXT NovaSPAN program seismic lines (after Deptuck and Kendall, 2012; Loudon et al., 2004).

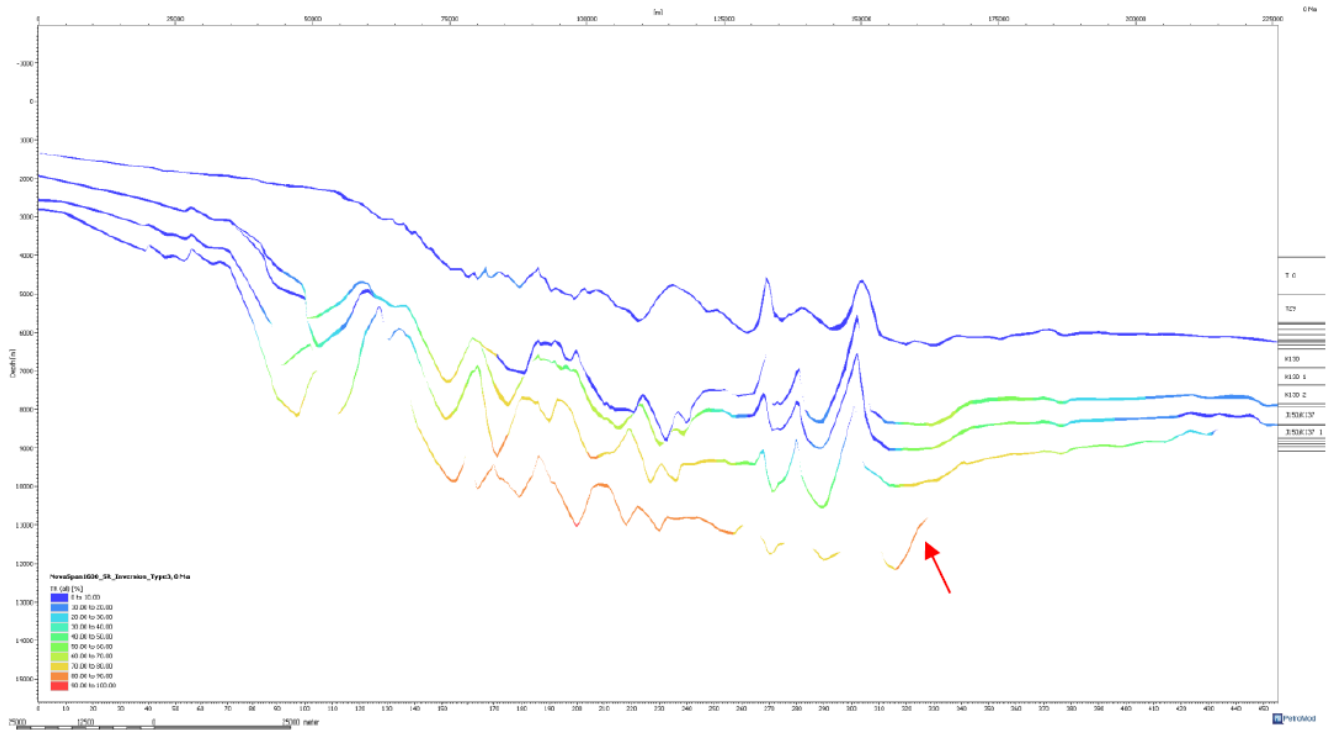


Figure 4. Modelling results for dip line LRV1-1600 run with Lower Jurassic source rock parameters of HI=200 mg HC/g TOC and TOC=3%. Red arrow indicates the track of the Lower Jurassic Source Rock through time.

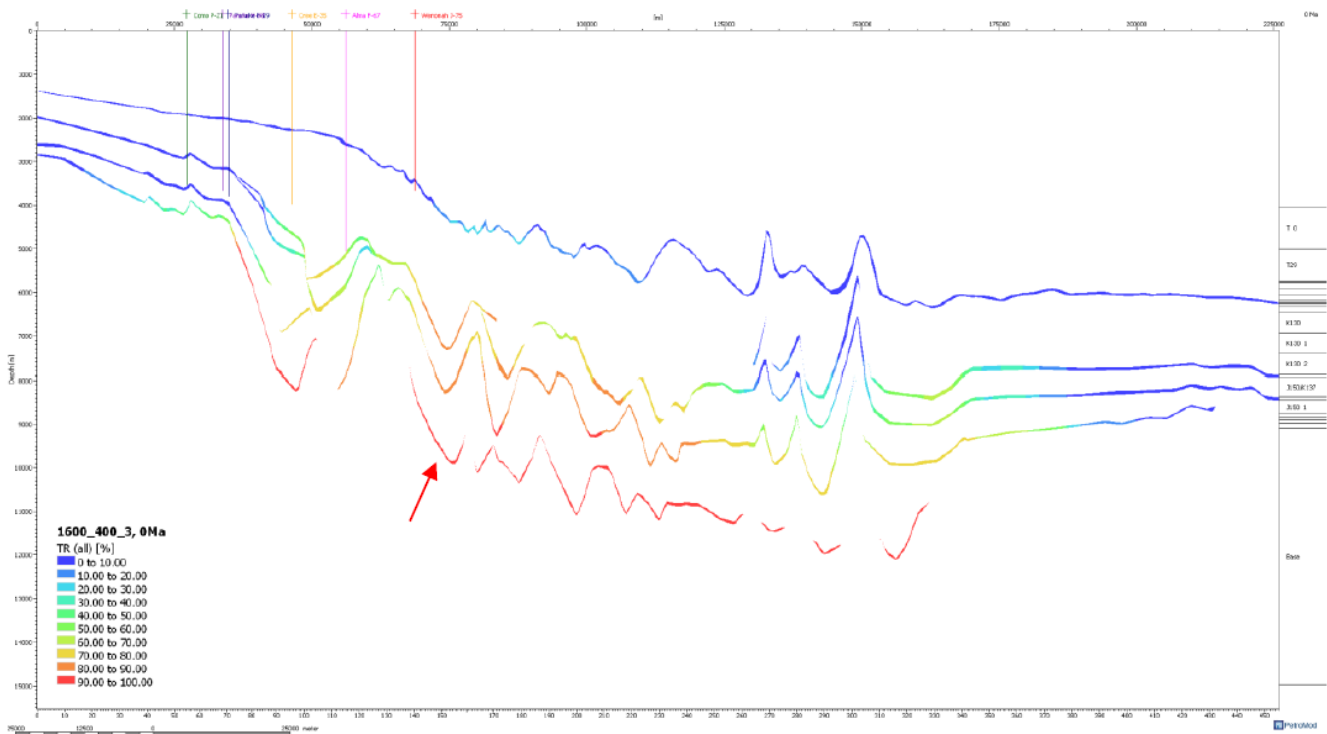


Figure 5. Modelling results for dip line LRV1-1600 run with Lower Jurassic source rock parameters of HI=400 mg HC/g TOC and TOC=3%. Red arrow indicates the track of the Lower Jurassic Source Rock through time.

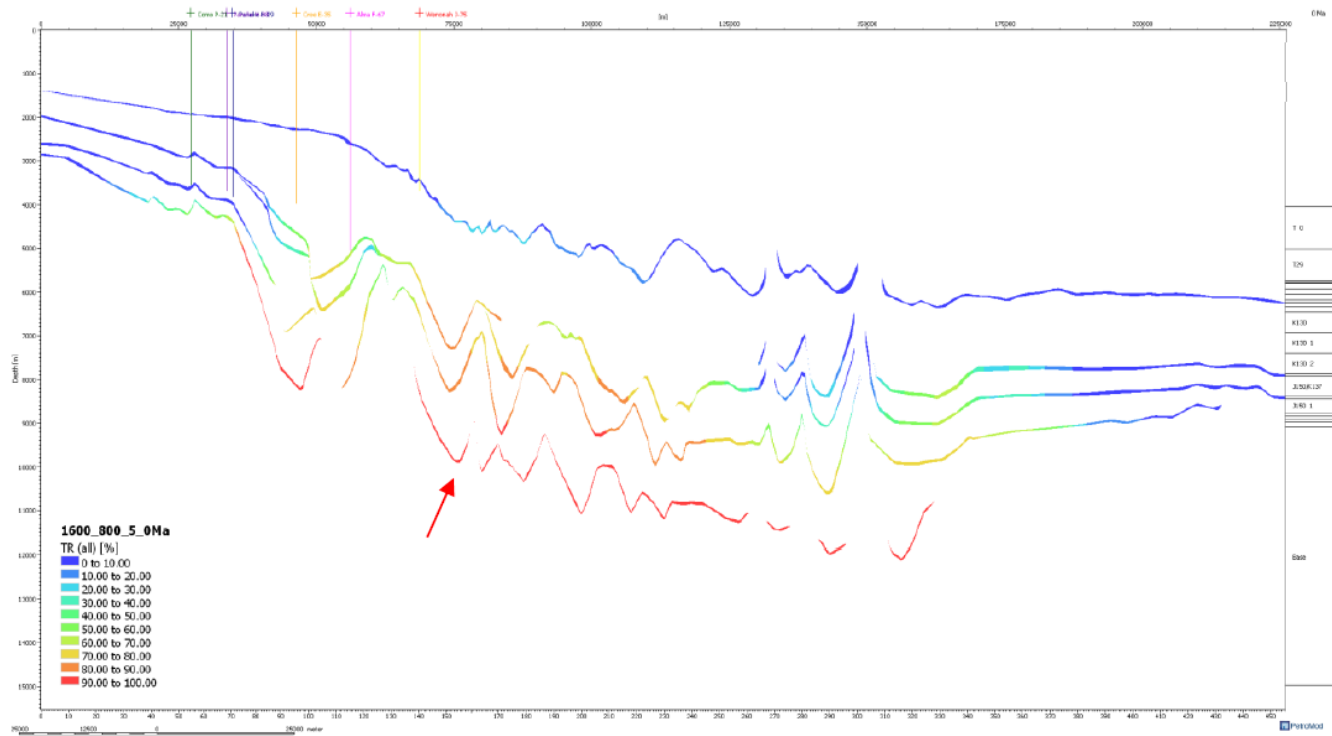


Figure 6. Modelling results for dip line LRV1-1600 run with Lower Jurassic source rock parameters of HI=800 mg HC/g TOC and TOC=5%. Red arrow indicates the track of the Lower Jurassic Source Rock through time.

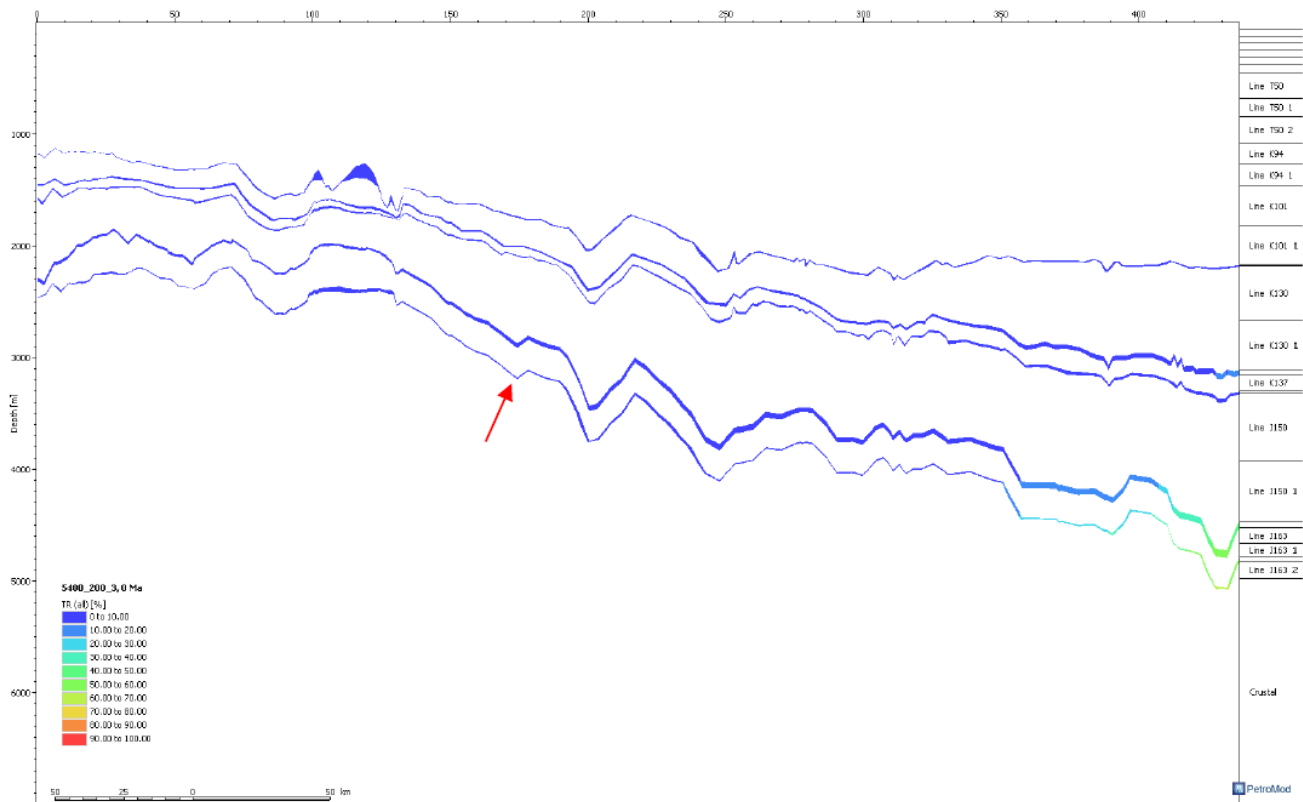


Figure 7. Modelling results for strike line LRV1-5400 run with Lower Jurassic source rock parameters of HI=200 mg HC/g TOC and TOC=3%. Red arrow indicates the track of the Lower Jurassic Source Rock through time.

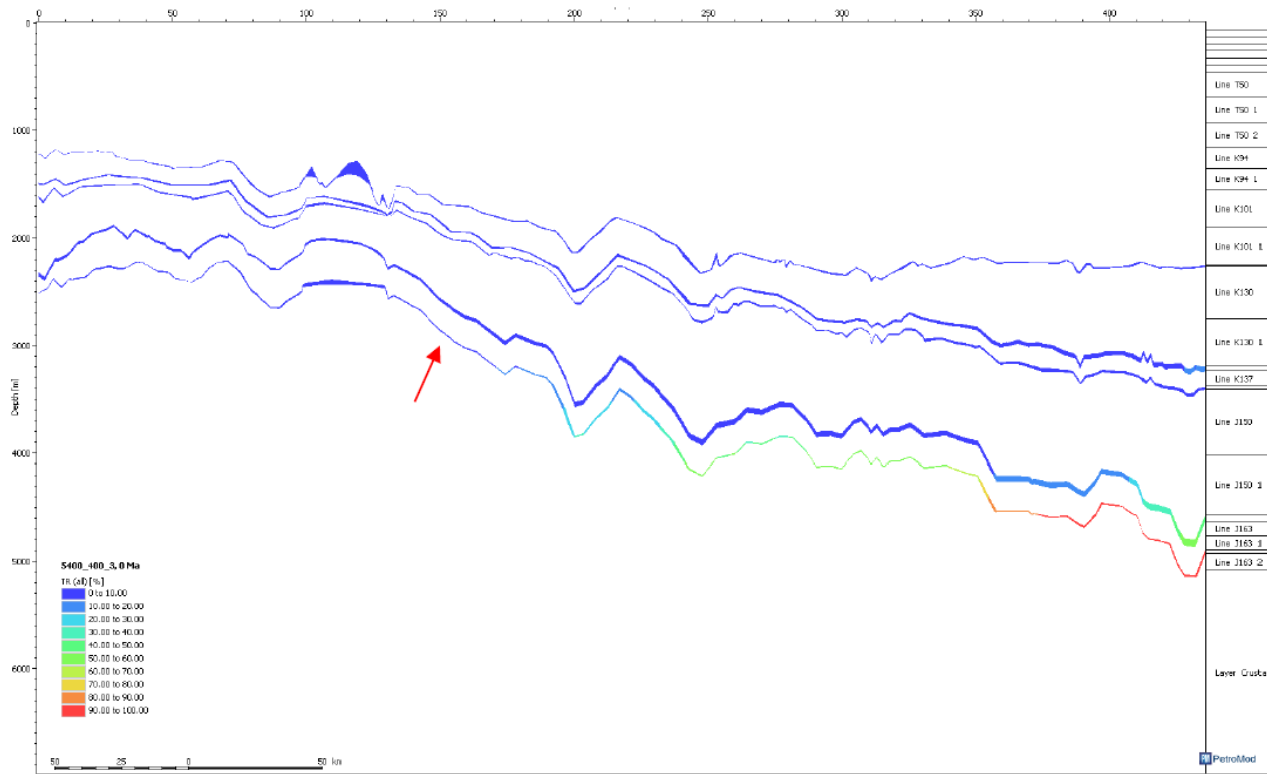


Figure 8. Modelling results for strike line LRV1-5400 run with Lower Jurassic source rock parameters of HI=400 mg HC/g TOC and TOC=3%. Red arrow indicates the track of the Lower Jurassic Source Rock through time.

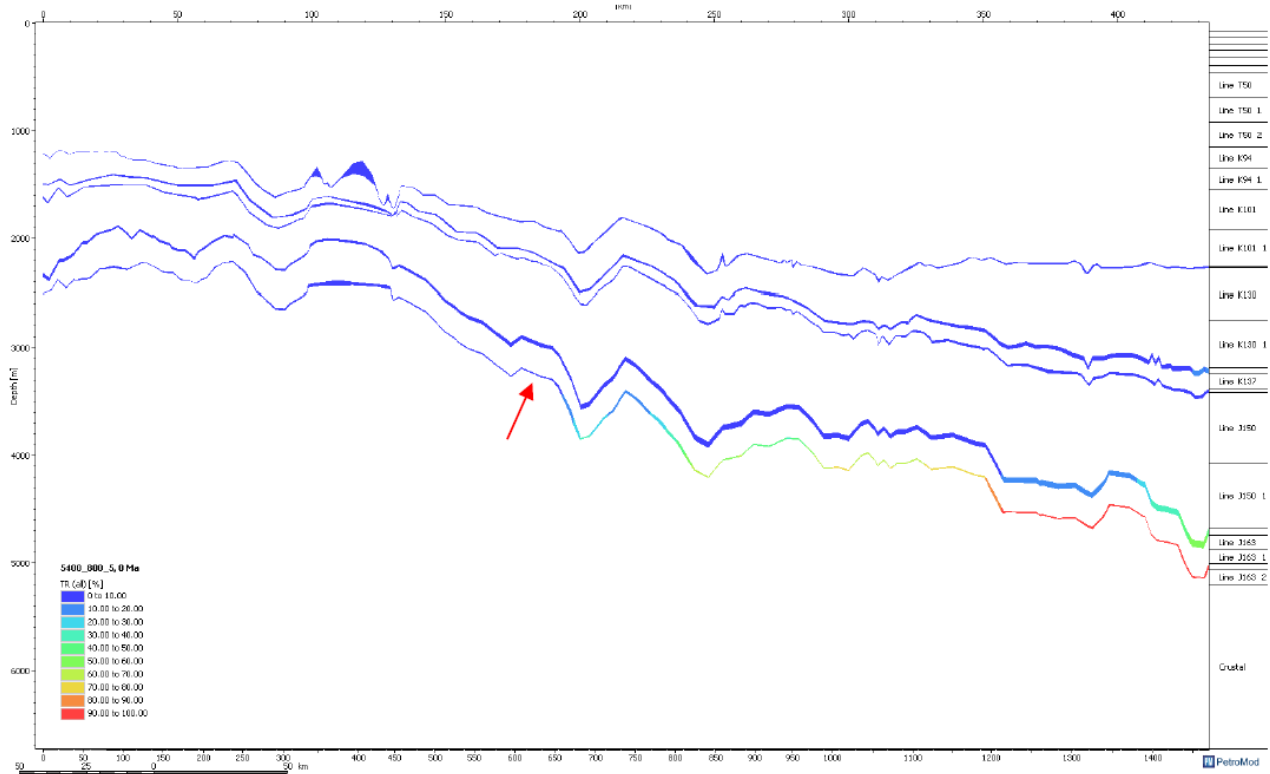


Figure 9. Modelling results for strike line LRV1-5400 run with Lower Jurassic source rock parameters of HI=800 mg HC/g TOC and TOC=5%. Red arrow indicates the track of the Lower Jurassic Source Rock through time.



Summary

The figures above represent the initial outputs of the simulation results for two seismic lines: LRV1-1600 (dip), and LRV1-5400 (strike). Source rock variables of total organic carbon (TOC) and hydrogen index (HI) were based on values from equivalent strata in the High and Middle Atlas of Morocco (e.g. Bodin et al., 2010; Sachse et al., 2012; Rodrigues et al., 2018). The following source rock variable combinations were used in the modelling: HI=200 mg HC/g TOC and TOC=3% (**Figures 4 and 7**); HI=400 mg HC/g TOC and TOC=3% (**Figures 5 and 8**); and HI=800 mg HC/g TOC and TOC=5% (**Figures 6 and 9**). We believe these reasonably reflect the range of potential source rock parameters that may have existed during deposition and subsequent maturation of organic-rich intervals along the Scotian margin.

Based on the simulated models, the Lower Jurassic rocks have different maturities within the different parts of the basin. In the slope and the abyssal area, modelled Lower Jurassic source rocks are mature and are within oil or gas window. On the shelf (and LaHave Platform), their maturity is variable depending on HI and TOC values. The source rock transformation ratio reaches a higher value as it goes into the abyssal area. The Lower Jurassic source rocks also have a higher transformation ratio in the eastern part of the basin, moving from immature to mature.

Acknowledgements

I would like to thank Professor Grant Wach for giving me this great opportunity to work on this research and encouraged me to pursue this project. And I would also like to express my thanks and appreciation to Carlos Wong, who contributed to many discussions and advice that helped resolving some of the most difficult problems. I would also like to acknowledge helpful suggestions from Dr. Ricardo L. Silva.

References

- Bodin, S., Mattioli, E., Fröhlich, S., Marshall, J.D., Boutib, L., Lahsini, S., and Redfern, J., 2010. Toarcian carbon isotope shifts and nutrient changes from the Northern margin of Gondwana (High Atlas, Morocco, Jurassic): Palaeoenvironmental implications. *Palaeogeography, Palaeoclimatology, Palaeoecology*, **297**, 377-390. <https://doi.org/10.1016/j.palaeo.2010.08.018>
- Canada-Nova Scotia Offshore Petroleum Board (CNSOPB), 2009. Call for Bids NS09-1 Information Package - Regional Geoscience Overview. http://www.callforbids.cnsopb.ns.ca/2009/01/regional_geoscience.htm
- Deptuck, M., and Kendell, K., 2012. Contrasting salt tectonic styles on the western versus central parts of the Scotian Margin, offshore Nova Scotia. Abstract, Atlantic Geoscience Society 39th Colloquium and Annual General Meeting 2013, *Atlantic Geology*, **49**, 26-27.
- Hantschel, T., and Kauerauf, A., 2009. *Fundamentals of basin and petroleum systems modelling*. Springer, Berlin, 404 p.
- Hermanrud, C. 1993. Basin modelling techniques-an overview. In: A.G. Dore, J.H. Auguston, C. Hermanrud, D.S. Stewart, and O. Sylta (eds), *Basin modelling: Advances and Applications*. Norwegian Petroleum Society, Special Publication, **3**, 1-34.
- Louden, K.E., Tucholke, B.E., and Oakey, G.N. 2004. Regional anomalies of sediment thickness, basement depth and isostatic crustal thickness in the North Atlantic Ocean. *Earth and Planetary Science Letters*, **224**(1-2), 193-211. doi: 10.1016/j.espl.2004.05.002.
- OETRA, 2011. Scotian Basin Play Fairway Analysis study. Nova Scotia. Department of Energy. Report 88-11-00, http://www.oera.ca/offshore-energy-research/geoscience/play-fairway-analysis/Play_Fairway_Analysis-atlas/



- Rodrigues, B., Mendonça Filho, J.G., Silva, R.L., Driss, S., Duarte, L.V. 2018. Palynofacies as an indicator of paleoenvironmental dynamics across the Early Toarcian in Middle Atlas Basin (Morocco). In: R.L. Silva, L.V. Duarte, and S. Seco (eds), Abstract book of the 2nd International Workshop on Toarcian Oceanic Anoxic Event, Coimbra 2018, Portugal, 73. ISBN: 978-989-98914-6-3
- Sachse, V.F., Leythaeuser, D., Grobe, A., Rachidi, M., and Littke, R., 2012. Organic geochemistry and petrology of a lower Jurassic (Pliensbachian) petroleum source rock from Ait Moussa, Middle Atlas, Morocco. *Journal of Petroleum Geology*, **35**, 5-23. <https://doi.org/10.1111/j.1747-5457.2012.00516.x>
-